CRANFIELD UNIVERSITY

HARIHARAN HANUMANTHAN

SEVERITY ESTIMATION AND SHOP VISIT PREDICTION OF CIVIL AIRCRAFT ENGINES

SCHOOL OF ENGINEERING

PhD

CRANFIELD UNIVERSITY
SCHOOL OF ENGINEERING

PhD Thesis

HARIHARAN HANUMANTHAN

SEVERITY ESTIMATION AND SHOP VISIT PREDICTION OF CIVIL AIRCRAFT ENGINES

Supervisor : Professor Riti Singh

October 2009

ABSTRACT

To sustain in the vibrant field of civil aviation, the aircraft and engine manufacturers are in the pursuit of delivering efficient systems with the best economics. In umpteen scenarios of growing interest, engine maintenance cost due to scheduled maintenance is of importance. The current research is focused on estimation of the maintenance factors, such as *severity* and *shop visit rate to* study the operational scenarios and concurrent technologies.

The severity, defined as relative engine damage is estimated by blending the aircraft performance, gas turbine performance, gas turbine design and life estimation methods towards transforming the thrust variation into life estimates, reflecting the severity on critical Life Limited Part (LLP) of an aircraft engine. The Shop Visit Rate (SVR) is predicted based on Exhaust Gas Temperature (EGT) margin consumption due to gas turbine performance degradation.

The severity studies reveal that Hight Pressure Turbine (HPT) blade and disc are critical, depicting engine severity. Lower thrust engine severity is dominated by cyclic damage (low cycle fatigue) and large thrust engines by steady state damage (creep). The operational factors, take-off derate and Outside Air Temperature (OAT) have more sensitivity on severity of aircraft engines. The use of climb derate, reduces the damage on large thrust engines considerably, especially for three shaft engines. Cooling effectiveness and thermal barrier coating are important technological factors for reducing the severity level.

The SVR prediction on lower and large thrust engines, depict the take-off EGT as a source for shop visits, governed by operational parameters such as take-off derate, OAT, trip length and engine wash. The engine aging curves are represented as Weibull distribution based on severity and SVR.

Severity estimation and shop visit prediction methodology, demonstrated through an integrated tool will serve as a decision making element for comparing competitive engines, operational strategies and engine technologies.

ACKNOWLEDGEMENTS

Any research is a process of flowering in the dimensions of knowledge and experience, driven by moments of inspiration, motivation and support, received with utmost gratitude.

My absolute gratitude is for Professor Riti Singh and Professor Pericles Pilidis for their seamless support and guidance, in one of the finest pursuits of my life.

Sincere appreciation to Dr Peng Ho for shaping the project and instilling growth to the potentialities.

I am much obliged to Professor HIH Saravanamuttoo, Carleton University for refining my technical knowledge.

Thanks to Dr Panagiotis Laskaridis. I am thankful to Jan Janikovic, Diego Ayuso Adanero, Maria Sanchez, research colleagues and MSc students. Special thanks to the Cranfield staff for the pleasant atmosphere and timely help by Gillian Hargreaves, Maria Negus, Claire Bellis, Sam Broe, Rachel Smith and Nicola Datt.

I owe much more to my mother H.Yasodha to my dear wife H.Sivashankari and my affectionate brother H.Balaji for tremendous patience and love.

I have tearfull gratitude to my loving father K.Hanumanthan and my friend Navaal Ramdin who would have taken pride in my accomplishments.

I am grateful to my family members and friends for the ceaseless support and affection.

"Happiness cannot be traveled to, owned, earned, worn or consumed. Happiness is the spiritual experience of living every minute with love, grace and gratitude."

Dennis Waitley

TABLE OF CONTENTS

ABSTRACT ..... **II**
ACKNOWLEDGEMENTS ..... **III**
TABLE OF CONTENTS ..... **IV**
LIST OF FIGURES ..... **VIII**
LIST OF TABLES ..... **XVI**
NOTATIONS ..... **XVIII**
ROMAN SYMBOLS XVIII
GREEK SYMBOLS XXI
ACRONYMS ..... **XXII**
GLOSSARY ..... **XXIV**
PREAMBLE TO CHAPTERS ..... **XXVI**
1 INTRODUCTION **1**
1.1 AIRCRAFT ENGINES 1
1.2 TURBOFAN COMPONENTS 3
1.3 AIRCRAFT ENGINE DESIGN PROCESS 5
1.4 MAINTENANCE AND RESEARCH FOCUS 9
2 RESEARCH PARADIGM **13**
2.1 OBJECTIVE 13
2.2 DEFINITION OF THE NEED – SEVERITY 14
2.2.1 Derate Severity Curve *14*
2.2.2 Operational and Technology Parameters for Severity Estimation *15*
2.3 DEFINITION OF THE NEED – SHOP VISIT PREDICTION 16
2.3.1 Operational Parameters for Shop Visit Prediction *17*
2.3.2 Aging Curves *18*
2.4 SEVERITY ESTIMATION AND SOFTWARE DESCRIPTION 18
2.5 SHOP VISIT PREDICTION AND SOFTWARE DESCRIPTION 23
2.6 AUTHORS CONTRIBUTION 26
3 AIRCRAFT AND GAS TURBINE PERFORMANCE **29**
3.1 AIRCRAFT PERFORMANCE 29
3.2 FLIGHT PATH ANALYSIS 32
3.3 SIMPLIFIED FLIGHT PATH ANALYSIS APPROACH 32
3.4 GAS TURBINE PERFORMANCE 37
4 GAS TURBINE DESIGN **45**
4.1 TURBINE BLADE SIZING 45
4.2 COMPRESSOR BLADE SIZING 47

4.3 Parametric Disc 49
4.4 Technological Factors 51
5 ANALYSIS 57
5.1 Finite Element Analysis 57
5.2 Turbine Blade Modeling 60
5.3 Disc Modeling 62
5.4 Heat Transfer Calculation 63
5.5 Thermal Analysis 65
5.6 Thermo-Mechanical Analysis 68
5.7 Analysis Output 70
6 LIFE ESTIMATION 71
6.1 Failure Modes 71
6.2 Life Estimation Methods 74
6.3 Damage Calculation 78
6.4 Severity 81
7 SHOP VISIT PREDICTION 83
7.1 Engine Maintenance 83
7.2 Engine Degradation 85
7.3 Shop Visit Prediction Method 87
7.4 Aging Curves 90
8 CASE STUDIES ON SEVERITY 93
8.1 Engine Models 93
8.2 Short Haul Flight – Reference Mission 94
8.3 Short Haul Flight – Operational Factors 105
8.4 Short Haul Flight – Technological Factors 111
8.5 Short Haul Flight – Derate Severity Curve 114
8.6 Long Haul Flight – Reference Mission 116
8.7 Long Haul Flight – Operational Factors 125
8.8 Long Haul Flight – Technological Factors 130
8.9 Long Haul Flight – Derate Severity Curve 133
8.10 Long Haul Flight – Operational Factors Study – Engine E84 and E95 135
8.11 Long Haul Flight – Operational Factors Study – Comparison of Engines 142
8.12 Severity Sensitivity Analysis on Operational Factors 149
8.13 Severity Case Studies Summary 153
9 MISCELLANEOUS CASE STUDIES ON SEVERITY 155
9.1 High Pressure Compressor Severity Estimation 155
9.2 Mesh Convergence Study 163
9.3 Tip Shroud Design on HPT Blade Life 163

9.4 BLISK DESIGN ON HPT LIFE 164
9.5 COMPARISON OF AN^2 APPROACH WITH SEVERITY ESTIMATION METHODOLOGY 166
9.6 MISCELLANEOUS CASE STUDIES ON SEVERITY – SUMMARY 168
10 CASE STUDIES ON SHOP VISIT PREDICTION 169
10.1 OVERVIEW ON SHOP VISIT RATE PREDICTION FOR ENGINE MODELS 169
10.2 DEGRADATION – CYCLE DEFINITION 170
10.3 SHORT HAUL FLIGHT – SHOP VISIT RATE PREDICTION FOR ENGINE E56 177
10.4 SHORT HAUL FLIGHT – OPERATIONAL FACTORS STUDY ON ENGINE E56 SHOP VISIT RATE 181
10.5 SHORT HAUL FLIGHT – AGING CURVE FOR E56 ENGINE 186
10.6 SHORT HAUL FLIGHT – EFFECT OF ENGINE WASH ON ENGINE E56 SHOP VISIT RATE 188
10.7 LONG HAUL FLIGHT – SHOP VISIT RATE PREDICTION FOR ENGINE E115 189
10.8 LONG HAUL FLIGHT – OPERATIONAL FACTORS STUDY ON ENGINE E115 SHOP VISIT RATE 192
10.9 LONG HAUL FLIGHT – AGING CURVE FOR ENGINE E115 196
10.10 LONG HAUL FLIGHT – EFFECT OF ENGINE WASH ON ENGINE E115 SHOP VISIT RATE 198
10.11 SHOP VISIT RATE PREDICTION SENSITIVITY ANALYSIS 199
10.12 SHOP VISIT RATE PREDICTION – SUMMARY 201
11 CONCLUSION 203
12 SCOPE FOR IMPROVEMENTS AND FURTHER RESEARCH 205
13 REFERENCES 209
APPENDIX A 219
APPENDIX B 221
APPENDIX C 223
APPENDIX D 225
APPENDIX E 227
APPENDIX F 229

LIST OF FIGURES

Figure 1.1 : Turbofan engine cross section. 3
Figure 1.2 : Aircraft engine product development process [11]. 6
Figure 1.3 : Elements of aircraft engine design. 7
Figure 1.4 : Fuel control system [9]. 9
Figure 1.5 : Major activities of MRO industry. 10
Figure 2.1 : Severity estimation process..... 19
Figure 2.2 : Shop vist prediction methodology layout. 24
Figure 3.1 : Physical forces on an aircraft. 30
Figure 3.2 : Thrust and power curve at sea level..... 31
Figure 3.3 : Thrust available (engine thrust) classification..... 33
Figure 3.4 : Engine thrust variation with COT according to hierarchy..... 34
Figure 3.5 : Thrust fraction variation during mission [102]. 34
Figure 3.6 : Design point calculation. 36
Figure 3.7 : Off-design calculation points. 37
Figure 3.8 : Gas turbine cycle and entropy diagram. 38
Figure 3.9 : Twin spool turbofan layout. 38
Figure 3.10 : Typical compressor characteristics. 40
Figure 3.11 : Typical combustor characteristics. 41
Figure 3.12 : Typical turbine characteristics. 42
Figure 4.1 : Simplified flow chart of turbine sizing. 47
Figure 4.2 : Disc designs used in gas turbines. 50
Figure 4.3 : Thermal barrier coating on turbine blade..... 53
Figure 4.4 : Pattern factor profile description. 55
Figure 5.1 : Finite element analysis layout. 58
Figure 5.2 : Linear element types. 59
Figure 5.3 : NACA profiles for turbine blade. 61
Figure 5.4 : HPT blade geometry and finite element model..... 62
Figure 5.5 : Geometry and finite element model of disc and blade-disc assembly. 63
Figure 5.6 : Heat transfer correlations on the HPT blade. 65
Figure 5.7 : Heat transfer correlations on the HPT disc. 65

Figure 5.7 : Metal temperature plot at take-off and top-of-climb for HPT..... 67
Figure 5.8 : Von Mises stress plot at take-off and top-of-climb for HPT. 70
Figure 6.1 : Fatigue life variation with strain amplitude..... 75
Figure 7.1 : Classification of engine maintenance. 84
Figure 7.2 : Causes for engine degradation. 85
Figure 7.3 : Shop visit defining parameters. 88
Figure 7.4 : Shop visit prediction methodology layout. 89
Figure 7.5 : Aging curve characteristics..... 91
Figure 8.1 : E56 engine thrust and altitude variation for 1.4 hrs trip mission. 95
Figure 8.2 : E56 engine HPT turbine entry temperature, mass flow rate and shaft speed vector variation for 1.4 hrs trip mission. 95
Figure 8.3 : E56 engine HPT blade and disc geometry. 96
Figure 8.4 : E56 engine HPT heat transfer correlation and flow mapping. .. 97
Figure 8.5 : E56 Engine finite element model. 97
Figure 8.6 : Heat transfer application on finite element model of E56 HPT. 98
Figure 8.7 : E56 engine HPT blade metal temperature at mission points.... 99
Figure 8.8 : E56 engine HPT disc metal temperature at mission points. ... 100
Figure 8.9 : E56 engine HPT structural model constraints and load..... 101
Figure 8.10 : E56 engine HPT blade Von Mises or equivalent stress plot at mission points. 102
Figure 8.11 : E56 engine HPT disc Von Mises or equivalent stress plot at mission points. 103
Figure 8.12 : E56 engine HPT blade and disc life consumption pattern. 104
Figure 8.13 : E56 engine HPT blade and disc life plots. 104
Figure 8.14 : E56 engine characteristics for variation in take-off derate (a) Exhaust gas temperature (b) Shaft speed scaling vector (c) Blade Severity (d) Disc Severity. 106
Figure 8.15 : E56 engine characteristics for variation in climb derate (a) Exhaust gas temperature (b) Shaft speed scaling vector (c) Blade Severity (d) Disc Severity. 107
Figure 8.16 : E56 engine characteristics for variation in cruise derate (a) Exhaust gas temperature (b) Shaft speed scaling vector (c) Blade Severity (d) Disc Severity. 108
Figure 8.17 : E56 engine characteristics for variation in OAT (a) Exhaust gas temperature (b) Shaft speed scaling vector (c) Blade Severity (d) Disc Severity. 109

Figure 8.18 : E56 engine characteristics for variation in airport altitude (a) Exhaust gas temperature (b) Shaft speed scaling vector (c) Blade Severity (d) Disc Severity. 110

Figure 8.19 : E56 engine characteristics for variation in cruise altitude (a) Exhaust gas temperature (b) Shaft speed scaling vector (c) Blade Severity (d) Disc Severity. 111

Figure 8.20 : E56 engine severity variation with blade cooling effectiveness (a) Blade severity (b) Disc severity. 112

Figure 8.21 : E56 engine severity variation with thermal barrier coating (a) Thickness (b) Thermal conductivity. 113

Figure 8.22 : E56 engine severity variation with pattern factor (a) Location (b) Magnitude. 114

Figure 8.23 : E56 engine derate severity curve for 1.4 hrs mission. 115

Figure 8.24 : E56 engine derate severity curves for trip lengths. 115

Figure 8.25 : E115 engine thrust and altitude variation for 4 hrs trip mission. 116

Figure 8.26 : E115 engine HPT turbine entry temperature, mass flow rate and shaft speed variation for 4 hrs trip mission. 117

Figure 8.27 : E115 engine HPT blade and disc geometry. 118

Figure 8.28 : E115 engine HPT heat transfer correlation and flow mapping. 118

Figure 8.29 : E115 engine HPT heat transfer coefficients and bulk temperature. 119

Figure 8.30 : E115 engine finite element model. 119

Figure 8.31 : E115 engine HPT blade metal temperature at mission points. 121

Figure 8.32 : E115 engine HPT disc metal temperature at mission points. . 121

Figure 8.33 : E115 engine HPT structural model constraints and loads. 122

Figure 8.34 : E115 engine HPT blade Von Mises or equivalent stress plot at mission points. 122

Figure 8.35 : E115 engine HPT disc Von Mises or equivalent stress plot at mission points. 123

Figure 8.36 : E115 engine HPT blade and disc life consumption plot. 124

Figure 8.37 : E115 engine HPT blade and disc life plots. 124

Figure 8.38 : E115 engine characteristics for variation in take-off derate (a) Exhaust gas temperature (b) Shaft speed scaling vector (c) Blade Severity (d) Disc Severity. 126

Figure 8.39 : E115 engine characteristics for variation with climb derate (a) Exhaust gas temperature (b) Shaft speed scaling vector (c) Blade Severity (d) Disc Severity. 127

Figure 8.40 : E115 engine characteristics for variation cruise derate (a) Exhaust gas temperature (b) Shaft speed scaling vector (c) Blade Severity (d) Disc Severity. 128

Figure 8.41 : E115 engine characteristics for variation in OAT (a) Exhaust gas temperature (b) Shaft speed scaling vector (c) Blade Severity (d) Disc Severity. 129

Figure 8.42 : E115 engine characteristics for variation in airport altitude (a) Exhaust gas temperature (b) Shaft speed scaling vector (c) Blade Severity (d) Disc Severity. 129

Figure 8.43 : E115 engine characteristics for variation in cruise altitude (a) Exhaust gas temperature (b) Shaft speed scaling vector (c) Blade Severity (d) Disc Severity. 130

Figure 8.44 : E115 engine severity variation with blade cooling effectiveness (a) Blade severity (b) Disc severity. 131

Figure 8.45 : E115 engine severity variation with thermal barrier coating (a) Thickness (b) Thermal conductivity. 132

Figure 8.46 : E115 engine severity variation with pattern factor (a) Location (b) Magnitude. 133

Figure 8.47 : E115 engine derate severity curve for 4 hrs mission. 134

Figure 8.48 : E115 engine derate severity curves for trip lengths 134

Figure 8.49 : E84 engine characteristics for variation in take-off derate (a) Exhaust gas temperature (b) Shaft speed scaling vector (c) Blade Severity (d) Disc Severity. 135

Figure 8.50 : E95 engine characteristics for variation in take-off derate (a) Exhaust gas temperature (b) Shaft speed scaling vector (c) Blade Severity (d) Disc Severity. 136

Figure 8.51 : E84 engine characteristics for variation in climb derate (a) Exhaust gas temperature (b) Shaft speed scaling vector (c) Blade Severity (d) Disc Severity. 136

Figure 8.52 : E95 engine characteristics for variation in climb derate (a) Exhaust gas temperature (b) Shaft speed scaling vector (c) Blade Severity (d) Disc Severity. 137

Figure 8.53 : E84 engine characteristics for variation in cruise derate (a) Exhaust gas temperature (b) Shaft speed scaling vector (c) Blade Severity (d) Disc Severity. 137

Figure 8.54 : E95 engine characteristics for variation in cruise derate (a) Exhaust gas temperature (b) Shaft speed scaling vector (c) Blade Severity (d) Disc Severity. 138

Figure 8.55 : E84 engine characteristics for variation in OAT (a) Exhaust gas temperature (b) Shaft speed scaling vector (c) Blade Severity (d) Disc Severity. 138

Figure 8.56 : E95 engine characteristics for variation in OAT (a) Exhaust gas temperature (b) Shaft speed scaling vector (c) Blade Severity (d) Disc Severity. 139

Figure 8.57 : E84 engine characteristics for variation in airport altitude (a) Exhaust gas temperature (b) Shaft speed scaling vector (c) Blade Severity (d) Disc Severity. 139

Figure 8.58 : E95 engine characteristics for variation in airport altitude (a) Exhaust gas temperature (b) Shaft speed scaling vector (c) Blade Severity (d) Disc Severity. 140

Figure 8.59 : E84 engine characteristics for variation in cruise altitude (a) Exhaust gas temperature (b) Shaft speed scaling vector (c) Blade Severity (d) Disc Severity. 140

Figure 8.60 : E95 engine characteristics for variation in cruise altitude (a) Exhaust gas temperature (b) Shaft speed scaling vector (c) Blade Severity (d) Disc Severity. 141

Figure 8.61 : E84 engine characteristics for variation in cruise Mach (a) Exhaust gas temperature (b) Shaft speed scaling vector (c) Blade Severity (d) Disc Severity. 141

Figure 8.62 : E95 engine characteristics for variation in cruise Mach (a) Exhaust gas temperature (b) Shaft speed scaling vector (c) Blade Severity (d) Disc Severity. 142

Figure 8.63 : Large thrust engines comparison for take-off derate characteristics (a) Blade severity (b) Disc severity (c) HPT severity. 143

Figure 8.64 : Large thrust engines comparison for climb derate characteristics (a) Blade severity (b) Disc severity (c) HPT severity. 144

Figure 8.65 : Large thrust engines comparison for cruise derate characteristics (a) Blade severity (b) Disc severity (c) HPT severity. 145

Figure 8.66 : Large thrust engines comparison for variation in OAT (a) Blade severity (b) Disc severity (c) HPT severity. 146

Figure 8.67 : Large thrust engines comparison for variation in airport altitude (a) Blade severity (b) Disc severity (c) HPT severity. 147

Figure 8.68 : Large thrust engines comparison for variation in cruise altitude (a) Blade severity (b) Disc severity (c) HPT severity. 148

Figure 8.69 : Large thrust engines comparison for variation in cruise Mach (a) Blade severity (b) Disc severity (c) HPT severity. 148

Figure 8.70 : Lower thrust engine severity sensitivity for operational factors (a) Blade severity (b) Disc severity (c) HPT severity. 150

Figure 8.71 : Large thrust engine severity sensitivity on operational factors (a) Blade severity (b) Disc severity (c) HPT severity. 152

Figure 9.1 : Geometric and finite lement model of HPC blade and disc. ... 156
Figure 9.2 : Heat transfer correlations on HPC blade and disc..... 156
Figure 9.3 : Metal temperature variation on HPC blade. 157
Figure 9.4 : Metal temperature variation on HPC disc..... 157
Figure 9.5 : Equivalent stress variation on HPC blade. 158
Figure 9.6 : Equivalent stress variation on HPC disc..... 158
Figure 9.7 : Life plots for HPC blade and disc. 159
Figure 9.8 : Life consumption pattern for HPC blade and disc. 159
Figure 9.9 : Severity variation with take-off, climb and cruise derate variation for HPC blade and disc. 161
Figure 9.10 : Severity variation with OAT and airport altitude for HPC blade and disc..... 162
Figure 9.11 : Severity variation with cruise altitude and Mach number for HPC blade and disc..... 162
Figure 9.12 : HPT blade life plots comparison for tip shroud effect. 164
Figure 9.13 : HPT life plots comparison for blisk design..... 165
Figure 9.14 : Take-off derate severity characteristics comparison for AN^2 approach and severity method for engine E56..... 167
Figure 10.1 : EGT margin consumption for engine E56 through degradation scaling. 172
Figure 10.2 : EGT Margin Consumption for engine E115 through degradation scaling 172
Figure 10.3 : EGT margin consumption due to individual component degradation for engine E56. 174
Figure 10.4 : EGT margin consumption due to individual component degradation for engine E115 175
Figure 10.5 : Weibull curve for degradation scale of engine E56. 176
Figure 10.6 : Weibull curve for degradation scale of engine E115. 176
Figure 10.7 : Component degradation variation with engine flight cycles for engine E56. 178
Figure 10.8 : Take-off EGT characteristics for first shop visit prediction of engine E56. 179
Figure 10.9 : Climb and cruise EGT characteristics for the shop visit prediction of engine E56. 180
Figure 10.10 : EGT characteristics with successive shop visit for engine E56 180
Figure 10.11 : Effect of take-off derate on shop visit interval of engine E56.. 182

Figure 10.12 : Shop visit rate variation with take-off derate for engine E56. . 182
Figure 10.13 : Effect of OAT on shop visit interval for engine E56. 183
Figure 10.14 : Shop visit variation with OAT for engine E56. 184
Figure 10.15 : EGT characteristics variation with trip lengths for engine E56. 185
Figure 10.16 : Shop visit characteristics of engine E56. 186
Figure 10.17 : Aging curves for engine E56. 187
Figure 10.18 : Comparison of EGT characteristics due to engine wash for engine E56. 188
Figure 10.19 : Component degradation with engine flight cycles for engine E115. 190
Figure 10.20 : Take-off EGT characteristics for engine E115. 191
Figure 10.21 : Climb and cruise EGT characteristics for engine E115. 191
Figure 10.22 : Take-off EGT variation with successive shop visits for engine E115. 192
Figure 10.23 : Effect of take-off derate on EGT characteristics for engine E115. 193
Figure 10.24 : Shop visit variation with take-off derate for engine E115. 193
Figure 10.25 : Effect of OAT on EGT characteristics for engine E115. 194
Figure 10.26 : Shop visit variation with OAT for engine E115. 194
Figure 10.27 : Effect of trip length on the EGT characteristics of engine E115. 195
Figure 10.28 : Shop visit characteristics for engine E115. 196
Figure 10.29 : Aging curves for engine E115. 197
Figure 10.30 : Comparison of EGT characteristics due to engine wash for engine E115. 198
Figure 10.31 : Shop visit rate sensitivity plots for operational parameters. 199
Figure 10.32 : Effect of engine wash for engine E56 and E115. 200
Figure A.1 : Turbomatch brick layout for engines (a) E56 (b) E115. 219
Figure B.1 : HPT flow path and blade sizing for E56. 221
Figure B.2 : HPT flow path and blade sizing for E115. 221
Figure B.3 : HPC flow path and blade sizing for E56. 222
Figure C.1 : Larson Miller curve for Inconel 718 [97]. 223
Figure C.2 : Larson Miller curve for R-41 (Rene 41) [90]. 223
Figure C.3 : Oxidation parameters for life estimation [79]. 223
Figure D.1 : MTBR data for engines (a) CFM56-7 [87] (b) GE90-115B [87].

..... 225
Figure D.2 : Redline temperatures for engines (a) CFM56-7 [34] (b) GE90-115B [34]. 225
Figure E.1 : Typical climb derate characteristics. 227
Figure F.1 : Graphical user interface of the tool. 229

LIST OF TABLES

Table 3.1 : Thrust fraction data for typical flight mission [102]. 35

Table 4.1 : Blade preliminary design assumptions for height and weight (root and post) based on the disc design [81]. 51

Table 5.1 : NACA profile mean line and thickness variation [31]. 61

Table 8.1 : Aircraft engine specification used for building the engine models. 94

Table 8.2 : Technology parameter settings. 94

Table 8.3 : Rene 41 and Inconel 718 material properties. 98

Table 8.4 : E56 engine HPT blade life summary. 103

Table 8.5 : E56 engine HPT disc life summary. 104

Table 8.6 : E56 engine severity estimation for the reference mission. 105

Table 8.7 : E115 engine HPT blade life summary. 123

Table 8.8 : E115 engine HPT disc life summary. 124

Table 8.9 : E115 engine severity estimation for the reference mission. ... 125

Table 8.10 : Lower thrust engine severity sensitivity values for operational factors. 150

Table 8.11 : Large thrust engines severity sensitivity values for operational factors. 152

Table 9.1 : Life estimates for HPC blade and disc. 160

Table 9.2 : Mesh convergence study for HPC blade and disc. 163

Table 9.3 : Tip shroud comparison on HPT blade life estimate. 164

Table 9.4 : Blisk comparison on HPT life estimate. 165

Table 9.5 : Comparison table on AN2 approach and severity method. 166

Table 9.6 : Comparison of AN^2 approach with severity method in capturing the turbine blade severity. 167

Table 10.1 : Engine models for shop visit study. 170

Table 10.2 : Degradation values for the performance model. 171

Table 10.3 : Degradation cycle definition of engine E56. 177

Table 10.4 : EGT margin settings for the shop visit prediction of engine E56. 178

Table 10.5 : Shop visit interval for engine E56 through shop visit prediction. 181

Table 10.6 : Age factor estimation as Weibull distribution with respect to

MSVR of engine E56. 187
Table 10.7 : Degradation cycle definition of engine E115. 189
Table 10.8 : EGT margin settings for shop visit prediction of engine E115. 189
Table 10.9 : Shop visit interval for engine E115 through shop visit prediction. 192
Table 10.10 : Age factor estimation as Weibull distribution with respect to MSVR of engine E115. 197
Table 10.11 : Shop visit rate sensitivity values for operational parameters. . 199
Table 10.12 : Effect of engine wash on lower and large thrust engine.. 200

NOTATIONS

Roman Symbols

Symbol	Description	Units
A	area of flow path at mid span of blade	m
bf	fatigue strength exponent	
Bi_m	Biot number for metal	
Bi_{tbc}	Biot number for thermal barrier coating	
c	specific heat capacity for metal	J/kg-K
C_a	axial flow velocity	m/s
C_{crp}	creep constant dependent on the material	
cf	fatigue ductility exponent	
C_{hc}	jet velocity of the cold stream	m/s
C_{jc}	jet velocity of the cold stream	m/s
C_{oxid}	oxidation life constant	
C_{oxid_c}	constant for parabolic oxidation law	
C_p	specific heat capacity at constant pressure	J/kg-K
C_w	whirl velocity	m/s
[D]	conductivity matrix or stiffness matrix	
d	depth of the oxidation - arrhenius equation	in
D	drag force	N
D_c	damage fraction due to low cycle fatigue	
D_s	damage fraction due to creep and oxidation	
E	Young's Modulus	Pa
G	gap ratio (cavity axial width to radius ratio)	
Gr	Grashoff number	
k_p	parabolic rate constant	g^2/cm^4-sec
K_{xx}	thermal conductivity in the corresponding direction	W/m-K
L	lift force	Newton [N]
{L}	matrix vector operator	
m	mass flow at the inlet	kg/s
m_c	mass flow rate of cold stream	kg/s
m_h	mass flow rate of hot stream	kg/s
n	specific ratio	
n_i	number of load cycles	
N	shaft speed	rev/s (or rpm)
N_i	low cycle fatigue life in corresponding load cycle	cycles

Symbol	Description	Units
N_s	shaft speed scaling value	
Nu	Nusselt Number	
P	Larson-Miller Parameter	
p	pressure distribution	Pa
P_{01}	stagnation pressure at inlet	Pascal [Pa]
P_{02}	stagnation pressure at compressor outlet	Pa
P_{03}	stagnation pressure at turbine inlet	Pascal [Pa]
P_A	power available	Watts [W]
Pr	Prandtl number	
P_R	power required	Watts [W]
Q	activation energy - Arrhenius equation	ft-lb/lb
R	gas constant - Arrhenius equation	ft/R
r	radius	m
RA	area reduction of stressed component	
r_c	radius of curvature	m
Re_c	Reynold's number over flat plate	
Re_d	Reynold's number over a circular cylinder	
Re_{hd}	Reynold's number for an hydraulic diameter	
Re_z	axial Reynold's number	
S	severity factor	
T	temperature	K
t	time	seconds [s]
T_{01}	stagnation temperature at inlet	Kelvin [K]
T_{02}	stagnation temperature at compressor outlet	K
$T_{0c,k}$	stagnation temperature of coolant at tap condition	K
$T_{0c,x}$	stagnation temperature of coolant at mixing zone	K
T_{0g}	stagnation temperature of inlet gas	K
T_A	thrust available	N
T_{aw}	adiabatic wall temperature	K
T_{ci}	coolant inlet temperature	K
t_{crp}	creep life	hrs
T_E	thrust force	N
t_f	total flight duration	
T_g	gas temperature	K
t_i	flight segment interval	
T_m	metal temperature	K

Symbol	Description	Units
t_m	thickness of the metal	m
$T_{m,ext}$	metal temperature external	K
$T_{m,int}$	metal temperature internal	K
T_{oxid}	oxidation temperature	F
t_{oxid}	oxidation life	hrs
T_R	thrust required	N
T_{t1}	static temperature at nozzle inlet	K
T_{t2}	static temperature at blade inlet	K
T_{t3}	static temperature at blade outlet	K
T_{tav}	average exit temperature	K
t_{tbc}	thickness of thermal barrier coating	m
T_{tin}	average inlet temperature	K
T_{tmax}	maximum exit temperature	K
T_w	temperature at the wall	K
U	mean blade speed	m/s
{V}	velocity vector for mass transport of heat	
V_∞	velocity of flight	m/s
V_A	velocity of aircraft along flight path	m/s
W_A	weight of Aircraft	N
W_{oxid}	weight gain per unit area due to oxidation	kg/m^2

Greek Symbols

Symbol	Description	Units
ΔT_{0S}	stagnation temperature difference between inlet and outlet	K
$[\sigma]$	stress vector	
$\{\varepsilon\}$	elastic strain vector	
$\{\varepsilon^{th}\}$	thermal strain vector	
$\Delta\varepsilon$	strain range	
$\Delta\varepsilon_{el}$	elastic strain range	
$\Delta\varepsilon_{p}$	plastic strain range	
α	air angle	degree
α_g	heat transfer coefficient	W/m^2K
α_x^{se}	thermal expansion coefficient in respective direction	1/K
β_1	angle of relative inlet velocity with respect to axial direction	degree
β_2	angle of relative outlet velocity with respect to axial direction	degree
ε	strain on the element	
ε_0	total cooling effectiveness	
ε_a	strain amplitude	
$\varepsilon_{c,int}$	internal flow cooling effectiveness	
ε_f'	fatigue ductility coefficient	
$\varepsilon_f^{'}$	true tensile ductility	
$\varepsilon_{f'}$	film cooling effectiveness	
ε_{ff}	true fracture ductility	
η_{cp}	compressor isentropic efficiency	
θ_w	the angle between the force due to weight of aircraft and lift direction	degree (or radian)
Λ	degree of reaction	
λ_c	cyclic damage rate fraction	
λ_{cp}	compressor work done factor	
λ_s	steady state damage rate fraction	
λ_t	total damage rate fraction	
λ_{tbc}	thermal conductivity of thermal barrier coating	W/mK
v_{xy}	major Poisson's ratio	
v_{yx}	minor Poisson's ratio	
ρ	density	kg/m^3
σ_f'	fatigue strength coefficient	
σ_u	ultimate tensile strength	Pa
φ	flow coefficient	
Ψ	stage loading coefficient	
ω	angular velocity	rad/s
Φ_c	cooling effectiveness	

ACRONYMS

Abbreviation	Description
2D (or 2-D)	Two Dimensional
3D (or 3-D)	Three Dimensional
APDL	Ansys Parametric Design Language
BR	By-pass Ratio
CAE	Computer Aided Engineering
COT	Combustor Outlet Temperature
EFC	Engine Flight Cycles
EFH	Engine Flight Hours
EGT	Exhaust Gas Temperature
EPFM	Elasto-Plastic Fracture Mechanics
FOD	Foreign Object Damage
HPC	High Pressure Compressor
HPT	High Pressure Turbine
LCF	Low Cycle Fatigue
LEFM	Linear Elastic Fracture Mechanics
LLP	Life Limited Part
MCrAIY	Molybdenum Chromimium Aluminium Yittria
MRO	Maintenance Repair Overhaul
MSVR	Mature Shop Visit Rate
MTBR	Mean Time Between Removal
NACA	National Advisory Comitte for Aeronautics
NASA	National Aeronautics and Space Administration
No_x	Nitrogen Oxides
OAT	Outside Air Temperature
OEM	Original Equipment Manufacturer
PF	Pattern Factor
SVR	Shop Visit Rate
TBC	Thermal Barrier Coating
TET	Turbine Entry Temperature
T-O (or TO)	Take off

GLOSSARY

Terminology	Definition
Aging curve	The variation of the maturity factor of the engine with engine flight hours based on the mature shop visit rate.
Age factor	The value obtained through weibull distribution representing the aging of the engine with engine flight hours.
Degradation scaling vector	The scaling value with respect to maximum level of component degradation.
Derate	Percentage reduction in the thrust from the rated thrust.
Exhaust Gas Temperature (EGT)	Indicates the temperature at the downstream end of the hot gas path as specified by the engine manufacturers.
E56	Two shaft turbofan similar to CFM 56-7.
E84	Two shaft turbofan similar to PW 4084.
E95	Three shaft turbofan similar to Trent 895.
E115	Two shaft turbofan similar to GE 90-115.
EGT Margin	Difference between exhaust gas temperature and redline temperature.
Life consumption pattern	The damage distribution pattern representing event based damage contribution in percentage towards total damage due to the failure mode for the minimum life zone.
Life Limited Part	The aircraft engine component life as specified by the engine manufacturers for tracking useful service life.
Life Plot	A contour plot showing the life of the component expressed as logarithmic value with hyphen as prefix and depicting the zone with minimum life as red colour and maximum life as blue colour.

Terminology	Definition
Long haul	The typical mission having long flight duration powered by large thrust engines. Twin aisle, wide body and large thrust signify long haul flights in the context of the current research.
Mature Shop Visit Rate (MSVR)	Defined by the EMCWG as the product of severity and shop visit rate.
OAT	Represents the outside air temperature at the different flight segments.
Post	The part of the disc between the blade roots.
Redline temperature	Exhaust gas temperature limit specified by the engine manufacturers with respect to the transient and continuous mode of operation.
Severity	Ratio of the engine damage for the new mission with respect to the reference mission.
Shaft speed scaling vector	Scaling value for the rated shaft speed.
Shop Visit Rate (SVR)	Ratio of number of shop visits to total engine flight hours, commonly represented per 1000 engine flight hours.
Short haul	The typical mission having short flight duration powered by lower thrust engines. Single aisle, narrow body and lower thrust signify short haul flights in the context of the current research.
Trip length	Mission duration in hours.
Weibull slope	The value of ξ in the weibull cummulative distribution function $(1-\exp(-(x/\gamma))^{\xi})$, where x is the value to evaluate the function and γ the rate parameter estimated from MSVR.

PREAMBLE TO CHAPTERS

The civil aviation is predominantly propelled by turbofans, as thrust generating device, meeting the needs of the transportation. Economics of the civil aviation is one of prime factors sought after during the different phases of aircraft useful life. The aircraft industry in the pursuit of providing feasible economics probe and look ahead towards the aspect of planned maintenance. The research is in providing an insight on the critical factors that define maintenance cost of an engine, occupying a major share in the operational cost of aircraft. The cost estimation involves two prominent factors, such as the severity and shop visit rate, defining the maintenance cost of aircraft engines. The chapters have been constructed towards the goal of achieving the two factors through methodologies built on engineering principles of gas turbine engine design to study the range of operational and technology oriented parameters impacting the severity and shop visit rate.

Chapter 1 : A formal introduction on the type of aircraft propulsion systems, followed by the details of turbofan construction and design has been briefly touched upon highlighting the importance of maintenance.

Chapter 2 : The research focus on severity and shop visit rate, and basic elements forming the methodology has been narrated. The fidelity parameters pertaining to the operational and technological scenario has been explained.

Chapter 3 : The aircraft and gas turbine performance being the backbone for the severity and shop visit estimation is dealt in. The flight path analysis, followed by the fundementals on gas turbine cycle, components and their performance, described in precise context.

Chapter 4 : The turbomachinery sizing principles for the turbine and compressor

blade in achieving the physical dimensions is detailed. The technology factors, such as cooling effectiveness, thermal barrier coating and pattern factor are captured in severity estimation.

Chapter 5 : The process of transforming, the gas turbine performance and design data into metal temperature and stress is covered as part of finite element analysis and heat transfer calculation.

Chapter 6 : Theories used for life estimation, based on the predominant failure modes, such as low cycle fatigue, creep and oxidation are ellaborated. The damage theory adopted for the research together with severity factor and its constituents are provided.

Chapter 7 : The aspects of maintenance dealing with the shop visit and aging curves has been explained. The steps involved in shop visit prediction through performance degradation mechanism, consuming the exhaust gas temperature margin are provided.

Chapter 8 : Case studies on severity for lower thrust and large thrust engines, used in short and long haul flights, subjected to parametric analysis on operational and technological parameters affecting the severity are explained.

Chapter 9 : The extension of the severity estimation method to high pressure compressor,mesh convergence, effect of tip shroud, effect of blisk and comparison with traditional AN^2 approach is available.

Chapter 10 : Case studies on shop visit prediction for lower thrust and large thrust engines, and the process of obtaining the Weibull distribution for the aging curve has been briefed.

Chapter 11 : In the conclusion chapter, the observations from the severity estimation and shop visit rate prediction for the lower thrust and large thrust

engines have been summarized.

Chapter 12 : The prospects for improvements, pertaining to the methodology, and further research for extending the severity estimation, in scenarios of interest for maintenance has been addressed.

Chapter 13 : Selected references of importance has been listed.

1 INTRODUCTION

In an attempt to globalization, the aviation has played a vital part to our civilization. The aviation as defined precisely being the science and technology of aircraft has reached unprecendented level of growth triggered by inspiration and great interest. The introduction of Flyer, in 1903 by Wright brothers, as a sustained controlled powered flight had been with the basic construction made out of spruce and carved wooden propellers, driven by gasoline fired reciprocating engine. Through the years of sustained effort by the engineering community, remarkable progress has been made in the domain of design, material, manufacturing and effective management that could transform the field of aviation. This is evident from the construction of airframes using light weight composite structure, having high specific strength and specific stiffness, and powered by advanced gas turbines as energy efficient propulsion systems for producing thrust. The purpose of this chapter is to provide a general introduction about the aircraft propulsion systems and the current technology. Followed by an overview of the aircraft engine design process to appreciate the basic elements that are responsible for a feasible configuration of the engine. The turbofan basic elements have been portrayed, as the research is mainly on different types of turbofans used for powering narrow and widebody aircraft. The closing part of this chapter, deals with the maintenance philosophy in aircraft engines, as the essential contribution of the research is on improving the maintenance insight, from the engine perspective.

1.1 Aircraft Engines

The basic purpose of aircraft engine is for producing thrust. The propulsion systems are varied in construction and configuration to meet the requirements of an aircraft. The common powering mechanism can be classified as

- Reciprocating engine
- Gas turbine engine
- Ramjet engine

The reciprocating type of engines works on otto power cycle, involving adiabatic compression of the working gas, constant volume heat addition, adiabatic expansion in producing work followed by constant volume heat rejection. They are widely used for powering propeller type aircraft and suitable for low altitude and low subsonic speed applications. The limitations of reciprocating engines are lower specific thrust and high specific weight.

The gas turbine engines types widely used in aircraft are

- Turboprop
- Turbofan
- Turbojet

The backbone of the gas turbine is the brayton power cycle with an ideal pattern of isentropic compression of the air in the compressor isobaric heat addition in combustor isentropic expansion in turbine and isobaric heat rejection in exhaust. The gas turbine engines have high specific thrust and low specific weight, suitable for range of altitudes up to 20000 m, and Mach numbers from subsonic to supersonic range. The different types of gas turbines, differ in the thrust producing element that in the case of turboprop, the gas turbine drives a propeller. The turbofan uses fan for cold stream thrust and exhaust nozzle for hot stream thrust to achieve the best specific fuel consumption and propulsive efficiency. The turbojet uses the exhaust nozzle for the thrust generation. The turboprop is limited to 5000 m and Mach number of the lower subsonic range of about 0.6, turbofans are widely operated up to 11000 m having transonic Mach number, and turbojet for supersonic speed and altitude of 20000 m. Due to different capabilities, making them suitable for different modes of application, turbojets due to supersonic and high altitude capability are apt for military application satisfying the throttle excursions for combat maneuvering. The turboprop and turbofan are used for mass transportation either as civil or cargo carriers. The turboprop due to low Mach number and high noise level have been limited in their application, as compared to turbofans which have low noise

and exhaust gas emmisions, satisfying the environmental regulations which are impacting the current designs.

The novel derived versions of the gas turbines such as unducted fans and propfans are seen as successors for next generation of narrow body aircraft. Hence advanced propulsion systems are looked upon for future aircraft, however sufficiently large lead time required in aviation industry depending on the niche and technology.

Among the distinct class of thrust generating systems are the application of pulse detonation, wave rotor and ramjet engines. The ramjet engine is most commonly used in missiles. This system works by continuous combustion of a compressed air enabled through the forward motion, suitable for high super sonic speed ranging from 3 to 5 Mach number. The pulse detonation and wave rotor are among the possibilities for future propulsion systems for the transonic civil aviation.

1.2 Turbofan Components

The turbofan, a varient of the jet engine is of prime interest as they are a monopoly in civil aviation. The turbofan that follows the brayton cycle has the basic elements of intake, compressor, combustor, turbine and exhaust nozzle.

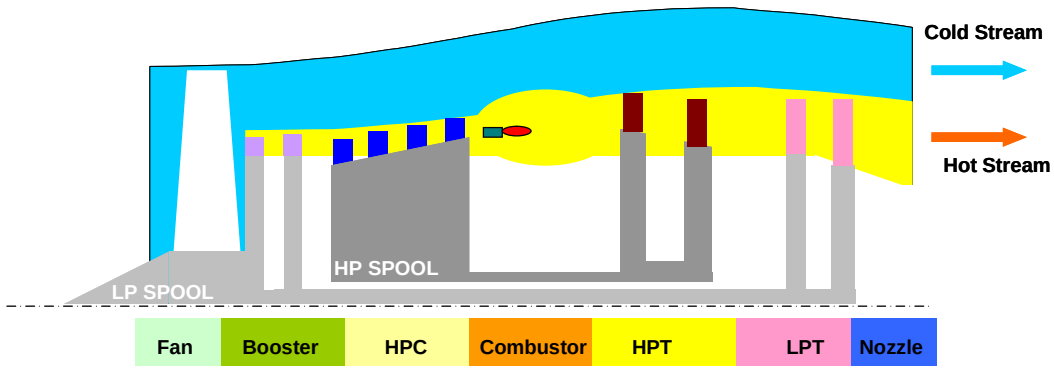

Figure 1.1 : Turbofan engine cross section.

Most current turbofans have two basic configurations depending on the shaft

system such as the

- Two shaft engine
- Three shaft engine

A turbofan requires, by basic construction, twin spool configuration to have low speed fan for accelerating a large mass of air, and high speed spool for high pressure end compression and work extraction. To achieve high aerodynamic efficiency and stable compressor operation, two major types of design have been used by the engine manufacturers, such as the variable stator vanes and three shaft system. The variable stator vanes ensures a stall free operation for the flight envelope. The three shaft system helps in having the intermediate spool rotate at a shaft speed lower than the high pressure spool, suitable for better compressor operability, and achieve high pressure ratios with less number of stages.

A two shaft system is said to have a low pressure spool and a high pressure spool. The low pressure spool connects the fan and booster to the low pressure turbine. The high pressure spool integrates the high pressure compressor and high pressure turbine. Air entering the intake is split into two streams, like the cold stream and hot stream. The fan pressure ratio which is the ratio of the fan outlet pressure to the inlet pressure, and by-pass ratio which is the ratio of the mass flow through the by-pass duct and the core are two major performance factors that are optimized to have a reduced fuel consumption.

The fan pressurizes the inlet air and the flow seperates into the cold stream and hot stream. The hot stream of air is further compressed through a booster that rotates at the same speed as the fan, or higher for a geared drive. The high speed spool with sufficiently large number of stages, helps in reaching the desired overall pressure ratio, defined as the ratio of compressor discharge pressure to the inlet pressure. The fuel is injected and ignited in the combustor

to release the heat energy to the high pressure air. The combustors have been incorporated with several advancements where the initial general configuration, such as the tube type have been transformed to tube-annular and now into annular combustor, suitable for the reducing the weight due to shorter length, and supplemented with suitable diffusers for the flame stability and complete combustion. Lean burn combustion technology has been widely used which ensures low NO_x levels inline with the emission regulations. The high pressure compressor is connected to one or two stages of the high pressure turbine that could withstand high temperatures through material and process advancements. The two important techniques of wider application for the turbine blades are the blade cooling and thermal barrier coating that have been critical for increasing the operational gas tempertures, and keeping the metal temperatures within acceptable limits. The low pressure turbine is to extract the useful work to drive fan and booster. The other purpose of the low pressure turbine is to provide an axial jet for developing the thrust. The nozzle in turbofans, can be mixed type or separate type, and as well a useful element for the reverse thrust mechanism. Flower nozzles are adopted in practice to reduce the noise level during take-off and landing. These engine components are subjected to design process to provide the desired functionality for feasible flight operation.

1.3 Aircraft Engine Design Process

The design of aircraft engines is the transformation of the engine specifications into products through a number of rigorous steps to ensure the level of performance, reliability, maintenance and certification standards. The process is the synergy of different fields aimed towards the realization of the product.

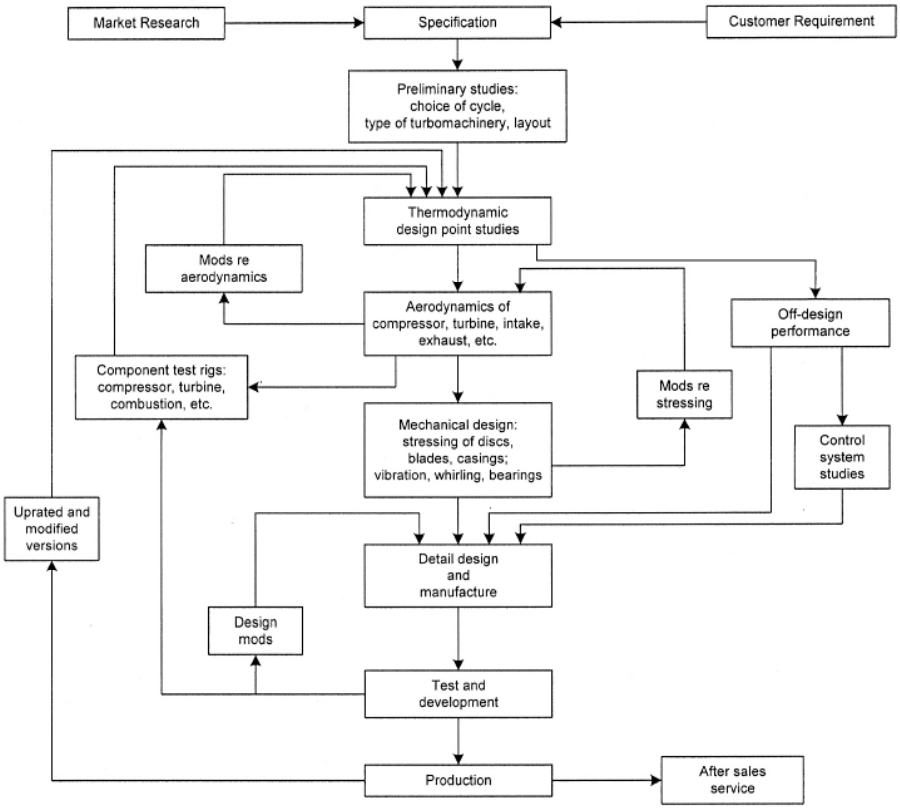

Figure 1.2 : Aircraft engine product development process [11].

The aircraft engine design [11] is strengthened predominantly by the domains such as

- Mechanical design
- Aerodynamic design
- Thermodynamic design
- Control system design

The mechanical design, takes into account the level of centrifugal stresses and thermal stresses on the components, and are kept at permissible level with optimized weight and expected life. The vibration behaviour is associated with the stiffness and mass of the system are designed to have the natural frequencies with sufficient margins from excitation frequencies to avoid resonance.

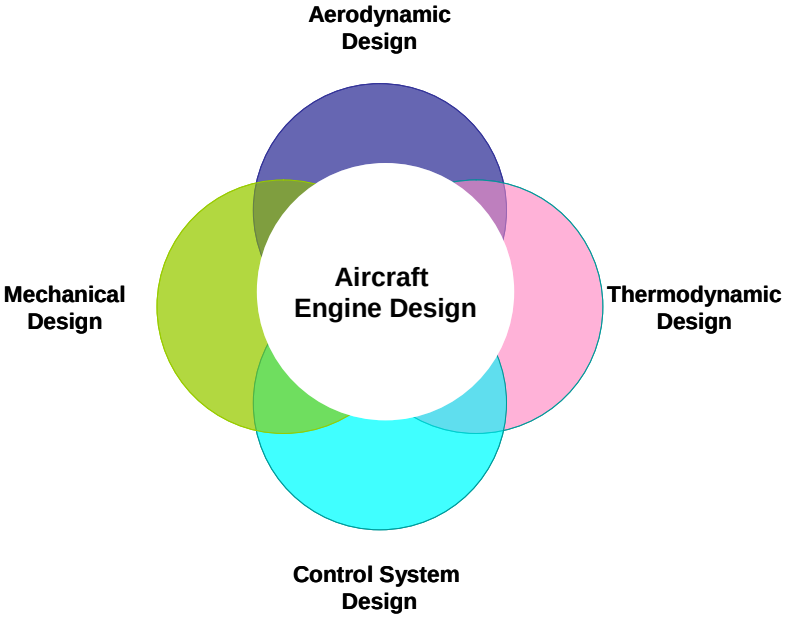

Figure 1.3 : Elements of aircraft engine design.

Material selection and manufacturing techniques are important in sustaining an optimal design, performing suitably during service. Major concerns regarding the material and manufacturing are the tolerancing of the designs, conformance with the critical to quality dimensions and consistent material properties to achieve a robust design.

Aerodynamic design deals with the required mass flow, pressure ratios, temperature, annulus area, rotational speeds and number of stages. The mass flow enables to achieve the desired level of thrust. The pressure ratios to achieve best thermal efficiency and reduce fuel consumption. The maximum cycle temperature, indicates the degree of work that can be extracted from the combustion gases through expansion in the turbine. Flow path for the thermodynamic changes in the properties and in sizing the components that are evaluated through the mechanical design process. The shaft speeds are with respect to the desired aerodynamic characteristics and feasible performance. Number of stages are consistantly reduced through the decades by highly loaded blade design. The 3-D aero design using computational fluid dynamics and use of optimized profile, result in reduced stages and number of rotating

blades, essentially reducing the weight of an aircraft engine and the fuel consumption.

Thermodynamic design is with respect to the selection of the gas turbine cycle parameters considered as zero level component design. The different trade-off studies are experimented, as the choice of parameters such as high pressure ratios and the turbine entry temperatures, pose technological challenges. These two parameters have been progressively moved upfront for gas turbines, in 1950's having a pressure ratio of 10 and Turbine Entry Temperature (TET) of 1100 K are now in the ball park of 40:1 to 50:1 and TET from 1800 K to 2000 K. These cycle requirements are made possible through the use of advanced techniques of design, material and manufacture that pushes the thresholds further up-line with an impetus of achieving lower fuel burn and emissions that dominate the current scenarios of gas turbine operation.

The control system design ensures the reliable gas turbine operation by providing

- Temperature limiting
- Speed limiting
- Power limiting
- Surge and stability

The commonly used control mechanism is the fuel control that is throttled to achieve the different fuel schedules for thrust generation. The fuel schedule and control helps to achieve the design and off-design behaviour of the gas turbine, and as well in limiting the temperature at the turbine that are restricted by the creep and rupture thresholds.

Through trade-off on different spheres, the design details are freezed in the detailed design phase, and are subjected to testing and validation with respect to the intended specification followed by production to meet the market

demands. During service there are always scope for improvements, upgraded through performance or design improvement programs .

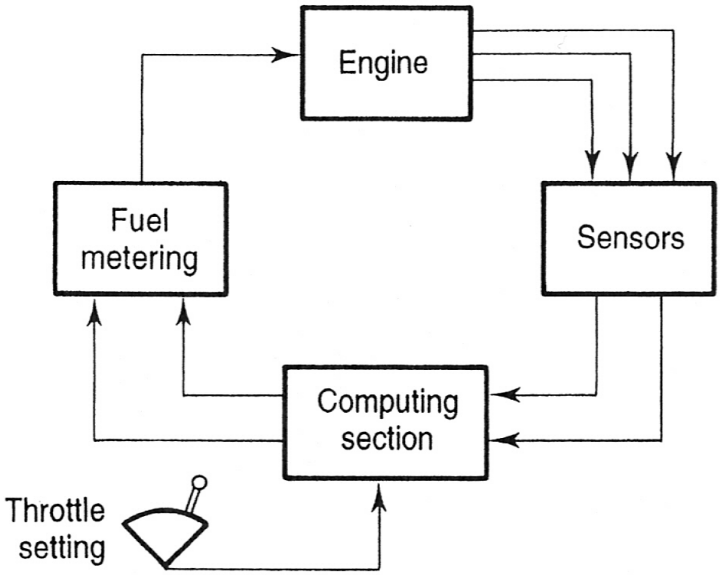

Figure 1.4 : Fuel control system [9].

1.4 Maintenance and Research Focus

The Maintenance Repair and Overhaul (MRO) segment has been key to reliable in-service aircraft fleet operation. The MRO activities can be classified into major scenarios such as

- Engine maintenance
- Line maintenance
- Component overhaul and repair
- Airframe maintenance
- Modifications

Engine maintenance occupies a large share of the MRO activities in restoring the engines to the required performance level and reliability. During the engine maintenance, the work scope is from dismantling the engine and its components, and building them back with repaired or new constituent parts,

hence depends on material and labour cost. The cost estimation for an engine maintenance are based on Shop Visit Rate (SVR), severity, type of the engine and maturity level in service life.

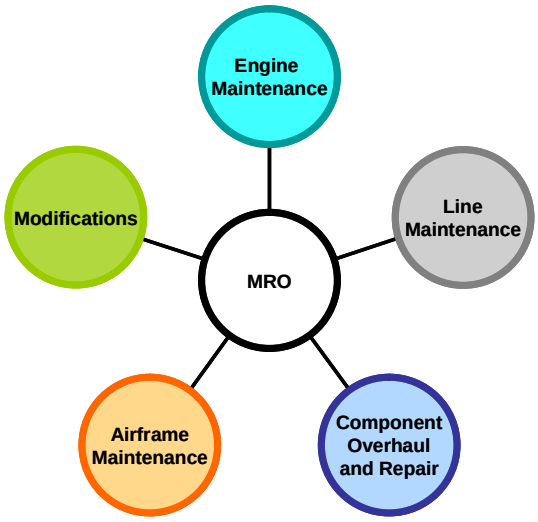

Figure 1.5 : Major activities of MRO industry.

The line maintenance deals with changing the aircraft components such as engine, auxiliary power unit, seal, landing gear and windshield. The other work scope involves structural repair, hydraulic leakage and repair of cargo loading system.

Component overhaul and repair involves testing, repair and overhaul of the aircraft components, and the time in restoring back to service is crucial.

Airframe maintenace involves structural inspection, testing, repair, rectification, corrosion control, weighing and painting for the airframe.

Modifications includes the restructuring of the aircraft interiors, engine modifications and other systems.

The requirements on the MRO, could be observed to be widespread, and result in the operational cost of the aircraft. The scope of the research is oriented

towards the engine maintenance.
As observed by the MRO industry, the engine maintenance involves higher proportion of the material cost, as compared to labour cost, while the airframe maintenance is more labour intensive.

The material cost for the engine maintenance, mainly depends on the severity and the age factor, defined for the engines, according to the thrust class. Hence the engine manufacturers, continuously strive to provide fuel efficient engines with reduced maintenance to have an edge in the competitive civil aviation market.

Hence the typical requirements for a propulsion system on the specification level has the major goals [13] such as

- Installed specific fuel consumption
- Direct operating cost
- Noise
- Emissions
- Performance retention

The direct operating cost is associated with the engine maintenance. The customers impacted by the maintenance are the airliners and focus has been on better on-wing life for reduced maintenance. The maintenance can be categorized, as planned and unplanned maintenance, based on the event leading to the shop visit. In-flight shutdown due to fuel leakage, vibration, abnormal oil consumption foreign object damage and quality escape due to defective parts from a batch, can lead to premature shop visit or removal from service are considered as unplanned maintenance. The life limited parts, EGT margin and specific fuel consumption which when approaches the limits specified by the engine manufacturers are due for a shop visit, considered as planned maintenance.

*Shop material cost = Age factor * Severity factor*Material cost* (1.1)

*Shop labour cost= Labour rate *Labour time* (1.2)

*Shop Visit Rate (SVR) = (Number of shop visits/Total engine flight hours)*1000 hrs* (1.3)

*Mature Shop Visit Rate = SVR * Severity factor* (1.4)

Age factor Maturity of the engine in service represented as Weibull curve.

Severity factor Relative engine damage.

The simplified maintenance cost equation 1.1 shows that it depends on age factor and severity factor. The age factor depicts, the maturity level in service through a Weibull curve based on the Mature Shop Visit Rate (MSVR). The severity factor is related to the engine damage, and defined as the ratio of the engine damage of the new mission with respect to a reference mission. The reference mission is defined according to Maintenance Repair and Overhaul (MRO) standards. Regarding the MSVR it is a product of severity factor and SVR (equation 1.4). The SVR is estimated by virtue of the shop visit interval to restore the performance and reliability as per the maintenance philosophy. The shop visit interval as observed in the industry is driven to a large extent by the phenomenon of Exhaust Gas Temperature (EGT) margin consumption through engine performance degradation. To comprehend the operational effects on the maintenance factors, such as the severity and SVR, dependent on the engine performance and design defining the engine maintenance cost is the prime objective in evolving the current research.

Hence the aircraft manufacturers have to make a suitable choice during engine selection, according to the thrust class, capable of providing the best economics, aimed at reduced engine maintenance cost. The maintenance cost needs to be competitive, from the airliners perspective that requires deeper understanding on maintenance factors, such as severity and SVR. The current research deals with the methodology for estimating the maintenance factors with respect to the operational scenarios and the engine technology.

2 RESEARCH PARADIGM

Civil aircraft industry with the spectrum of challenges have focus on engine maintenance cost, governing the fleet operational economics and regulations. To comprehend and analyse maintenance factors that define engine maintenance cost is of paramount importance to enhance the perspective at the conceptual (engine selection) and operational phase of civil aircraft. The pursuit of this research is towards the estimation of the maintenance factors through gas turbine engine design methodology to study scenarios of interest, impacting the maintenance cost. The maintenance factors are the severity dependent on relative engine life consumption, and Shop Visit Rate (SVR) based on gas turbine peformance degradation. This chapter aims at the journey towards the proposed methodology and pertinent research activities to substantiate the unique methodology, satisfying the industry requirement for further insight on engine maintenance.

2.1 Objective

The research paradigm can be simplified into eventual goal statements of two spheres. The objective of severity estimation dwelling on methodology for

- Derate-severity curves of lower thrust and large thrust engines.
- Effect of operational and technological parameters impacting severity.

The operational parameters of concern are the derates at take-off, climb and cruise. The other factors, such as Outside Air Temperature (OAT), airport altitude, cruise altitude and cruise Mach number. The most critical component that define the engine severity is the High Pressure Turbine (HPT). The design of the HPT depends on technological factors, such as the cooling effectiveness, thermal barrier coating thickness, thermal conductivity of the coating, pattern factor and profile are incorporated as part of the studies.

The other objective is in predicting the shop visit rate, driven by exhaust gas temperature (EGT) margin consumption due to performance degradation of the components. In the realm of shop visit rate the objectives are :

- Shop visit rate prediction due to EGT margin consumption.
- Effect of operational parameters on the shop visit rate.
- Aging curves.

The operational factors of importance for shop visit rate are the take-off derate, OAT and trip length. The current operational strategy of engine wash has been considered, inorder to identify the effect on the SVR for the civil aircraft engines.

2.2 Definition of the Need – Severity

The airliners operate on a variety of geograhical and operational scenarios, more focussed on the operational cost in a greater retrospect, as compared to the initial cost of aircraft. The operational cost of an aircraft can be broadly attributed to the airframe and the engine. The engine maintenance cost, part of the operational cost is fundamentally characterized by MRO, a community of aircraft manufacturers, engine manufacturers and contractors, defining the standards for maintenance cost estimation. The perspective of an aircraft manufacturer is limited to the operational demands, in terms of the flight performance whereas the dynamics of engine life consumption, dependent on thrust requirement is of interest.

2.2.1 Derate Severity Curve

The derate and severity, can be looked upon as the relationship, between the thrust requirement at take-off and the degree of life consumption. The take-off derate is crucial in terms of the mechanical integrity of the engine subjected to the design limits, in terms of the permissible stresses and temperature. The take-off derate is the percentage reduction in the take-off thrust, based on the aircraft weight and airport conditions. The different airports, impose a different thrust requirement, due to the OAT, altitude, runway length etc., affecting the

engine performance reflecting on the net thrust. The MRO categorizes the engines, as lower thrust engines and large thrust engines with the threshold value of 34000 pounds net thrust per engine. This classification suits the design of the aircraft, as called by the narrow body aircraft using lower thrust engines, and wide body with large thrust engines. Irrespective of the engine configuration, they are said to generate a common characteristics of derate-severity curves, falling under the same thrust class. The severity is a term that refers to the engine damage. The severity is defined as a ratio of the new mission damage to the reference mission damage and the MRO has defined the reference mission as follows.

- Lower thrust engines – T-O derate 10% – Trip length 1.4 hrs –18 °C OAT
- Large thrust engines – T-O derate 10% – Trip length 4 hrs –18 °C OAT

Hence for different levels of thrust, the intensity of damage is expressed as the ratio with respect to the reference mission. For a lower thrust engine operating at 10 % T-O derate with a trip length of 1.4 hrs operated at 18 °C OAT has a severity value of unity and the life as specified in the Life Limited Part (LLP) list. The operational requirements of the airlines demand different levels of derate, and gets reflected on the severity value. The fact to be observed is the level of severity decreases with increasing derate as it results in lowering the stress and temperature on the engine. A value of severity less than unity has a magnifying effect on component life whereas a value more than unity diminishes the critical part life. The severity as represented on the damage scale is the inverse of the component life and hence the behaviour of decreasing severity with increasing derate.

2.2.2 Operational and Technology Parameters for Severity Estimation

The operational and technology parameters have to be incorporated to address the scenarios of usage and the level of technology. On the operational domain,

the significance of the derate which is the percentage reduction in thrust from the rated thrust is to be studied at three critical segments of the flight path, such as the take-off, climb and cruise. Most often the take-off impose maximum shaft speed and maximum temperature to meet the required velocity of flight. Hence as part of the flight path analysis, the derate at take-off, climb and cruise are made parametric to generate the desired severity characteristics.

The airport conditions, such as altitude and outside air temperature are prone to reduce the thrust, as it affects the mass flow and pressure ratio in the process of maintining the expected level of thrust, the combustion temperature is raised by pumping in more fuel. This makes the turbine entry temperature and the shaft speed to be increased, associated with the rise in the severity of the critical components. The other factors considered are the cruise Mach number and altitude for the severity studies.

The technology parameters are temperature offset mechanisms, due to blade cooling, thermal barrier coating, pattern factor and profile. The technology parameters are important to reduce the severity on the component by reducing the metal temperature. Hence the technology parameter have been incorporated in the severity estimation.

The value of severity is factored into engine material maintenance cost estimation (equation 1.1), while the labour cost is as per the industry norms of MRO.

Hence a methodology needs to be developed taking into account the operational and technology parameters for the severity estimation of the critical components signifying engine severity.

2.3 Definition of the Need – Shop Visit Prediction

The term shop visit in this research is with respect to planned maintenance.

The shop visit is attributed to the EGT margin conumption has been deciphered as part of this research. The EGT margin consumption depends on the performance degradation characteristics of the engine components. The component performance parameters are the efficiency and mass flow, influencing the thrust. Irrespective of the component degradation, the thrust level needs to be maintained that leads to increasing fuel flow, and rise in exhaust gas temperature. Hence the EGT margin, specified by the engine manufacturers for reliable and efficient engine operation is continuously reduced with engine flight hours, due to degradation.

The prediction of the flight hours to meet the shop visit is based on the degradation of the components with cycles of operation. The engine flight hours in consuming the EGT margin predicts the shop visit interval and with the successive EGT margin restoration, the engine shop visit interval differs yielding the shop visit rate of the aircraft engine. The shop visit rate is one of the factors in depicting the term used in MRO industry as Mature Shop Visit Rate (MSVR).

Hence the objective of severity through life estimation and the shop visit through performance degradation mechanism is vital to estimate the MSVR (equation 1.4) of an aircraft engine.

2.3.1 Operational Parameters for Shop Visit Prediction

The shop visit rate of an aircraft engine has dependence on the factors, such as the ratio of EFH/EFC (Engine Flight Hours/Engine Flight Cycles) or the average trip length, OAT and take-off derate. The trip length has the effect on the shop visit, as the degradations are defined on the basis of cycles, hence the engine flight hours for the shop visit gets scaled accordingly. The OAT, an evinronmental agent governs the exhaust gas temperature affecting the shop visit interval. The other prominent element is the take-off derate that is normally the peak temperature of the mission, reducing the EGT margin with engine degradation has been studied. The shop visit prediction methodology, needs to

include the operational parameters along with the component degradation.

2.3.2 Aging Curves

The maintenance cost, lies in the estimation of the age factor, (equation 1.1) with respect to the engine flight hours. The age factor, varies between 0 to 1, based on the service life of an aircraft, commonly referred to as the aging curves. The aging curves as per the MRO practice is a Weibull curve with the slope of 1.5, spreading to the entire life in service. The shop visit rate together with the severity determines the MSVR, and represents the characteristic aging of the components for maintenance cost estimation. The aging curves are of two major classes one being the material and the other being the labour cost. The labour is based on the MRO standards followed in terms of the time and effort. The current research addresses only the material aspect that is based on SVR and severity level.

2.4 Severity Estimation and Software Description

The severity and shop visit prediction are essentially different domains, but of interest for the industry. The severity, as is explained to be a factor representing the degree of life consumption by virtue of the operational demands. The latter on shop visit prediction is in the perspective of the component performance degradation, affecting the shop visit interval.

The art of achieving the life of the engine components has been more of proprietary in nature, as the crictical components, involved are the hot section parts where sufficiently ingenious level of technology is under application to make the engine manufacturers stay ahead in the market. However the focus of the research is in the estimation of severity which is a relative life estimation.

The integrated lifing analysis tool, as developed by Tinga et al. [80] which outlines the elements necessary for the life estimation of the gas turbine component, especially for the turbine blade.

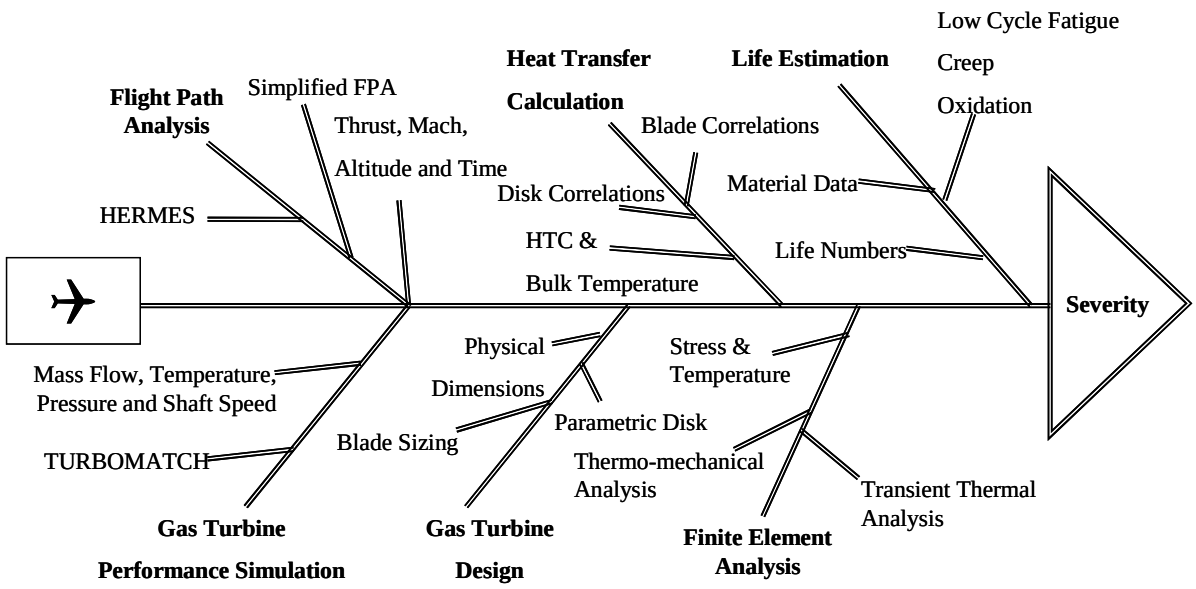

Figure 2.1 : Severity estimation process.

The work done by Saurez et al. [76] on condition monitoring system for aircraft engines fall in similar lines. The tools and methods followed are the exact design process, as an engine manufacturer pursues. Hence the requirement to estimate severity, as defined by Strabylla et al. [72] to be the ratio of the damage of a new mission with respect to a reference mission, hence the relative ratio is of importance. The damage is inverse of the component life as per the linear damage rule. The severity depends on damage calculation and damage on life estimation of the component.

The framework of the current method is in transforming a flight path data into an estimate on life, and are compared with respect to changes in operational parameters to capture the factor of severity. As the purpose is to predict the severity trends, using a numerical approach, and help the decision making process on the maintenance aspects of the civil aircraft engines. The proposed methodology, needs to synchronize a number of numerical simulation programs and software codes that could transform a flight path data into a component severity.

The severity estimation process (Figure 2.1) involves the following steps:

- Flight path analysis for a typical civil aviation mission to obtain the thrust, altitude and Mach number variation .
- Gas turbine performance calculation is used for design point and off-design conditions as defined by thrust, altitude and Mach number variation. Mass flow rate, temperature, pressure and shaft speed are inferred as outputs from the simulation.
- Gas turbine design based on turbomachinery rules being adopted to size the turbine blade while the disc geometry from the equivalent engine cross-section. The turbine sizing is estimated from the design point (take-off) data of the gas turbine performance simulation.
- The heat transfer coefficients at the blade and disc are estimated based on standard correlations using the thermodynamic properties and physical dimensions.
- Finite element analysis is employed for transient thermal analysis with the estimated heat transfer coefficients and bulk temperatures at the mission points. Thermo-mechanical analysis has been carried out with thermal load as metal temperature and mechanical load by virtue of the shaft speed for the mission points. The outputs from the finite element analysis are the metal temperature and stress variation during the flight mission being utilised for the life estimation.
- The turbine blade and disc life for the modes of failure such as low cycle fatigue, creep and oxidation are obtained through theoretical life estimation methods dependent on metal temperatures, stresses and material properties. The life values are converted to damage fractions using the linear damage theory. The damage fractions are availed for the severity estimation.
- Severity, the ratio of total damage due to reference mission to the total damage due to the new mission is estimated for the turbine blade and disc as part of studies on operational and technological factors.

The Hermes, Cranfield in-house aircraft performance software, or simplified flight path analysis code, could be utilized for capturing the typical flight mission

common to civil aviation. The flight events right from taxi-out to taxi-in, involves various levels of thrust, needs to be simulated using the proposed program. The operational strategy of the airlines have to be duly addressed with a parametric form of the required features incorporated in the simplified flight path analysis code. The different parametric studies, involving operational and technological factors have to be integrated, as part of the software layout. The output of the flight path analysis program are the thrust, altitude and Mach number with respect to time.

The flight path data, specifies the design and off design points of the gas turbine performance. Turbomatch, a Cranfield gas turbine performance software is used in translating the flight mission data into the properties of the fluid across the engine. The gas properties and shaft speed data are basic inputs for the thermal and mechanical behaviour of the components.

The physical dimensions are important as they depict the inertia of the structure, and the forces generated by virtue of its operation. As observed in the aviation industry where the hot section components, comprise the most critical elements that are sensitive towards the maintenance aspects. The rotating components, suffer a high level of distress as compared to stationary components. In the current study only the turbine especially the high pressure turbine blade and disc assembly have been investigated for the severity estimation, and extended to high pressure compressor blade and disc. The turbine blade and compressor blade, sized using the turbomachinery design process. The disc geometry is replicated from the engine cross-section using a parametric model driven by input dimensions. An excel based input for the Matlab code has been developed for sizing and interfacing with different programs.

The physical dimensions of the blade and the disc together with the properties of the fluid at their proximity, determines the heat transfer coefficient and bulk temperature using standard correlations. A Matlab code has been developed to

estimate the thermal loads for the engine mission points.

Ansys, the commercial finite element analysis software has been utilized for predicting the thermal and mechanical behaviour of the blade and the disc assembly. A parametric code has been developed using APDL (Ansys Parametric Design Language) to build finite element model, apply loads and boundary conditions, perform analysis and extract the outputs through postprocessing in an automated manner.

The thermal model is constructed and analyzed with estimated heat transfer coefficients and bulk temperatures for the different sections of the components. Transient thermal analysis is carried out to capture the time dependent metal temperature variation, associated with the engine mission points. The response of the blade metal surface to fluctuating flow path conditions leads to thermal shock on the turbine blades. The transient blade metal temperature forms the basis of the thermal load for the structural model.

Subsequent to the thermal analysis, a thermo-mechanical analysis is carried out for estimation of the stress levels in the components. The two fundamental loads of concern for this preliminary model are the blade metal temperature and the shaft speed. The gas bending stresses have been ignored as they contribute less than 10 % towards the resultant stress in the components. The von mises stress or the equivalent stress and the metal temperatures are extracted for the mission points, using the postprocessing script that are fed into the life estimation routines.

A life estimation Matlab program is used to estimate the life numbers under three critical modes of life consumption, namely low cycle fatigue, creep and oxidation. The inputs for the life estimation are the stresses and the metal temperatures, along with the material coefficients and properties. The severity is obtained through the relative damage ratio as defined.

The complete process, starting from the flight path analysis, upto the severity estimation is integrated to enable parametric studies, varying operational and technological factors.

2.5 Shop Visit Prediction and Software Description

As envisaged, the shop visit is of two major types [102] one being the scheduled and latter an unscheduled. The research is about the scheduled shop visit where exhaust gas temperature margin has been the driving factor for the engine shop visit. The shop visit interval is based on the life limits of the critical components, especially the turbine blade. Normally designed to endure much longer and provide life until every atom has been consumed. However performance is critical for achieving the fuel efficient system for best economics and reduced emissions, hence the EGT has been tracked for estimating the shop visit. In aviation industry, the engines with the larger EGT margin, signify reduced shop visits. The engine manufacturers desire to have a feasible margin and often incorporated changes through performance improvement programs. The life limits is an outcome of the design, manufacturing and material whereas the EGT margin depends on the component performance degradation characterisitics.

In most of the engine monitoring systems, the exhaust gas temperatures are observed with respect to redline temperature, at transient and continuous mode of operation. The take-off temperature, indicates the highest temperature among the transient temperatures. The climb and cruise temperatures are compared with the continuous exhaust gas temperature. As the exhaust gas temperature approaches the redline temperature, an eventual shop visit is said to occur.

The key factor is the degradation of the individual components, causing changes in the mass flow and decrease in efficiency. The degradations are varied in nature, either as changes in clearance or fouling of the blades etc. are considered to impact the performance of the engine, and hence an increase in

the EGT to maintain the thrust for feasible flight operation. The typical degradation values as observed in turbofans are used as a basis for the estimation of the EGT margin reduction, represented on the cycles, suitably converted to the engine flight hours, depending on the trip length.

The shop visit rate of the engine based on EGT margin reduction, depends on factors such as the OAT, EFH/EFC, take-off derate and engine wash. Hence a parametric feature is built with the required operational factors, influencing the shop visit of the engine.

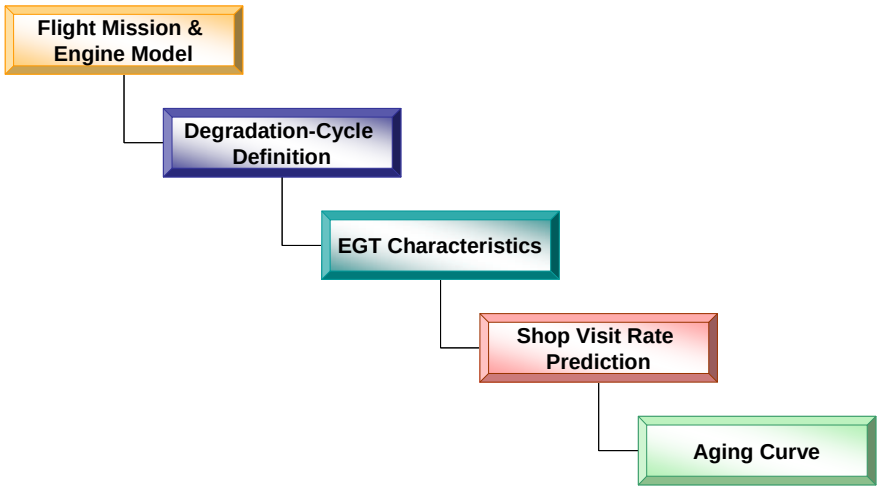

Figure 2.2 : Shop vist prediction methodology layout.

The shop visit prediction methodology (Figure 2.2) involves the following steps:

- Flight mission common to civil aviation is simulated through flight path analysis providing the thrust, altitude and Mach number variation. The gas turbine performance model of the engine with the degradation capability based on component maps are utilised to estimate the thermodynamic properties across the engine as mass flow rate, temperature, pressure and shaft speed.
- The variation of the component degradation with respect to engine flight cycles are simulated as changes in the mass flow rate and component efficiency.

- The exhaust gas temperature variation is observed for the degradation cycle definition, at take-off, climb and cruise of the flight mission. The maximum exhaust gas temperature specified for the engine during the transient and continous conditions are the thresholds for identifying the shop visit interval, observed as a cross over in exhaust gas temperature characteristics. The subsequent shop visit intervals are inferred with respect to different EGT margins.
- The shop visit interval or maintenance interval could be represented as shop visit rate being an inverse of the maintenance interval expressed for every 1000 engine flight hours.
- The changes in the engine life as severity impacting the engine flight cycles and the shop visit rate governing the maintenance interval are the basis for the Mature Shop Visit Rate (MSVR) estimation of the engine. The MSVR is represented as a Weibull curve indicating the maturity of the engine during its useful service life on an aircraft referred to as the aging curve.

The shop visit prediction methodology is constructed with the basic elements of the flight path analysis and gas turbine performance degradation. The flight path analysis is in defining the flight mission, and especially the thrust characteristics. The gas turbine performance simulation is to predict the exhaust gas temperature with respect to the engine degradation-cycle definition. The EGT characteristics represented with respect to the engine flight hours reveals the shop visit interval and cascaded into the parameter of the SVR. The SVR and the severity factor are used for estimating the MSVR, represented as a Weibull curve, indicating the maturity of the engine with respect to its useful service life is the engine aging curve.

The shop visit prediction methodology involves organizing the inputs, such as an excel sheet with the mission definition, component degradation, EGT redline temperatures, and frequency of engine wash. Turbomatch, an engine performance simulation code is used to perform the calculation for predicting

the exhaust gas temperature, based on component degradation, being tracked during the flight mission. The calculation is performed for the degradation-cycle definition, yielding EGT characteristics of the engine. The software that integrates the flow of information is Matlab. This software is equipped with mathematical functions and interfacing features suitable for both shop visit prediction and severity estimation studies with the benefit of summarizing and retrieving data from excel files. This facilitates ease of analyzing the data and representing them as suitable characteristics.

2.6 Authors Contribution

The engine maintenance cost as inherent in the aviation industry, and a term most often looked upon in civil aviation will play a crucial role in engine selection, suitable for an aircraft. Currently the civil aviation industry, depend more on the experts to compare the engine manufacturer's competitive designs, and operational strategies. The methodology with its uniqueness in integrating the aircraft and gas turbine behaviour will serve as a decision making tool for engine selection, and capture operational trends through comprehensive studies. Hence the current research is a step forward to address the maintenance of aircraft engines through an integrated view binding the operational parameters with core drivers, such as severity and shop visit rate.

The contribution towards the severity are

- Development of a unique methodology to estimate severity.
- Capability to observe the effect of operational and technological factors on severity.

The severity characteristics with respect to the thrust is of value in maintenance cost estimation. The aircraft manufacturers, need a methodology to estimate and to observe the relative sensitivity on severity of the engines having different designs. The challenging situation pertaining to severity estimation is in

phrasing a methodology which could transform the information available in the public domain into the severity characteristics comparable with MRO curves. The severity as observed to be a ratio of the life with respect to the predominant life consumption modes, lies in the realm of design process of the engine components. The design process of the components are complex and iterative, involving the design practices observed over the years of development and application. The basic turbomachinery rules are the backbone with technological know-how, continuously upgraded to satisfy the current challenges. Hence the research relies on the basic turbomachinery rules and formulation that are available in the public domain to bring out the characteristics of severity, relative to the temperature and stress variation of the components. The process followed walks closer to the actual design process but on a less detailed scale suitable to the available information and timeline.

The second phase of the contribution is on shop visit rate, being a phenomenon governed by the peformance variation, by virtue of the component degradation. The shop visit is predicted, based on the EGT margin deterioration with engine flight hours, tending to redline temperatures, specified as the operational limits for ensuring engine reliability and acceptable performance. The research is confined to scheduled shop visit, as compared to the unscheduled shop visit caused due to abnormalities in the design, performance, manufacturing and inspection leading to unexpected shop visit or engine removal from service. The shop visit rate is specified by the engine manufacturers by assuming degradations observed on similar engines. During service, the engine is subjected to temperature variations and are continuously monitored with respect to the redline temperatures. The exhaust gas temperature data has been used as a signature of the engine health. Considerable research has been done on condition monitoring and diagnostics for understanding the degradation characteristics. However the effort in this research is with the objective of using assumed levels of degradation to estimate the SVR, and to capture the significance of operational factors.

Hence the contribution towards shop visit rate are

- Demonstration of methodology to predict shop visit rate.
- Identification of the impact due to operational factors on shop visit rate.

The complex factors of severity and shop visit rate have been ordained through simplified integrated methods, tieing up different design envelopes of the engine into a common sphere. To analyse and comprehend aircraft engines and scenarios of interest through severity characteristics for better engine maintenance perspective will be the unique contribution through the current research.

3 AIRCRAFT AND GAS TURBINE PERFORMANCE

An aircraft has an essential balance of performance and design. The science dealing with aircraft motion is commonly referred to as flight mechanics. The embodiment of flight mechanics are the disciplines, such as aircraft performance, aircraft stability and control, and flight simulation. The design and operating parameters, such as take-off, climb and the typical requirements of feasible flight are governed by four fundamental forces: lift, drag, thrust and weight. The purpose of this chapter is in highlighting the parameters involved in aircraft performance which is reflected as a thrust, altitude and Mach number variation with time. The different levels of thrust for feasible flight is met by implementing an engine that satisfies the requirements adequately. The changes in the thrust is achieved by the turbofan through important control parameters, such as the shaft speed and combustor outlet temperature. Hence the concern of this chapter is on aircraft performance and gas turbine performance that form the basis for inputs to severity estimation and shop visit prediction.

3.1 Aircraft Performance

The interaction of a body in a fluid medium is dealt in the study on aerodynamics. The aircraft as it progresses, in the free stream is subjected varying pressure distribution and shear stress distribution, especially the wing that gives rise to a force and a moment on the structure. The physical forces experienced are classified as lift, drag, thrust and weight.

Lift (L)	The force perpendicular to the flight path direction
Drag (D)	The force parallel to the flight path direction
Weight (W_A)	The force acting downward towards the centre of the earth
Thrust (T_E)	Force inclined to the flight path direction

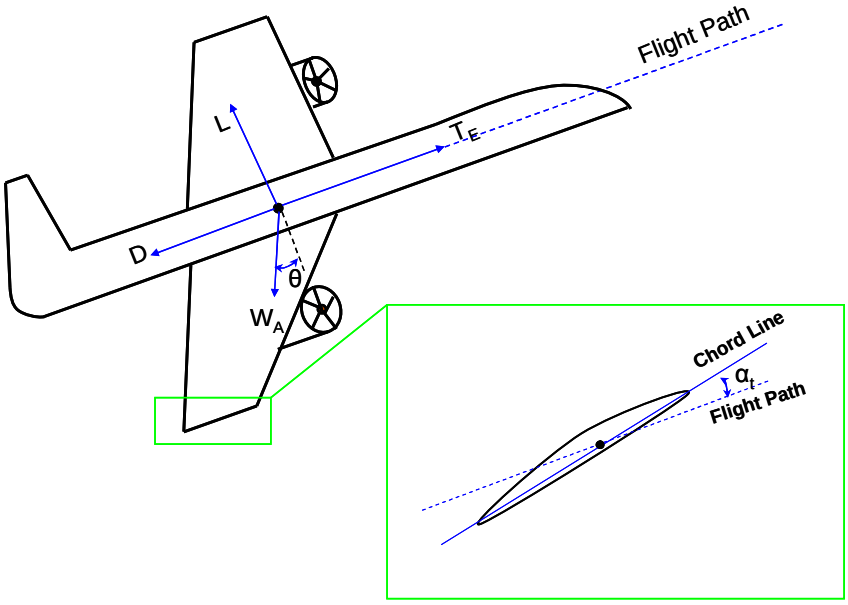

Figure 3.1 : Physical forces on an aircraft.

$$T_E \cos\alpha_T - D - W_A \sin\theta = m\frac{dV_A}{dt} \tag{3.1}$$

$$L + T_E \sin\alpha_T - W_A \cos\theta = m\frac{V_A^{\,2}}{r_c} \tag{3.2}$$

The above equations 3.1 and 3.2 are the equations of motion for an aircraft during accelerated flight [1].

The required thrust is varied in nature due to the operational scenarios such as

- Constant speed, level altitude
- Constant speed, changing altitude
- Variable speed at level altitude
- Variable speed and changing altitude

There are two basic kinds of thrusts of interest one being the required thrust by virtue of aerodynamics of the aircraft, and the other form is the available thrust

developed by the propulsion system. The propulsion system under consideration is turbofan that produces a fairly constant thrust with respect to the free stream velocity.

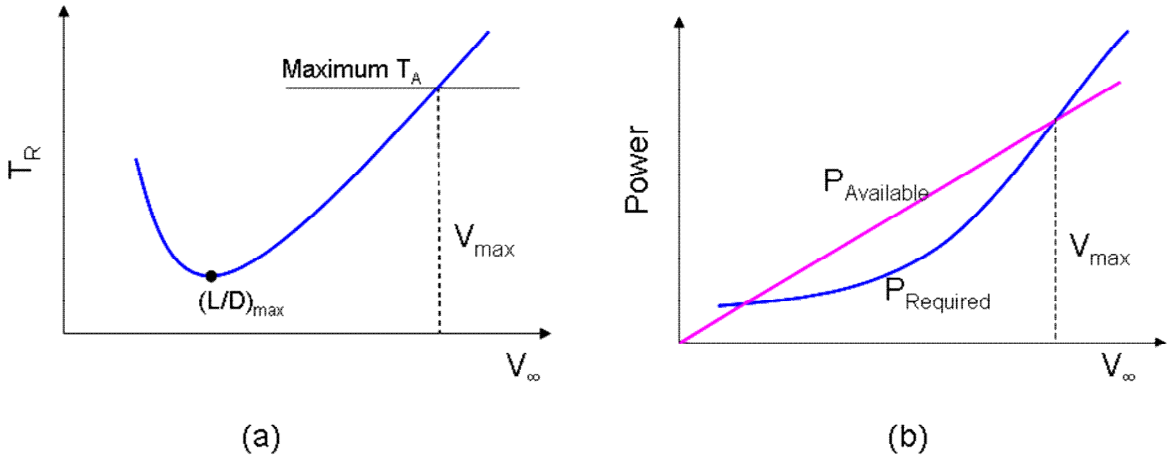

Figure 3.2 : Thrust and power curve at sea level.

$$P_R = T_R V_\infty \quad (3.3)$$

$$P_A = T_A V_\infty \quad (3.4)$$

P_R Power required [Watts]

P_A Power available [Watts]

T_R Thrust required [N]

T_A Thrust available [N]

V_∞ Free stream velocity [m/s]

The thrust characteristics [1] of an aircraft at a constant altitude, shows a decreasing thrust, until the L/D ratio reaches a maximum value, and increases with increasing velocity. The maximum velocity of the flight is limited by the intersection of the P_A and P_R. The process involved in the estimation of the P_A and P_R or otherwise T_A and T_R are on a different basis. The required thrust, being totally a function of the pressure and shear stress distribution on the body due to the flow field whereas the available thrust is a characteristics of the engine, in converting the energy of fuel into heat through combustion into a high

velocity or high mass flow exhaust to create the propulsive force.

3.2 Flight Path Analysis

The flight path analysis is the process of depicting the thrust, altitude and Mach number variation with time. A flight mission comprises of events such as
Taxi out – Take-off – Climb – Cruise – Descent – Approach – Landing – Reverse thrust – Taxi-in.

Each of the flight segment has a unique requirement in terms of thrust, due to the maneuvers that demand different level of thrust, mathematically represented through the equations of motion for aircraft. However the engine thrust or the available thrust is characterized by the gas turbine performance. The flight path analysis forms the initial step towards realizing the severity. The thrust, altitude and Mach variation with time, driven by the design of the aircraft is adequately satisfied by the engine performance. Hence the synergy between the aircraft performance and engine performance is pivotal.

3.3 Simplified Flight Path Analysis Approach

In the preceeding parts the significance of required thrust and available thrust have been brought to our perspective. Fundamentally the flight path simulation, can be carried out in two distinct ways one totally relying on the equations of motions of the aircraft where the prediction of the take-off performance, rate of climb, cruise speed, range and landing performance are determined as a function of lift, drag, altitude and velocity. The other point of view is from the engine perspective to deliver thrust fractions which forms a simplified approach in simulating the flight path. The Cranfield in-house flight path simulation code Hermes works on the basis of former approach to capture the thrust characteristics and interacting with engine performance in checking the suitability. This simulation will require the design details of the aircraft and the engine, supplemented with thrust characteristics from the in-house gas turbine performance code Turbomatch. In reference [102], a radically different approach has been used for life estimation and works on a simplified scale of

inputs, producing the flight path characteristics. Hence a Matlab code has been developed to mimic the process that bears distinct advantages, such as integration with the life estimation process, basic engine information, standardized approach of flight path simulation, customization for the range of case studies of interest complacent for the current research.

Thrust as specified by the engine manufacturers can be identified as certified thrust and uncertified thrust. The certified thrust, includes the maximum take-off thrust and continous thrust, specified at the sea level together with the flat rating temperature. The uncertified thrust are those corresponding to the top of climb and cruise conditions, specified at the cruise altitude.

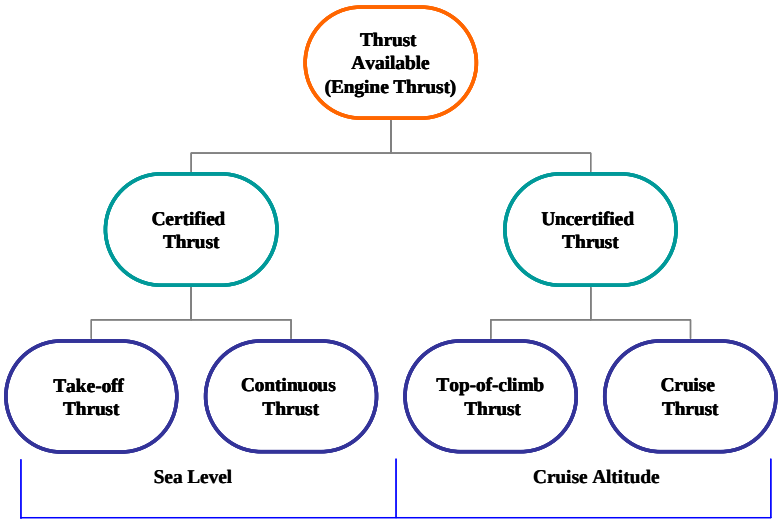

Figure 3.3 : Thrust available (engine thrust) classification

The engine manufacturers information on the thrust are used as a primary input for the thrust characteristics of the mission. The hierarchy of the thrust is as provided in Figure 3.3 where take-off is the highest thrust followed by the continous thrust. The top-of-climb and cruise thrust, fall under the lower level of the thrust, due to the altitude effects that causes a decrease in the air density, and thrust being proportional to the density decreases accordingly. The take-off thrust is phenomenally high to couteract the large drag forces and inertia to get the aircraft velocity beyond the stall velocity for lift-off. The climb thrust that

ensures the rate of climb negotiating the large amount of drag forces as compared to lift.

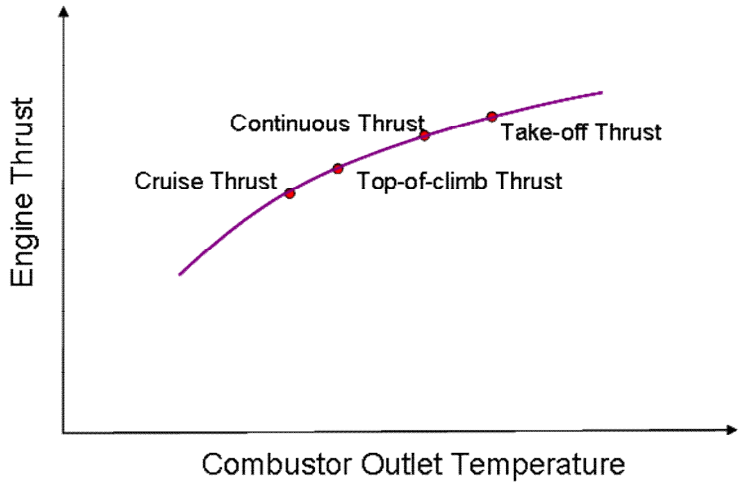

Figure 3.4 : Engine thrust variation with COT according to hierarchy.

The aircraft mission is respresented as a thrust fraction of the maximum take-off thrust at sea level.

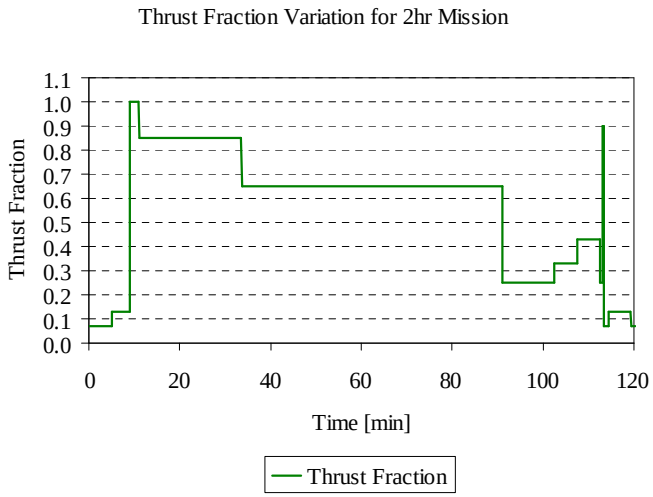

Figure 3.5 : Thrust fraction variation during mission [102].

The simulation of the flight path from an engine perspective requires a gas turbine performance simulation for which the in-house code, Turbomatch has been used. The process of estimating the thrust variation, as per the gas turbine performance, requires a design point simulation satisfying the engine

specification, and followed by each and every flight segment, being simulated as an off-design condition.

Mission Phase	Segment	Thrust Fraction	Time[min]	Mach
Ground idle	1	0.07	5.0	0.00
Taxi	2	0.13	4.0	0.00
Take off	3	1.00	2.0	0.38
Maximum Climb	4	0.85	22.5	0.80
Maximum Cruise	5	0.65	57.5	0.80
Flight Idle	6	0.25	11.5	0.65
Loiter	7	0.33	5.0	0.50
Approach	8	0.43	5.0	0.30
Flight Idle	9	0.25	0.5	0.10
Reverse Thrust	10	0.90	0.3	0.00
Ground idle	11	0.07	1.0	0.00
Taxi	12	0.13	5.0	0.00
Ground idle	13	0.07	1.0	0.00

Table 3.1 : Thrust fraction data for typical flight mission [102].

The pre-requiste of the Turbomatch is a suitable engine model, built using the building blocks called the bricks of the software code duly capturing the engine thermodynamics.

This capability of gas turbine performance using Turbomatch is tied up with the thrust fractions using the Matlab code. The simulations of interest as per the structure of the code are

- Design point estimation
- Thrust variation with COT at sea level
- Thrust variation with COT at sea level and flat rating temperature
- Thrust variation with COT at cruise altitude
- Thrust variation with COT at cruise altitude and flat rating temperature

These characteristic curves, determine the design point Combustor Outlet Temperature (COT) together with the other off design COT, represented through suitable thrust fractions. The thrust variation at cruise altitude has been considered to estimate the top-of-climb and cruise COT, closer to the engine specifications, and it is fairly observed that the thrust fractions of the different engines do not necessarly follow the same ratio are varied in nature, due to

design philosophy chosen by the engine manufacturers.

The flat rating temperature simulations are to estimate the threshold of the COT, beyond which the thrust is reduced, as the temperatures are limited by the maximum blade temperature, as per the design practice.

The design point calculation is carried out by increasing the COT, until the take-off thrust is achieved. Often the engine specifications, provide the mass flow rate at the take-off condition, hence the design point is done at the take-off, however depends on the availability of the data for the engine in the public literature.

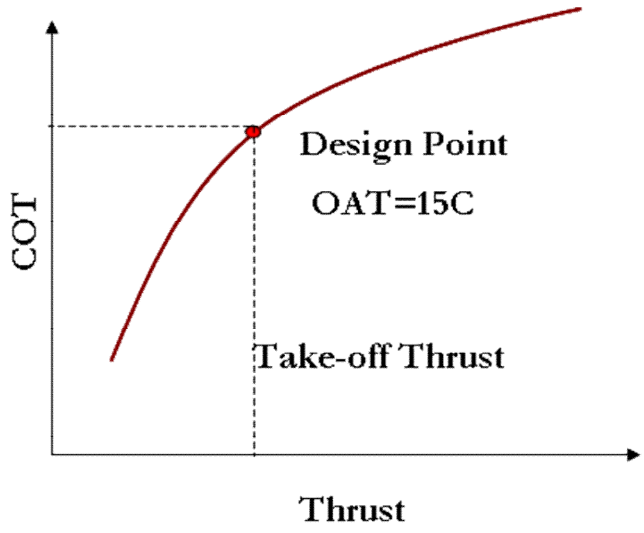

Figure 3.6 : Design point calculation.

The off-design COTs are estimated through two curves one at the sea level, and the other at cruise altitude and cruise Mach number. These two thrust characteristics are used to map the thrust fractions of the engine, at the different flight segments, giving rise to the corresponding COT. The upper bound thrust versus COT curve is generated by simulating off design conditions at the flat rating temperature. The thrust versus COT curves, define the essential design and off design points for the flight path simulation and are processed in sequence to generate the flight path characteristics. The Turbomatch

generates for the corresponding COT, the thrust, mass flow total temperature total pressure and shaft speed variation.

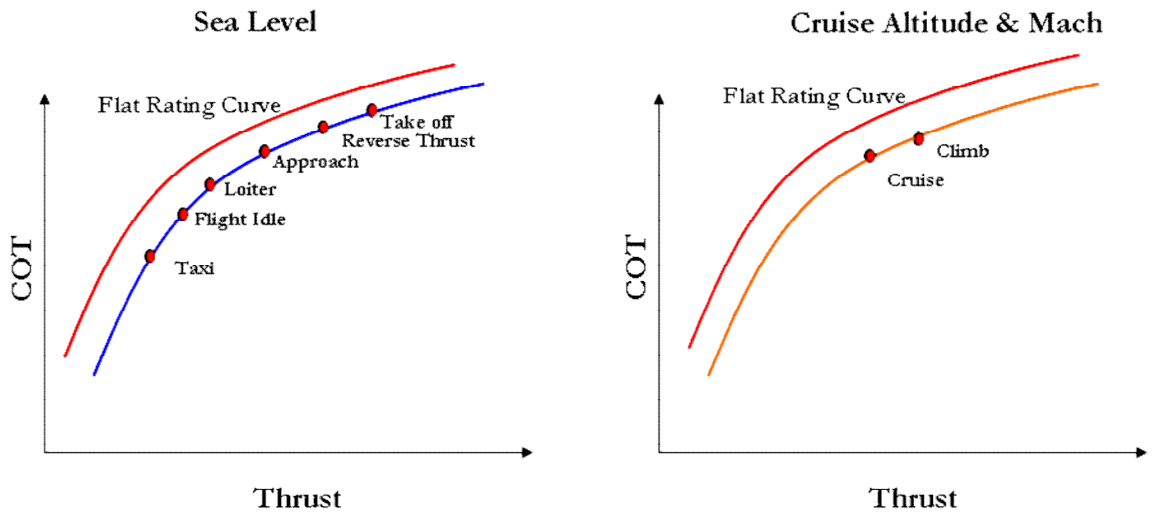

Figure 3.7 : Off-design calculation points.

3.4 Gas Turbine Performance

The gas turbine performance is the thermodynamics involved, as the energy is transformed from fuel with high calorific value burned to provide heat energy following the brayton cycle. The essential components of a gas turbine used for the aircraft engines, includes an inlet, compressor, combustor, turbine and exhaust nozzle. The inlet with the prime functionality of reducing the pressure loss as the air flows towards the face of the compressor, and then subjected to multiple stages of compression process, increasing the pressure and temperature. The high pressure air is said to undergo the combustion process releasing heat, raising the temperature of the working fluid, at constant pressure assuming low pressure loss in an ideal cycle. The high temperature and high pressure air is converted into mechanical energy, by expanding through the turbine blades, and finally through the exhaust nozzle. The cycle involves the following steps.

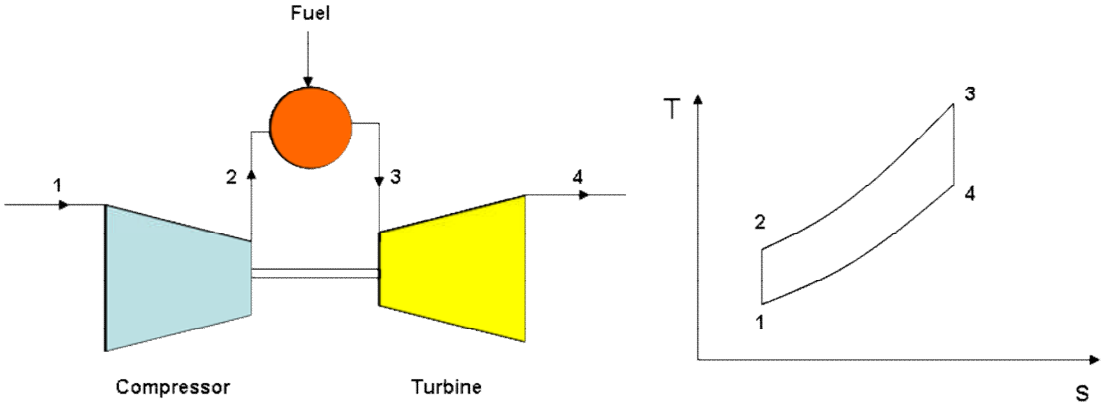

Figure 3.8 : Gas turbine cycle and entropy diagram.

- 1→2 Isentropic compression – Compressor
- 2→3 Isobaric heat addition – Combustor
- 3→4 Isentropic expansion – Turbine
- 4→1 Isobaric heat exhaustion – Exhaust

Hence the essential components for a gas turbine cycle [66] are the inlet for conducting the air stream, compressor which raises the pressure ratio, combustor for conversion of chemical energy into heat energy, turbine to convert heat and pressure energy into shaft power, and finally an exhaust to generate a jet of air creating the thrust. The type of gas turbine that the research is focussed upon is turbofan that follows a similar configuration but having two streams of airflow.

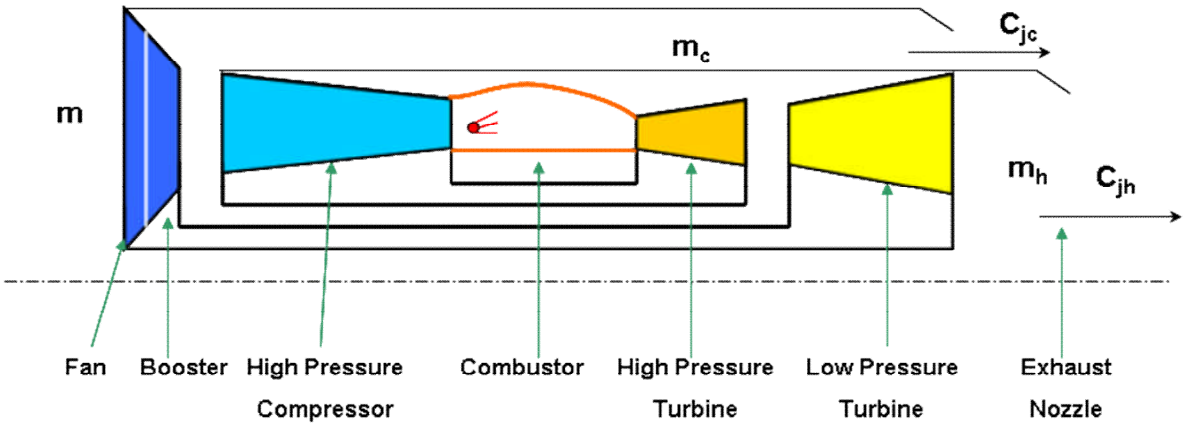

Figure 3.9 : Twin spool turbofan layout.

The schematic layout of a twin spool turbofan has been depicted in Figure 3.9. The individual components have unique characteristics serving the intended purpose, and brief description has been furnished.

By-Pass

The turbofan has a by-pass duct that seperates the flow into cold stream and hot stream. By-pass ratio is the terminology for the splitting of the flow, defined as the ratio of the cold stream air (m_c) to the hot stream air (m_h).

$$BR = \frac{m_c}{m_h} \tag{3.5}$$

The modern classification of the turbofans have been based on the by-pass ratio. The by-pass ratio closer to unity is used for military applications, and between 5 to 10 for the civil aviation. In an effort to increase the propulsive efficiency and minimized fuel burn, the by-pass ratio has been increased suitable to the design thrust.

Fan

The thrust produced by a turbofan, due to two streams of jet are named as cold thrust generated by the cold stream, and hot thrust generated by the core flow for separate nozzles, and have a combined effect in mixed nozzles. The fan is a specialized form of compressor to produce pressure ratio and accelerate a large mass of air, responsible for producing the cold thrust, and a pressurized air to the core flow.

The fan pressure ratio and the by-pass ratio are optimized [52] to minimize the fuel consumption which plays a crucial role for the long range aircraft that spend considerable amount of time in the cruise.

Booster

The booster helps in stepping up the pressure ratio, at the low pressure end of

the compressor. It has been observed that the engine manufacturers specification combine the pressure ratio due to fan and booster, and call them as the fan pressure ratio. In this research, it is considered as a separate stage of compressor, also called as low pressure compressor that rotate at the shaft speed of the low pressure turbine.

High Pressure Compressor

The fact that high overall pressure ratio, minimizes the fuel consumption has been the necessary impetus, by the engine manufacturers to achieve high values. The overall pressure ratio has been phenomenally improved through 3D aerodynamic design of the blades, and reducing the number of stages of compression, as compared to its predecessors. The overall pressure ratio is fairly at 40:1 and approaching 50:1. Each stage is a combination of rotor and stator vanes. The increasing temperature along the compressor, reduces the density, and hence a converging flow path is adoped to maintain the axial velocity. The passage between the blades have a diverging flow enabling an increase in the pressure, leading to higher pressure ratio.

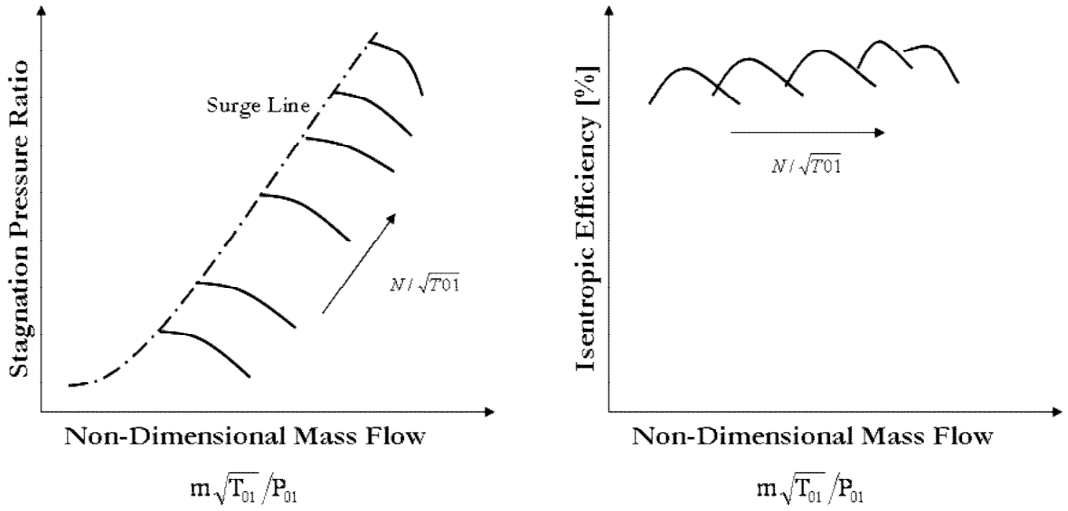

Figure 3.10 : Typical compressor characteristics.

The compressor during its operation are often faced with two limitations, being the surge and the choking behaviour that are detrimental to the performance, lowering the efficiency of the compressor. Hence a suitable running line is built by the engine manufacturers, concurrent with their design practice of specifying a surge margin. These behaviours are part of the compressor map is depicted in two basic forms, as the stagnation pressure ratio versus non-dimensional flow, and isentropic efficiency versus non-dimensional flow.

Combustor

The combustor technology has transformed from mere conversion of energy of the fuel into the possiblities of high combustion efficiency, low pressure loss, flame stability, reduced NO_x levels and lean burn technology. During the design phase, as this component bridges the compressor with the turbine, the compressed air axial velocity and mass flow from the compressor is suitably handled to have flame stability, a stoichiometric combustion with high combustor efficiency and lower pressure loss. The combustor can be split into four zones. The inlet zone where a dump or aerodynamic diffuser is used to reduce the velocity of the flow to the acceptable limits for stable combustion.

The primary zone where the fuel and a stoichiometric proportion of air is mixed for complete combustion that is followed by successive cooling and mixing holes to add the parts of air as the flame progresses, until a suitable profile factor has been achieved.

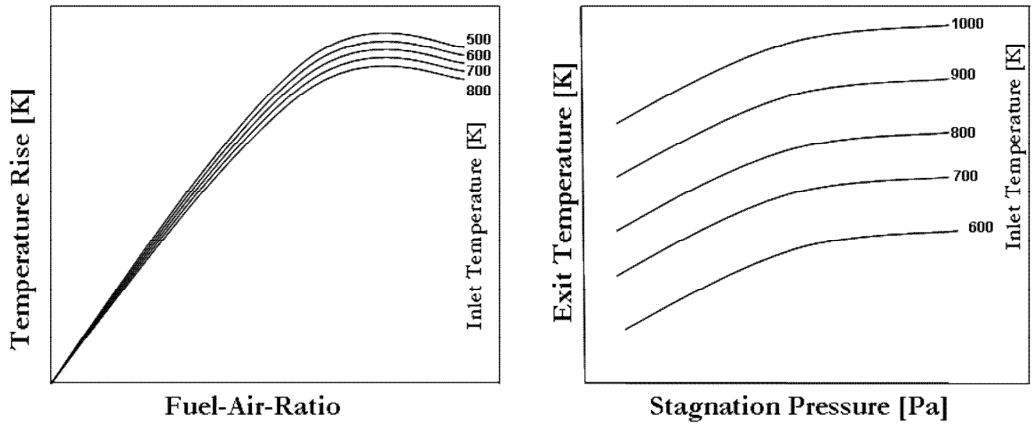

Figure 3.11 : Typical combustor characteristics.

High Pressure and Low Pressure Turbine

The purpose of converting, the heat and pressure energy into shaft rotation is performed, using the turbine. Most of the aircraft engines have one or two stages of high pressure turbine and several stages of low pressure turbine. The high pressure turbine technology is towards highly loaded turbine blade, able to withstand high energy conversion with reduced number of stages, and tolerant towards sufficiently high temperatures as high as 1800 K, and are currently limited by the capability of the material. The technological factors of cooling effectiveness and thermal barrier coating are in use for the purpose of offsetting the blade metal temperatures to the allowable limits of the single crystal alloys, used widely in the industry. The requirement to withstand high temperature has propelled the advancement in materials, from polycrystal alloys into bidirectionally solidified, and recently to single crystals, in providing high thermal stablility for the material through strengthening materials along the highly loaded direction. Each stage of the high pressure turbine is comprised of a nozzle to redirect the flow towards turbine blade with the required range of incidence angles. The first stage nozzle is choked to avoid flow instablities being transmitted from the preceding sections of the gas turbine.

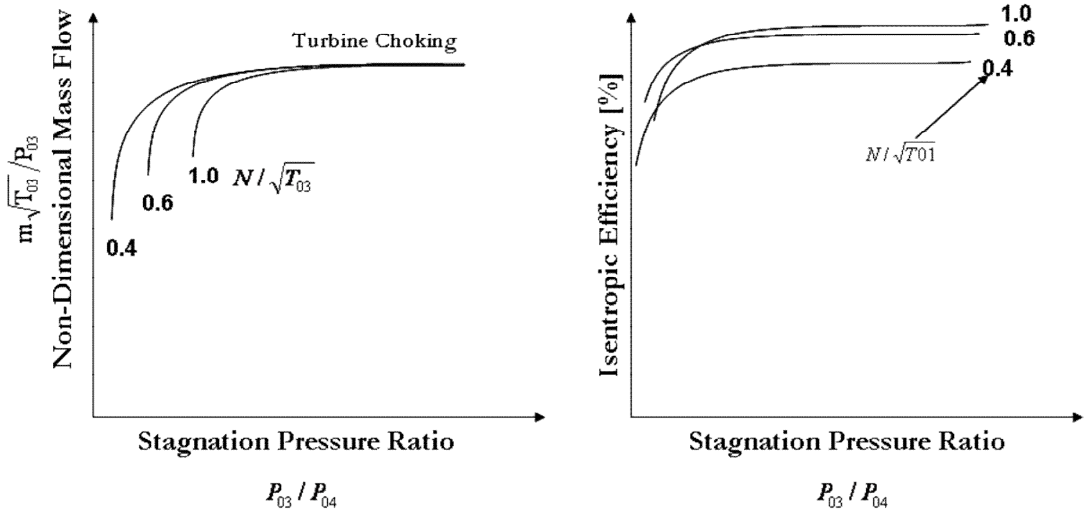

Figure 3.12 : Typical turbine characteristics.

The turbine section has a diverging flow path in allowing the hot gases to expand to extract more work, and the passages between the blades are converging, causing large temperature drop. Hence requires less number of stages for expansion, as compared to compression process that adds less temperature rise per stage in the latter stages, as the flow goes uphill of the pressure line. The high pressure turbine drives the high pressure compressor and rotates at much higher shaft speed. The low pressure turbine drives the booster and fan hence rotate at lower shaft speed and experience a lower temperature.

The turbine characteristics are normally represented by turbine non-dimensional mass flow versus turbine pressure ratio, and the turbine isentropic efficiency versus turbine pressure ratio. The curves depict that the efficiency remains constant, over a wide range of speed by virtue of the accelerating flow, and most of the turbines are designed to have a choked flow at the nozzle which brings all the curves of $N/\sqrt{T_{03}}$, follow the same line for increasing turbine pressure ratio.

Exhaust Nozzle

The turbofans are desgined in two different configurations, the mixed nozzles where the cold stream and hot stream are mixed, and the latter design is that of separate exhausts. The nozzles supports the functionality of providing the desired thrust, using a convergent propelling nozzle, and other requirements of thrust reversal, noise suppression using flower nozzle are adopted to meet the stringent airport regulations. The performance of the exhaust nozzle is that of convergent nozzle characteristics, handling range of flow.

The performance traits of the components are simulated using Turbomatch for obtaining the thermodynamic and shaft speed variation, during the flight mission.

4 GAS TURBINE DESIGN

Gas turbine design is the process of building the hardware configuration through turbomachinery principles, supported by the shape, function and manufacturing techniques. The need for the turbine design, in terms of obtaining the physical dimensions is required for estimating the stresses and blade metal temperature to derive the severity. This chapter follows the fundemental rules, laid out in design of turbomachinery, as available in different sources and large part of the formulations are from references [20], [31], [52] and [66]. The components having low life numbers are often the hot-section components. The other thumb rule is, the stator components except aerofoils of aircraft engines are designed for the entire service life of the aircraft, while the rotor and aerofoil components are replaced at intervals through the shop visit, in getting back the performance and life of the components. This obviously shifts our focus on highly loaded parts, in terms of temperature and shaft speed, the high speed spool suffers from such a combination. Hence the current chapter deals about sizing the high pressure turbine and compressor, and disc through a parametric modeling. The turbine blade has technological factors that enable to achieve the life limits. The factors such as cooling effectiveness, thermal barrier coating and profile factor are discussed in the concluding section.

4.1 Turbine Blade Sizing

The physical dimensions of the blade is of importance for the estimation of the thermal and mechanical response, under a transient mission. The dimensions are derived from the flow path sizing of the High Pressure Turbine (HPT) section. Often the HPT is a single stage or a maximum of two stages which is sufficient to rotate the high pressure compressor, due to accelerating flow between the blade passages. The turbine blade design is governed by parameters such as stage loading coefficient, flow coefficient, degree of reaction, blade and air angles.

The stage loading coefficient is the ratio of the stagnation enthalpy drop to the kinetic energy imparted.

$$\psi = \frac{2C_p \Delta T_{0s}}{U^2} \tag{4.1}$$

The stage loading coefficient is required to be between 2 and 5 for suitable energy conversion having high turbine efficiency.

The flow coefficient another design parameter, being the ratio of axial flow velocity to the tangential velocity at the blade tip is a value that is held between 0.8 to 0.9 for optimal efficiency, and depends on the blade and air angles.

$$\varphi = \frac{C_a}{U} \tag{4.2}$$

The degree of reaction is normally a proportion of the static temperature drop across the rotor to the temperature drop across the stage.

$$\Lambda = \frac{T_{t2} - T_{t3}}{T_{t1} - T_{t3}} \tag{4.3}$$

T_{t1} Static temperature at turbine stage nozzle inlet

T_{t2} Static temperature at turbine stage blade inlet

T_{t3} Static temperature at turbine stage blade outlet

The degree of reaction is kept in the zone of 0.4 to 0.5, wherein the blade behaviour is neither purely impulse type or reaction type making it suitable for axial flow machines.

The turbine blades are normally sized for the take-off, having the maximum mass flow and have to withstand high stresses due to shaft rotation. Hence a Turbomatch performance simulation has been run for the engine models to obtain the turbine inlet and outlet conditions for take-off. Based on the AN^2 (product of annulus area and square of the rotational speed) limit, the maximum height of the blade could be estimated, comparing dimensions on the engine cross-section diagram. The use of maximum height of the blade enables minimizing the stages of the turbine, quintessential for the aircraft engines

aimed at reducing the weight. The exit area estimation through the AN^2 approach as well fixes the flow coefficient. If it is the first stage of the turbine, the nozzle is designed to be choked that gives the optimum blade loading coefficient, and suitably sized to meet the blade angles with respect to the limits of the angles and degree of reaction. A simplified flow chart is represented in the Figure 4.1 highlighting the important design factors for sizing.

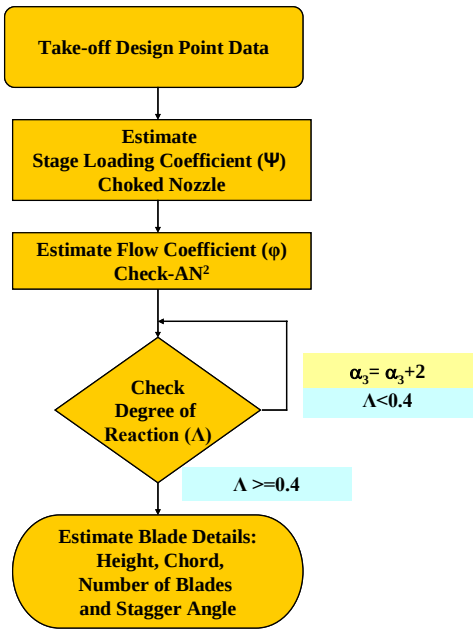

Figure 4.1 : Simplified flow chart of turbine sizing.

The reference [81] based on the preliminary design point of view, the expected mass and height of the root and shank are estimated based on the aerofoil mass and height (Table 4.1).

4.2 Compressor Blade Sizing

As part of the high speed spool, the high pressure compressor last stages are exposed to higher temperatures and shaft speed prone to failure by fatigue. The compressor flow path is sized to achieve the required pressure ratio without flow instabilities such as surge and choking. The compressor design mainly follow three basic configurations, such as constant mean radius design, constant inner radius, and constant outer radius. Hence a parametric sizing

code has been developed to capture the different design configurations. The critical element for the sizing of the compressor blade is the temperature rise per stage, iterated to achieve the satisfactory requirements of the De Haller number that is kept above 0.72 for establishing allowable diffusion.
The temperature rise per stage is calculated using the equation.

$$\Delta T_{0s} = \frac{\lambda_{cp} U C_a (\tan\beta_1 - \tan\beta_2)}{C_p} \tag{4.4}$$

The total temperature rise is based on the polytropic equation

$$T_{02} = T_{01}\left[\frac{p_{02}}{p_{01}}\right]^{\frac{n-1}{n\eta_{cp}}} \tag{4.5}$$

Hence from the above two equations, the feasible number of stages could be estimated and checked for compatability with respect to De Haller number for the individual stages. The common use of the sizing philosophy is the repeating stage design.

The radial equilibrium equation is given as

$$\frac{1}{\rho}\frac{dp}{dr} = \frac{C_w^2}{r} \tag{4.6}$$

The degree of reaction, depends on the blading assumption, such as free vortex design, exponential design and first power design, according to the whirl velocity distribution along the blade height. It is observed that when the degree of reaction becomes 0.5 all the designs yield identical whirl distribution, hence normally adopted to achieve closer to this number.

The other design strategies are in terms of maintaining a constant hub, mean and tip radius. A constant inner diameter is chosen for the industrial gas turbines, and constant outer diameter designs are used for minimum number of stages as in aircraft engines. The temperature rise per stage, degree of reaction, and the De Haller number, specify the required blade angles and

hence the design of the individual stages of the compressor. The sizing of the high pressure compressor is carried out for the design point calculation data, corresponding to the top-of-climb where the maximum pressure ratio is achieved with respect to the mission points and the shaft speed almost near to the take-off condition. The process is iterated for the feasibility of the stages, and to the type of design of the engine manufacturers, in terms of reference radius for the design.

4.3 Parametric Disc

The disc system of an aircraft engine, designed to withstand the centrifugal forces due to rotation of the blades is influenced by the objective of minimum weight, expected life and safety demands. The disc system have different shapes suitable to rim loads and functionality. As part of design practice, they are to satisfy a number of criterions, such as hoop burst under overspeeds, crushing strength at overspeed, fatigue life suitable to the mission and optimized weight to reduce fuel burn. The scope of the current focus is limited to life estimation on a relative basis for severity, hence the disc configurations are reproduced, from the engine cross-sections of the engine manufacturers. The disc system, occupying the major amount of weight of an aircraft engine, can be segmented into three categories [81] such as

- Cylindrical disc
- Web shaped disc
- Hyperbolic disc

The shape has unique features and purpose, in minimizing the weight of the disc system. The ideal form of disc system for most of the application and a common point of reference is a cylindrical disc. The adaptations of the web and hyperbolic disc are with respect to magnitude of the rim loads that are suitably designed to have the radial and hoop stress pattern to be within the expected levels for reaching the feasible life.

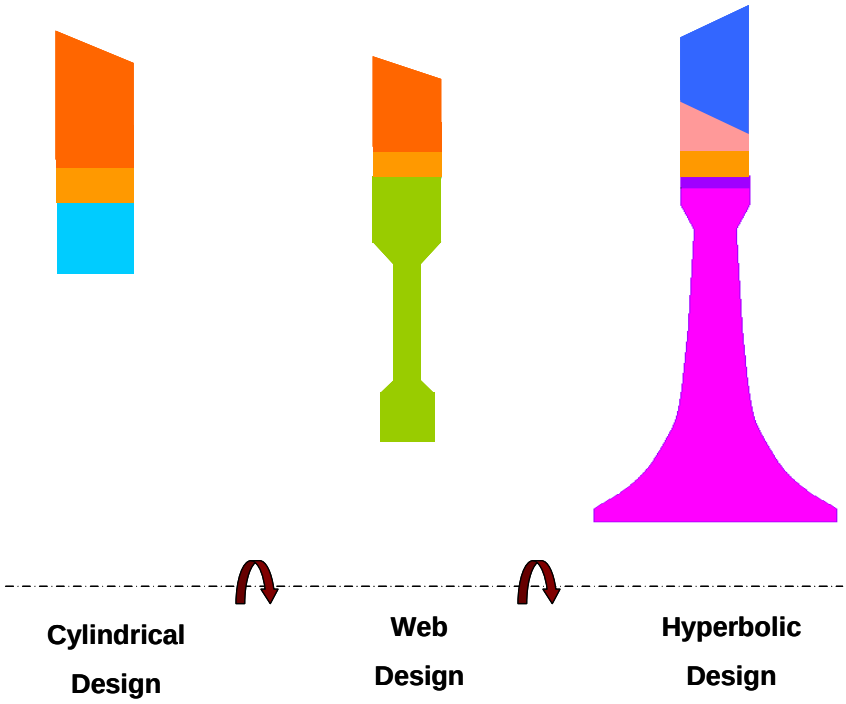

Figure 4.2 : Disc designs used in gas turbines.

The cyclindrical discs are commonly used in the first few stages of the compressor. The web shaped discs are widely used, in the last stages of the low pressure compressor, high pressure compressor and low pressure turbine. The hyperbolic disc is eventually used for the high pressure turbine, and for three shaft systems on the intermediate stage. The shape is one of the optimization on the basis of minimizing the weight by keeping the stresses such as the radial and hoop within design limits.

Most of the disc systems for aircraft engines are subjected to fatigue where it has been observed a substantial portion of life is exhausted in the nucleation or the crack initiation, where the link between surface cracks and sub-critical cracks of the region are developed. The other observation is that for high strength materials, having higher yield strength exhibit less resistance in the crack propagation, hence the design of discs are confined to the crack initiation phase.

A parametric automation has been developed to capture the different design configurations of the disc system. The reference [79] has been used for the estimation of the blade root and blade shroud dimensions. The dimensions for the disc at the critical locations are based on the engine cross-section that helps in capturing the profile of the design, adopted by the engine manufacturers. The exact design of the disc system, involves optimization with respect to material, shape, weight and stress levels is a vast area and would require material data of proprietary nature and design practices of the engine manufacturers, beyond the current scope and time.

Cylindrical			Web			Hyperbolic		
Blade root height	**Blade root weight**	**Post weight**	**Blade root height**	**Blade root weight**	**Post weight**	**Blade root height**	**Blade root weight**	**Post weight**
17.60%	20%	10%	25%	20%	20%	53.85%	50%	20%
Aerofoil height	Total blade weight	Total blade weight	Aerofoil height	Total blade weight	Total blade weight	Aerofoil height	Total blade weight	Total blade weight

Table 4.1 : Blade preliminary design assumptions for height and weight (root and post) based on the disc design [81].

The shaft rotation and the influence of blade mass on the disc leads to two major types of stresses, primarily the radial stress due to the outward force by the rotation, and the stress in the circumferential direction called as the hoop stress. In addition to the above loading, there are torsional and bending moment, but insignificant as compared to these major forces. Though the disc involves a 3-D structure, as it forms a rotating component, it is made to be axisymmetric to minimize balancing issues, and to have the centre of gravity as close as possible to the engine axis. The disc is designed with different shapes to suit the operation and its nature of loading. The major factor that defines the different shapes is in optimizing the weight of the engine that inturn helps in achieving fuel economy.

4.4 Technological Factors

Turbine design over the decades of progress have been designed to withstand sufficiently high temperatures, as high as 1800 K aiming at higher thermal efficiency is beyond the stability of turbine blade materials. Hence a number of technology parameters have been promising, in sustaining a proper operation of

the turbine blade through temperature offset mechanism on magnitude and profile.

Cooling Effectiveness

The cooling effectivness [29] provides the temperature offset, by using the compressed air at lower temperature for blade cooling that establishes a convective film layer over the metal surface. The measure of cooling effectiveness [41] is a ratio of the temperature difference between the gas and blade metal temperature to that of temperature difference between gas and coolant temperature. The cooling effectiveness is a critical parameter, as a balanced amount of coolant air to be used which is the quantity of compressed air without useful work, hence leads to loss in the overall efficiency. In this research activity the cooling effectiveness is simulated as a temperature drop on the bulk temperature at the interaction of the metal with the gas.

$$\Phi_c = \frac{T_g - T_m}{T_g - T_{ci}} \tag{4.7}$$

Φ_c cooling effectiveness

T_g gas temperature [K]

T_m average metal temperature [K]

T_{ci} coolant inlet temperature [K]

The value of cooling effectiveness [53] varies in current engines between 0.5 to 0.7 with different techniques for cooling. The internal cooling where the coolant travels through the turbine blade through radial holes or channels are simple among the cooling configurations. The film cooling is one where a fluid film is developed through the use of closely-spaced holes and are efficient in providing a higher cooling effectiveness of 0.6. The highly efficient version of the blade cooling is the use of effusion cooling with the porous surfaces builds the necessary film, and have significantly high level of cooling effectiveness upto 0.7. However each type of cooling system has its advantages and disadvantages associated with the design. The effusion cooling being the most effective system, but has manufacturing difficulties, as well loss in aerodynamic

efficiency, hence not favoured for the current engines. The internal and film cooling, impose less challenges, but require larger volume of cooling flow to achieve the effectiveness of effusion cooling. The choice of the blade cooling technology requires trade-off studies on thermal efficiency, aerodynamic efficiency, manufacturability, cost and without compromise on reliability.

Thermal Barrier Coating

The thermal barrier coating [103] is a means of lowering the metal temperature through a layer of low conductivity material. The coating constituents are two layers with the external layer being the thermal barrier coating having lower thermal conductivity, and a bond coat beneath for oxidation resistance. The thermal barrier coating material, widely used in aircraft engine turbine blades is yittria stabilized zirconia. The bond coat for the purpose of oxidation and corrosion resistance are aluminides and MCrAlY [98]. The temperature offset through the coating, helps in reducing the amount of cooling flow, improving the efficiency of the cycle, and as well in improving the creep life [3].

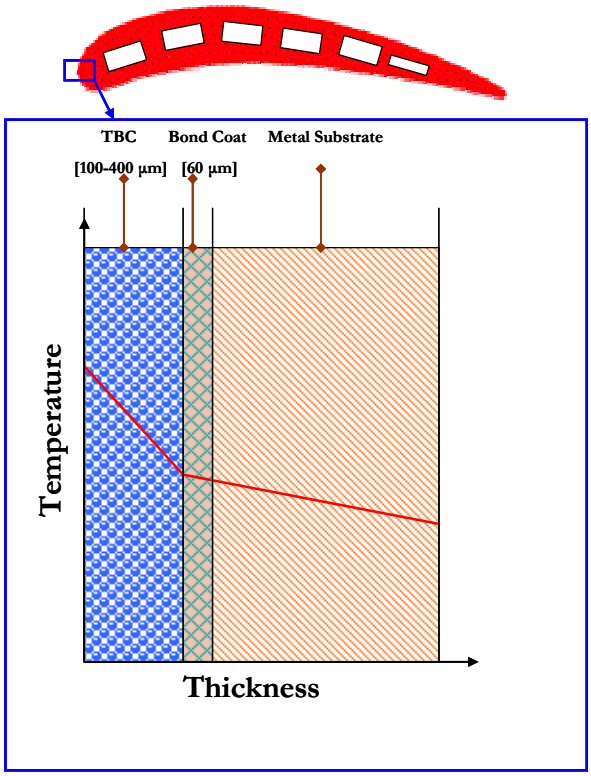

Figure 4.3 : Thermal barrier coating on turbine blade.

However the low cycle fatigue and thermal fatigue, become the limiting factor on such designs, due to difference in the response of the ceramic and metal substrate leading to high compressive stresses, tending to cracks at the thermally grown oxide layer. The typical thickness [66] of the TBC varies from 100 μm to 400 μm and for the bond coat of 60 μm. The thermal conductivity of the thermal barrier coating and thickness are critical for reducing the temperature.

The methodology adopted for the heat flux transfer from the gas to the cooled turbine blade is that in reference [5] and [82]. The heat transfer model can be represented through the following equations.

$$Bi_{tbc} = \frac{T_w - T_{m,ext}}{T_{aw} - T_w} = \frac{\alpha_g t_{tbc}}{\lambda_{tbc}} \tag{4.8}$$

$$Bi_m = \frac{T_{m,ext} - T_{m,\text{int}}}{T_{aw} - T_w} = \frac{\alpha_g t_m}{\lambda_m} \tag{4.9}$$

$$\varepsilon_0 = \frac{T_{0g} - T_{m,ext}}{T_{0g} - T_{0c,k}} \tag{4.10}$$

$$\varepsilon_{c,\text{int}} = \frac{T_{0c,x} - T_{0c,k}}{T_{m,\text{int}} - T_{0c,k}} \tag{4.11}$$

$$\varepsilon_f = \frac{T_{0g} - T_{aw}}{T_{0g} - T_{0c,x}} \tag{4.12}$$

The equations are solved by assuming $\varepsilon_{c,\text{int}} = 0.7$ and $\varepsilon_f = 0.4$ with assumed technology level for cooling effectiveness that gives the temperature drop by virtue of the thermal barrier coating.

Pattern Factor And Profile

The pattern factor [52] which is the ratio of the temperature difference between maximum combustor outlet and average outlet temperature to the difference between average outlet and inlet combustor temperature. This factor has impact on the life of the turbine blade, as the location of the maximum

temperature is predominantly designed to fall on the region of less stress to maximize life. Hence in the current research, the profile has been identified having five segments along the radial height of the blade.

$$PF \equiv \frac{T_{t\max} - T_{tav}}{T_{tav} - T_{tin}} \tag{4.13}$$

T_{tmax} maximum measured exit temperature (local) [K]

T_{tav} average of all temperatures at exit plane [K]

T_{tin} average of all temperatures at inlet plane [K]

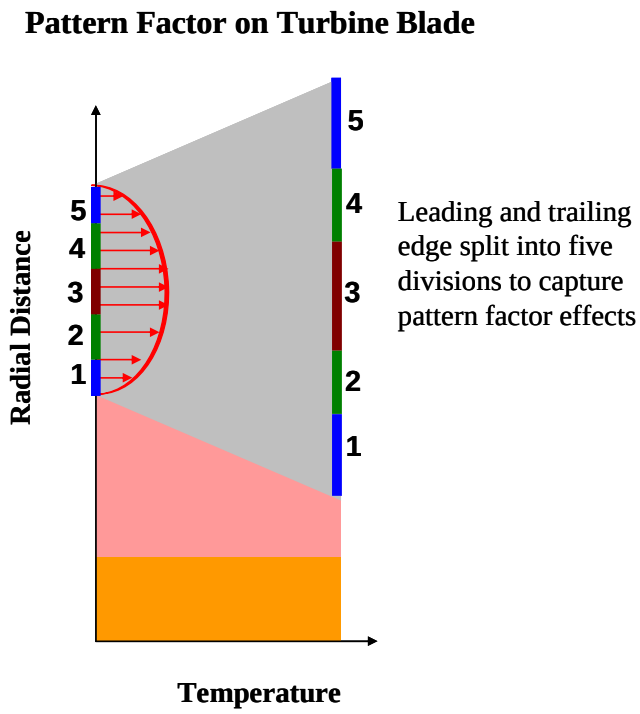

Figure 4.4 : Pattern factor profile description.

5 ANALYSIS

The analysis deals with the numerical simulation of the components, depicting the response to changes in thermal and mechanical loads. The essential steps to follow from the design of the blade and the disc is in capturing the blade metal temperature and stresses during the mission. The metal temperature spread is a transient response to the varying gas temperatures and flow rate, establishing a convective heat transfer on the metal surface. This by virtue of thermal properties of the material and thermal load observed as a temperature response to the thrust variations during the mission points. The temperature together with the shaft speed variation, dictates the stress level in the component. The temperature response of the structure is captured using the numerical simulation technique of finite element analysis, and further for predicting the stress level through thermo-mechanical analysis. The finite element analysis requires, an estimate of the thermal loads on the component that are obtained through the heat transfer calculation. This chapter deals with the intermediate process that transforms the mission, performance and design data into the temperature and stress on the components towards the goal of life estimation.

5.1 Finite Element Analysis

The thermal and mechanical behaviour of structures have been to a large extent subjected to the use of finite element analysis, a numerical simulation technique to predict the thermal and mechanical response. A number of commercial Computer Aided Engineering (CAE) packages are in use among the industry and research groups. The software Ansys has been adopted as it offers parametric programming features, such as the use of Ansys Parametric Design Language (APDL) and blends with Matlab a base platform software for the current research supporting the integration. However other competitive packages could be applied as they will serve the purpose. The process involved is in transforming a geometric model into grids

represented, as an assembly of mass and stiffness of the system, at the discretized level that through progression, builds the entire structure under consideration. The commercial packages are equipped with capabilities of simulating complicated geometry, coupled effects and non-linearlities in the analysis. The fundamental phases of finite element analysis are preprocessing, solution and postprocessing.

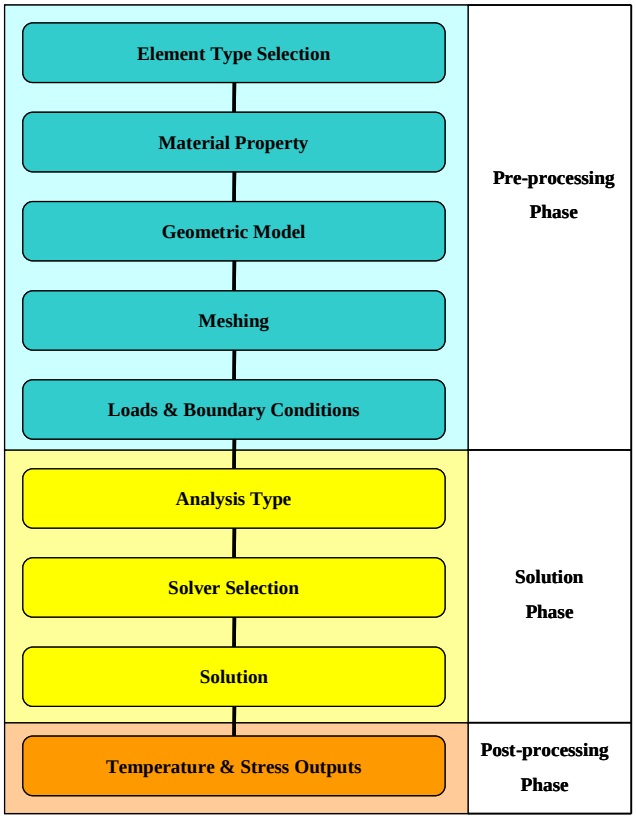

Figure 5.1 : Finite element analysis layout.

The preprocessing phase is initiated through the selection of the appropriate element type which bears the element definition. The element is the basic entity used in the process of discretization of the continuum. Element is characterized by an assembly of nodes conforming to the mathematical formulation of the domain under consideration. The domain discretization is driven by two distinct methods such as h-method and p-method. The h-method uses linear elements, where the edges have two nodes, and the number of elements are progressively increased to an optimal number, suitable for the

domain commonly referred to as the mesh convergence. The p-method is pertaining to the order of the element where the edges are defined by more than two nodes, hence quadratic or polynomial in characteristics and mesh convergence is achieved through higher order elements. For thermal and thermo-mechanical analysis, being the current scope, the linear elements or the h-method is used as the domain involves small deformation. The p-method is used in situations of large deformation and have better convergence for such domains.

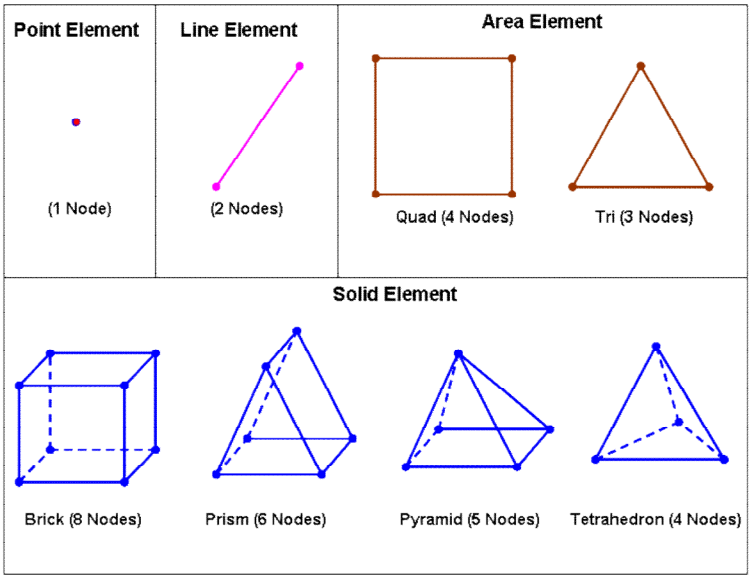

Figure 5.2 : Linear element types.

Plane 42, an Ansys area element has the features of plane element with thickness option, and as well for axi-symmetric features, making it ideal for the turbine blade and the disc model. The 2-D geometry is generated using the APDL for parametric modeling of the turbine blade and the disc, compatible for different engines. The thermal and mechanical material properties are incorporated as part of the material definition. Meshing, a discretization process of the geometric model using the nodes and element are done using two approaches, such as the mapped meshing and free meshing. The load for the thermal model is the the heat transfer coefficient and bulk temperature. The structural model is subjected to the constraints to avoid rigid body motion, and loads such as the metal temperature and angular velocity. The gas bending

forces are ignored, as they have less significance in magnitude, as compared to centrifugal forces, and stiffer blades due to less blade height for the high speed spool making it less prone to bending, as compared to the low speed spool.

The solution phase is in identification of the type of analysis for the estimating the response of the structure. Transient thermal analysis is used for obtaining the temperature profile across the blade and disc assembly. For the mechanical response, a thermo-mechanical analysis is performed for the mission points with the temperature profile corresponding to the transient thermal response together with the shaft speed as angular velocity. An appropriate solver is chosen for the problem to estimate the response for the different load steps corresponding to the mission.

The postprocessing is in retrieving the response of the system, as temperature and stress plots, or data values. Metal temperatures and Von Mises stresses are extracted for further calculation involving the life estimation.

The entire process from the geometric model creation till postprocessing is automated through APDL code with the input from Matlab generated data files and churned down to stress and temperature for the nodes, and the output is streamlined with the Matlab life estimation code.

5.2 Turbine Blade Modeling

The turbine blade consists of the root, shank and aerofoil. The sizing of the blade provides the data on the aerofoil. The reference [81] dealing on the preliminary disc optimization specifies the approximate blade root and shank dimensions, in terms of volume and height, used as an estimate for the blade mass calculation acting as a rim load for the disc. Based on the common geometry of the blade shank and root, the volume and height are mathematically dealt to estimate the thickness at different sections using suitable assumptions. The aerofoil sizing that provides the blade height and chord is fitted into the standard profiles [31] such as A_3K_7 or $B_1E_1I_1$. Aerofoil

profile A_3K_7 finds application at the first stage of turbine for high loading. $B_1E_1I_1$ is symmetrical profile conventionally used for lower loading and suitable for last stages of high pressure turbine.

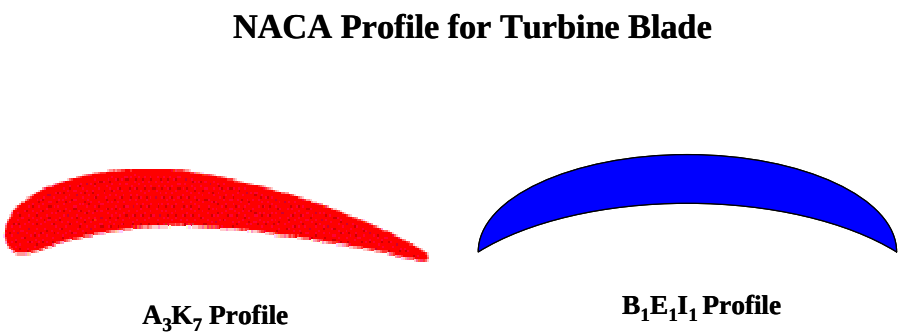

Figure 5.3 : NACA profiles for turbine blade.

A_3K_7				$B_1E_1I_1$			
Mean Line		Thickness		Mean Line		Thickness	
x_c [%]	y_c [%]	x_t [%]	y_t [%]	x_c [%]	y_c [%]	x_t [%]	y_t [%]
0	0.00	0	0.00	0	0.00	0	0.00
1.25	0.84	1.25	3.47	1.25	0.72	1.25	2.58
2.5	1.43	2.5	4.97	2.5	1.25	2.5	3.28
5	2.36	5	6.92	5	2.13	5	4.04
10	3.69	10	9.01	10	3.48	10	5.01
15	4.60	15	9.83	15	4.51	15	5.59
20	5.22	20	10.00	20	5.29	20	7.00
25	5.62	25	9.90	25	5.86	25	8.06
30	5.85	30	9.61	30	6.26	30	9.03
35	5.94	35	9.11	35	6.51	35	9.73
40	5.90	40	8.59	40	6.64	40	10.00
45	5.75	45	7.91	45	6.65	45	9.73
50	5.52	50	7.15	50	6.55	50	9.01
55	5.20	55	6.34	55	6.34	55	8.02
60	4.81	60	5.50	60	6.02	60	6.91
65	4.37	65	4.66	65	5.55	65	5.85
70	3.87	70	3.85	70	4.98	70	5.00
75	3.33	75	3.09	75	4.33	75	4.31
80	2.75	80	2.41	80	3.68	80	3.62
85	2.13	85	1.83	85	2.82	85	2.94
90	1.49	90	1.39	90	1.95	90	2.25
95	0.80	95	1.10	95	0.95	95	1.56
100	0.00	100	0.00	100	0.00	100	0.00
Expressed as % of the chord length							

Table 5.1 : NACA profile mean line and thickness variation [31].

The blade, a 3-D dimensional geometry would consume computational time, not convenient for preliminary life estimation, making it computationally costlier. Hence a modeling technique with computational effort and time, concurrent with preliminary design needs to be employed. The practice of using plane element with thickness which mimics the 3-D model on a 2-D with the only limitation of not capturing the stagger angle and out of plane loads is a useful approach for the preliminary life estimation. The Ansys element library [85], having a comprehensive collection of element types for different applications, provides Plane 42 for capturing thickness variation on a plane element. This element has the feature of the axi-symmetric option, hence can be applied for modeling the disc geometry for the predicting the thermal and mechanical behaviour.

HPT Blade Geometry and Mesh

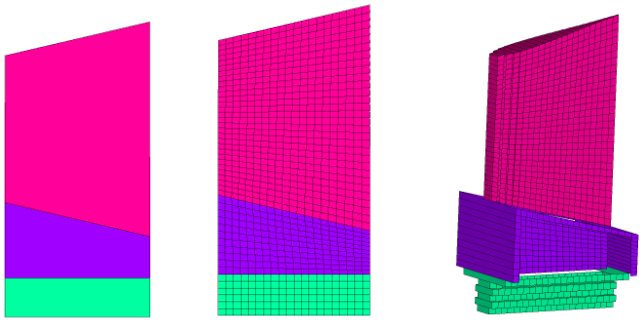

Figure 5.4 : HPT blade geometry and finite element model.

5.3 Disc Modeling

The disc broadly classified, as cylindrical, web and hyperbolic are axi-symmetric in geometry. This gives the possibility of using axi-symmetric option for the Plane 42 element saving considerably on the numerical computation. The axi-symmetric elements are effective in simulating the geometry which are revolved structures upon the axis of rotation, can be represented as 2-D cross-sections. Hence the need for 3-D model is redundant and reduces the number of elements and nodes. The disc with the feature for accomodating the blade root, differs from the axi-symmetric nature due to the fir-tree slots. The mechanism for retaining the axi-symmetry for such regions, relies on the use of orthotropic

properties, especially for the material youngs modulus. A flow through mesh or mapped mesh is applied for the disc geometry. The number of elements at the blade root region is mapped with the disc interface for tieing up the nodes using coupled degrees of freedom. The coupled degrees of freedom for the thermal model is the temperature, while for the structural model the displacement along the engine axial and radial direction are coupled.

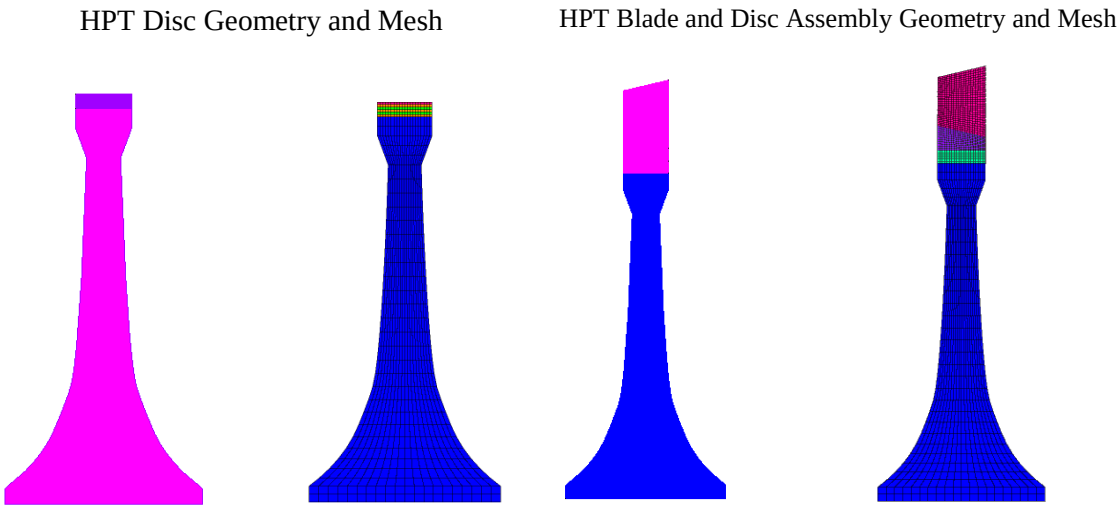

Figure 5.5 : Geometry and finite element model of disc and blade-disc assembly.

5.4 Heat Transfer Calculation

The heat transfer to the gas turbine component has three fundemental modes, such as the conduction, convection and radiation. The conduction and convection being the dominant modes for the blade and disc has been estimated using the standard correlations. The metal temperature of the blade and the disc involves the calculation of the heat transfer coefficients for the different segments of the turbine. The estimation of the blade metal temperature involves different flows, leading edge uses the circular cylinder correlation, trailing edge uses the flat plate correlation, as the trailing edge tapers down to a minimum thickness. The channel correlation applied at the tip region of the blade. The shank forms the cavity flow to seal off the secondary flow. The disc region has different cavity flow patterns, such as axial through flow, radial outflow, according to the flow arrangements adopted by the engine

manufacturers.

The circular cylinder stagnation point correlation for the leading edge [53]:

$$Nu = 1.14\,\mathrm{Re}_d^{\,0.5}\,\mathrm{Pr}^{0.4} \tag{5.1}$$

Flat plate turbulent flow correlation for trailing edge [53]:

$$Nu = 0.029\,\mathrm{Re}_c^{\,0.8}\,\mathrm{Pr}^{0.33} \tag{5.2}$$

Tip channel flow correlation:

$$Nu = 0.023\,\mathrm{Re}_{hd}^{\,0.8}\,\mathrm{Pr}^{0.4} \tag{5.3}$$

Axial through flow cavity correlation [59]:

$$Nu = 0.050 G^{0.38}\,\mathrm{Re}_z^{0.15}\,Gr^{0.31} \tag{5.4}$$

Radial outflow cavity correlation [59]:

$$Nu = 0.267 Gr^{0.286} \tag{5.5}$$

Nu	Nusselt number
Re_d	Reynolds number over the cylinder
Re_{hd}	Reynolds number over the hydraulic diameter
Re_z	Reynolds number along the axial direction
Pr	Prandtl number
G	Gap Ratio
Gr	Grashoff number

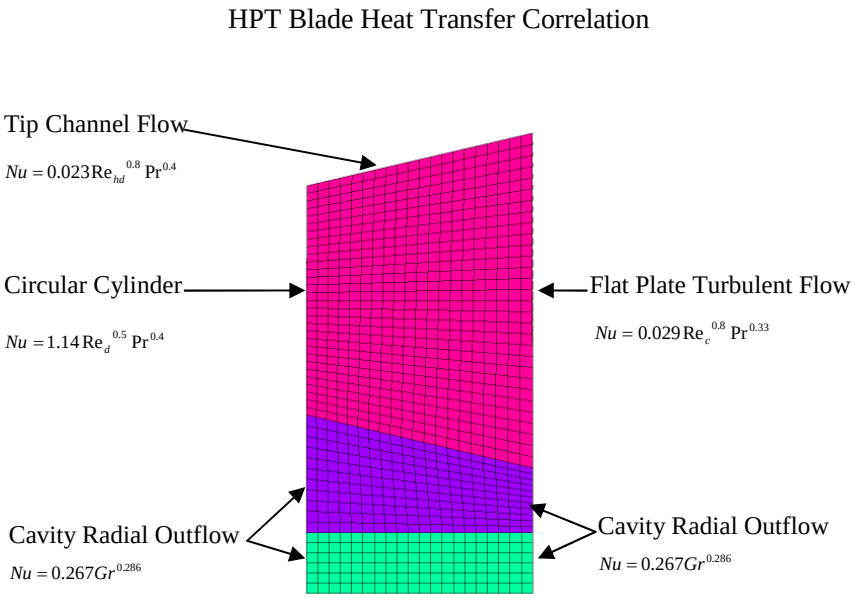

Figure 5.6 : Heat transfer correlations on the HPT blade.

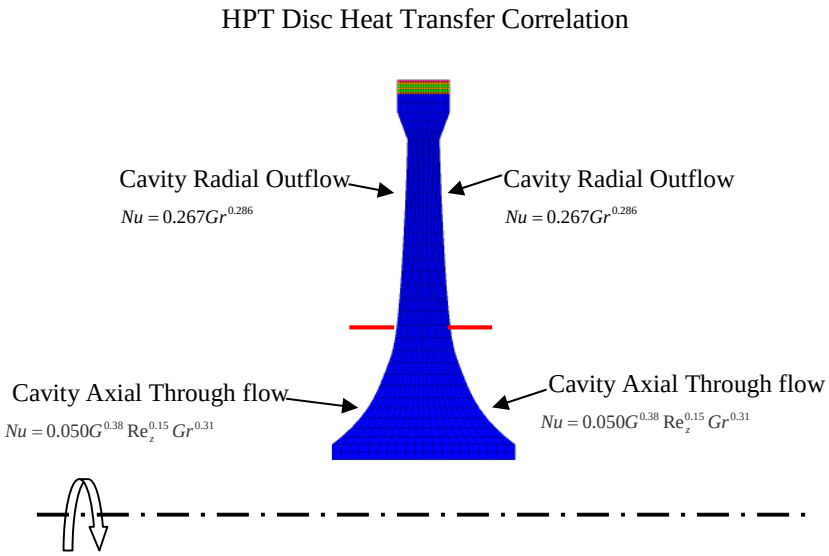

Figure 5.7 : Heat transfer correlations on the HPT disc.

5.5 Thermal Analysis

The thermal analysis is to obtain the blade metal temperature dependent on conduction and convection. The aircraft engine mission with thrust variation, undergoes changes in the gas path properties at the different components, based on the performance characteristics. The thermal response of the component varies with the gas properties and as well with time. Hence a

transient thermal analysis is carried out to predict the metal temperatures during the mission. The heat transfer calculation carried out in Matlab is provided as input thermal load for the different segments of the blade and the disc geometry. The thermal material properties, such as the thermal conductivity, specific heat capacity and density of the material are provided part of material definition. The properties used for the analysis are temperature dependent, as the component is subjected to wide range of operational temperatures. The coupled degrees of freedom is applied for the coincident nodes of the blade and the disc. The initial loadstep corresponding to the taxi segment is considered as the steady state condition for the initial temperature spread and solved cummulatively with respect to time for the transient behaviour.

The mathematical formulation involved in the finite element analysis is based on the fundemental equation of thermodynamics [85] (Ansys Theory Manual).

$$\rho c\left(\frac{\partial T}{\partial t}+\{V\}^T\{L\}T\right)+\{L\}^T\{Q\}=\ddot{Q} \tag{5.6}$$

ρ density of the material

c specific heat capacity

T temperature

t time

{L}= $\begin{Bmatrix}\frac{\partial}{\partial x}\\ \frac{\partial}{\partial y}\\ \frac{\partial}{\partial z}\end{Bmatrix}$ = vector operator

{V}= $\begin{Bmatrix}V_x\\ V_y\\ V_z\end{Bmatrix}$ = velocity vector for mass transport of heat

$$\{Q\}=[D]\{L\}T \tag{5.7}$$

$$[D] = \begin{bmatrix} K_{xx} & 0 & 0 \\ 0 & K_{yy} & 0 \\ 0 & 0 & K_{zz} \end{bmatrix} = \text{conductivity matrix}$$

K_{xx}, K_{yy} and K_{zz} ,the thermal conductivity of the material in the element x, y, z directions.

The equation can be reconstructed as

$$\rho c\left(\frac{\partial T}{\partial t} + V_x\frac{\partial T}{\partial x} + V_y\frac{\partial T}{\partial y} + V_z\frac{\partial T}{\partial z}\right) = \ddot{Q} + \frac{\partial}{\partial x}\left(K_x\frac{\partial T}{\partial x}\right) + \frac{\partial}{\partial y}\left(K_y\frac{\partial T}{\partial y}\right) + \frac{\partial}{\partial z}\left(K_z\frac{\partial T}{\partial z}\right) \tag{5.8}$$

For the mission points the finite element model with the temperature dependent properties, heat transfer coefficient and bulk temperature with coupled temperature at the blade-disc interface is solved for different load steps. The temperature response obtained are the required blade and disc metal temperatures. In Ansys, the temperature response of the blade and disc assembly, can be applied as the temperature load for the structural model by reading from the results file generated at the end of the solution phase. The metal temperature, serves the purpose of the thermal load on the structural model, and for estimating the material properties during the life estimation.

HPT Metal Temperature Plot

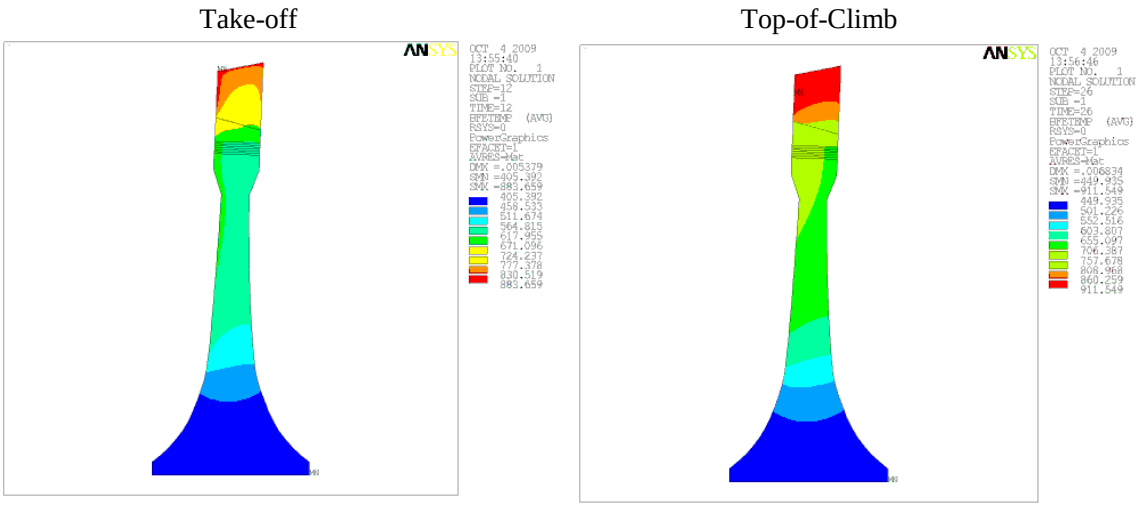

Figure 5.7 : Metal temperature plot at take-off and top-of-climb for HPT.

5.6 Thermo-Mechanical Analysis

The structural model is achieved by flipping the element type from thermal to structural, thereby the degrees of freedom is changed from temperature to structural displacement. The mechanical properties such as the Young's modulus, Poisson's ratio, shear modulus, density varying with temperature is assigned to the elements. The loads on the structural model are the temperature and angular velocity. The temperature is read from the results file generated from the transient thermal analysis. The angular velocity is applied through shaft speed scaling vector obtained from the performance calculation for the shaft speed. The engine specification provides the shaft speed in rpm which is converted to radians/s.

$$\omega = \frac{2\pi N}{60} * N_s \tag{5.9}$$

ω angular velocity in radians/s

N shaft speed in rpm at 100% speed.

N_s shaft speed scaling value

The angular velocity and the temperature, from the thermal analysis were applied, and the analysis performed for the time points considered for the simulation.

$$\{\sigma\} = [D]\{\varepsilon\} \tag{5.10}$$

$\{\sigma\}$ stress vector

$[D]$ stiffness matrix

$\{\varepsilon\}$ elastic strain vector

The equation 5.10 [85] (Ansys Theory Manual) can be rewritten in terms of the total strain as

$$\{\varepsilon\} = \{\varepsilon^{th}\} + [D]^{-1}\{\sigma\} \tag{5.11}$$

$$\{\varepsilon^{th}\} = \Delta T \begin{bmatrix} \alpha_x^{se} & \alpha_y^{se} & \alpha_z^{se} & 0 & 0 & 0 \end{bmatrix}^T \tag{5.12}$$

α_x^{se} secant coefficient of thermal expansion in the x direction of the element.

$$\Delta T = T - T_{ref} \tag{5.13}$$

T Temperature of the location in Kelvin

T_{ref} Reference temperature in Kelvin

The inverse of stiffness matrix is the flexibility matrix given as

$$[D]^{-1} = \begin{bmatrix} 1/E_x & -\upsilon_{xy}/E_x & -\upsilon_{xz}/E_x & 0 & 0 & 0 \\ -\upsilon_{yx}/E_y & 1/E_y & -\upsilon_{yz}/E_y & 0 & 0 & 0 \\ -\upsilon_{zx}/E_z & -\upsilon_{zy}/E_z & 1/E_z & 0 & 0 & 0 \\ 0 & 0 & 0 & 1/G_{xy} & 0 & 0 \\ 0 & 0 & 0 & 0 & 1/G_{yz} & 0 \\ 0 & 0 & 0 & 0 & 0 & 1/G_{xz} \end{bmatrix}$$ = Flexibility matrix

E_x Young's modulus in the x direction [Pa]

v_{xy} major Poisson's ratio

v_{yx} minor Poisson's ratio

G_{xy} Shear modulus in the xy plane [Pa]

The structural model with the metal temperature and shaft speed as angular velocity is simulated for the mission points to estimate the stress at the different time points. The disc needs to be simulated for an assembly of blades while the model has incorporated only one blade for the simulation, hence based on the mass of the blade and its centre of gravity, the centrifugal forces are calculated. The total blade force due to (total number of blades-1) number of blades is applied on the interface nodes of the blade root and the disc.

Two scenarios are of concern for the turbine blade, especially the tip shroud and the blisk configuration that are in current practice among the engine manufacturers. The tip shroud effect is simulated as a centrifugal radial force, assuming 10 % of the blade mass at the tip radius. The blisk configuration is achieved by merging the nodes of the model at the blade root region overlapping the disc.

The life estimation methods for super alloys, rely on the equivalent stress on the component, commonly referred to as the Von Mises stress which is a resultant

HPT Von Mises Stress Plot

Take-off

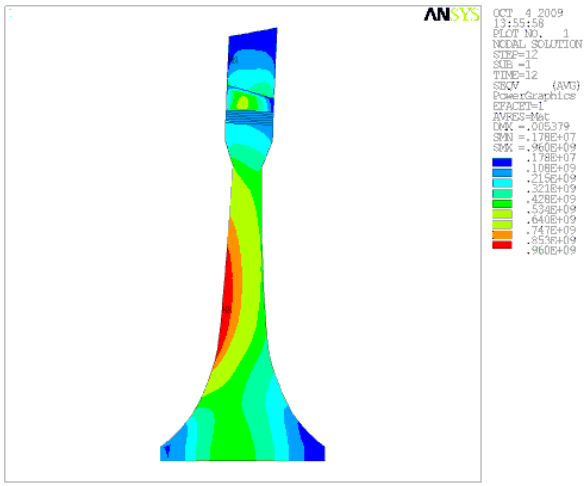

Top-of-Climb

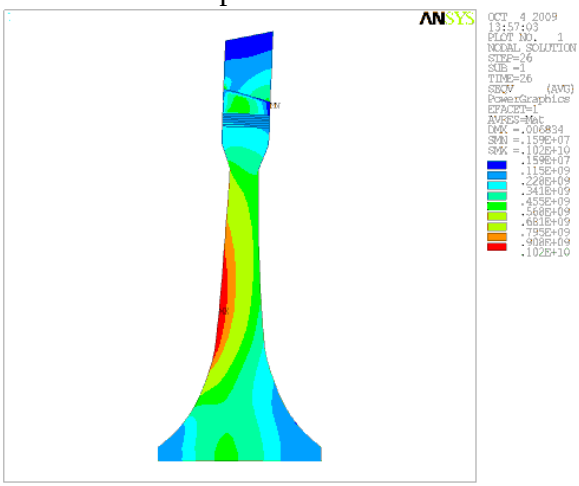

of the principal stresses.

Figure 5.8 : Von Mises stress plot at take-off and top-of-climb for HPT.

5.7 Analysis Output

The transient thermal and thermo-mechanical analysis, provides two basic values for the mission points, such as the blade metal temperature and Von Mises or equivalent stress. This data is retrieved for the mission points, at the nodes comprising the finite element model, and the geometric location for producing the lifing plots with the geometry of the model. The data is utilized for the estimation of the low cycle fatigue using method of universal slopes, creep using Larson Miller approach and oxidation through Arrhenius equation.

6 LIFE ESTIMATION

The gas turbine components are designed to deliver the expected performance level with deformations and stresses kept within the acceptable limits or design limits. The life of a component is defined based on the fundamental modes of failure leading to non-conformance in terms of functionality or intended purpose. The factors pertinent in gas turbines having great influence are the stresses and temperature limiting the component life. The aircraft engines as observed in the previous chapter, undergo thrust excursions especially ramping up from taxi to maximum take-off thrust. Every flight segment imposes a dynamic loading on to the critical components leading to damage accumulation. For prediction of the life of the components, based on the modes of failure have constituent theories or methods have been proven to be reliable over the years of application through testing and validation. This chapter is to capture the failure modes commonly observed in gas turbines and the critical ones limiting the life of the component. From fairly large number of failure modes the critical modes are captured using the widely used approaches. As the load pattern is of spectrum loading where the means of representing or estimating the life is through methods of cumulative damage has been explored in the context of the current research. The process involved in converting the life into damage fractions is represented in the severity calculation as explained in the concluding part.

6.1 Failure Modes

Mechanical failure of the structure is the change in size, shape, material properties of a structure or machine leading to unsatisfactory performance in its intended function. The failure happens through four fundamental behaviours [10] such as

- Elastic
- Plastic

- Rupture
- Material change

The factors that induce mechanical failure can be broadly looked upon as due to

- Force
- Temperature
- Time
- Reactive environment

In gas turbines, the inducing factors are the shaft rotation in creating a centrifugal force, the bending force due to pressure difference across the blades are the force inducers having fluctuating amplitude, during the mission. Due to maximum cycle temperature, the components are exposed to the threshold of material temperature limits, and have demanded growth in material, cooling and coating technology. The super alloys known for withstanding high temperature through advancements have transformed polycrystal blades into bidirectionally solidified and with the current technology to single crystal, providing greater temperature stability and improved strength. The components are optimized to minimize mass for reduction in total weight, thereby stresses are pushed to their limits, so as to achieve lower fuel conumption without compromising on the reliability. In the literatures on aircraft engine failures, the most commonly observed phenomenons ([25], [44], [47], [48], [49]) are low cycle fatigue, high cycle fatigue, creep and oxidation.

Fatigue

Fatigue is considered as sudden and catastrophic seperation of the engine part into two or more pieces due to the fluctuating loads or deformation over a period of time, as per the classical definition. There are two phases in fatigue failure, such as crack initiation and crack propagation, and it is truly a surface phenomenon. The failure that happens after sufficiently large number of cycles such as 100000 cycles are considered to be high cycle fatigue. The

mechanism [17] of damage is in spending 90 % of the life in the crack initiation, and 10 % in crack propagation to failure, making them more catastropic in nature due to abrupt failure. Unlike high cycle fatigue, the low cycle fatigue involves, 10 % life consumed in crack initiation and 90 % in crack propagation, giving clear indication of the progress to failure, in terms of the crack detection. The low cycle fatigue failure is characterized by failure in less than 100000 cycles. Hence the critical components prone to failure by low cycle fatigue are specified as life limited parts, represented on the cycles basis. The current research deals with low cycle fatigue, as it is one of critical phenomenon, limiting life of the component, as compared to high cycle fatigue.

Creep

Due to high operational temperatures, closer to the material limits, the other common mode of failure is due to the creep. Anelastic deformation leading to body type of failure involving bulk deformation, as compared to fatigue which is a surface phenomenon. The primary inducers are the temperatures above homologous temperature, nearly 40 % of the melting point of the material, subjected to the stresses. The plastic deformation accrues over a period of time, leading to accumulated dimensional changes causing lack of ability to perform its intended function. The creep behaviour [10] is through three major stages.

- Transient or Primary creep – rate of creep strain decreases
- Steady state or Secondary creep – rate of strain is virtually constant
- Tertiary creep – creep strain rate increases until the terminal rupture or creep rupture.

Oxidation

The hot gas path components are exposed to distress due to depletion of the oxide layer that takes considerable period of time, causing material loss at a slower mode. Suitable alloying and oxidation coatings, reduce catastropic oxidation where the oxidation deviates from linear kinetics into a rapid,

exothermic reaction at high temperatures. The reaction rate is a critical factor defining the oxidation characteristics and in most of the metals follow a parabolic oxidation rate [21].

$$W_{oxid}^2 = k_p t + C_{oxid\_c} \quad (6.1)$$

Where W_{oxid} is the weight gain per unit area, t is time, k_p the parabolic rate constant, and C_{oxid_c} is a constant.

6.2 Life Estimation Methods

Theoretical life prediction, capturing the different modes of failure have been extensively used in the design phase of the components, supplemented by validation with test results. The objective of the research has been to capture relative effects of operational scenario and technology factors on the life of the component, hence a numerical life estimation has been adopted. The fundamental modes of interest are the low cycle fatigue, creep and oxidation, and the associated theoretical estimation techniques have been dealt in detail. Several theories have been proposed for predicting the life of the component, and choice of the theory adopted for the current research is based on the wide application of the methods and availability of the material data.

Low Cycle Fatigue

The stress fluctuations are inherent in aircraft engines and the components have been identified to fail due to such variations. The stress variations have significant impact on the components are realized through manufacturing techniques that have flaws or defects or as surface finish. These discontinuities, when subjected to stress fluctuations, grow in proportion to the pattern and sequence of load on the component. Fundamentally the theoretical approaches can be classified as stress method, strain method and fracture method. The stress method involves prediction for cyclic loading with the strain cycles limited to elastic range, and are considered as a methodology to predict the high cycle fatigue. In contrast to the stress method, the strain method

invovles, relatively high cyclic loads and significant plastic strains which gives low number of cycles, and are considered as a low cycle fatigue or strain controlled fatigue. The fracture mechanics approach deals with crack propagation due to localized plastic deformation which starts with an appreciable crack length (1mm) and estimates the life to reach a crictical crack length. The fracture mechanics is further classified as linear elastic fracture mechnics (LEFM) and Elasto-Plastic Fracture Mechanics (EPFM) based on the state of stress considered for the failure.

There are a number of theories proposed for the low cycle fatigue calculation, but only a few are widely used, as the different theories depend on fatigue failure data which often for superalloys used in aircraft engine hot section are confidential. Hence most of the research that are aimed at generic studies are based on approaches, like method of universal slope. This method is quite prominent as it has been revealed that with the tensile test data, the fatigue life can be estimated without requiring detailed fatigue data, such as the fatigue exponents and fatigue coefficients.

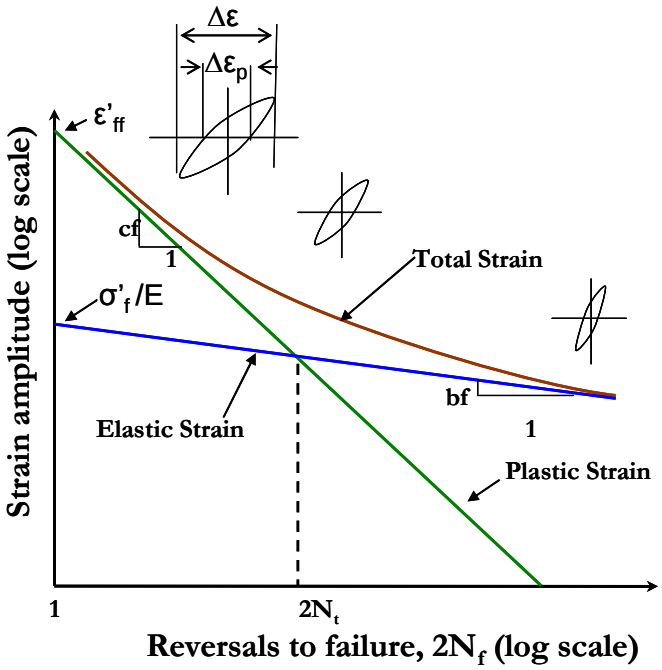

Figure 6.1 : Fatigue life variation with strain amplitude.

The fundamental strain life equation [74] is given as

$$\frac{\Delta\varepsilon}{2} = \varepsilon_a = \frac{\Delta\varepsilon_e}{2} + \frac{\Delta\varepsilon_p}{2} = \frac{\sigma_f'}{E}(2N_f)^{bf} + \varepsilon_{ff}'(2N_f)^{cf} \quad (6.2)$$

$\Delta\varepsilon/2$ = strain amplitutde total = ε_a

$\Delta\varepsilon_e/2$ = strain amplitutde elastic = $\Delta\sigma/2E=\sigma_a/E$

$\Delta\varepsilon_p/2$ = strain amplitude plastic =$\Delta\varepsilon/2 - \Delta\varepsilon_e/2$

$\Delta\sigma/2$ = stress amplitude = σ_a

ε_{ff}' fatigue ductility coefficient

cf fatigue ductility exponent

σ_f' fatigue strength coefficient

bf fatigue strength exponent

E modulus of elasticity [Pa]

The Figure 6.1 shows that as the total strain when it remains elastic, sufficiently large number of cycles to failure is evident, normally above 10^5 cycles. When the strain cycling range increases, the failure happens at low number of cycles predominantly less than 10^5 cycles. The intercept with the y-axis, specifies the fatigue coefficients of the strain life equation, and the slopes corresponding to the elastic and plastic strain, define the fatigue exponents bf and cf respectively.

The method of universal slope [48] is an adaptation of the basic strain life equation, fitted for fairly large number of specimens of different materials and through regression analysis providing the fatigue exponents and fatigue coefficients considered constants, needs only the tensile test data for the strain life estimation. Hence unlike the conventional approaches, it does not require the fatigue data for the material under consideration.

$$\Delta\varepsilon = 3.5\frac{\sigma_u}{E}(N_f)^{-0.12} + \varepsilon_{ff}^{\,0.6}(N_f)^{-0.6} \quad (6.3)$$

σ_u ultimate tensile strength [Pa].

ε_{ff} true fracture ductility (universal tensile test data).

ε_{ff} ln(1/(1-RA))

RA area reduction of stressed component.

The equation 6.3 requires a newton raphson iteration to yield the life of the component, and will reduce to simplified equations when the strain is totally elastic to the first part, and when it is largely plastic to the second part. Hence the universal testile test data that is available in the public domain for some of the superalloys, can be capitalized using the method of universal slope.

Creep

The creep, a bulk deformation phenomenon leading to failure, at sufficiently high temperatures, more than the homologous temperature of the material. The common approach in the industry to estimate the creep life is by the Larson Miller approach [11] which is derived from the Arrhenius equation.

$$P = \frac{T}{1000}(\log_{10} t_{crp} + C_{crp}) \tag{6.4}$$

P Larson Miller parameter
T temperature [K]
t_{crp} time to creep failure [hrs]
C_{crp} constant dependent on the material

The Larson Miller approach has a unique advantage in terms of the simplicity of the approach. There are other approaches such as Theta method, Orr-Sherby-Dorn, Goldhoff-Sherby, White-Le May, Manson-Succop and Manson–Haferd for the creep life estimation. The approaches capitalize on the isostress lines, based on the assumptions has led to different methods of estimating the creep life. By far the Larson Miller approach is the most successful of the *rate process theory* where the stress, temperature and time, can be effectively represented as a characteristics based on the isostress behaviour.

Oxidataion

The gas path that experiences large mass flow of air and combustion products, exposing the material to high temperature causing depletion of the oxide layer on a continuous scale. There had been a number of pioneering work on the oxidation life estimation, and the approach adopted by Swaminathan et al. [79],

in correlating the blade metal temperature to the depth of the oxidation, built on the Arrhenius equation, and on the assumption that the oxidation layer builds in a parabolic manner as observed in the case of metals to a larger extent.

$$\left[\log C_{oxid} - \log(d^2/t_{oxid})\right] * \left[T_{oxid} + 460\right] = Q/R \tag{6.5}$$

$\log C_{oxid}$	constant
d	depth of oxidation front [in]
t_{oxid}	oxidation life [hrs]
T_{oxid}	temperature [F]
Q	activation energy [ft-lb/lb]
R	gas constant [ft/R]

The aircraft engine components are preferably out of alloys and each element has an affinity towards oxidation, and have complexity when two or more metals part of the composition, leading to oxide layer formation. In the initial phases, the oxide layer growth is fairly linear because the mechanism is through the transport of the reactants, and once the layer becomes sufficiently thicker, the chemical kinetics shifts towards the diffusion, following a parabolic pattern. Hence the above equation adequately used to capture the oxidation life of the coatings that extend the service life of the critical components. In the case of turbine blade, the thermal barrier coating not only as a layer to lower blade metal temperature, as well a protective layer improving the oxidation life. The thermal barrier coating is layed over a bond coat on the parent material whereas the useful life extended by the thermal barrier coating is much higher as compared to its substrates hence only the coating thickness has been considered for the estimation.

6.3 Damage Calculation

The aircraft mission is one of highly variable load pattern and are broadly looked upon as a spectrum loading. The conventional life estimation process are for a unique amplitude of the stress and temperature to include the effects of the high variation in the load pattern, the damage theories are effective. The load pattern is split into a number of simplified situations where life estimation

equations are employed to estimate life and damage fraction on a piecewise fashion, and are cummulatively added to estimate the resultant life.

The Palmgren-Miner hypothesis or linear damage theory is the first among the damage theories, predicts failure when the damage fractions appraoch a value of unity. The damage fraction [10] corresponding to certain stress level is proportional to the ratio of the cycles of operation to that of cycles to failure.

$$D_{c1} + D_{c1} + ... + D_{ci-1} + D_{ci} \geq 1 \quad (6.6)$$

$$D_{ci} = \frac{n_i}{N_i} \quad (6.7)$$

$$\frac{n_1}{N_1} + \frac{n_2}{N_2} + ... + \frac{n_{i-1}}{N_{i-1}} + \frac{n_i}{N_i} \geq 1 \quad (6.8)$$

$$\sum_{j=1}^{i} \frac{n_j}{N_j} \geq 1 \quad (6.9)$$

n_i number of load cycles
N_i life [cycles]
D_c damage fraction

The other damage theories to predict life of the component under spectrum loading are [10] :

- Henry cumulative damage theory
- Gatts cumulative damage theory
- Corten-Dolan cumulative damage theory
- Marin cumulative damage theory
- Manson double linear damage rule
- Marco-Starkey cumulative Damage Theory

As compared to the above theories, the most common theory is the linear damage rule which is a simplistic approach with fairly the same level of reliability of life prediction, as compared to other theories. The linear damage

theory has limitations, in terms of the load sequence, where the effects are ignored, the metals subjected to higher load followed by a low amplitude have higher life as compared to a load pattern of lower amplitude followed by a higher load. The linear damage theory considers each and every point, as independent events which in reality depends on the load sequence, due to the zone plastified in setting up compressive stress at the crack tip will demand more tensile load to overcome the compressive stress at the crack tip.

The equation 6.9 holds good for the phenomenon of the low cycle fatigue which is dependent on the cycles to failure. The failure due to creep and oxidation are hours limited, hence the damage equation is specified, in terms of the time for the event to the component life in hours.

$$\frac{t_{e1}}{t_{s1}} + \frac{t_{e2}}{t_{s2}} + ... + \frac{t_{ei-1}}{t_{si-1}} + \frac{t_{ei}}{t_{si}} \geq 1 \qquad (6.10)$$

$$D_{s1} + D_{s2} + ... + D_{si-1} + D_{si} \geq 1 \qquad (6.11)$$

t_e time duration of the event [hrs]
t_s life estimated due to creep or oxidation [hrs]
D_s damage fraction

The conversion of the life into the damage, provides the possibility of combining the damage due oxidation and creep as a steady damage mechanism, while the low cycle fatigue causes cyclic damage mechanism.

To estimate life, the stresses obtained through the thermo-mechanical analysis are elastic stresses that are transformed to elasto-plastic through the application of the Neuber's rule [15] to account for situations of plastic strain during the mission.

6.4 Severity

Severity as defined in the reference [72] represented as the ratio of the damage of the new mission with respect to the reference mission. The severity is factored into maintenance cost estimation for the engine, as it is attributed to degree of life consumption, based on the chosen thrust level of the operation, commonly referred to as the derate. As aircraft engines with the functionality of developing thrust which causes the change in the temperature and shaft speed, defining the degree of damage are represented as the derate-severity curves by the MRO.

The damage is broadly incurred by two modes, steady state loading and cyclic loading, influencing the failure characteristics of the engine components.

Mathematically can be written as

$$(\lambda_t)_r = (\lambda_c)_r + (\lambda_s)_r \quad (6.12)$$

$$(\lambda_t)_n = (\lambda_c)_n + (\lambda_s)_n \quad (6.13)$$

λ_t Total damage fraction

λ_c Cyclic damage fraction

λ_s Steady state damage fraction

$(\lambda_t)_r$ Total damage for the reference mission

$(\lambda_t)_n$ Total damage for the new mission

Normalizing the above equation by dividing both the sides by $(\lambda_t)_r$

$$(S_t)_r = (S_c)_r + (S_s)_r = 1 \quad (6.14)$$

$$(S_t)_n = (S_c)_n + (S_s)_n \quad (6.15)$$

S = Severity

The severity has two parts towards total severity. The cyclic part capturing the

low cycle fatigue and steady part in a collective manner the modes creep and oxidation. The damage pattern due to cyclic and steady part changes with the type of the engine design and application. The aircraft can be categorized as narrow body and wide body serving the airline industry for two different kinds of operation especially the short haul and long haul flights. The short haul flights have frequent take-off and landing are limited by cyclic damage, while the long haul flights due to longer mission are subjected more of steady damage. Hence the severity estimation is suitable for the lower thrust and large thrust engines, and effective parameter to capture the damage on a relative basis, meeting the industry practice.

The other significance of using the severity is in understanding the effect of operational parameters due to changes in mission impacting the critical life limiting component. The combination of the severity together with the cummulative damage theories, explores the life consumption of the components on the basis of the individual events, and in totality strengthening the methodology.

7 Shop Visit Prediction

Aircraft engine as part of the design matrix has many objectives, in the process of realizing the product. The engine maintenance has been occupying a larger interest, among the airliners, as the operational cost plays a decision making role, in the choice of the aircraft and its engine. The engine manufacturers with the field data and through the design practice have evolved the maintenance strategies, suitable to the aircraft. However from the view of the aircraft manufacturers, when the choice of the engine has to be made are based on selected pieces of information from the engine manufacturers, as the art of designing to meet the expected shop visit interval is proprietary. This chapter is about describing the engine degradation phenomenon leading to shop visits, and the characteristic aging curves that are used for maintenance cost estimation.

7.1 Engine Maintenance

The engine maintenance [102] is a means of restoring the performance and design to the expected levels of functionality and reliability. The loss in the performance and design intent, can be due to expected or unexpected events. This defines the maintenance, as the scheduled maintenance and unscheduled maintenance. The scheduled maintenance is controlled by the life limits of the critical components from the design point of view, and the exhaust gas temperature margin from the view of performance. An aircraft engine is essentially, a perfect balance of design and performance, and have to be competitive meeting stringent standards and regulations.

The situation of un-scheduled maintenance are due to events of abnormality from the usual mode. Foreign Object Damage (FOD) happens, in the event of bird ingestion, but the level of damage incurred is less serious and can be put back into service through suitable replacement of the blades. The other forms of FOD are ice and runway debris passing through the engine during the

ground maneuvers at the airport. The hardware deterioration is observed during the borescope inspection and chip collection which in certain severe operating conditions, reveal abnormal rates of deterioration. Such a situation is commonly observed, due to sand ingestion leading to erosion of blades, reducing the useful life of the engine. The high level of oil consumption is yet another form of failure that will lead to a flight shutdown, and removal of the engine, due to possible reasons of leakage in bearings, oil lines and coking of the bearings. On rare occassions, there might be an engine removal, due to the identification of batch of defective parts from a manufacturing process.

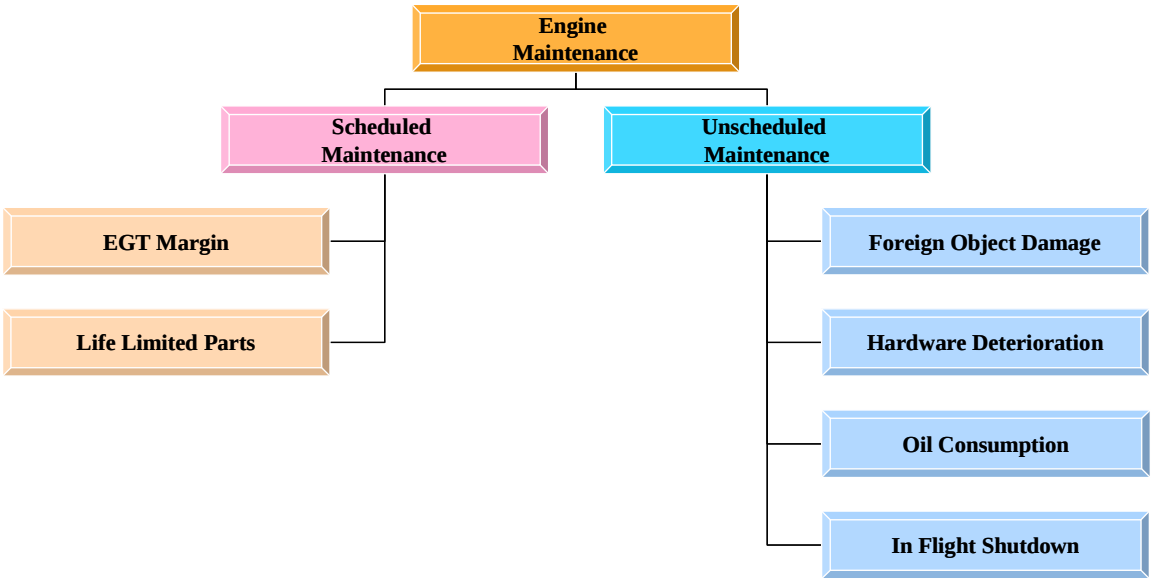

Figure 7.1 : Classification of engine maintenance.

The current research is in predicting the shop visit due to scheduled maintenance. The scheduled maintenance, as observed either due to life limits or EGT margin are in the retrospect of estimation. However the life limits of the components are to be maintained, designed with sufficient factor of safety to yield the specified number of cycles or hours, and have to be retained in a legal sense. Hence the focus has been to determine the exhaust gas temperature margin deterioration pattern as been observed in the industry, as the key indicator to predict the shop visit interval for the engines. The exhaust gas temperature is one of the signatures of the engine health, and the limits are

specified as redline temperature by the engine manufacturers to identify the proximity for shop visit. The change in the EGT with the flying hours is closely related to the performance of the individual components. With the flying hours the EGT increases due to component degradation.

7.2 Engine Degradation

Degradation is an unavoidable parsitic loss parameter of the engine with its usage over a period of time. The degradation happens, as the engine is an assembly of moving and stationary parts, during its mission is exposed to wear and tear. There is an initial wearing of the components, until suitable clearances are developed, and then proceeds with gradual wearing of the components.

The causes of degradation [39] are multifold, from either a FOD and to the extent of turbine nozzle bowing. In a broader sense, the degradation can be considered due to different sources as furnished in Figure 7.2.

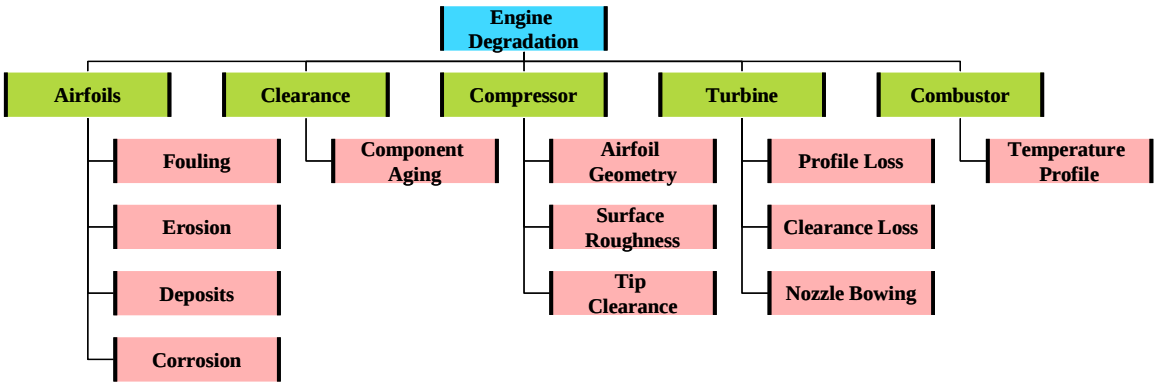

Figure 7.2 : Causes for engine degradation.

The degradation has a larger toll with respect to the rotating components, where the aerofoil and clearance, dictates the loss in the performance.

The aerofoil, a component contributing towards the aerodynamic behaviour, achieving the required mass flow rate and efficiency has four major sources of degradation, such as fouling, erosion, deposits and corrosion. Fouling is the

increase in the surface roughness, due to the build of dirt, causes aerodynamic loss by reducing the mass flow and efficiency. The dirt accumulation is larger in the initial phase, and due to the centrifugal force and mass flow, does not allow the growth to increase beyond a certain level, hence a slower rate of dirt accumulation is observed. To minimize the degradation, the engine is subjected to washing. Erosion is the process of removal of material, from the surface of the component, due to the abrasive nature of the impinging objects that increases the profile loss. The deposits, change the geometric shape of the gas flow path at the compressor and turbine. Corrosion is the chemical decomposition affecting the surface quality. The changes, in the geometry, surface roughness and erosion, can lead to issues of improper transitioning of the flows, from laminar to turbulent. This causes, heat transfer imbalance, increased boundary layer, and flow seperation, affecting the aerodynamics of the aerofoil, closely related to the mass flow changes and component efficiencies.

The clearance is the gap between the rotating and stationary components, where the tip clearance is pivotal to achieve the desired level of component efficiency. The clearances are maintained, by design and through control mechanisms, driving the cooling flows for the casing. Due to aging of the components, wearing of the tip the clearance pattern starts deviating from the actual design, and leading to tip leakage losses.

The fan, booster and high pressure compressor, due to field operation are prone to changes, as pointed out in aerofoil and clearance degradation. The major drivers, affecting the flow capacity and the efficiency are the tip clearance, surface roughness and aerofoil profile

The turbines, such as the high pressure turbine and low pressure turbine, over the time in operation, develop the degradation characteristics of clearance loss, profile loss and nozzle bowing affecting the performance, and increasing the EGT.

The combustor as it is free from moving components have less impact due to degradation, and the observed phenomenon of the shift in the temperature profile, due to the blockage of the cooling and mixing holes, leading to loss in the turbine effficiency.

Hence the degradation patterns, leading to more losses and penalty are observed as, changes in efficiency and flow capacity are considered as health parameters of the engine. From the performance end, the corresponding change in efficiency and flow capacity leads to increase in the EGT, as the aircraft engines are intended to maintain the same level of thrust, irrespective of the degradation, hence normally compensated by increasing the fuel flow. The increasing fuel consumption and the corresponding increase in the EGT are monitored as against the EGT limits specified by the engine manufacturers. The proximity to the EGT limits is an indication for the expected shop visit according to the maintenance norms.

7.3 Shop Visit Prediction Method

The scope of the research is in developing a method to predict the scheduled shop visit. The information and inputs for predicting the shop visit are to be based on the level of details available in open literature. As enunciated, the exhaust gas temperature tracking is used as a means of predicting the shop visit. The balance between the life limits and the EGT margin is made by the engine manufacturers. The life limits are in the realm of the design of the component, whereas the EGT is the performance parameter. Often the aircraft engines have scheduled shop visits to restore the EGT margin, because the performance level degrades much faster than the life of the component built to endure. As per the design practice, the turbine blade remains the limiting life number defining the shop visit interval, while the disc or shaft system are designed to have nearly twice the blade life, suitable for replacement on alternative shop visits.

Figure 7.3 : Shop visit defining parameters.

For the exhaust gas temperature tracking, as it involves the performance calculation for the engine, the Cranfield in-house software Turbomatch has been employed to carry out the performance calculation. A Matlab code has been developed to run iterations with different level of component degradation characteristics. The structure of the shop visit prediction code is depicted in the Figure 7.4. The degradation characteristics as in reference [42] which was employed on a typical turbofan has been utilized for the shop visit prediction. The component degradation has been specified for different levels of degradation through scaling, based on the exposure to the environmental conditions that impact them. The degradation characteristics for the individual components have been adopted and simulation runs are performed, by tracking the exhaust gas temperature, according to engine, where the measurement locations are varied, and are based on the choice of the engine manufacturers.

The EGT tracking is implemented with respect to the component degradation varying with engine cycles. The upper bound of the cycles is the limiting value of the critical life limited part of the aircraft engine.

The intersection of the EGT curve with the redline temperature indicates the expected first shop visit. There are two limits for redline temperature according to the mode of operation, as transient redline temperature during take-off and continuous redline temperature during climb and cruise.

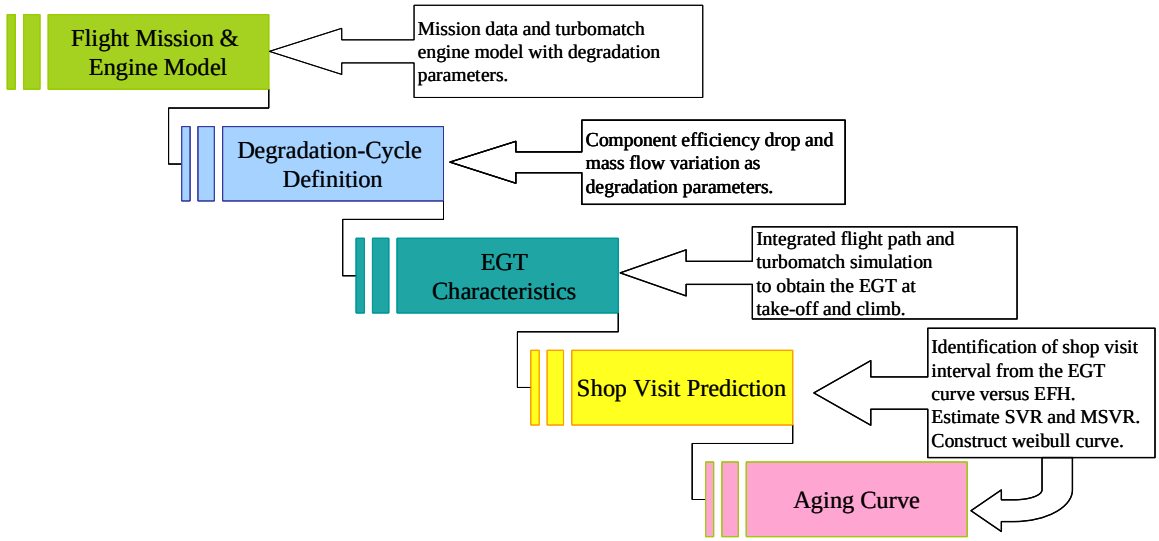

Figure 7.4 : Shop visit prediction methodology layout.

Hence the EGT is tracked at the take-off with respect to the transient redline temperature, and the average temperature during climb and cruise are compared with continuous redline temperature. The take-off being the significant source of maximum thrust, moves closer to the maximum redline temperature. From the EGT versus the engine flight hours, shows the progression of the temperature towards the redline temperature. Infact a similar characteristics for every shop visit, as the components are replaced restoring the margin. The only deviation is an absolute recovery is impossible, as during shop visit only the life limited parts are replaced, whereas the casing remains intact for the entire service life of the aircraft, and depends on the strategy of the engine manufacturers. As the new components start with a different clearance pattern offsets the EGT margin according to the components being replaced. Hence the engine undergoes, a similar cycle of degradation, but a different EGT margin, reducing the shop visit interval as compared to the first shop visit. The degradation cycle is repeated with different EGT margins to estimate the successive shop visit interval, inorder to estimate the shop visit rate.

The effect of engine wash providing EGT margin benefits has been considered, by offsetting the EGT, based on the engine wash frequency, extending the shop visit interval.

The shop visit rate is mathematically represented as

*Shop Visit Rate =(number of shop visits/Total engine flight hours)*1000hrs* (7.1)

The shop visit rate is the tendency for the shop visit for every 1000 engine flight hours, as adopted by the MRO industry, depicting the maintenance. An airliner has a wide range of fleets with different destinations and trip lengths, and are normally represented on an averaged basis for the entire fleet. The individual aircraft engines will have different degradation pattern, as it is highly a function of the tolerancing of the components attributed to manufacturing, and environmental conditions.

In this research the shop visit prediction is based on EGT characteristics, driven by degradation cycle definition for typical turbofan, adapted to the type of the engine, and the effect of the operational parameters and engine wash has been studied.

7.4 Aging Curves

The MRO use the terminology of the mature shop visit rate which transcends to the aging curve. The mature shop visit rate is the product of the engine severity factor and shop visit rate. The understanding behind the use of severity factor is the basic degradation cycles are represented with respect to the life limits in cycles, and these life limits vary with the derate of the engine, hence the use of severity together with the shop visit rate, precisely addressed through the terminology of the mature shop visit rate.

*Mature Shop Visit Rate = Severity * Shop Visit Rate* (7.2)

Inorder to estimate the maintenance cost of the engine during its service, the aging curves are derived, and are distinct for every MSVR. The aging curves are represented by Weibull distribution with the slope of 1.5, as chosen by the MRO to identify the age factor of the engine with the engine flight hours. The

aircraft engine reaches the value of unity, at the end of accumulated service life with the specified number of shop visits as designed. The variation of age factor having Weibull slope of 1.5, captures the succesive shop visit interval, as observed at the maintenance shop floor.

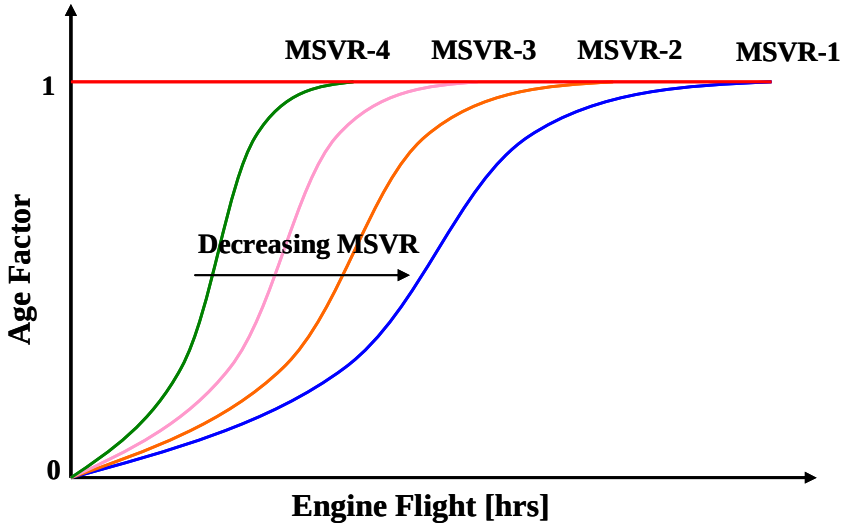

Figure 7.5 : Aging curve characteristics.

8 CASE STUDIES ON SEVERITY

The methodology involving aircraft performance, gas turbine performance, gas turbine design and lifing for severity estimation have been applied for engines, used in short haul and long haul flights. The short haul flights (narrow body aircraft) have distinct pattern of operation as compared to long haul flights (wide body aircraft). The take-off derate versus severity characteristics has been demonstrated for the engines of the different thrust class to compare with the trends of MRO curves, used for maintenance cost estimation. From the operational front, the take-off, climb and cruise derate studies have been conducted to identify the sensitivity on severity. The other operational parameters such as the OAT, airport altitude, cruise altitude and cruise Mach number have been considered for the investigation. The technological factors, such as cooling effectiveness, thermal barrier coating thickness and conductivity, pattern factor and profile, impacting the severity have been demonstrated. The operational and technological factors of significance have been addressed through characteristics generated from parametric studies in the perspective of severity, impacting the maintenance cost of an aircraft engine.

8.1 Engine Models

The engine models subjected to the case studies have been corresponding to lower thrust and large thrust class. For a lower thrust class, an engine with less than 34000 lb take-off thrust per engine has been chosen used for short haul flights. The large thrust (> 34000 lb take-off thrust per engine) engines have competitive designs hence three different engines have been considered for the case study.

For the short haul aircraft powered by E56 engine that is a two shaft configuration and the specification resembles CFM 56-7. Under the large thrust

Aircraft Engines for Severity Study					
		Lower Thrust	Large Thrust		
Parameter	**Units**	**E56**	**E84**	**E95**	**E115**
Spool		2	2	3	2
Fan Diameter	m	1.5494	2.377	2.794	3.256
Mass Flow	kg/s	355	1157	1208	1641
By- pass Ratio		5.1	6.41	5.8	8.9
Pressure Ratio		32.8	34.2	41.6	42
T-O Thrust	N	121430	385928	422600	512880
Shaft Speed	rpm	15183	10850	10611	11292
Overspeed	%	105	100	100	121
Cimb Thrust	N	26520	71667	79605	99565
Cruise Thrust	N	24376	62275	60500	98488

Table 8.1 : Aircraft engine specification used for building the engine models.

category the engine E84 is similar to PW 4084, E95 similar to Trent 895 and E115 similar to GE 90-115B. E84 and E115 has a two shaft configuration while E95 has a three shaft configuration.

The reference mission for short haul flights is 1.4 hrs mission at OAT of 18 °C and take-off derate of 10 %. For long haul flights the reference mission is 4 hrs trip length, 18 °C OAT and 10 % take-off derate. The reference mission for the individual thrust class has been defined by MRO that serves as a reference point for the severity estimation.

The technology parameters or factors are maintained at an appropriate settings (Table 8.2) for the operational studies. The pattern factor location is identified through the five divisions of the blade leading and trailing edge, and numbered in sequence with increasing radius and the value 3 indicates the third segment having maximum temperature.

Technology Parameter Settings				
Cooling effectiveness	**TBC Thickness**	**TBC Thermal Conductivity**	**Pattern Factor**	**PF Location**
0.7	200 microns	2	0.1	3

Table 8.2 : Technology parameter settings.

8.2 Short Haul Flight – Reference Mission

The narrow body aircraft that are effective over shorter trip length has been worked out using the severity estimation methodology. The aircraft

performance calculation using the simplified flight path analysis code, depicting the thrust, altitude and Mach number variation with respect to time for a commerical aircraft mission.

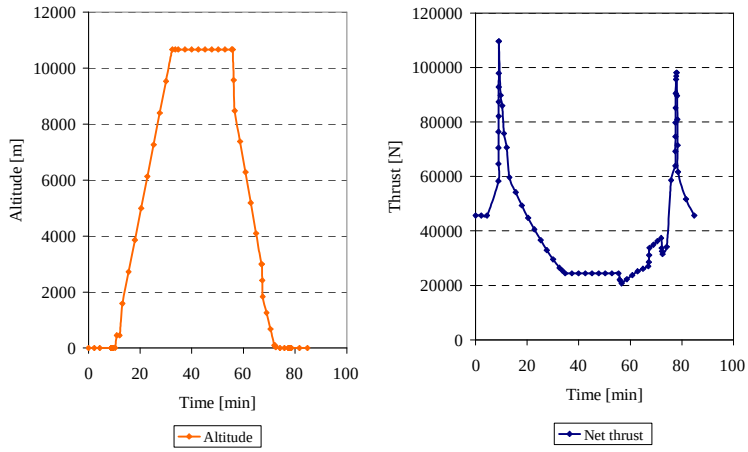

Figure 8.1 : E56 engine thrust and altitude variation for 1.4 hrs trip mission.

The Turbomatch model (Appendix A) representing the engine specification E56 is built for the gas turbine performance calculation, satisfying the thrust, altitude and Mach number variation with respect to time. The mass flow rate, temperature, pressure and non-dimensional shaft speed has been estimated for the gas turbine components. The characteristics for the HPT is as in Figure 8.2.

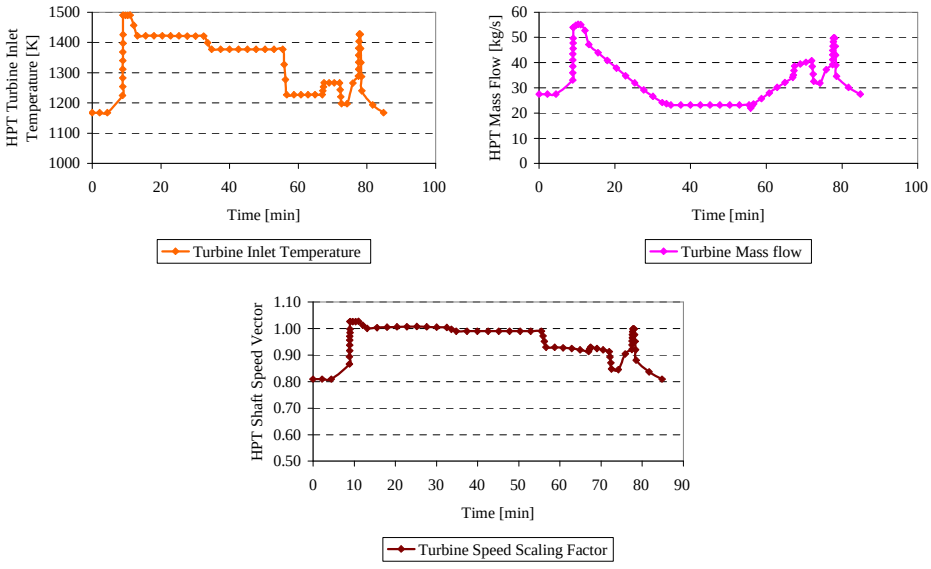

Figure 8.2 : E56 engine HPT turbine entry temperature, mass flow rate and shaft speed vector variation for 1.4 hrs trip mission.

For the HPT blade, the sizing code is used to estimate the blade dimensions (Appendix B). Disc dimensions are obtained from an engine cross-section of the equivalent engine. The data used for sizing the turbine blade corresponds to the take-off condition.

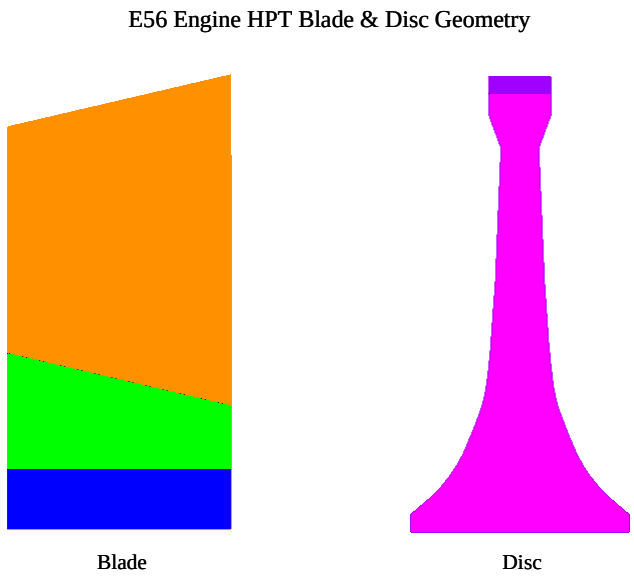

Figure 8.3 : E56 engine HPT blade and disc geometry.

The heat transfer calculation module, estimates the heat transfer coefficients and the bulk temperatures that will form the thermal load, at the boundary of the finite element model.

The finite element model built through the APDL code has been illustrated in Figure 8.5. The blade, though a 2-D plane model, takes into account the thickness variation of the aerofoil, root and shank regions. The number of elements used in the model are 1700 having 1827 nodes. The elements in the finite element model are optimized using the mesh convergence study based on life estimates of the component.

E56 Engine HPT Blade & Disc Thermal Correlation and Flow Tag Mapping

Location	Thermal correlation	Flow Tag
B_1	1	1
B_2	1	1
B_3	1	1
B_4	1	1
B_5	1	1
B_6	3	1
B_7	2	2
B_8	2	2
B_9	2	2
B_10	2	2
B_11	2	2
B_12	4	4
B_13	4	4
B_14	4	4
B_15	4	5
B_16	4	5
D_1	5	3
D_2	5	3
D_3	4	4
D_4	4	4
D_5	4	4
D_6	5	3
D_7	5	3
D_8	5	3
D_9	4	5
D_10	4	5
D_11	4	5

Thermal Correlation	
Circular Cylinder	1
Flat Plate	2
Gap	3
Cavity Radial Outflow	4
Cavity Axial Outflow	5

Flow Tag	
Turbine Inlet	1
Turbine Outlet	2
Disk Bore Cooling	3
Disk Front Cooling	4
Disk Aft Cooling	5

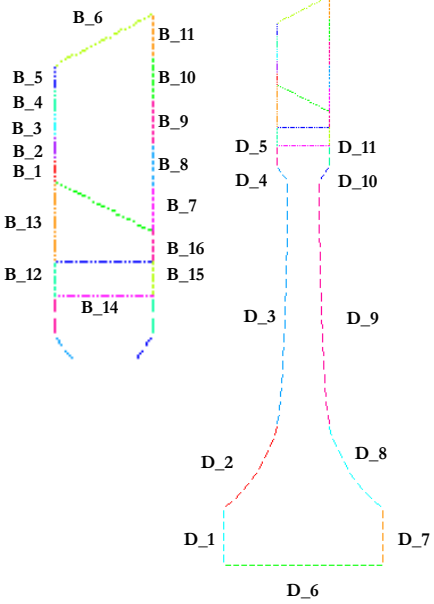

Figure 8.4 : E56 engine HPT heat transfer correlation and flow mapping.

E56 Engine HPT Blade & Disc Finite Element Model

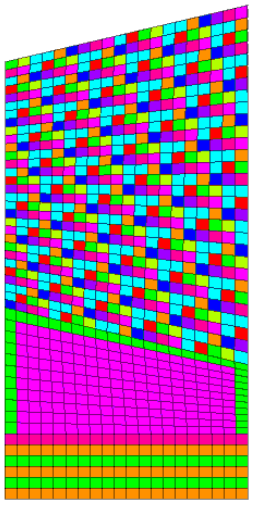

Blade – 2D View

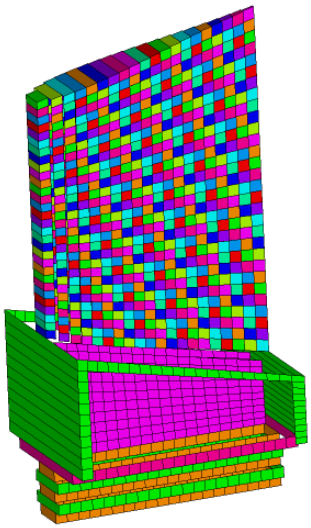

Blade – 3D View

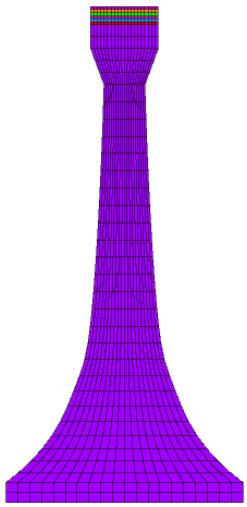

Disc

Figure 8.5 : E56 Engine finite element model.

The material properties used for the analysis are as provided in Table 8.3. The blade is assigned Rene 41 and disc with Inconel 718.

Rene41 Material Properties											
Temperature [K]	300	366	589	811	922	1033	1144				
Youngs Modulus [Pa]	2.18E+11	2.14E+11	2.02E+11	1.88E+11	1.79E+11	1.71E+11	1.6E+11				
Temperature [K]	300	366	589	811	922	1033	1144				
Poissons Ratio	0.31	0.31	0.31	0.31	0.31	0.31	0.31				
Temperature [K]	300	366	589	811	922	1033	1144				
Density [kg/m^3]	8249	8249	8249	8249	8249	8249	8249				
Temperature [K]	366	589	811	922	1033	1144	1255	1366			
Coefficient of Thermal Expansion [1/K]	1.21E-05	1.26E-05	1.35E-05	1.40E-05	1.48E-05	1.58E-05	1.67E-05	1.78E-05			
Temperature [K]	422	589	811	922	1033	1144					
Thermal Conductivity [W/m-K]	11.5	14.7	18.9	21.1	23.2	25.2					
Temperature [K]	294	366	478	588	698	813	923	1033	1143	1253	
Specific Heat [kJ/kg-K]	400	400	395	420	440	420	460	480	500	525	

Inconel 718 Material Properties											
Temperature [K]	294	366	477	589	700	811	922	1033	1144	1227	
Youngs Modulus [Pa]	2.08E+11	2.05E+11	2.02E+11	1.94E+11	1.86E+11	1.79E+11	1.72E+11	1.62E+11	1.27E+11	7.80E+10	
Temperature [K]	294	366	477	589	700	811	922	1033	1144	1227	
Poissons Ratio	0.284	0.284	0.284	0.284	0.284	0.284	0.284	0.284	0.284	0.284	
Temperature [K]	294	366	477	589	700	811	922	1033	1144	1227	
Density [kg/m^3]	8220	8220	8220	8220	8220	8220	8220	8220	8220	8220	
Temperature [K]	294	366	477	589	700	811	922	1033			
Coefficient of Thermal Expansion [1/K]	1.28E-05	1.28E-05	1.35E-05	1.39E-05	1.42E-05	1.44E-05	1.51E-05	1.60E-05			
Temperature [K]	478	588	698	813	923	1033	1143	1253	1363		
Thermal Conductivity [W/m-K]	11.8	13.7	15.6	17.7	19.7	21.5	23.3	25.3	27.2		
Temperature [K]	294	366	478	588	698	813	923	1033	1143	1253	1363
Specific Heat [kJ/kg-K]	420	460	500	525	545	565	585	625	670	710	710

Table 8.3 : Rene 41 and Inconel 718 material properties.

E56 Engine HPT Blade and Disc Heat Transfer Coefficient & Bulk Temperature

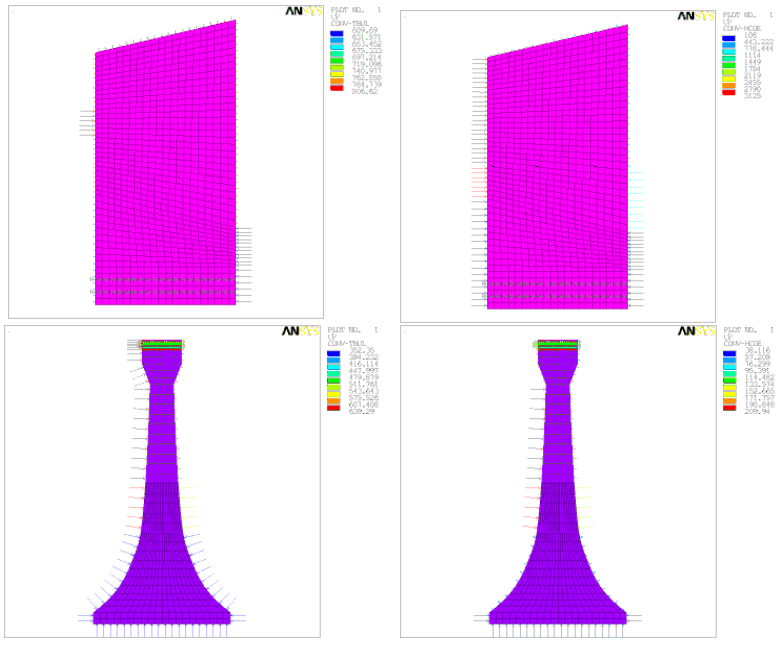

Figure 8.6 : Heat transfer application on finite element model of E56 HPT.

The transient thermal analysis conducted on the blade and disc assembly has the loads on the boundary as heat transfer coefficients and bulk temperature.

The bulk temperature is estimated from the gas temperatures by taking into account cooling effectiveness, thermal barrier coating, pattern factor and temperature profile.

E56 Engine HPT Blade Metal Temperature Variation

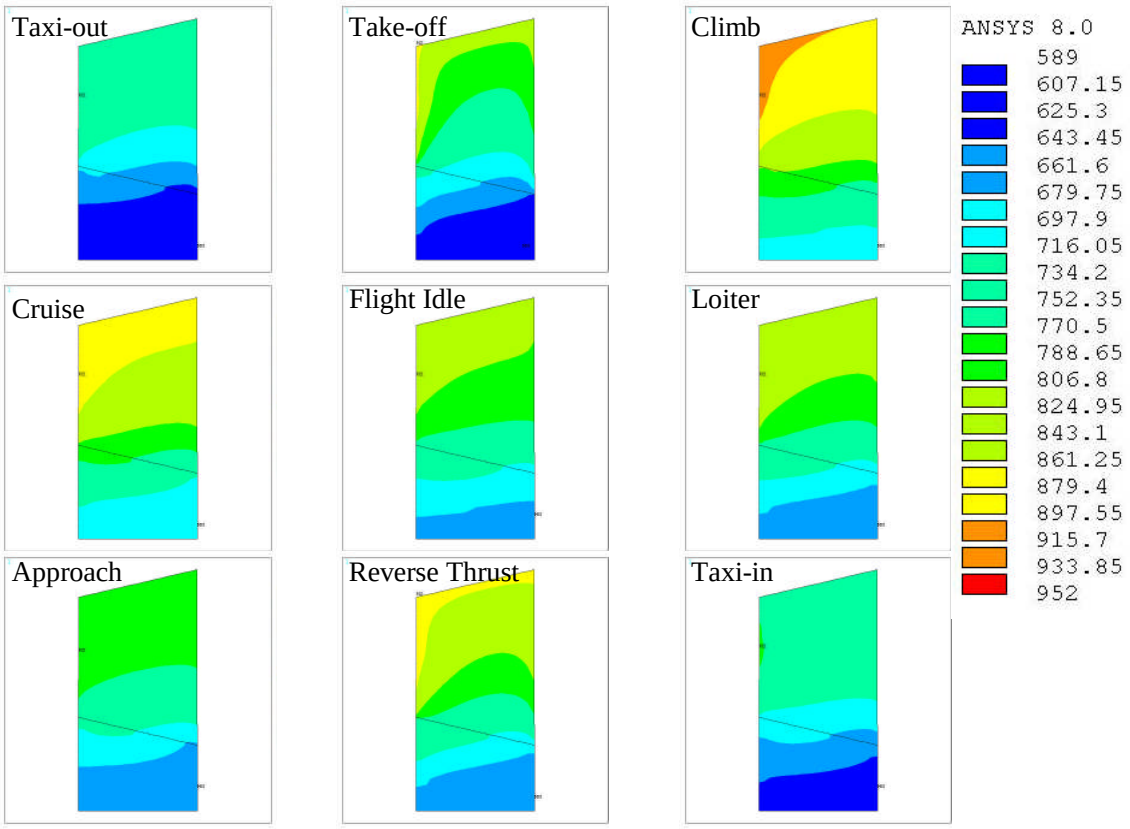

Figure 8.7 : E56 engine HPT blade metal temperature at mission points.

E56 Engine HPT Disc Metal Temperature Variation

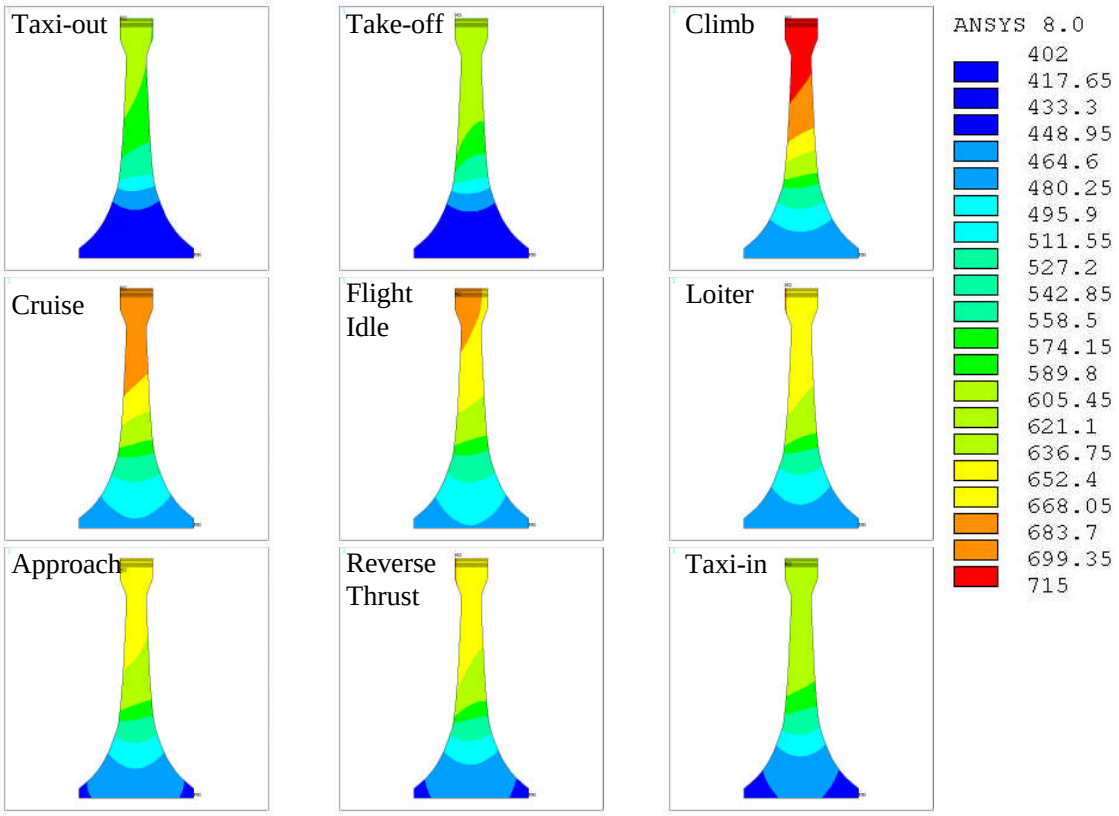

Figure 8.8 : E56 engine HPT disc metal temperature at mission points.

The temperature variation during the mission, plotted for the critical segments to observe the metal temperatures.

The structural model is depicted in the Figure 8.9. The interface nodes of the blade and disc have a coupled degrees of freedom, and radial force due to the (total number of blades-1) blades has been applied to simulate the net blade force on the disc. The temperature and the angular velocity are applied as loads for the thermo-mechanical analysis as per the mission points.

E56 Engine HPT Blade and Disc Structural Model Loads and Constraints

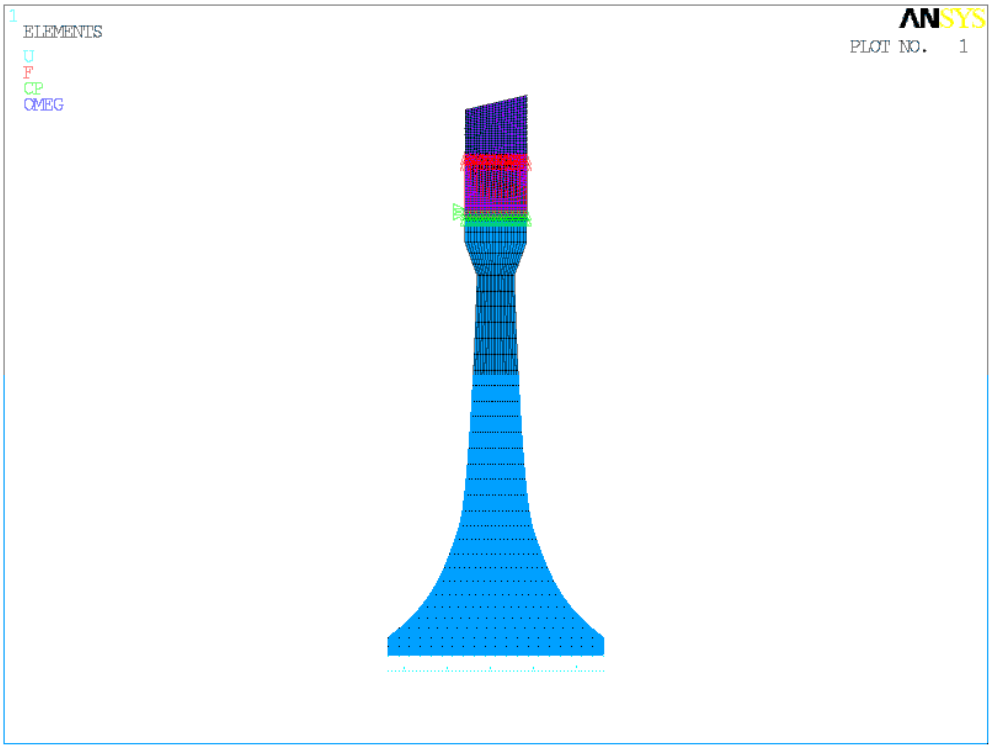

Figure 8.9 : E56 engine HPT structural model constraints and load.

The Von Mises stress or equivalent stress variations are plotted for the critical mission points.

E56 Engine HPT Blade Equivalent (Von Mises) Stress Variation

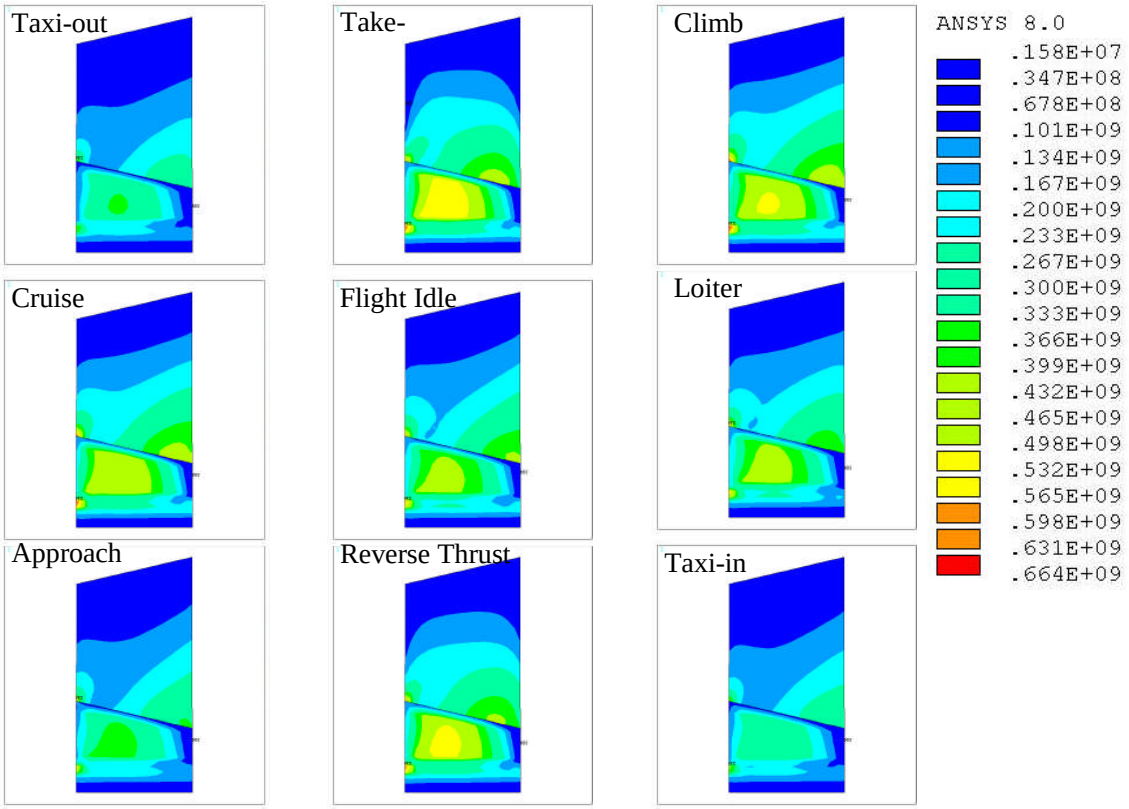

Figure 8.10 : E56 engine HPT blade Von Mises or equivalent stress plot at mission points.

E56 Engine HPT Disc Equivalent (Von Mises) Stress Variation

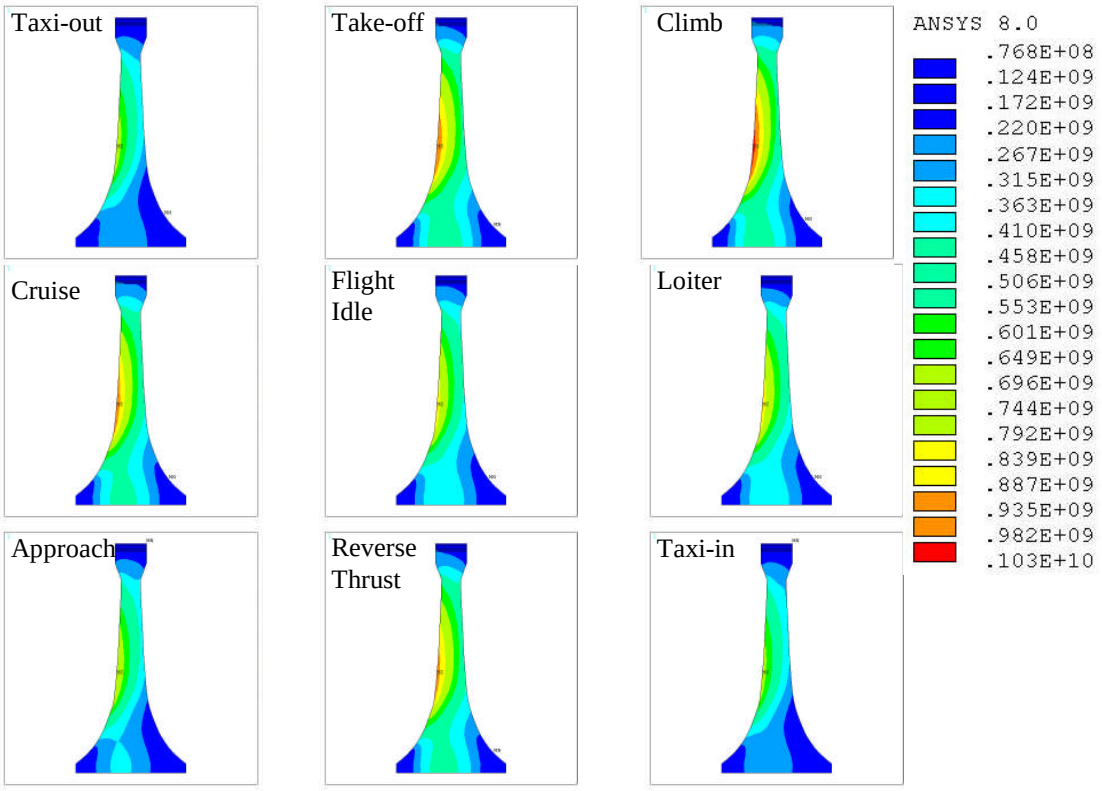

Figure 8.11 : E56 engine HPT disc Von Mises or equivalent stress plot at mission points.

The life estimates based on low cycle fatigue, creep and oxidation have been tabulated for the blade (Table 8.4) and the disc (Table 8.5).

HPT Blade			
	Low cycle Fatigue	**Creep**	**Oxidation**
Units	cycles	hrs	hrs
Blade Life	6.44E+05	2.71E+07	9.45E+11
Take-off Life Consumption[%]	13.73	0.00	10.80
Climb Life Consumption [%]	24.44	80.31	74.31
Cruise Life Consumption [%]	31.25	19.60	13.74
Descent Life Consumption [%]	12.08	0.09	0.47
Landing Life Consumption [%]	18.50	0.01	0.68

Table 8.4 : E56 engine HPT blade life summary.

HPT Disc			
	Low cycle Fatigue	**Creep**	**Oxidation**
Units	cycles	hrs	hrs
Blade Life	1.10E+04	3.50E+08	3.55E+10
Take-off Life Consumption[%]	18.24	0.02	0.18
Climb Life Consumption [%]	36.30	83.92	63.48
Cruise Life Consumption [%]	18.99	15.91	32.20
Descent Life Consumption [%]	8.52	0.13	3.23
Landing Life Consumption [%]	17.95	0.02	0.92

Table 8.5 : E56 engine HPT disc life summary.

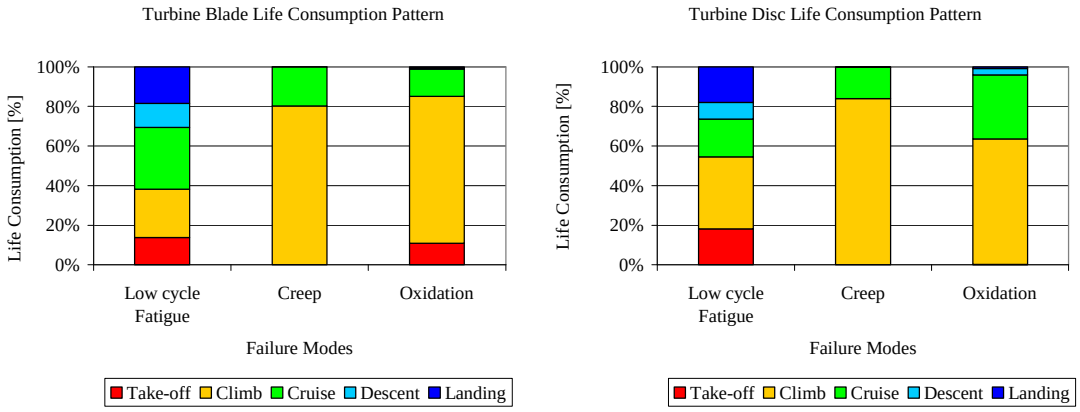

Figure 8.12 : E56 engine HPT blade and disc life consumption pattern.

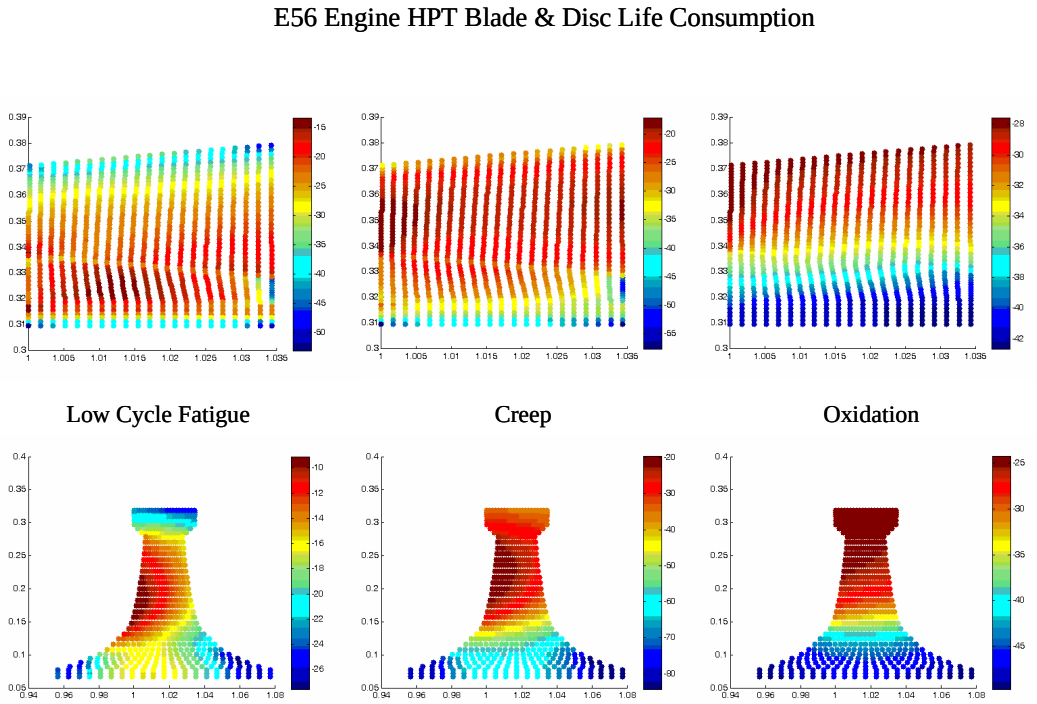

Figure 8.13 : E56 engine HPT blade and disc life plots.

The low cycle fatigue is said to have a minimum value among the failure modes for the blade and the disc. The Figure 8.12 shows the percentage of life consumed at the different flight segments. For indicating the life consumption the total damage has been estimated corresponding to minimum life of the component and the different events that are represented as a set of mission points are summed up to find the event damage and the contribution towards total damage expressed as a percentage. The Figure 8.13 shows the life values expressed as a logarithmic value with hyphen as prefix range from a minimum value indicated as red colour and blue for maximum value. The most affected zones are indicated by the red colour and have the limiting value under the respective modes of failure.

The low cycle fatigue blade life plot indicates the worse areas at the shank region and at the blade-shank interface. The creep plot shows limiting zone at the leading edge and trailing edge mid span. The leading edge becomes the limiting zone for the oxidation mode of failure. The disc due to low cycle fatigue is prone to failure at the forward end of the hyperbolic profile, creep near the rim region, and oxidation at the rim region experiencing high temperature during the mission.

The Table 8.6 shows the severity calculation for the reference mission, and a similar process is followed for the studies on different operational and technological factor variation.

Trip Length [hrs]	T-O Derate [%]	Blade Cyclic Severity	Blade Steady Severity	Blade Severity	Disc Cyclic Severity	Disc Steady Severity	Disc Severity	Average Cyclic Severity	Average Steady Severity	Average Severity
1.4	10	0.97	0.03	1.00	1.00	0.00	1.00	0.98	0.02	1.00

Table 8.6 : E56 engine severity estimation for the reference mission.

8.3 Short Haul Flight – Operational Factors

The operational factors influence the severity on the components. The derate at take-off, climb and cruise have been investigated through parametric studies. The other significant factors of great interest are the OAT, airport altitude, cruise altitude and cruise Mach number are observed on the sensitivity over severity

factor. The characteristics are substantiated through the plots of exhaust gas temperature and the shaft speed scaling vector for the corresponding parametric studies. The exhaust gas temperature and shaft speed, change with respect to operational factors at different segments, changing the life consumption, and hence the severity.

Effect of Take-Off Derate

The derate is a widely used strategy to reduce the maintenance cost of aircraft engines. The derate being the percentage reduction in thrust, reduces the peak temperature and shaft speed for the flight mission. The take-off is a demanding segment where the maximum temperature and shaft speed are utilized to achieve a feasible take-off. Hence the common practice has been in specifying the take-off derate, as an important factor that dictates the severity level on the HPT. Hence a parametric study has been carried out, by varying the take-off derate from -10% to 20%, while the other operational and technological factors have the same settings. The take-off derate results in an associated change in the maximum temperature and shaft speed, hence the severity curves are inline with the EGT and shaft speed scaling vector plot (normalized shaft speed) with respect to the take-off derate.

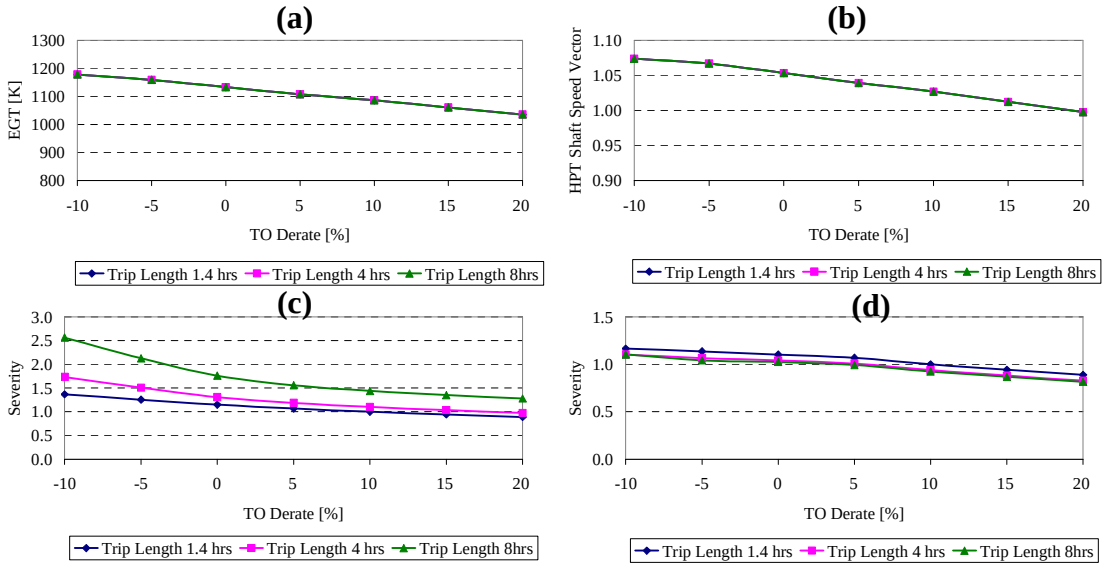

Figure 8.14 : E56 engine characteristics for variation in take-off derate (a) Exhaust gas temperature (b) Shaft speed scaling vector (c) Blade Severity (d) Disc Severity.

The take-off derate has significant impact on the severity. The derates at other flight segments, such as the climb and the cruise condition has been studied to bring out their importance.

Effect of Climb Derate

The climb plays the second critical role for the short haul flights as considerable amount of time is spent in climb and descent. The engine manufacturers propose climb derate strategy [18] to save the engine life. The proposed strategy involves, the use of climb derate upto a certain altitude called as taper altitude, and ramp up to 0 % derate (top-of-climb thrust) at a higher altitude referred to as the washout altitude (Appendix E).

The climb derate study has been conducted for various taper and washout altitude. The severity reduces with increasing climb derate however is not impacted by the taper and washout altitude.

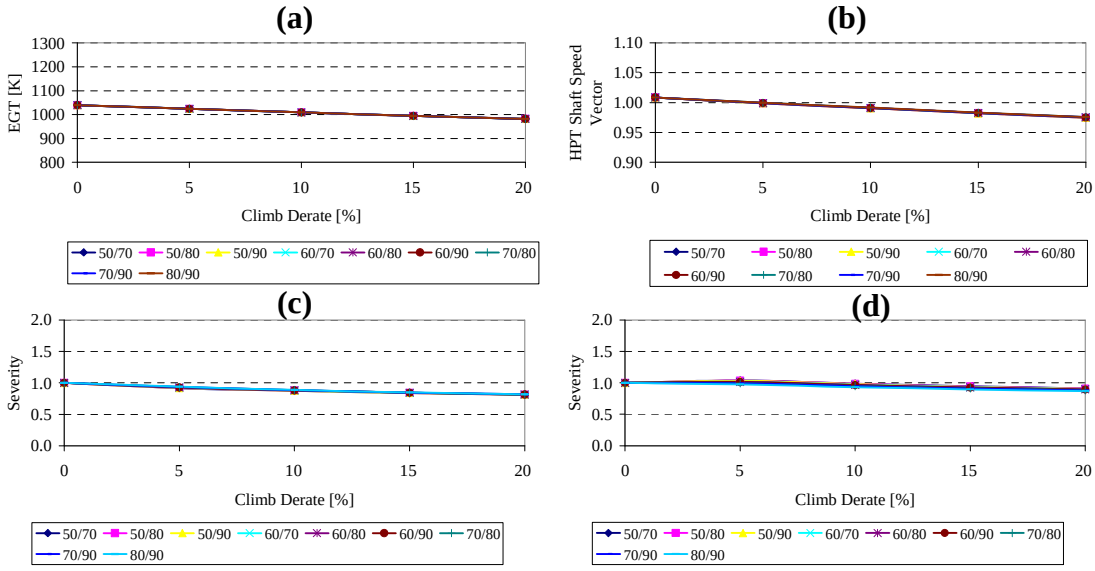

Figure 8.15 : E56 engine characteristics for variation in climb derate (a) Exhaust gas temperature (b) Shaft speed scaling vector (c) Blade Severity (d) Disc Severity.

Effect of Cruise Derate

The cruise derate will have less importance, as the temperature and shaft

speed scaling vector are lower, as compared to the take-off and climb. However to identify the change in severity, a parametric study for cruise derate from 0 % to 20% has been carried out, shows severity characteristics are flatter.

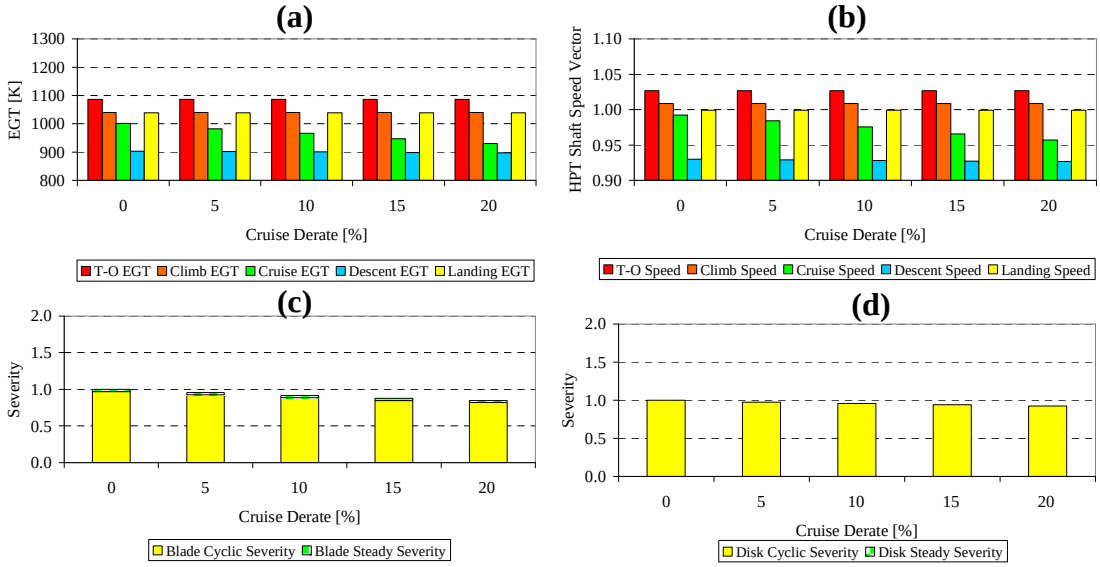

Figure 8.16 : E56 engine characteristics for variation in cruise derate (a) Exhaust gas temperature (b) Shaft speed scaling vector (c) Blade Severity (d) Disc Severity.

Effect of Outside Air Temperature

The gas turbines are fundementally sensitive with respect to the OAT, as the changes in the inlet condition of the air, changes the thrust produced by the engine. The airliners use higher derate for the zones operated at high OAT to minimize the damage on the engine. The engine manufacturers use a flat rating upto a certain OAT with the scope of increasing the combustor temperature to account for the reduction in the thrust, however beyond the flat rating temperature, an eventual reduction in the thrust is followed, due to the design temperature limit for the components. The OAT is varied from 0 °C to 40 °C, however different temperature ranges could be studied, as per the city pairs for the mission.

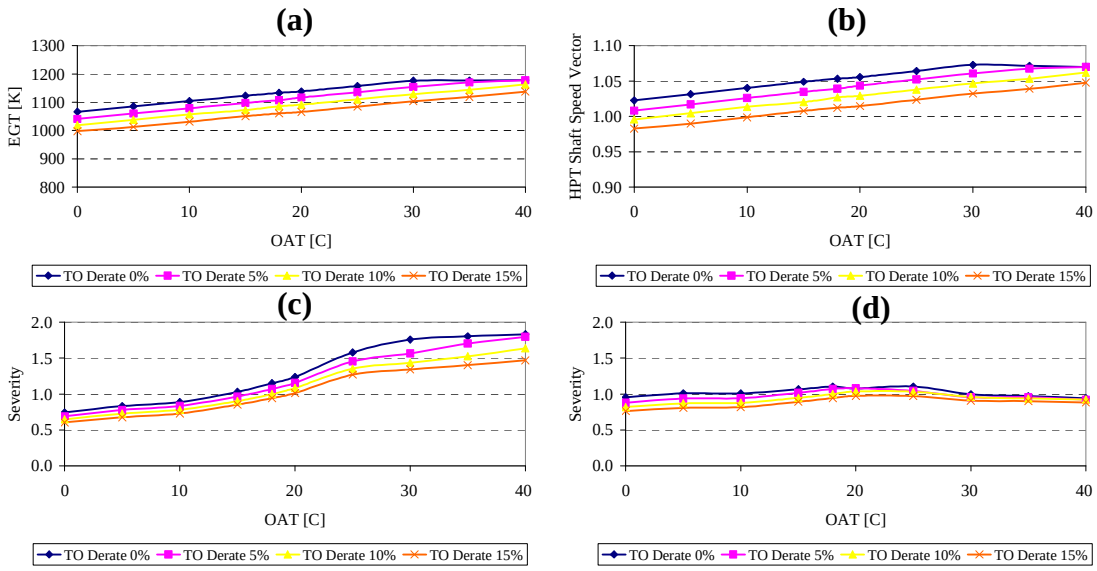

Figure 8.17 : E56 engine characteristics for variation in OAT (a) Exhaust gas temperature (b) Shaft speed scaling vector (c) Blade Severity (d) Disc Severity.

The increase in OAT increases the EGT and the shaft speed. This causes an increase in the severity with increasing OAT until the flat rating temperature, beyond which the trend becomes flatter, showing constant level of damage.

Effect of Airport Altitude

The altitude remains a factor changing with the airports in different continents. The change in the altitude affects the level of thrust, hence it is important to

study the severity trends for the lower thrust engines operated at different geographical regions. The increase in the altitude reduces the thrust as the density of air reduces hence an amount of derate is used suitable to the airport. The altitude variation for the parametric analysis is from sea level to 1600 m.

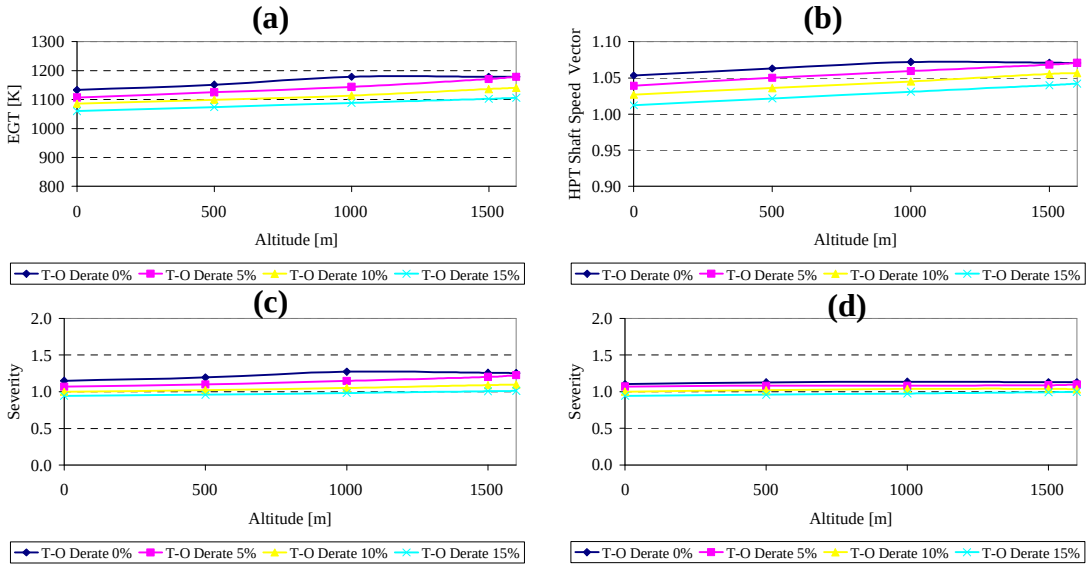

Figure 8.18 : E56 engine characteristics for variation in airport altitude (a) Exhaust gas temperature (b) Shaft speed scaling vector (c) Blade Severity (d) Disc Severity.

With increasing airport altitude, the severity of the blade increases while the disc severity has less sensitivity. For increasing take-off derate the blade severity is observed to incur less damage. Hence the use of take-off derate is beneficial for the aircraft engines operated at airports of higher altitude.

Effect of Cruise Altitude & Cruise Mach

The cruise altitude and Mach number has been considered under the operational factors to be studied. The cruise altitude is varied between 8000 m to 11500 m and conducted for Mach number varying between 0.7 and 0.8. In maintaining the cruise thrust, at different altitudes and Mach numbers, the severity level of the blade and disc has been observed to increase due to the associated increase in the EGT and the shaft speed. However cruise altitude and Mach number are optimized based on the aircraft and engine performance to achieve the best specific fuel consumption and propulsive efficiency.

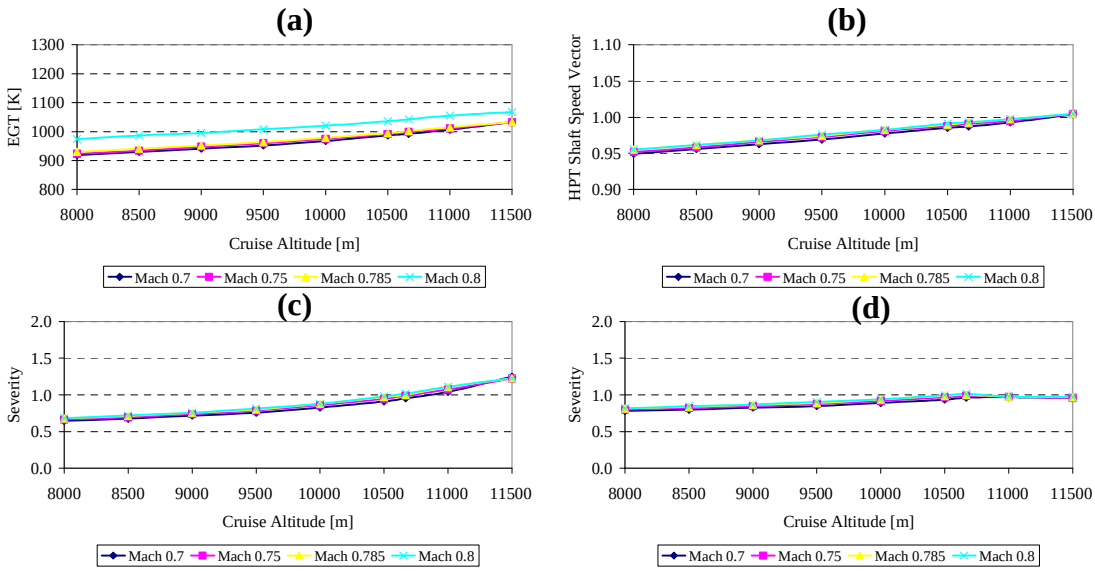

Figure 8.19 : E56 engine characteristics for variation in cruise altitude (a) Exhaust gas temperature (b) Shaft speed scaling vector (c) Blade Severity (d) Disc Severity.

8.4 Short Haul Flight – Technological Factors

The technological factors such as cooling effectiveness, thermal barrier coating, pattern factor and profile, affect the degree of life consumption, as these factors change the metal temperature. The metal temperature is prominent for failures such as the creep and oxidation and as well for low cycle fatigue.

Cooling Effectiveness

The advanced aircraft engines use sufficient cooling for the nozzle and turbine blades to withstand high cycle temperatures. The cooling effectiveness is a temperature offset mechanism through the use of air at lower temperature, passing through the turbine cooling holes or slots, reducing the metal temperatures to operate within the metallurgical limits. A parametric study has been conducted by varying the cooling effectiveness to obtain the relative sensitivity on the severity for the reference mission.

The cooling effectiveness of lower value shows tremendous increase in the severity. This is basically due to the phenomenon of creep, dominating for lower cooling effectiveness, and shifts into low cycle fatigue as the the value of

the cooling effectiveness is increased. The creep life has high level of response with temperature, showing large severity values and progressively lowered with increasing cooling effectiveness. Hence cooling effectiveness is one of the important technological factors to reduce the severity level on the component.

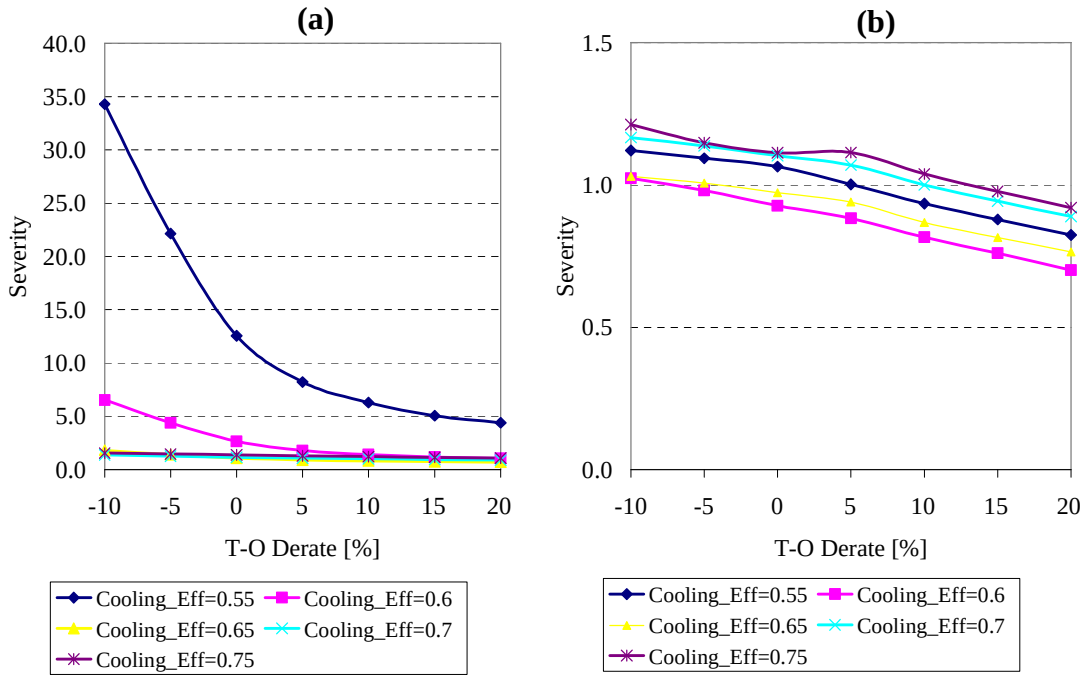

Figure 8.20 : E56 engine severity variation with blade cooling effectiveness (a) Blade severity (b) Disc severity.

Thermal Barrier Coating

The use of yittria stabilized zirconia, a ceramic coating, allows the reduction of the metal temperature by using the lower thermal conductivity of the coating material. The coatings are common practice in the aircraft engines that facilitates the use of higher turbine entry temperature. The two factors which govern the thermal barrier coating are the coating thickness and thermal conductivity of the material have been varied to observe the changes in severity of the component.

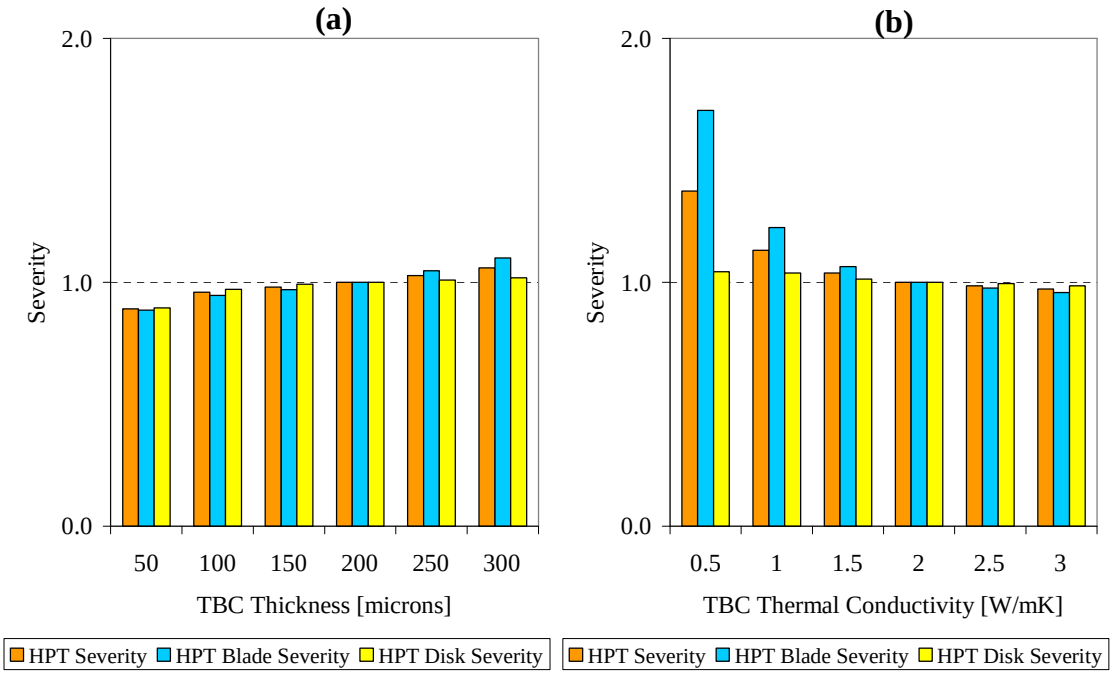

Figure 8.21 : E56 engine severity variation with thermal barrier coating (a) Thickness (b) Thermal conductivity.

The use of cooling effectiveness of 0.7 for the study has shifted the pattern of life consumption to low cycle fatigue. The increasing thickness and decreasing thermal conductivity studies, shows detrimental effect due to the thermal shock, affecting the low cycle fatigue life. However for lower values of cooling effectiveness, it will indicate decrease in the severity when the limiting mode shifts to creep. This has been observed for the large thrust engines, where creep becomes the limiting phenomenon, and shows reduction in severity with respect to thermal barrier coating thickness and thermal conductivity.

Pattern Factor and Profile

The pattern factor is a measure of the peak temperature experienced by the nozzle and turbine blades. The pattern factor has been incorporated in the methodology to appreciate the different combustor designs. A parametric study has been aimed to capture the changes in severity with the pattern factor and different temperature profiles.

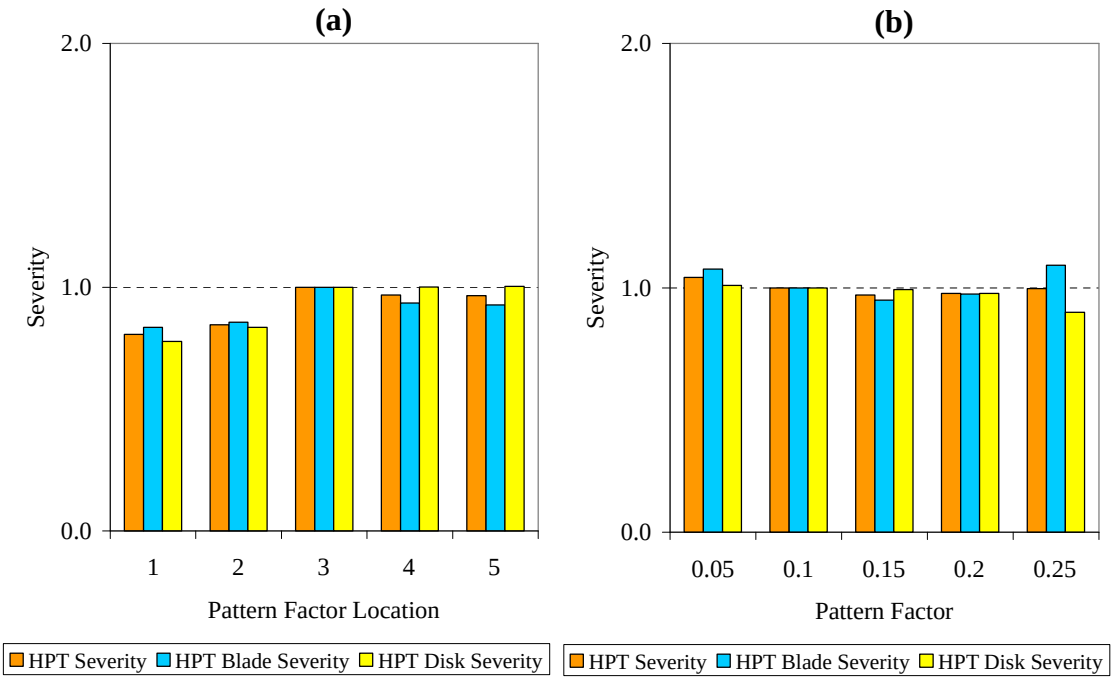

Figure 8.22 : E56 engine severity variation with pattern factor (a) Location (b) Magnitude.

The pattern factor shows less sensitivity due to the use of better cooling effectiveness. The pattern factor and location will have greater significance, when creep becomes the critical life consumption mode as observed in large thrust engines .

8.5 Short Haul Flight – Derate Severity Curve

The derate severity curve has been the basis for the maintenance cost estimation for the aircraft engines as established by the MRO. The severity characteristics for the various take-off derates, represented for different trip lengths is the typical MRO curve for an engine. The severity factor is observed from the cooling effectiveness study with the individual curves for different cooling effectiveness are represented with respect to its own reference mission rather than the reference mission for cooling effectivness of 0.7, and averaged to obtain the resultant derate-severity. The reference mission of 1.4 hrs trip length, 10 % take-off derate and 18 °C OAT is normalized to a severity value of unity. Hence the derate severity curve can be defined as a single point reference curve, and the severity values expressed with respect to the reference mission.

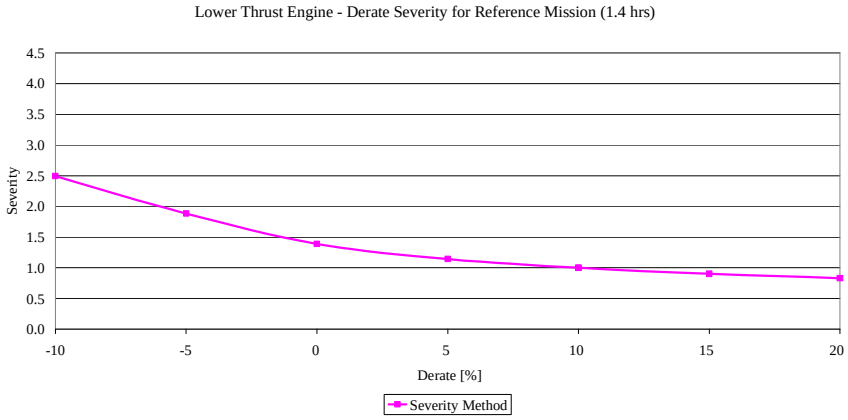

Figure 8.23 : E56 engine derate severity curve for 1.4 hrs mission.

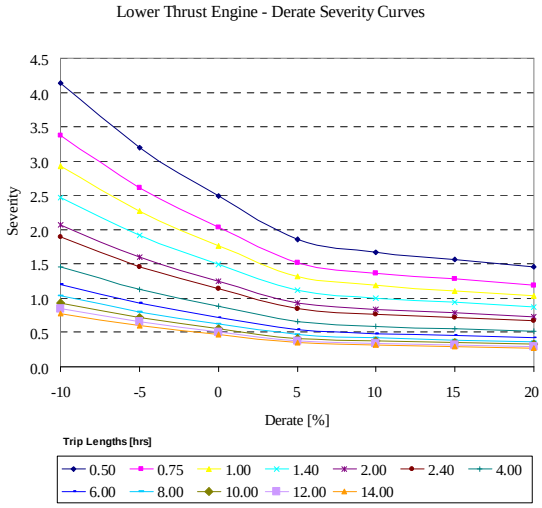

Figure 8.24 : E56 engine derate severity curves for trip lengths.

The shorter trip lengths show more severity, as the limiting life consumption mode is the low cycle fatigue, a phenomenon that is based on cycles of operation. A typical take-off and landing includes one cycle. Hence for shorter trip lengths, a number of take-off and landing is involved, consuming larger part of the low cycle fatigue life. Hence the severity for short trip lengths are more as compared to longer trip lengths. The severity has more steepeness in the zone of -10 to 10 % take-off derate, as the component is subjected to sufficiently high temperatures and shaft speed, and with the reduction in the thrust beyond this zone fall in the severity is much flatter. This is evident from the fatigue life curves that has a similar characteristics, showing more gradient

near the zone of maximum strain range, and becomes flatter for the smaller strain ranges.

The reference mission curve has been compared with the MRO curve, and a good agreement is observed in Figure 8.23. This indicates the methodology of estimating the severity by the engine manufacturers could be captured with help of fundemental techniques and information available in the public domain. An overlay plot has been provided for the different trip lengths comparing MRO and severity estimation method curves available in Figure 8.24.

8.6 Long Haul Flight – Reference Mission

The wide body aircraft used for long haul flights has been analyzed to estimate the severity of the high pressure turbine blade and disc. The flight path analysis using the simplified aircraft performance code has been utilized for thrust, altitude and Mach number variations with respect to time for a typical civil aviation mission.

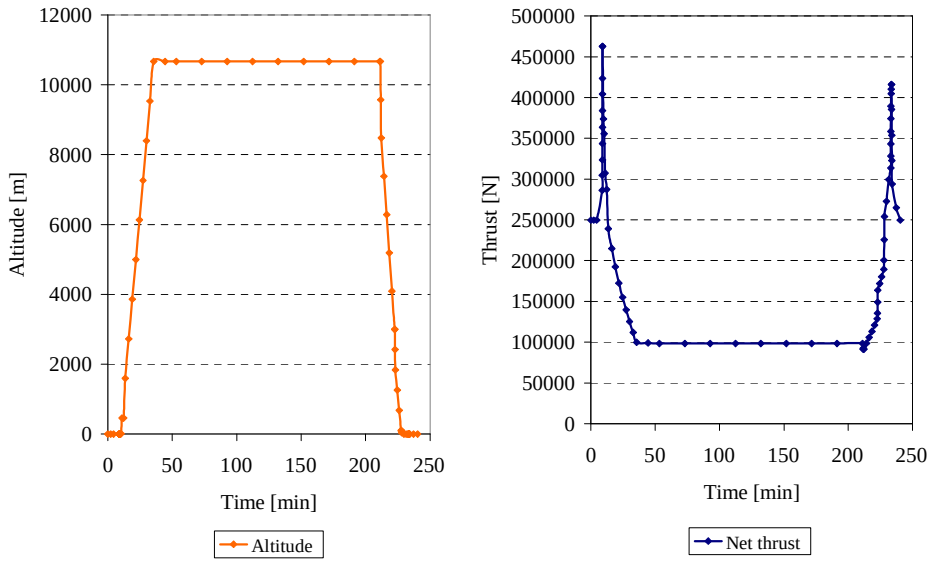

Figure 8.25 : E115 engine thrust and altitude variation for 4 hrs trip mission.

The engine used under the large thrust category is constructed as Turbomatch performance model (Appendix A) representing the specification of E115. To

simulate using gas turbine performance as design and off design conditions with respect to thrust, altitude and Mach number variation. The mass flow rate, temperature, pressure and non-dimensional shaft speed are retrieved for the gas turbine components for further calculation.

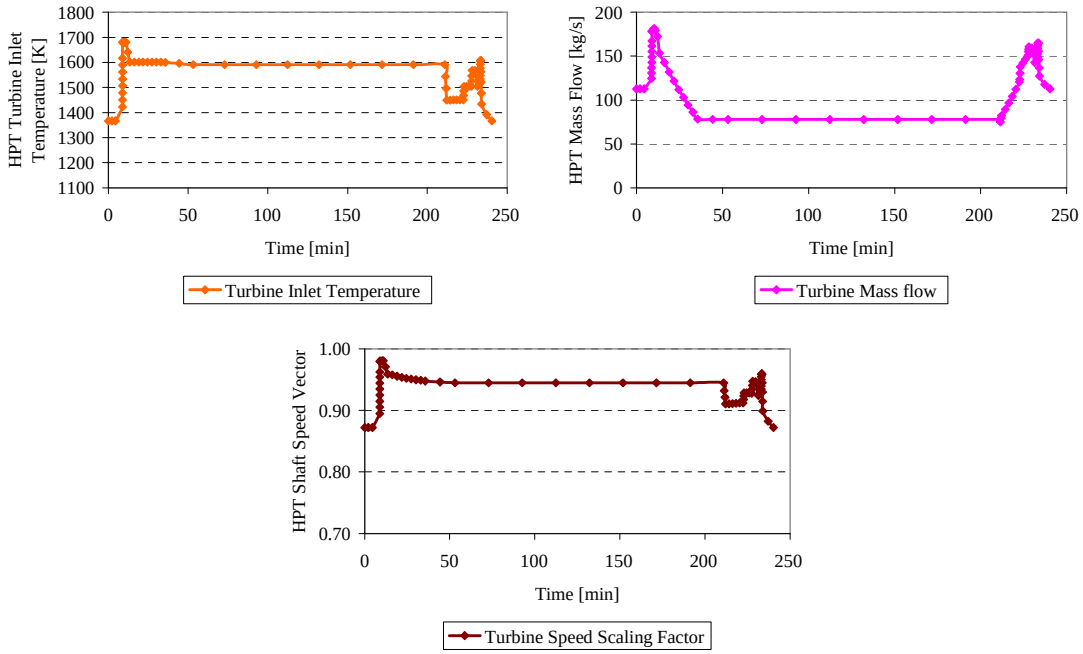

Figure 8.26 : E115 engine HPT turbine entry temperature, mass flow rate and shaft speed variation for 4 hrs trip mission.

Turbomachinery sizing is carried out on the high pressure turbine blade to estimate the physical dimensions (Appendix B) using the Matlab code. Disc is built from the cross-section drawing of an equivalent engine. The high pressure turbine blade is sized based on the take-off condition.

The heat transfer calculation module, estimates the heat transfer coefficients and the bulk temperatures for the transient thermal analysis. The mapping of the flow tag and the thermal correlation for the different segments of the high pressure turbine blade and the disc is used during the heat transfer estimation.

E115 Engine HPT Blade & Disc Geometry

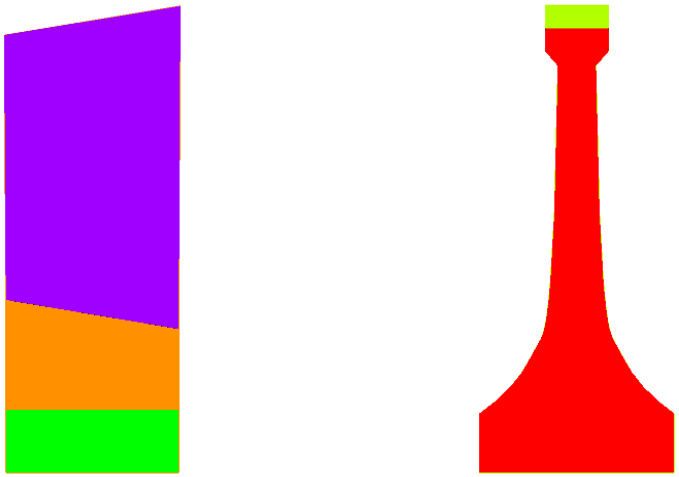

Blade Disc

Figure 8.27 : E115 engine HPT blade and disc geometry.

E115 Engine HPT Blade & Disc Thermal Correlation and Flow Tag Mapping

Location	Thermal correlation	Flow Tag
B_1	1	1
B_2	1	1
B_3	1	1
B_4	1	1
B_5	1	1
B_6	3	1
B_7	2	2
B_8	2	2
B_9	2	2
B_10	2	2
B_11	2	2
B_12	4	4
B_13	4	4
B_14	4	4
B_15	4	5
B_16	4	5
D_1	5	5
D_2	5	5
D_3	4	4
D_4	4	4
D_5	4	4
D_6	5	3
D_7	4	5
D_8	4	5
D_9	4	5
D_10	4	5
D_11	4	5

Thermal Correlation	
Circular Cylinder	1
Flat Plate	2
Gap	3
Cavity Radial Outflow	4
Cavity Axial Outflow	5

Flow Tag	
Turbine Inlet	1
Turbine Outlet	2
Disk Bore Cooling	3
Disk Front Cooling	4
Disk Aft Cooling	5

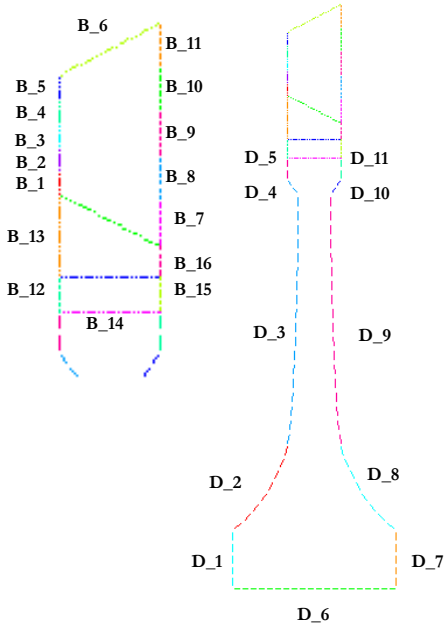

Figure 8.28 : E115 engine HPT heat transfer correlation and flow mapping.

E115 Engine HPT Blade and Disc Heat Transfer Coefficient & Bulk

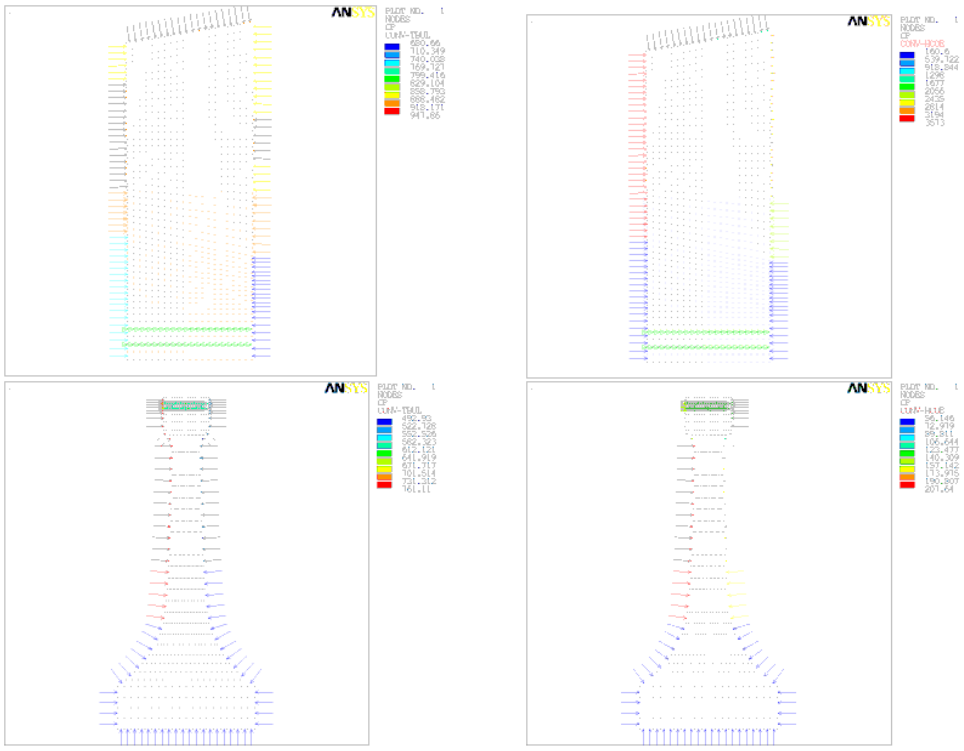

Figure 8.29 : E115 engine HPT heat transfer coefficients and bulk temperature.

E115 Engine HPT Blade & Disc Finite Element Model

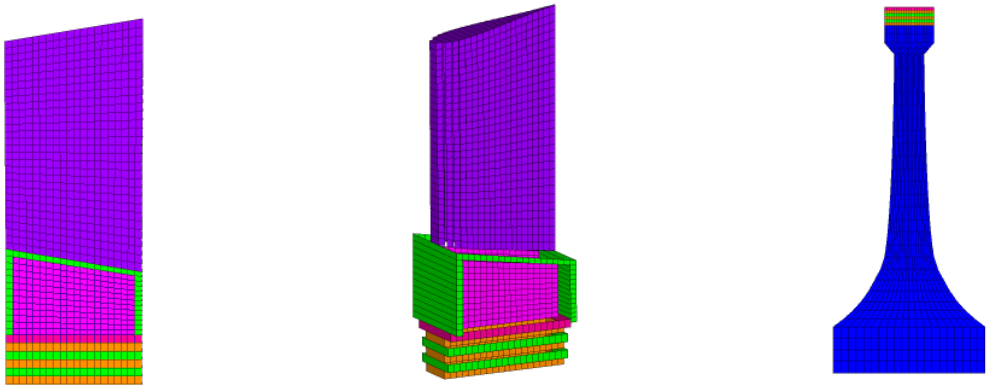

Blade – 2D View | Blade – 3D View | Disc

Figure 8.30 : E115 engine finite element model.

The finite element model built through the APDL code has been illustrated. The blade with the thickness variations at the root, shank and aerofoil is modeled using the 2-D plane element with thickness capability. The number of elements used in the model are 1720 having 1848 nodes. The number of elements in the finite element model, optimized using the mesh convergence study with respect to the life of the component.

The HPT turbine blade uses, Rene 41 material properties and the disc with Inconel 718, as provided in Table 8.3. Single crystal super alloys and other super alloys are used for aircraft engine turbine blade and disc, but most of the properties are proprietary data of the manufacturers. Hence the materials available in the open literature has been applied for the analysis.

The transient thermal analysis conducted on the blade and disc assembly with the heat transfer coefficients and bulk temperature, estimated at the mission points. The bulk temperature is changed from the gas temperatures due to cooling effectiveness, thermal barrier coating, pattern factor and temperature profile.

The metal temperature for the blade and the disc has been plotted for the critical segments of the flight in Figure 8.31 and Figure 8.32.

The structural model is illustrated in the Figure 8.33. The coupled degrees of freedom have been used for tieing up the interface nodes of the blade and disc. The radial force due to the (total number of blades-1) blades has been applied to simulate the net blade force on the disc. The temperature and the angular velocity are applied, as load for the thermo-mechanical analysis, simulating the mission points.

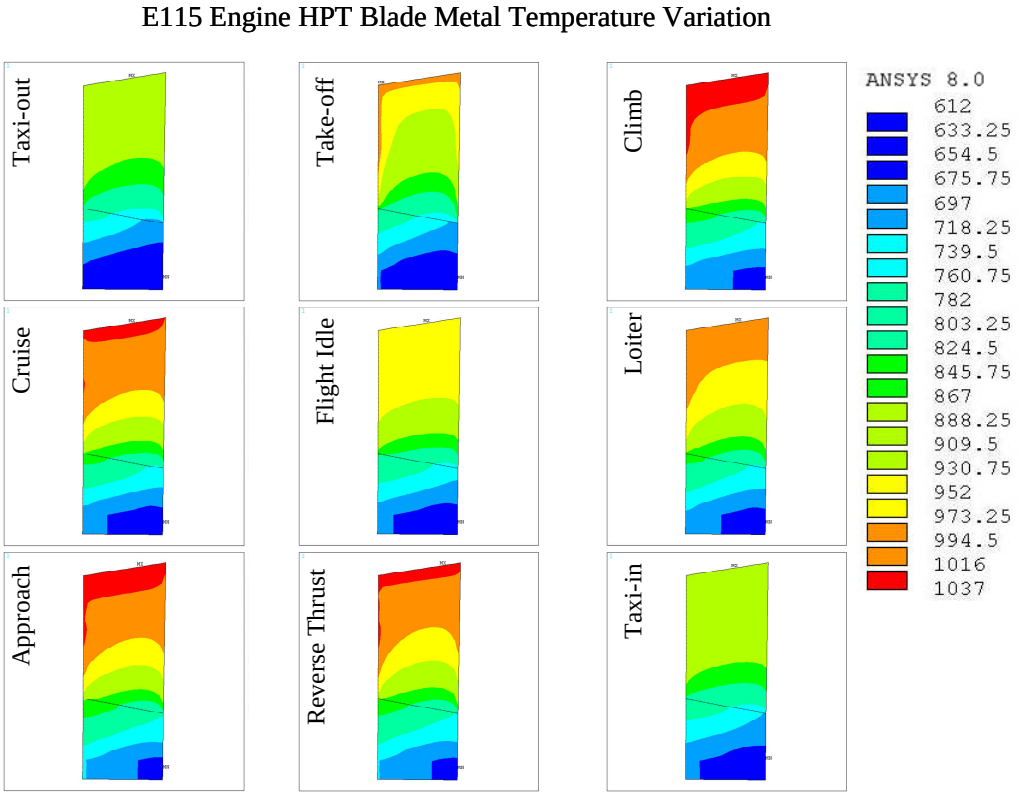

Figure 8.31 : E115 engine HPT blade metal temperature at mission points.

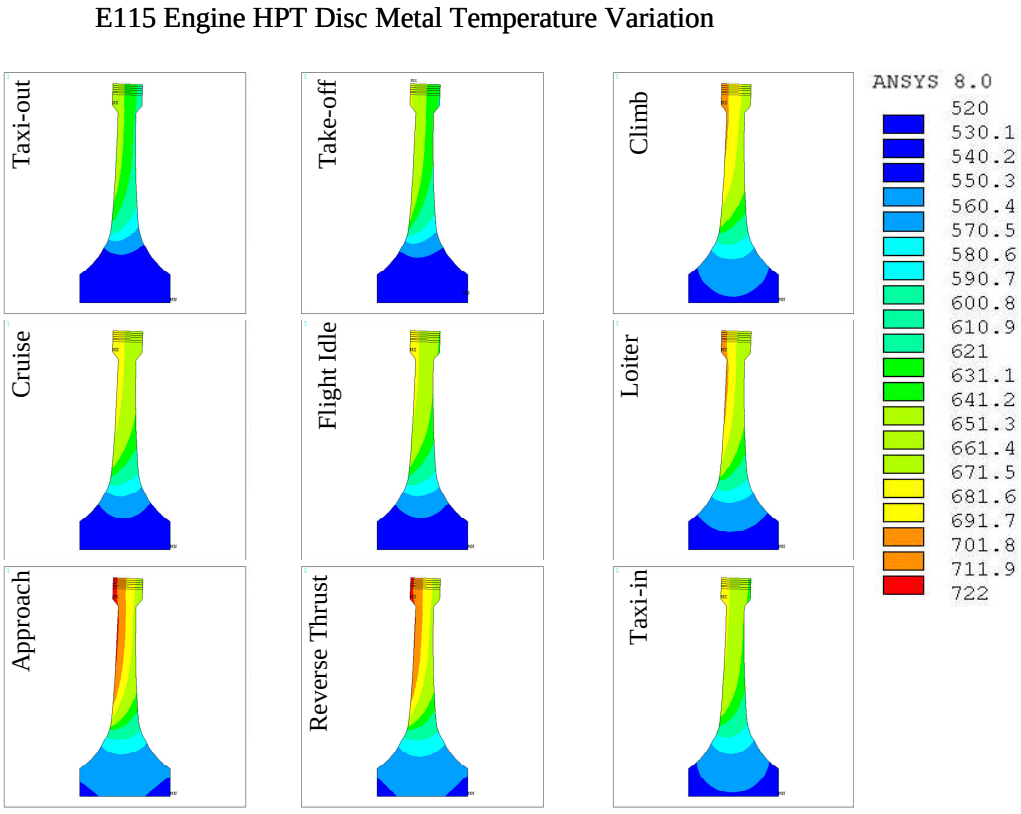

Figure 8.32 : E115 engine HPT disc metal temperature at mission points.

E115 Engine HPT Blade and Disc Structural Model Loads and Constraints

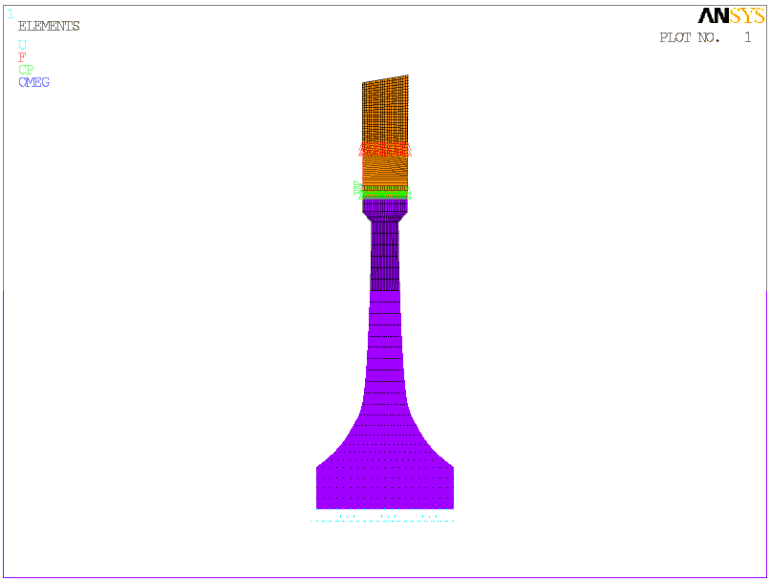

Figure 8.33 : E115 engine HPT structural model constraints and loads.

E115 Engine HPT Blade Equivalent (Von-Mises) Stress Variation

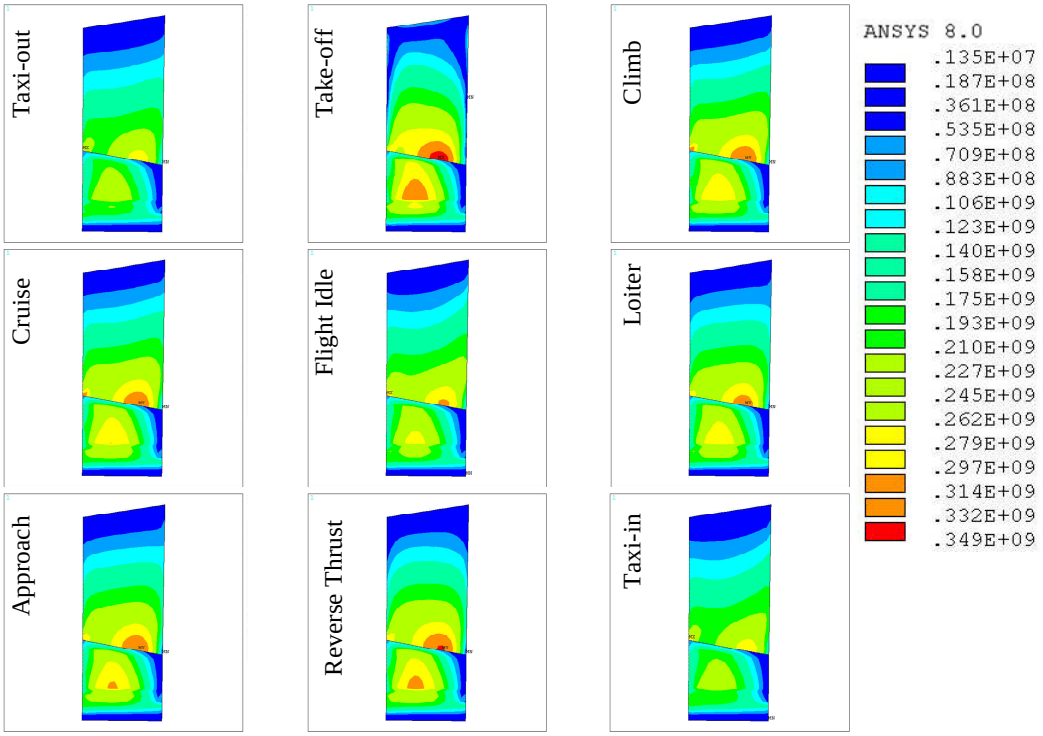

Figure 8.34 : E115 engine HPT blade Von Mises or equivalent stress plot at mission points.

E115 Engine HPT Disc Equivalent (Von-Mises) Stress Variation

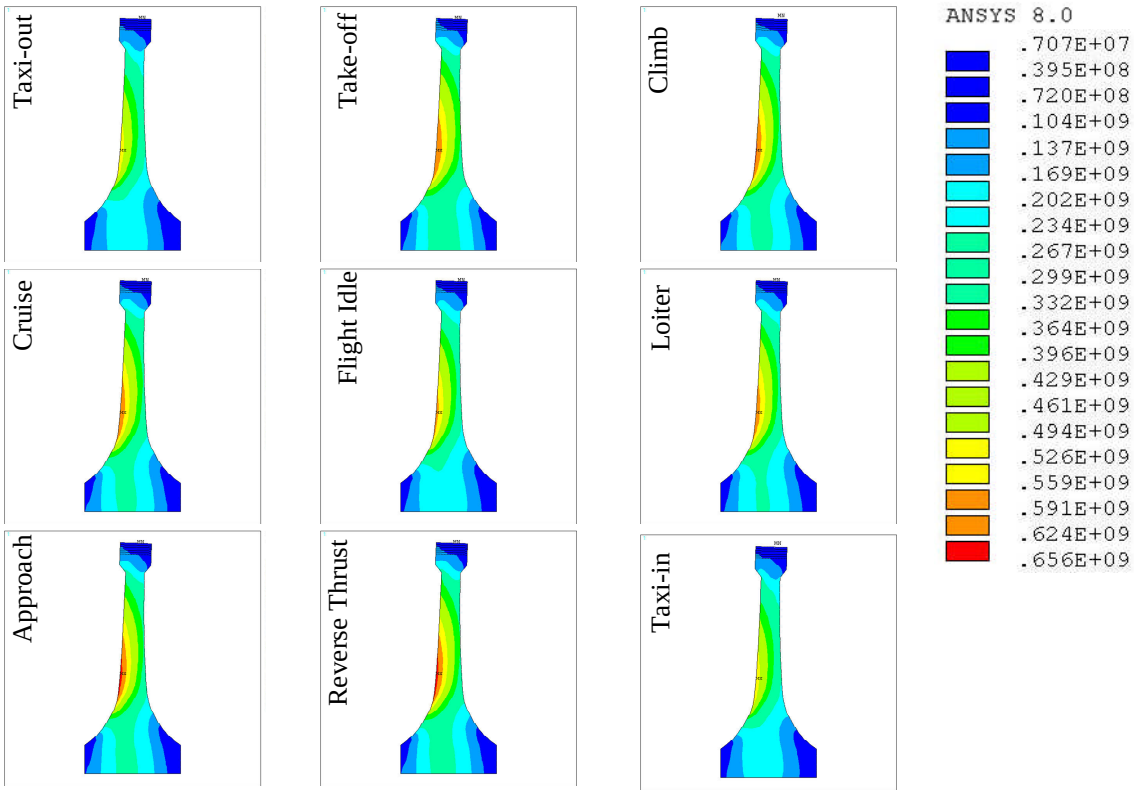

Figure 8.35 : E115 engine HPT disc Von Mises or equivalent stress plot at mission points.

The Von Mises stress for the critical mission points has been shown in Figure 8.34 and 8.35.

HPT Blade			
	Low cycle Fatigue	**Creep**	**Oxidation**
Units	cycles	hrs	hrs
Blade Life	1.03E+08	1.61E+04	1.18E+09
Take-off Life Consumption[%]	23.65	0.84	4.04
Climb Life Consumption [%]	18.83	76.55	27.30
Cruise Life Consumption [%]	16.36	6.49	64.58
Descent Life Consumption [%]	12.49	1.91	1.38
Landing Life Consumption [%]	28.67	14.21	2.69

Table 8.7 : E115 engine HPT blade life summary.

HPT Disc			
	Low cycle Fatigue	**Creep**	**Oxidation**
Units	cycles	hrs	hrs
Blade Life	2.43E+05	7.58E+09	1.20E+10
Take-off Life Consumption[%]	16.39	1.94	1.38
Climb Life Consumption [%]	23.59	75.89	39.89
Cruise Life Consumption [%]	13.73	8.25	41.43
Descent Life Consumption [%]	12.37	2.00	5.26
Landing Life Consumption [%]	33.91	11.92	12.04

Table 8.8 : E115 engine HPT disc life summary.

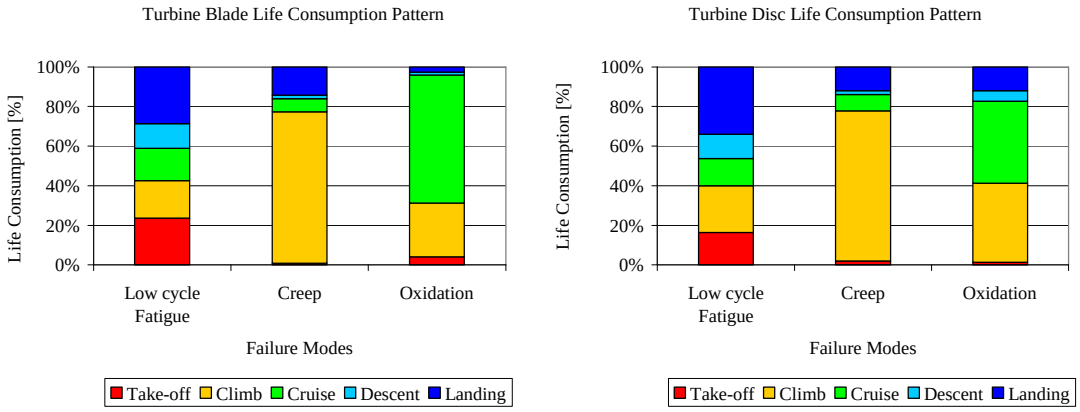

Figure 8.36 : E115 engine HPT blade and disc life consumption plot.

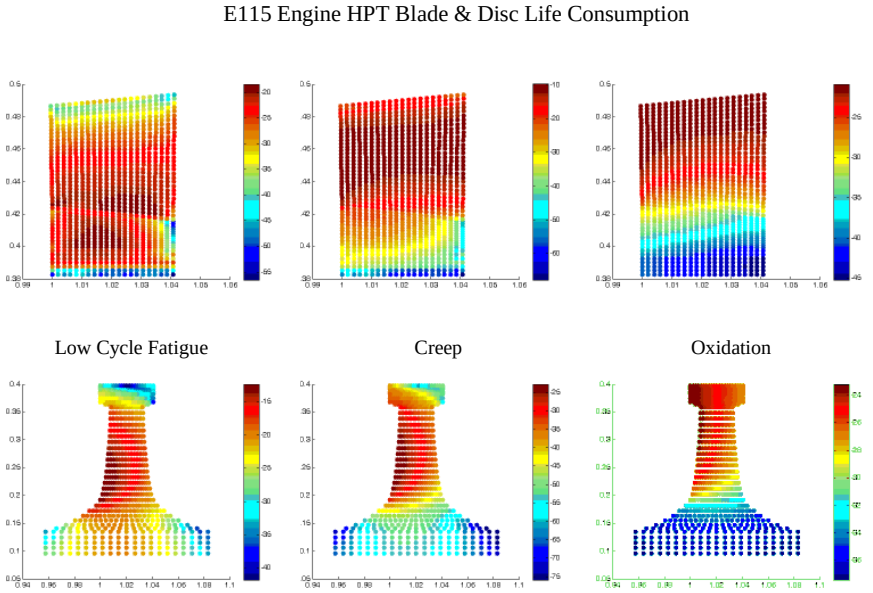

Figure 8.37 : E115 engine HPT blade and disc life plots.

The limiting values of the life for the different modes is provided in Table 8.8 and 8.9. The creep life is said to have a minimum value among the failure mode for the blade and the disc is life limited due to low cycle fatigue. The Figure 8.36 shows the percentage of life consumed at the different flight segments. The damage due to the events in the flight mission collectively represented by a set of mission points have been cumulatively added with respect its damage for the mission points and expressed as a percentage of the total damage with respect to the limiting life value for the individual failure modes. The Figure 8.37 indicates the life values across the component with respect to its failure mode. The values are in a logarithmic scale with hyphen as a prefix. The minimum life zone is indicated by the red colour and the maximum life zone by the blue colour. The minimum life zone corresponds to the limiting value of life with respect to the individual modes of failure.

Blade low cycle fatigue life plot reveals the shank and the blade-shank interface as failure zones experiencing high stress fluctuations. The creep is evident at the mid span of the blade and oxidation along the leading edge and tip region. The disc low cycle fatigue plot indicates the failure zone at the hyperbolic surface of the forward end and for creep it moves towards the rim region. The oxidation pattern is inline with the temperature profile on the disc.

Trip Length [hrs]	T-O Derate [%]	Blade Cyclic Severity	Blade Steady Severity	Blade Severity	Disc Cyclic Severity	Disc Steady Severity	Disc Severity	Average Cyclic Severity	Average Steady Severity	Average Severity
4	10	0.00	1.00	1.00	1.00	0.00	1.00	0.50	0.50	1.00

Table 8.9 : E115 engine severity estimation for the reference mission.

The Table 8.10 shows the severity calculation for the reference mission for engine E115, and a similar process is followed for the case studies, aimed at different operational and technological factor variation.

8.7 Long Haul Flight – Operational Factors

The long haul flights equipped with large thrust engine is analyzed based on the E115 engine model. The derates, OAT, airport altitude, cruise altitude and cruise Mach number are viewed in the perspective of the severity for the large

thrust engines. The severity characteristics are supplemented with exhaust gas temperature and the shaft speed scaling vector (normalized shaft speed) changes for better understanding. The exhaust gas temperature and shaft speed trends reflect the level of severity on the component that influence operational factors, at the different segments of the flight path.

Effect of Take-off Derate

The derate is commonplace in aircraft engine maintenance strategy. The derate being the percentage reduction in thrust, reduces the maximum temperature and shaft speed for the flight mission. The take-off is a demanding segment where significantly high temperature and shaft speed are utilized to achieve a feasible take-off. Hence the common practice is in specifying the take-off derate as an important factor indicating the severity level experienced. A parametric study has been carried out by varying the take-off derate from -10% to 20% while the other operational and technological factors have the same settings.

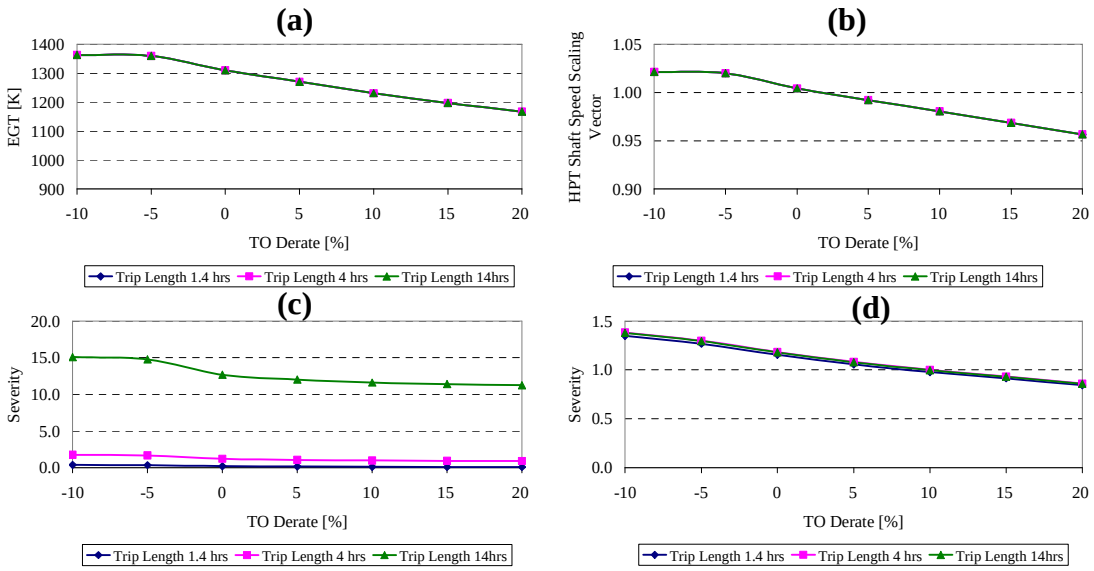

Figure 8.38 : E115 engine characteristics for variation in take-off derate (a) Exhaust gas temperature (b) Shaft speed scaling vector (c) Blade Severity (d) Disc Severity.

The take-off derate results in associated changes in the maximum temperature

and shaft speed, hence the severity curves are supplemented with the EGT and shaft speed scaling vector plot with respect to the take-off derate. The increasing take-off derate reduces the severity level and more phenomenal near the bump zone of one engine-off condition in the event of failure considered as -10 % take-off derate. The severity characteristics changes into a mode of constant damage beyond 10 % take-off derate as observed.

Effect of Climb Derate

The climb derate study (Appendix E) has been in similar respect to the short haul flights. The severity characteristics for engine E115, representing the large thrust engine is observed to be beneficial strategy, reducing the blade and disc severity. But has greater sensitivity on blade, and the influence of the taper and washout altitude is of litte significance with repect to the trends extracted from the climb derate study.

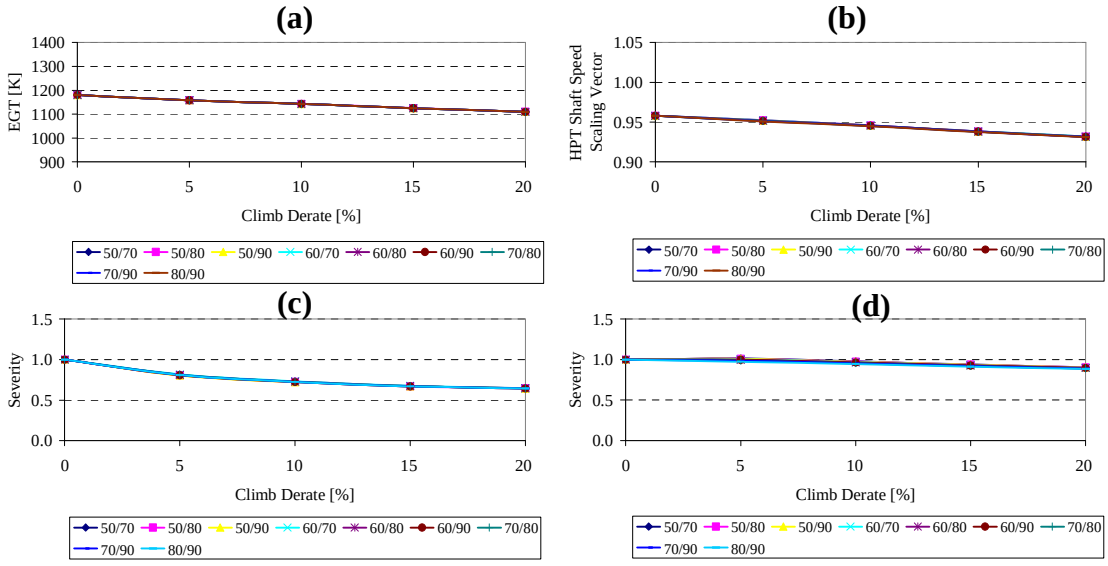

Figure 8.39 : E115 engine characteristics for variation with climb derate (a) Exhaust gas temperature (b) Shaft speed scaling vector (c) Blade Severity (d) Disc Severity.

Effect of Cruise Derate

The cruise derate is studied in similar respects to the take-off and climb derate. The large thrust engine E115 shows, reduction in the severity level, as the limiting mode of failure is creep that is sensitive with the temperature to a larger

extent. Hence the cruise derate will be suitable strategy for improving two shaft large thrust engines with high by-pass ratio, however fuel economy will receive more importance for longer mission.

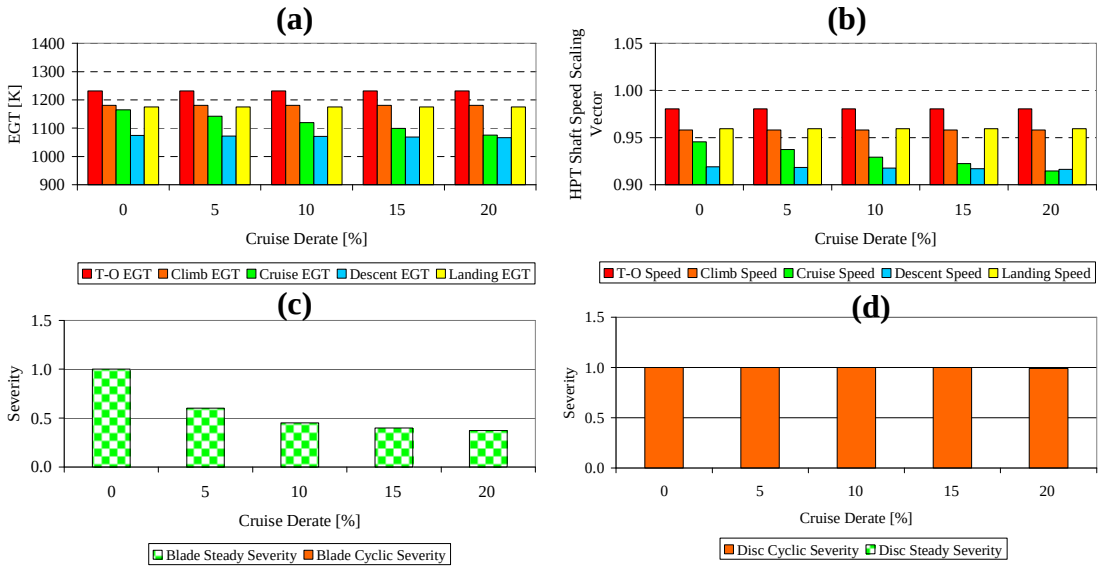

Figure 8.40 : E115 engine characteristics for variation cruise derate (a) Exhaust gas temperature (b) Shaft speed scaling vector (c) Blade Severity (d) Disc Severity.

Effect of Outside Air Temperature

The sensitivity with respect to the OAT has been narrated for the lower thrust engine, and holds good for the large thrust engines. The OAT is varied from 0 °C to 40 °C to observe the impact on the engine severity. The trends indicate tremendous increase in the severity beyond 20 °C, and the blade severity is dominant, as observed in the different studies, depicting the engine severity.

Effect of Airport Altitude

The airport altitude influences the take-off thrust as operated at different geographical regions. The parametric study involves varying the airport altitude corresponding to the take-off from 0 m to 1600 m. The study shows that the impact of the airport altitude could be considerably reduced by increasing the take-off derate, as observed for the lower thrust engines, and have similar behaviour for the large thrust engines.

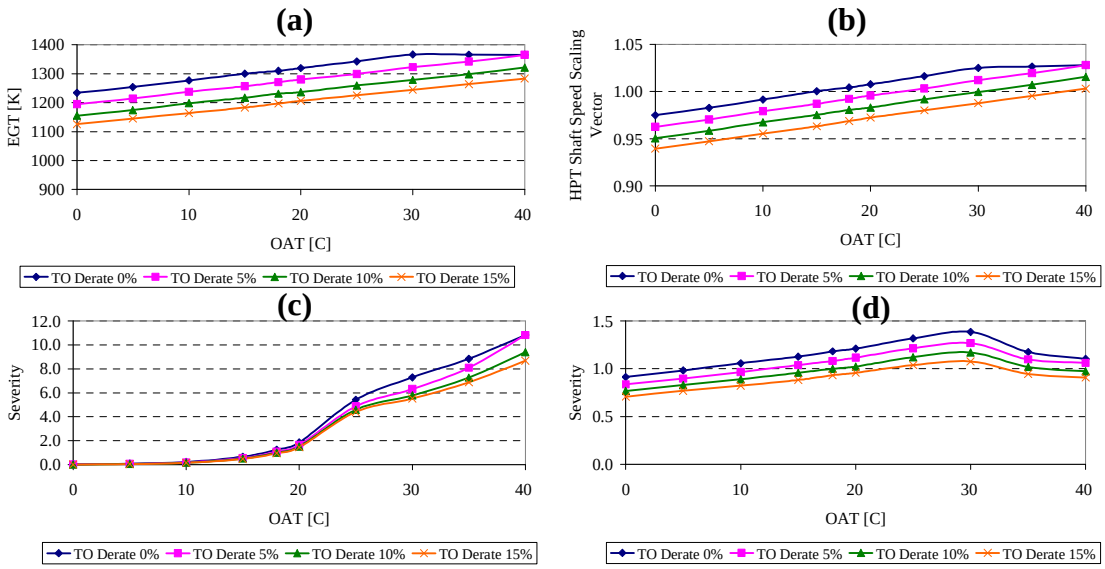

Figure 8.41 : E115 engine characteristics for variation in OAT (a) Exhaust gas temperature (b) Shaft speed scaling vector (c) Blade Severity (d) Disc Severity.

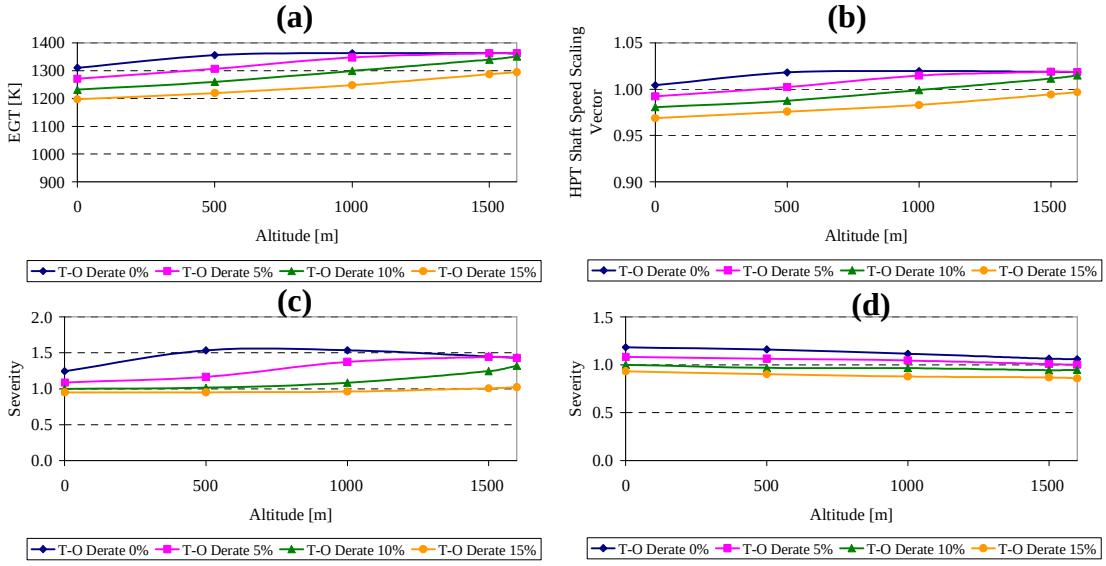

Figure 8.42 : E115 engine characteristics for variation in airport altitude (a) Exhaust gas temperature (b) Shaft speed scaling vector (c) Blade Severity (d) Disc Severity.

Effect of Cruise Altitude & Cruise Mach

The cruise altitude and Mach number has been varied to obtain the severity characteristics. A continues rise in the severity has been observed with increasing cruise altitude and Mach number for the engine E115. The severity is more for the cruise altitude and Mach number, beyond the engine manufacturers specification.

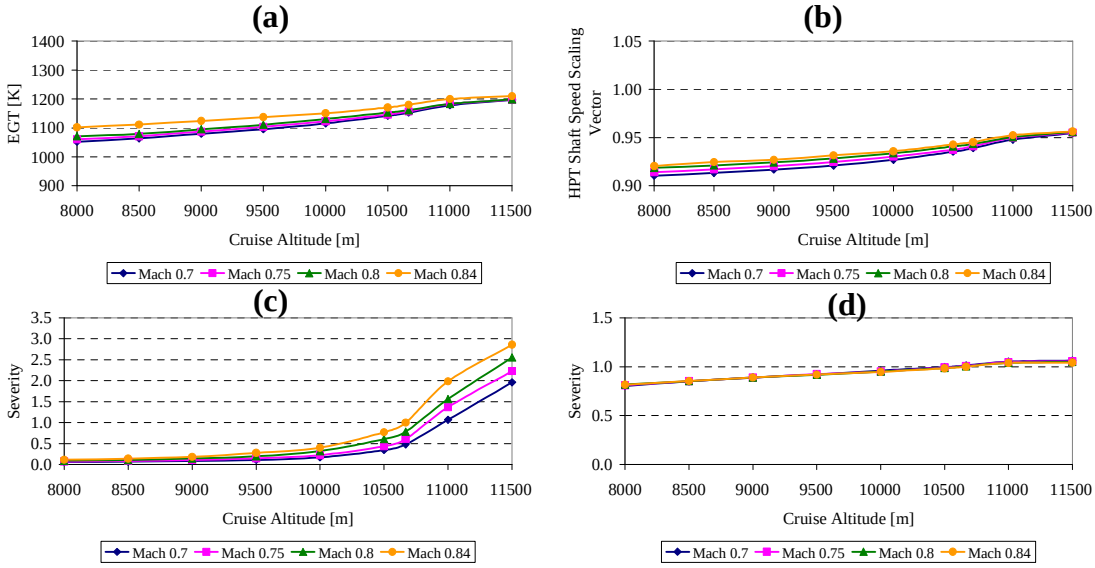

Figure 8.43 : E115 engine characteristics for variation in cruise altitude (a) Exhaust gas temperature (b) Shaft speed scaling vector (c) Blade Severity (d) Disc Severity.

8.8 Long Haul Flight – Technological Factors

The technological factors have been explored in the context of the long haul flights for the engine E115.

Cooling Effectiveness

The cooling effectiveness is a governing factor for the level of severity as observed in the study on lower thrust engines, and the argument could be extended for the large thrust engines. The increase in the cooling effectiveness, reduces the metal temperatures, and hence phenomenal improvement in the life, reducing the severity, as observed through the parametric analysis. The cooling effectiveness of 0.7 has been used for the reference mission, a sufficiently high value, however to enable the use of material, such as Rene 41 that has lower temperature limits, as compared to

the single crystal alloys and its properties are not available in open literature.

It could be observed that cooling effectiveness is responsible for lowering the severity, and a significant factor in the hands of the engine manufacturers to satisfy the industry needs.

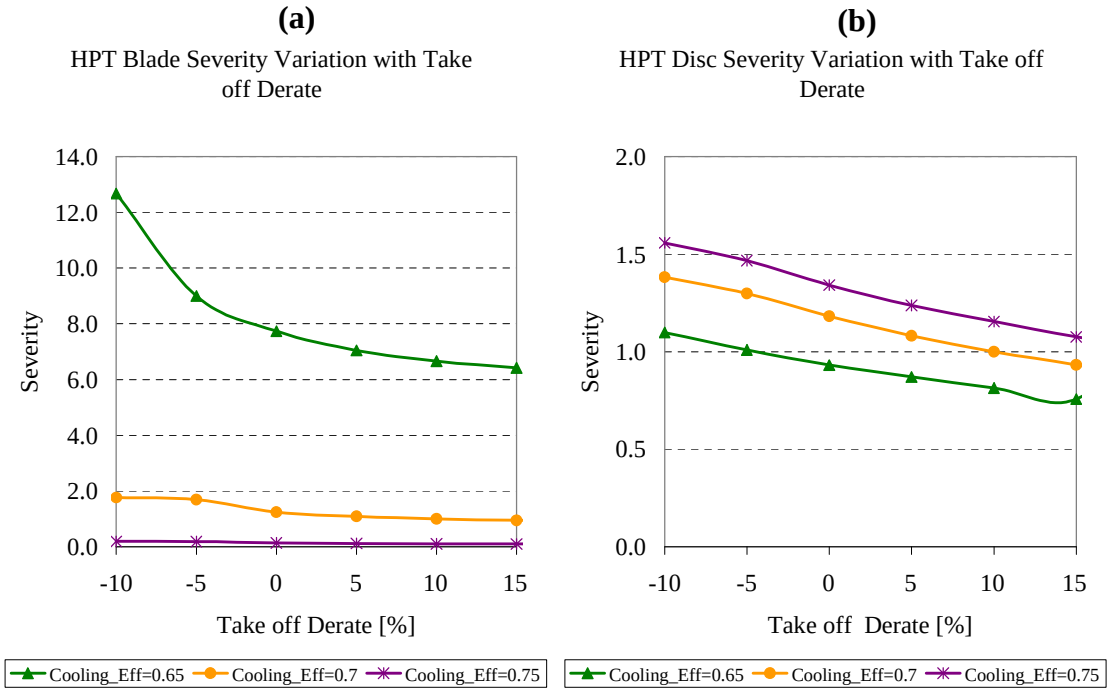

Figure 8.44 : E115 engine severity variation with blade cooling effectiveness (a) Blade severity (b) Disc severity.

Thermal Barrier Coating

The variation of the coating thickness and thermal conductivity, studied on the severity of engine E115. The increase in the coating thickness, sufficiently reduces the severity level on the blade due to temperature offset, and the limiting mode of failure being creep has greater sensitivity on the temperature. The thermal conductivity study shows that the metal temperatures are increased, and associated increase in the severity of the component .

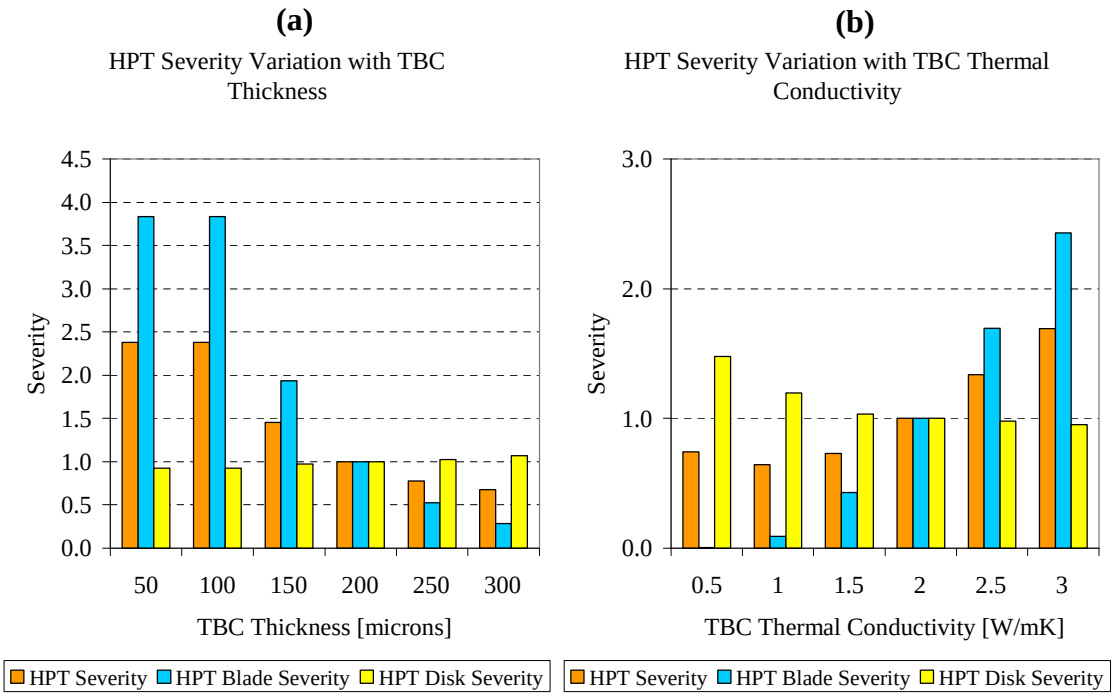

Figure 8.45 : E115 engine severity variation with thermal barrier coating (a) Thickness (b) Thermal conductivity.

Pattern Factor and Profile

The pattern factor and its profile has been studied for the large thrust engine E115. The pattern factor is varied between 0.05 to 0.25, and the location of the maximum temperature shifted to the different zones of the blade in the radial direction. The value of 1 indicates the hub radius and numbered sequentially till 5, indicating the tip region.

The pattern factor shows substantial increase in the severity level on the blade, due to the creep limiting mode, magnified due to the increase in the peak temperature.

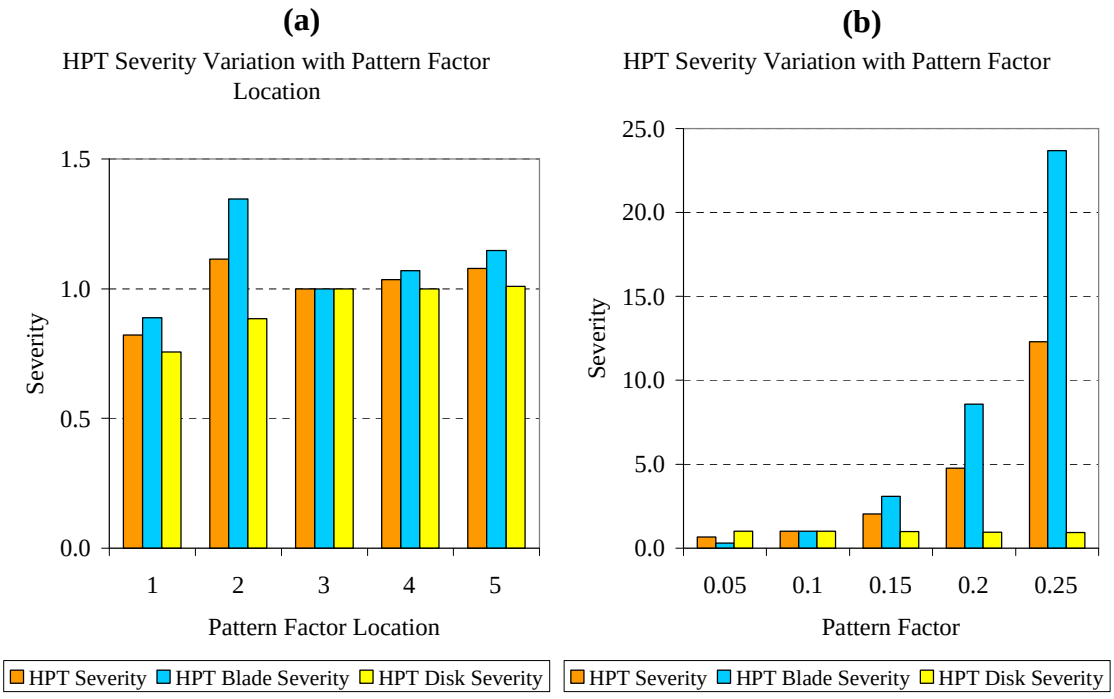

Figure 8.46 : E115 engine severity variation with pattern factor (a) Location (b) Magnitude.

8.9 Long Haul Flight – Derate Severity Curve

The derate severity curve could be developed using the severity methodology as established by the MRO. The reference mission of 4 hrs trip length, 10 % take-off derate and 18 °C OAT is normalized to a severity value of unity . With this single point reference mission, the variation in the take-off derate for various trip length has been observed.

The derate-severity curves for large thrust engines are much flatter, as compared to the lower thrust engines, as the limiting mode is creep that is dependent on the engine flight hours. The reference mission severity trend predicted through the methodology follows the MRO industry observation of decreasing severity with increasing take-off derate.

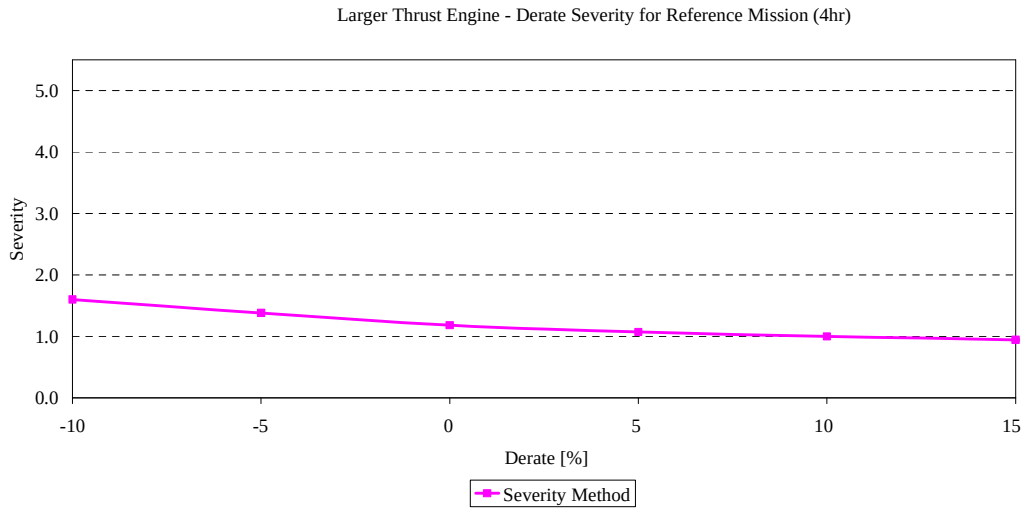

Figure 8.47 : E115 engine derate severity curve for 4 hrs mission.

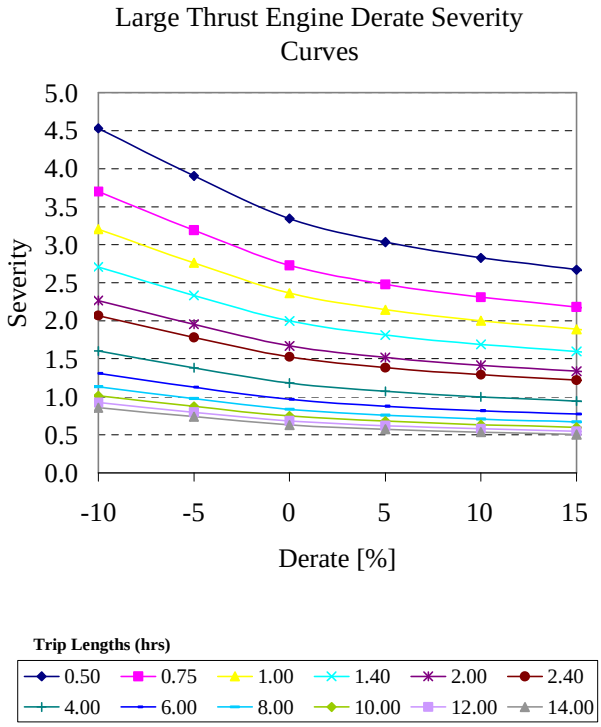

Figure 8.48 : E115 engine derate severity curves for trip lengths.

8.10 Long Haul Flight – Operational Factors Study – Engine E84 and E95

The competitive long haul flight application has been further explored with engine models of E84 and E95 having challenging designs with respect to operational factors. The parametric studies involving the operational factors are conducted by keeping the technological factors constant.

Effect of Take-off Derate

The take-off derate study with the change in the derate from -10 % to 20 % has been conducted for the severity estimation. The severity curve falls steeply between -10 % to 10 % derate. The trends become much flatter for derates over 10 %. EGT and shaft speed are inline with the observations on the severity for the two engines.

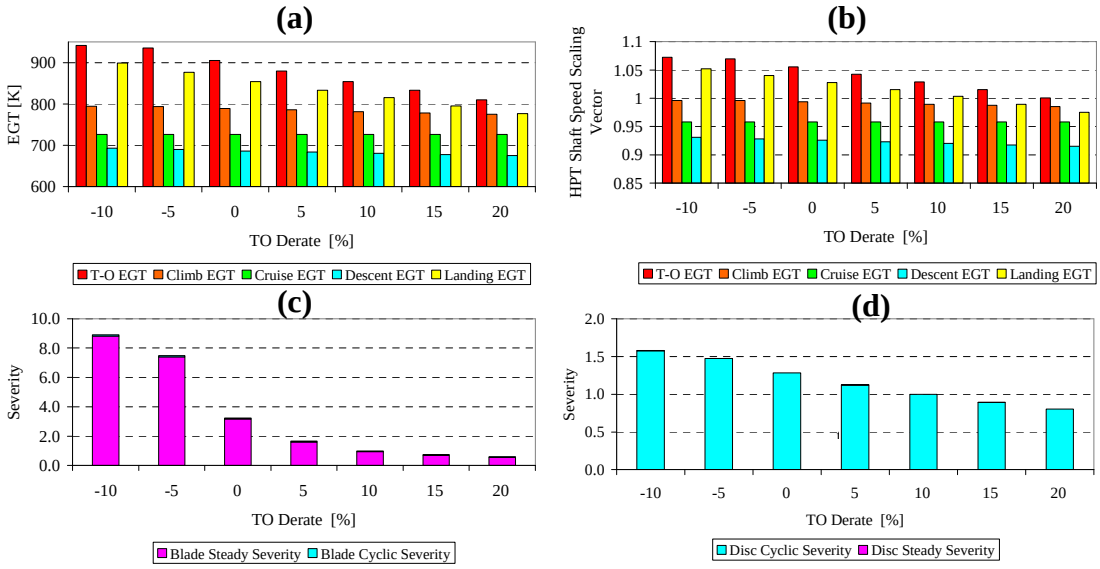

Figure 8.49 : E84 engine characteristics for variation in take-off derate (a) Exhaust gas temperature (b) Shaft speed scaling vector (c) Blade Severity (d) Disc Severity.

Effect of Climb Derate

The effect of climb on long haul flights has been carried out, by varying the climb derate at certain taper and washout altitude for the two shaft configuration of engine E84, and the three shaft configuration of E95. The severity study indicates, three shaft design with climb derate has lower severity, as compared

to the two shaft design. Hence will have appreciable benefits on three shaft designs.

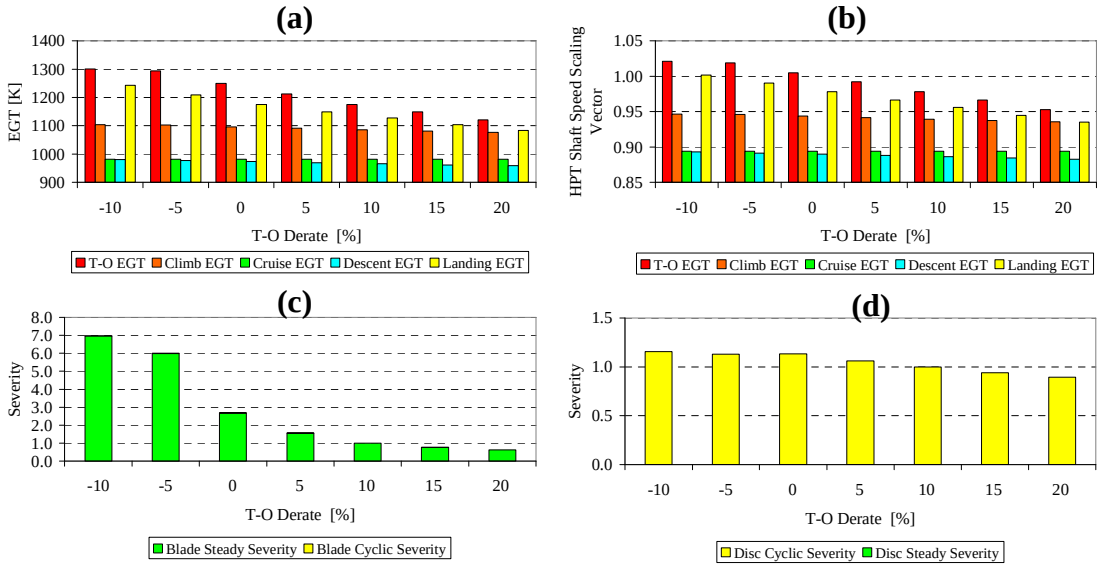

Figure 8.50 : E95 engine characteristics for variation in take-off derate (a) Exhaust gas temperature (b) Shaft speed scaling vector (c) Blade Severity (d) Disc Severity.

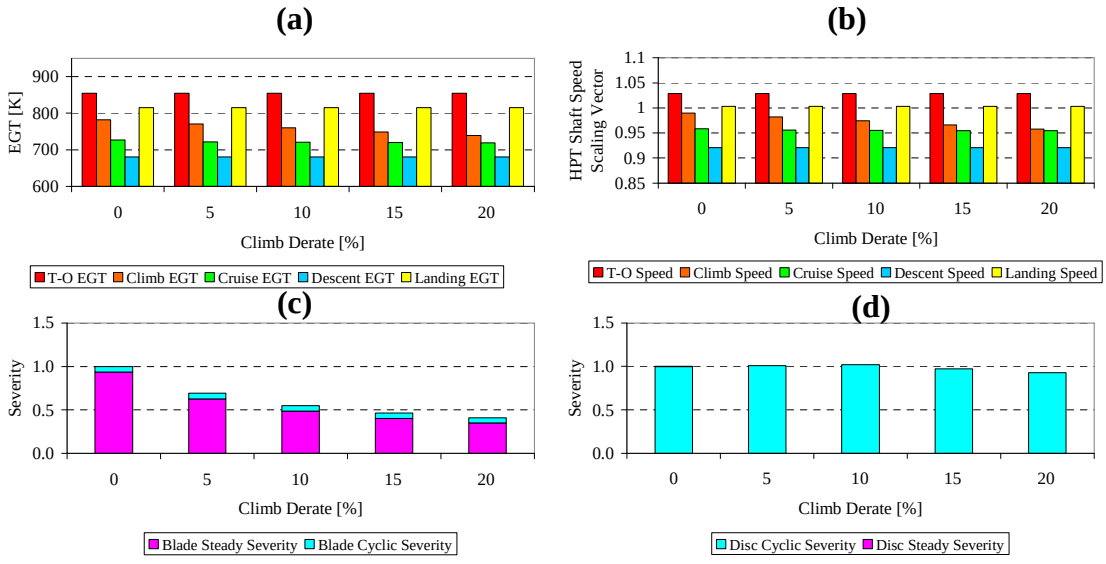

Figure 8.51 : E84 engine characteristics for variation in climb derate (a) Exhaust gas temperature (b) Shaft speed scaling vector (c) Blade Severity (d) Disc Severity.

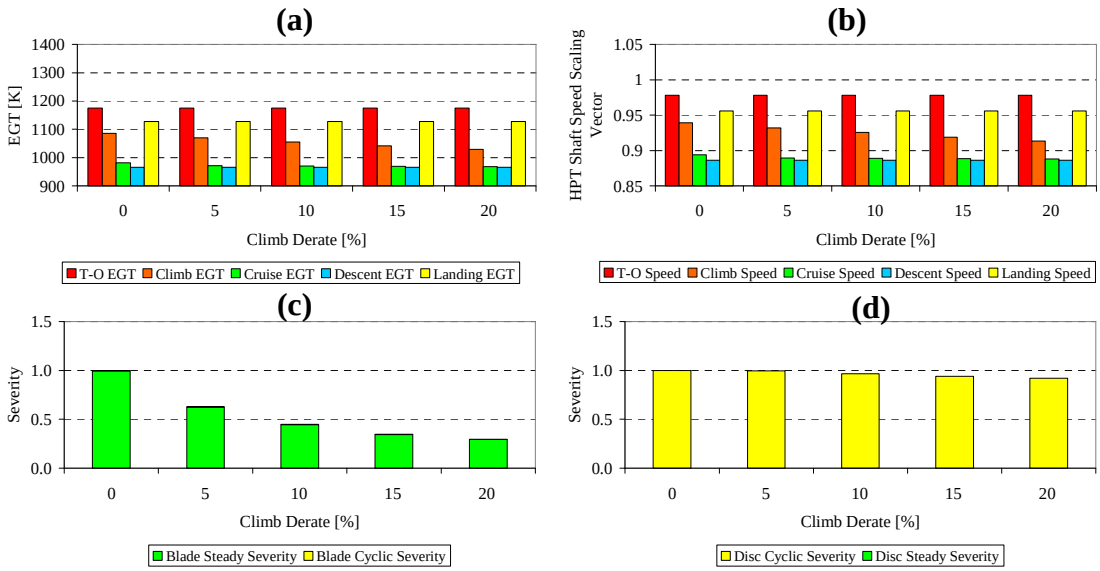

Figure 8.52 : E95 engine characteristics for variation in climb derate (a) Exhaust gas temperature (b) Shaft speed scaling vector (c) Blade Severity (d) Disc Severity.

Effect of Cruise Derate

The cruise derate has been changed, between 0 % to 20 % for possible benefits, in their use for the large thrust engines, as part of their mission. The decrease in the severity is not appreciable, and will not be of much significance for the large thrust engines E84 and E95.

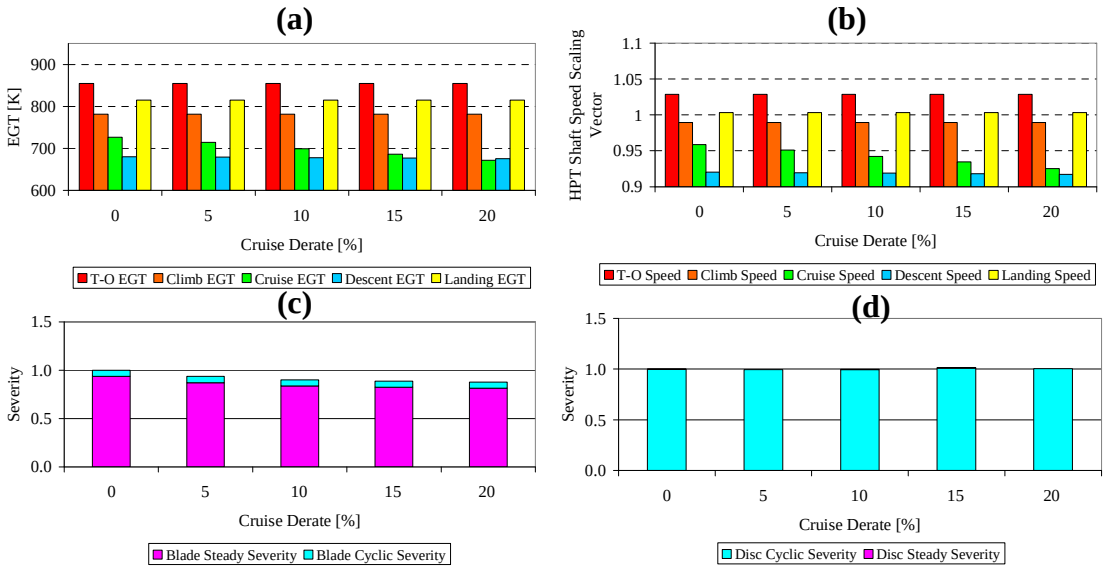

Figure 8.53 : E84 engine characteristics for variation in cruise derate (a) Exhaust gas temperature (b) Shaft speed scaling vector (c) Blade Severity (d) Disc Severity.

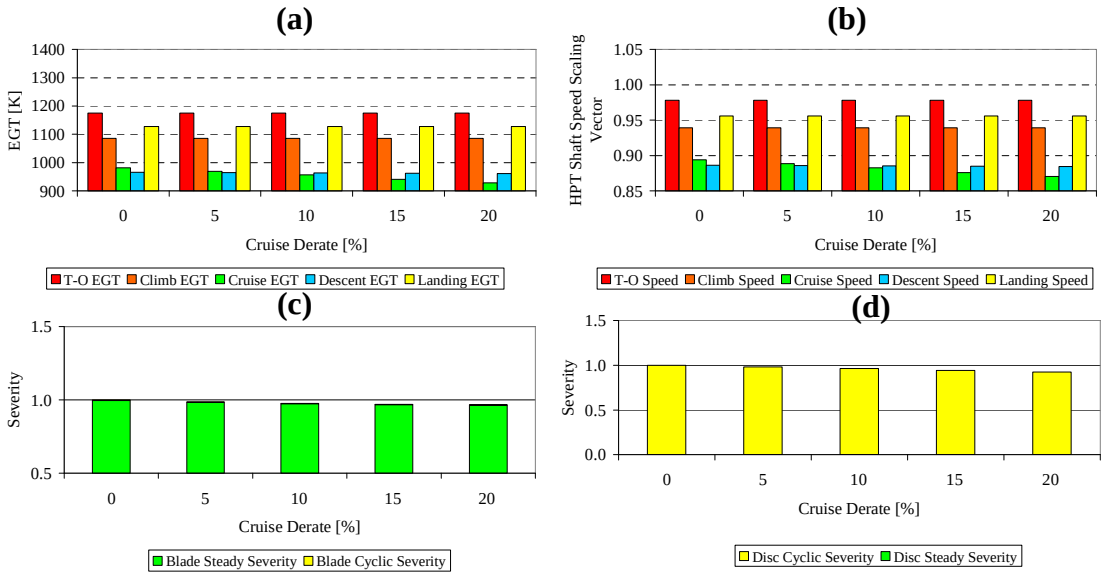

Figure 8.54 : E95 engine characteristics for variation in cruise derate (a) Exhaust gas temperature (b) Shaft speed scaling vector (c) Blade Severity (d) Disc Severity.

Effect of Outside Air Temperature

The effect of the OAT on the two engine models, indicates a continuous increase in the severity, and higher for the engine E84, as compared to E95. The technology level for the different engines differ in reality, the required severity level is based on cooling effectiveness and thermal barrier coating.

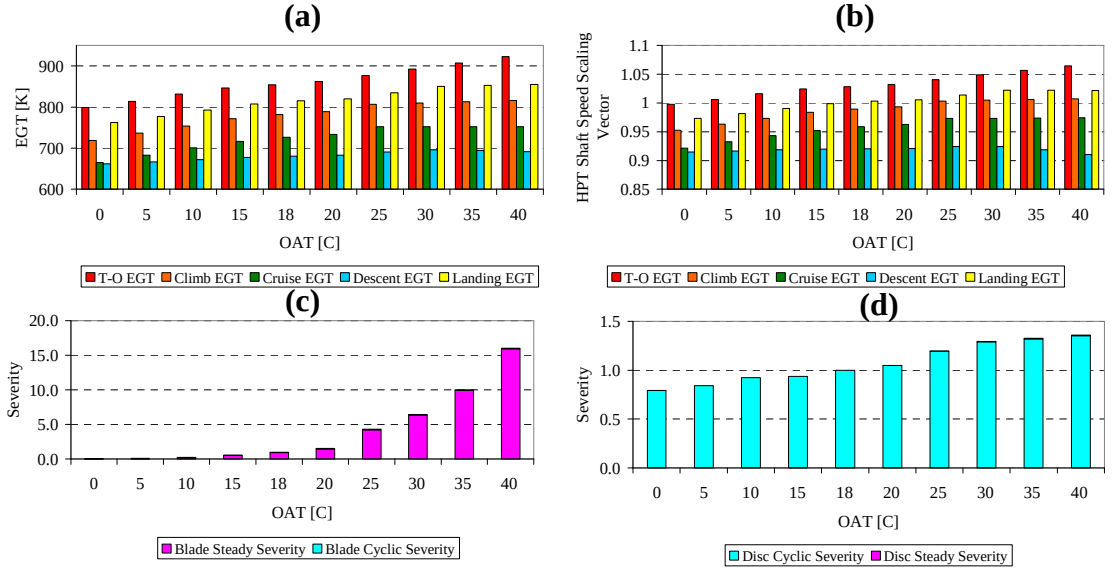

Figure 8.55 : E84 engine characteristics for variation in OAT (a) Exhaust gas temperature (b) Shaft speed scaling vector (c) Blade Severity (d) Disc Severity.

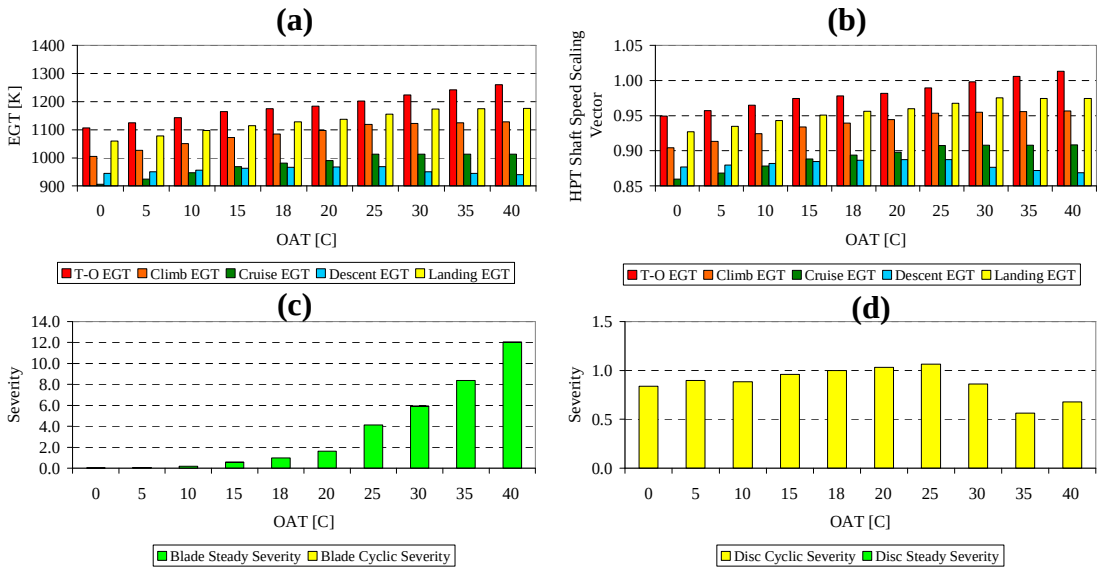

Figure 8.56 : E95 engine characteristics for variation in OAT (a) Exhaust gas temperature (b) Shaft speed scaling vector (c) Blade Severity (d) Disc Severity.

Effect of Airport Altitude

The airport altitude has been studied from sea level to 1600 m for the large thrust engines that indicates increasing severity with increasing altitude. The severity level could be reduced, as suggested for lower thrust and large thrust engines through increasing the take-off derate.

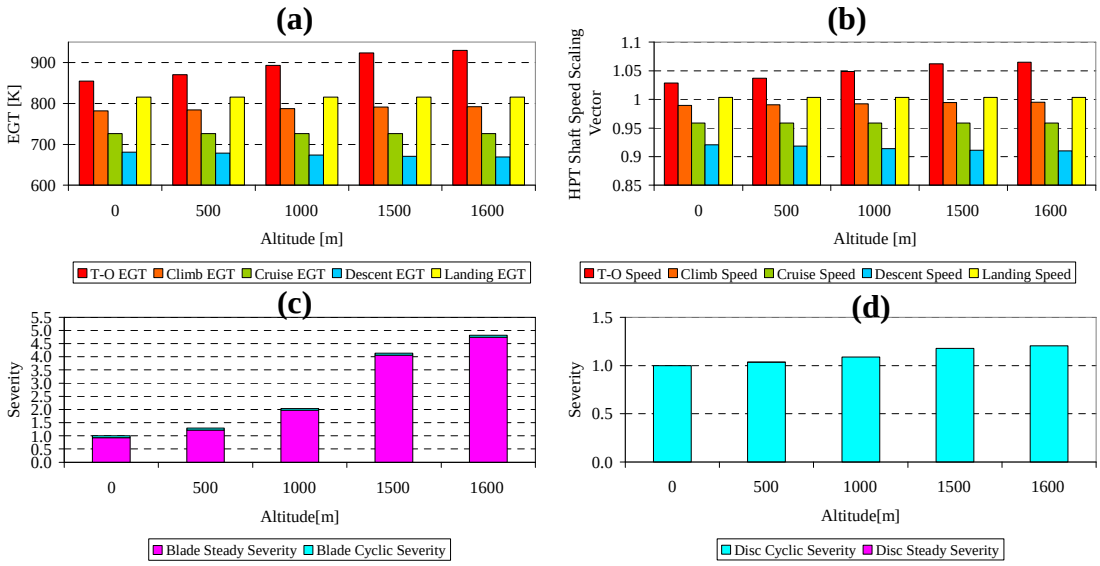

Figure 8.57 : E84 engine characteristics for variation in airport altitude (a) Exhaust gas temperature (b) Shaft speed scaling vector (c) Blade Severity (d) Disc Severity.

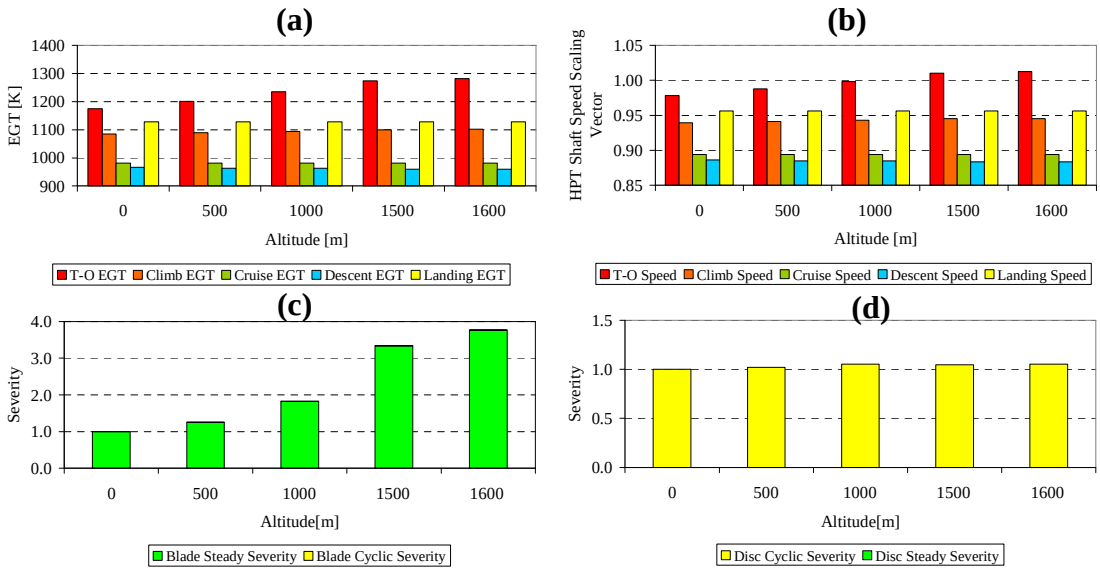

Figure 8.58 : E95 engine characteristics for variation in airport altitude (a) Exhaust gas temperature (b) Shaft speed scaling vector (c) Blade Severity (d) Disc Severity.

Effect of Cruise Altitude & Cruise Mach

The cruise parameters for the large thrust engines has been varied to identify the operational sensitivity on the severity which reveal a monotonous increase in blade severity, in similar respects for both the designs.

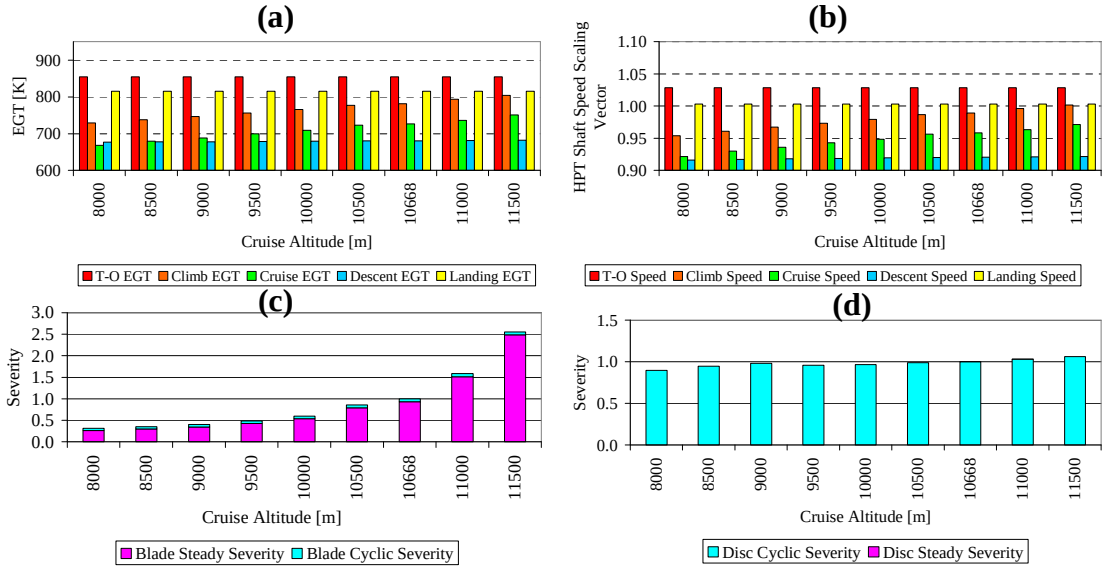

Figure 8.59 : E84 engine characteristics for variation in cruise altitude (a) Exhaust gas temperature (b) Shaft speed scaling vector (c) Blade Severity (d) Disc Severity.

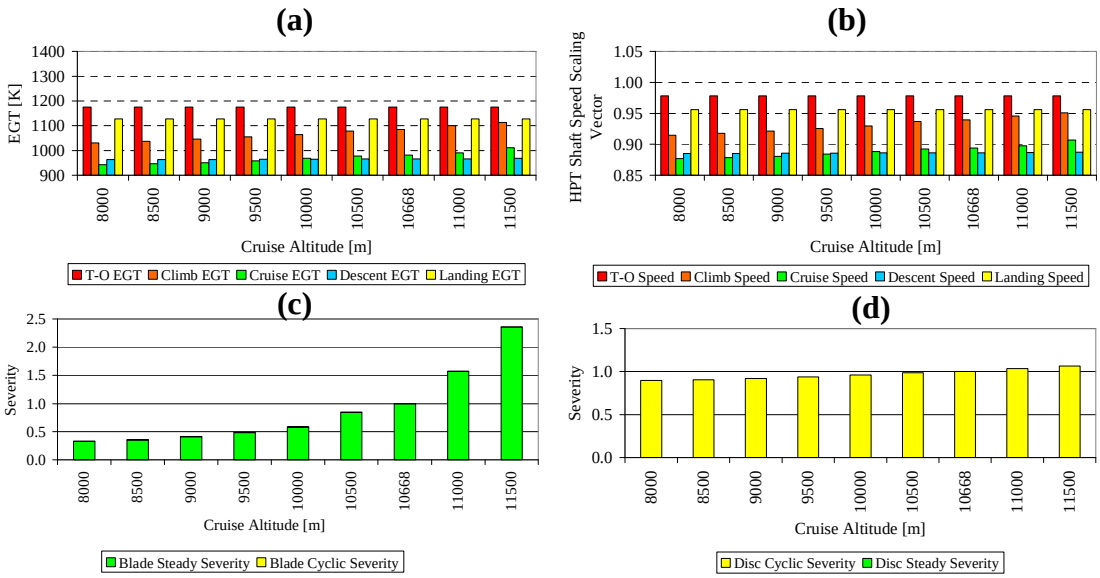

Figure 8.60 : E95 engine characteristics for variation in cruise altitude (a) Exhaust gas temperature (b) Shaft speed scaling vector (c) Blade Severity (d) Disc Severity.

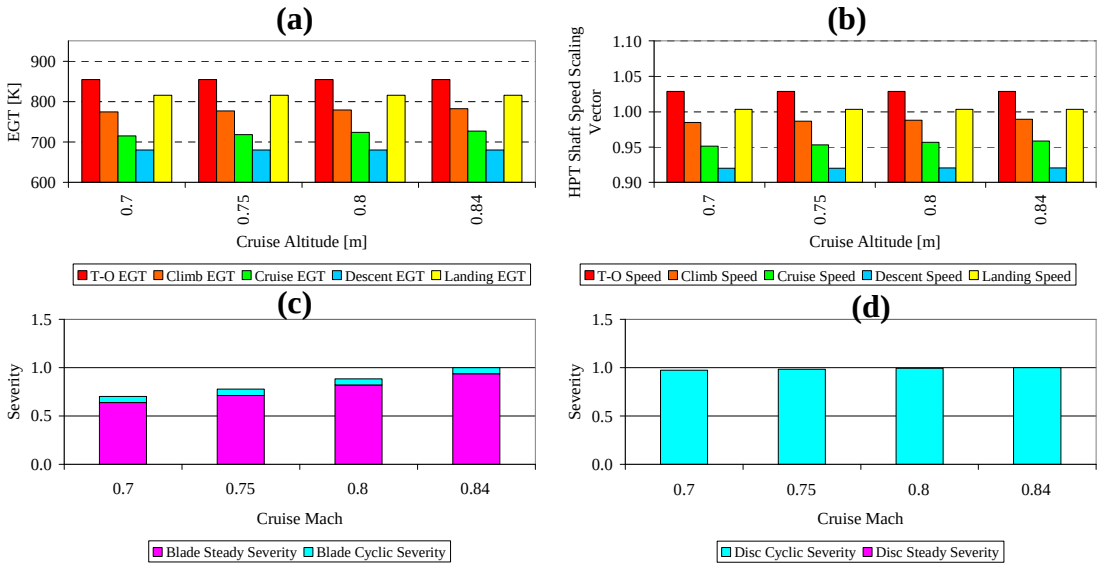

Figure 8.61 : E84 engine characteristics for variation in cruise Mach (a) Exhaust gas temperature (b) Shaft speed scaling vector (c) Blade Severity (d) Disc Severity.

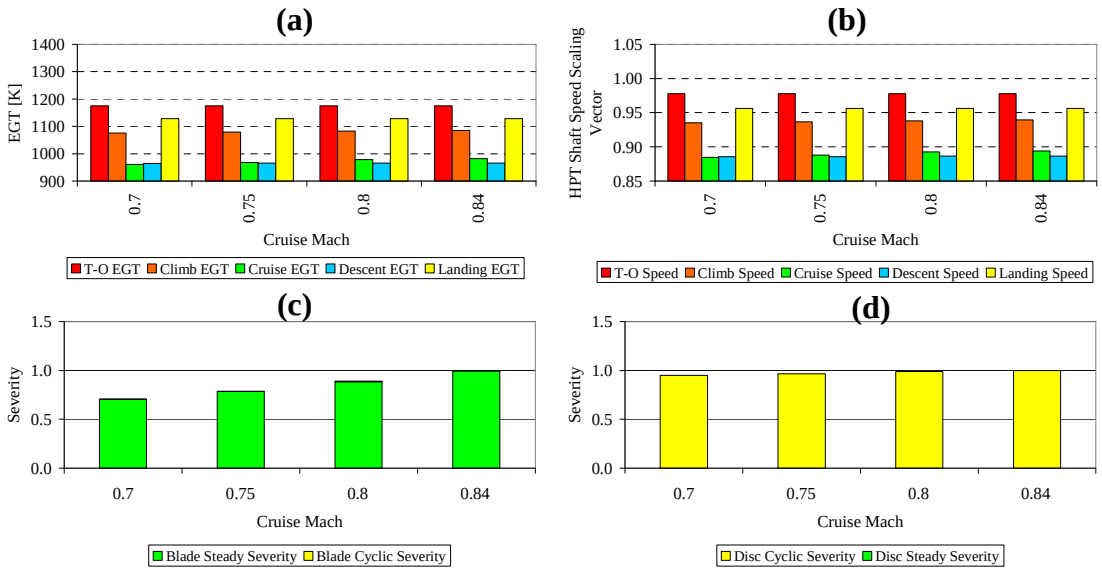

Figure 8.62 : E95 engine characteristics for variation in cruise Mach (a) Exhaust gas temperature (b) Shaft speed scaling vector (c) Blade Severity (d) Disc Severity.

8.11 Long Haul Flight – Operational Factors Study – Comparison of Engines

The wide body aircraft operated with large thrust engines have different design philosophies, adopted by the engine manufacturers. The engine E115 with two shaft design has variable stator vanes for the compressor stability and high pressure ratio, having the largest take-off thrust. The engine E95, a three shaft design for compactness to reduce weight, enabled by achieving high pressure ratio due to three levels of shaft speed has been explored and compared. The engine E84 that has lower thrust among this category is a two shaft configuration. Hence three engines operated at different level of thrust, using intricate designs has been compared to comprehend the behaviour with respect to operational factors and its impact on HPT blade severity, HPT disc severity and an average represented as HPT severity, being of paramount importance for insight on civil aviation.

Effect of Take-off Derate

The take-off thrust, a significant factor governing the temperature and shaft speed is pertinent in the severity trends. This factor is more impactful on the

HPT turbine blade, as compared to the disc. The change in the severity as observed with the different engines, shows much flatter response for E115. However for the comparison same level of technology factors such as cooling effectiveness, thermal barrier coating and pattern factor are used for the analysis. The different engine manufacturers use suitable technological factors to reduce the sensitivity level.

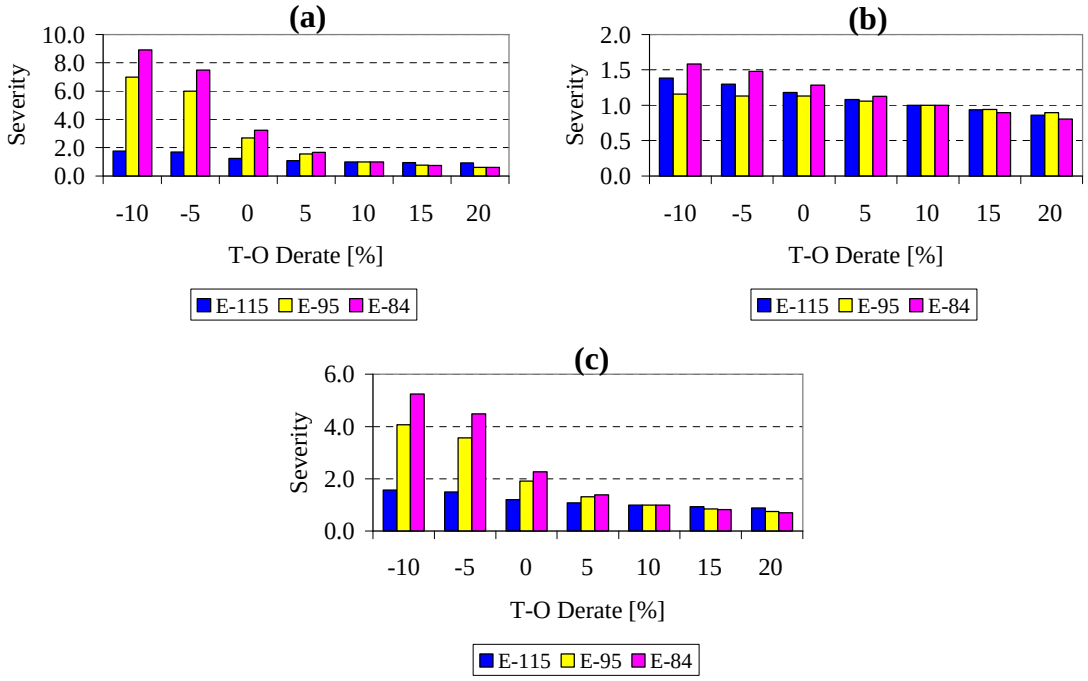

Figure 8.63 : Large thrust engines comparison for take-off derate characteristics (a) Blade severity (b) Disc severity (c) HPT severity.

Effect of Climb Derate

As the focus has been in lowering the maintenance cost, the segments apart from take-off have been receiving due importance. In the demand for the thrust of an aircraft, the climb thrust is important in reaching the cruise altitude. The engine manufacturers have done interesting studies highlighting the importance of using the climb derate. The three engines are compared on a similar derate strategy that reveal three shaft configurations have lower severity, and hence more benefits to be availed as compared to two shaft designs.

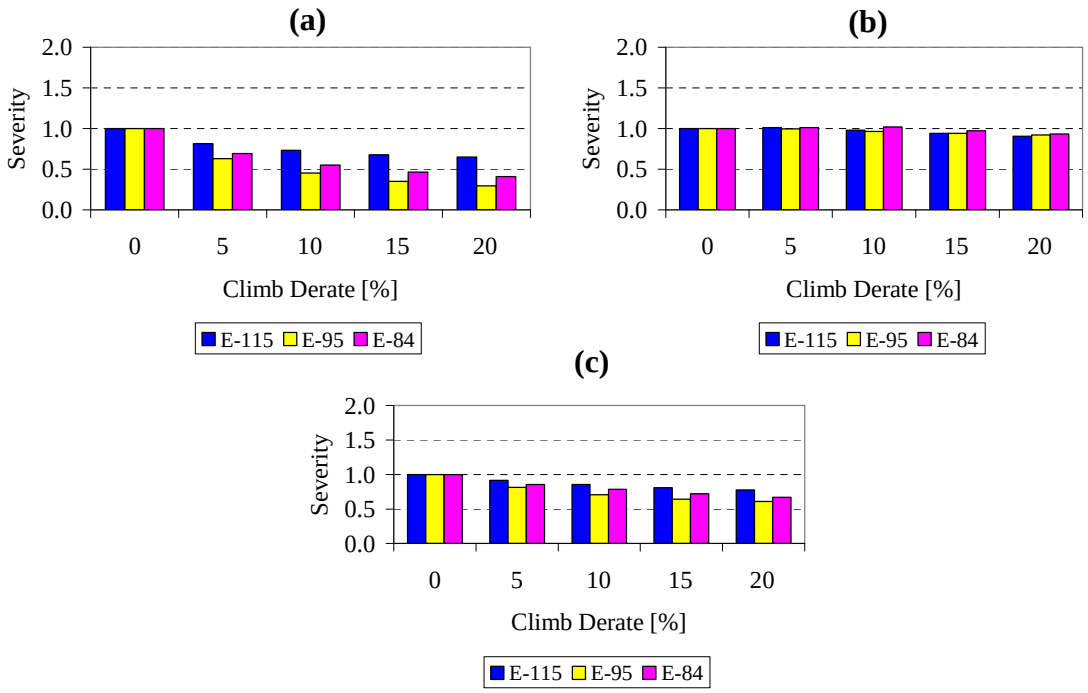

Figure 8.64 : Large thrust engines comparison for climb derate characteristics (a) Blade severity (b) Disc severity (c) HPT severity.

Effect of Cruise Derate

The twin aisle aircraft used on the long range missions have larger slice of time spent at cruise. The use of derate at cruise will play a part on severity as the turbine blade life is creep limited for large thrust engines. The E115 and E84 engines respond to the cruise derate, in a similar fashion as they have a two shaft design and severity is more sensitive to large by-pass engines among these configurations.

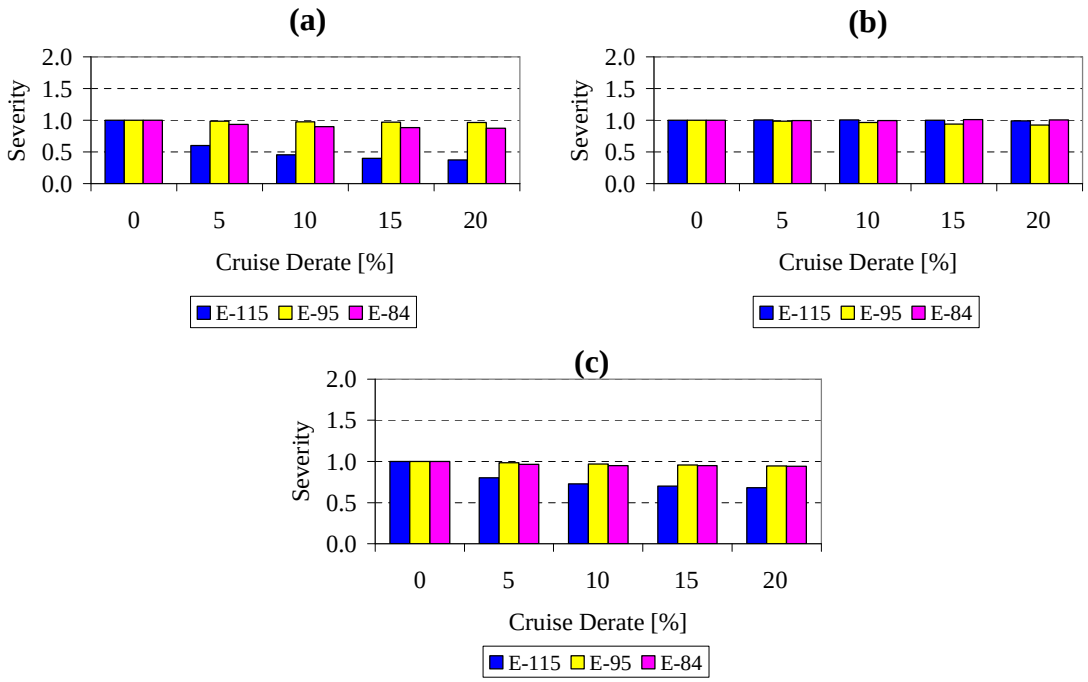

Figure 8.65 : Large thrust engines comparison for cruise derate characteristics (a) Blade severity (b) Disc severity (c) HPT severity.

Effect of Outside Air Temperature

The response of the large thrust engines with respect to the influencial parameter of OAT will be of much interest with airliners. The characteristics of the three engines have similar trends, and the sensitivity can be levelled up through the choice of technological factors.

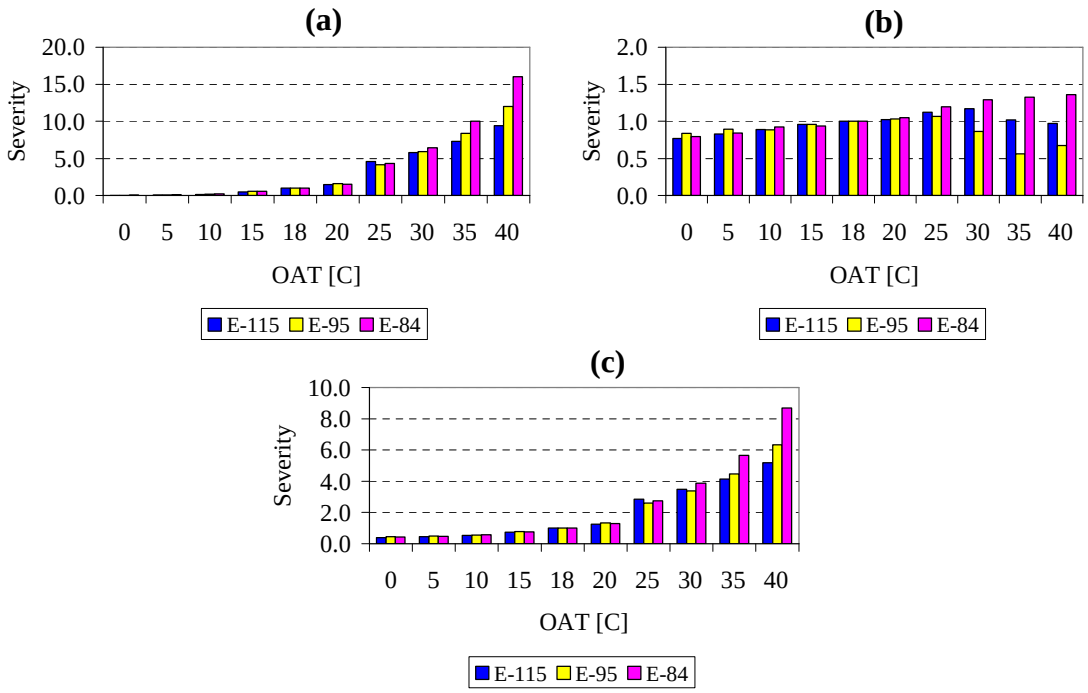

Figure 8.66 : Large thrust engines comparison for variation in OAT (a) Blade severity (b) Disc severity (c) HPT severity.

Effect of Airport Altitude

The severity increase with respect to the altitude is consequent in the thrust characteristics with altitude, where the E115 shows strong points in lowering the severity. This can be attributed to large by-pass flow among the compared engines. The airport altitude does not have much impact on disc severity for the three designs.

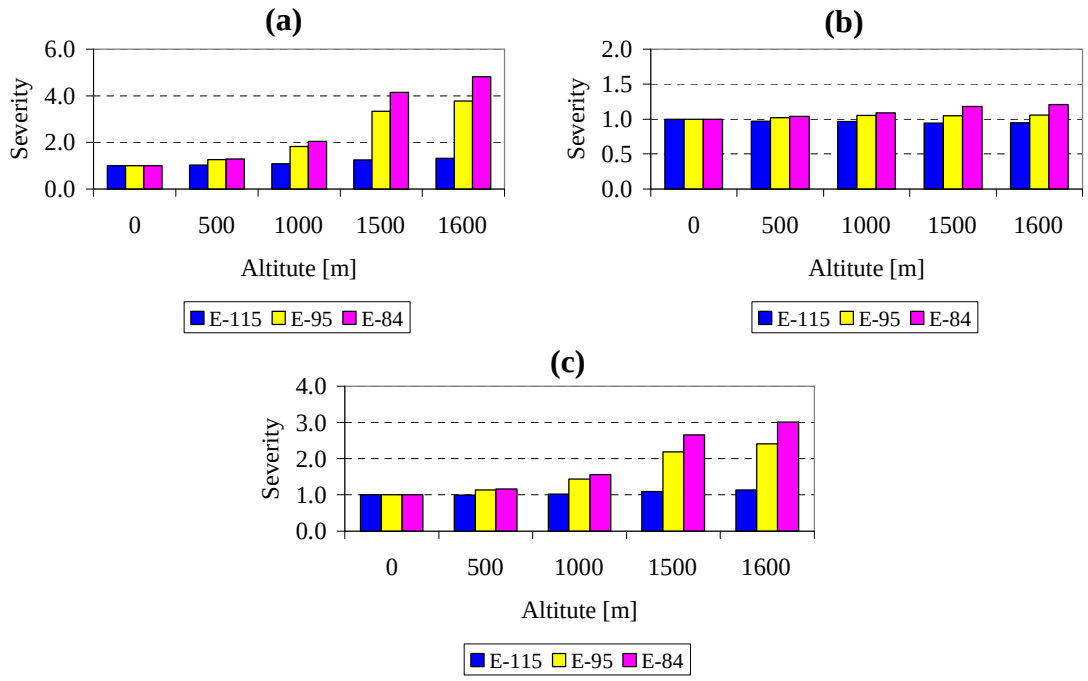

Figure 8.67 : Large thrust engines comparison for variation in airport altitude (a) Blade severity (b) Disc severity (c) HPT severity.

Effect of Cruise Altitude & Cruise Mach

Through the studies varying the cruise altitude keeping the same level of cruise thrust has been investigated. The engines have the severity increasing with altitude due to constraint of use in same thrust settings. The Mach number at cruise altitude reveals lower severity at lower Mach number. The use of lower Mach number away from the optimal value will penalize the fuel consumption hence not feasible in the economical perspective.

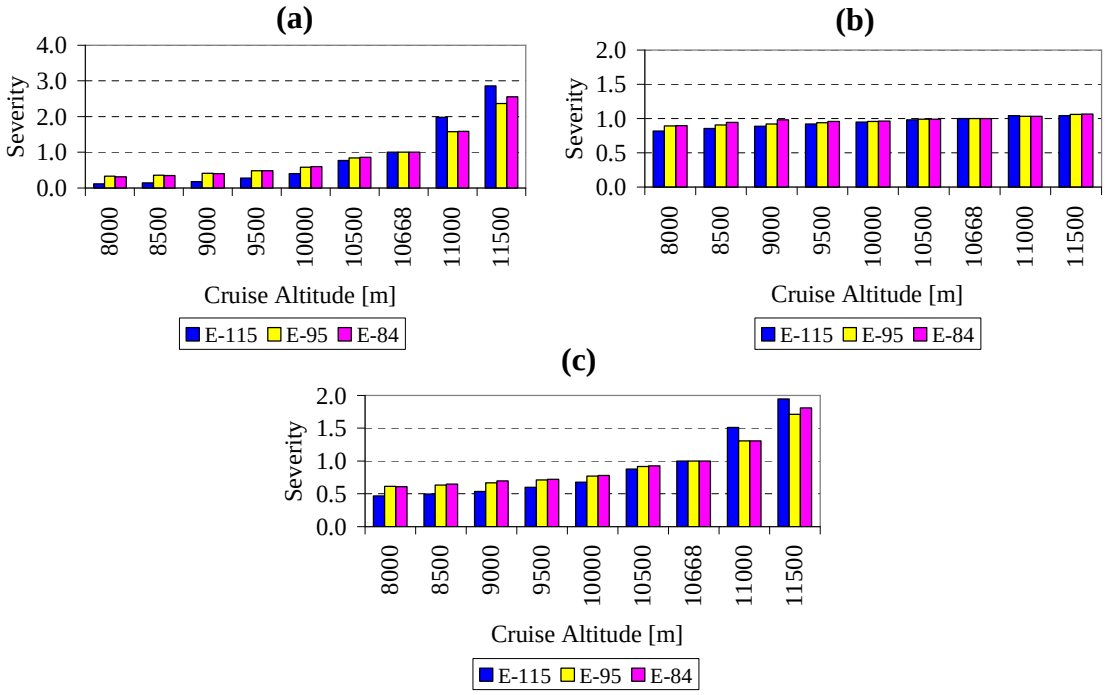

Figure 8.68 : Large thrust engines comparison for variation in cruise altitude (a) Blade severity (b) Disc severity (c) HPT severity.

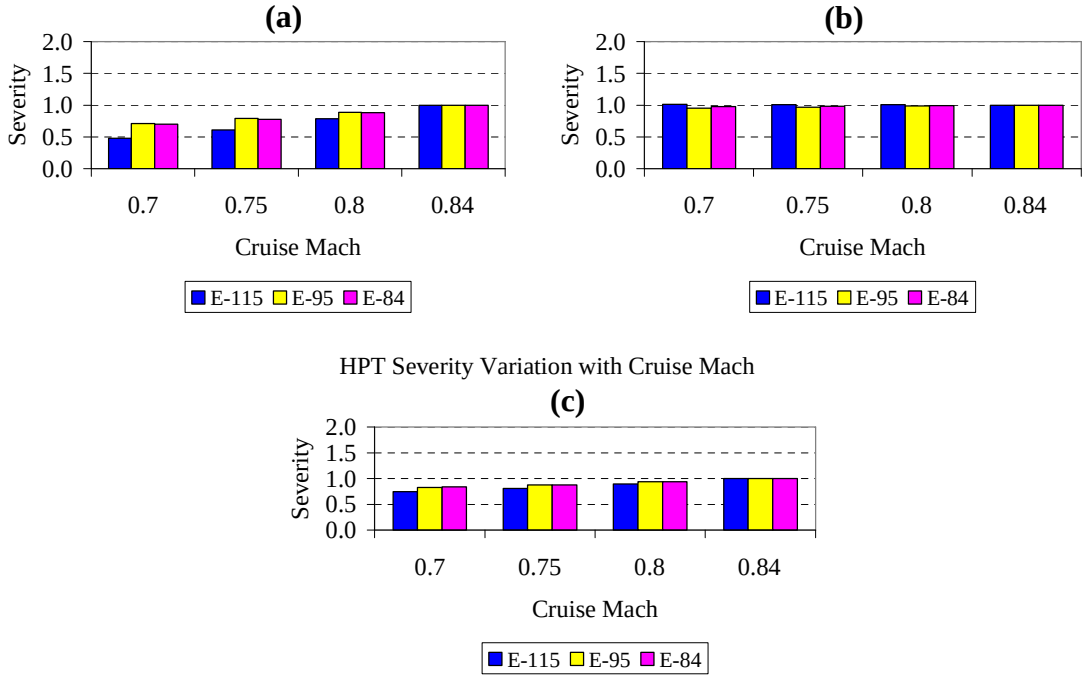

Figure 8.69 : Large thrust engines comparison for variation in cruise Mach (a) Blade severity (b) Disc severity (c) HPT severity.

8.12 Severity Sensitivity Analysis on Operational Factors

The operational factors through parametric studies have been portrayed in the characteristic curves. For better insight on the relative scale with each other, an attempt has been to bring out the sensitivity of all factors, and quantify the changes on a linear basis. The variation in severity with respect to operational factors follow a higher order curve, however a linear curve fitting has been performed for simplicity and facilite comparison.

The sensitivity analysis observations are with respect to the engine models, E56 under lower thrust class, and E115, E95 and E84 under the large thrust category. The technological factors are maintained constant for the parametric analysis on the operational factors.

The HPT blade and the disc have been analyzed to depict the engine severity and the trends have followed closely with respect to MRO curves.

Lower Thrust Engines

- HPT blade and disc severity has a dominant part of cyclic damage induced by low cycle fatigue as compared to steady state damage due to creep and oxidation.
- Take-off derate and OAT are critical operational factors impacting the severity of the engine.
- The effect of airport altitude on severity could be minimized by the use of suitable take-off derate.
- The use of climb and cruise derate will yield marginal benefits on the life of the blade and the disc.
- The increase in the cruise altitude and Mach number in keeping the same thrust level will reduce the life of the blade and the disc.

The change in the severity for the lower thrust engine is available in Table 8.10.

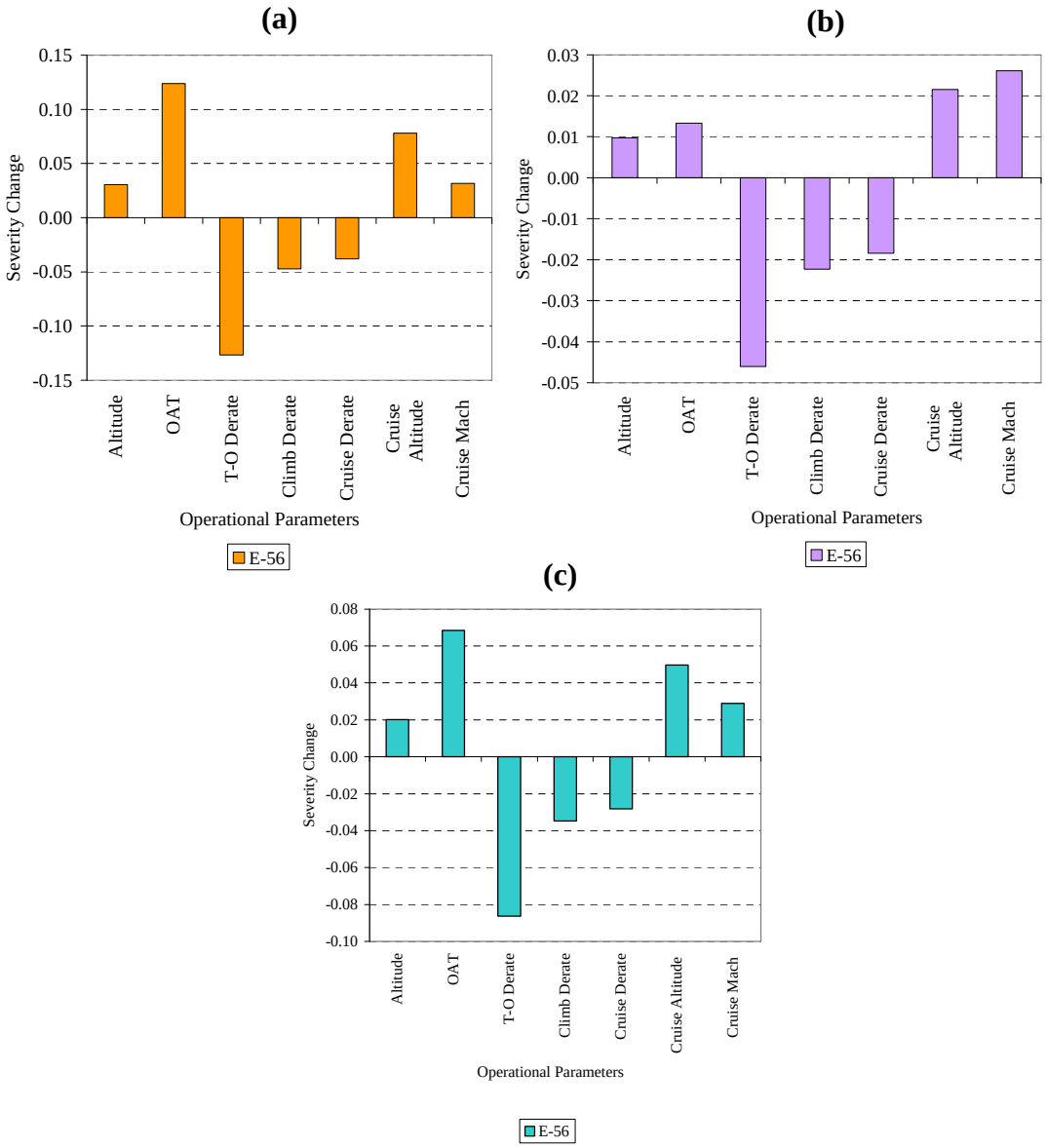

Figure 8.70 : Lower thrust engine severity sensitivity for operational factors (a) Blade severity (b) Disc severity (c) HPT severity.

E56 HPT		
Operational Parameters	Increment value	Severity Change
Altitude [m]	500	0.020
OAT [C]	5.00	0.069
T-O Derate [%]	5	-0.086
Climb Derate [%]	5	-0.035
Cruise Derate [%]	5	-0.028
Cruise Altitude [m]	500	0.050
Cruise Mach	0.05	0.029

Table 8.10 : Lower thrust engine severity sensitivity values for operational factors.

Large thrust Engines

- HPT blade is life limited by creep while the disc is life limited by low cycle fatigue.
- Take-off derate and OAT are important factors affecting the severity of the engine.
- Largest by-pass ratio engines have flatter response on severity with respect to operational factors.
- The effect of airport altitude on severity could be levelled up by the use of suitable take-off derate.
- The use of climb derate will improve the disc life by more margin as compared to blade.
- The climb derate will be more significant for three shaft engine severity as compared to two shaft engines.
- The increase in the cruise altitude and Mach number will be detrimental for the engine life.
- Two shaft engines with largest by-pass ratio have lower severity for increase in cruise altitude and Mach number.

The change in the severity for the large thrust engine is available in Table 8.11.

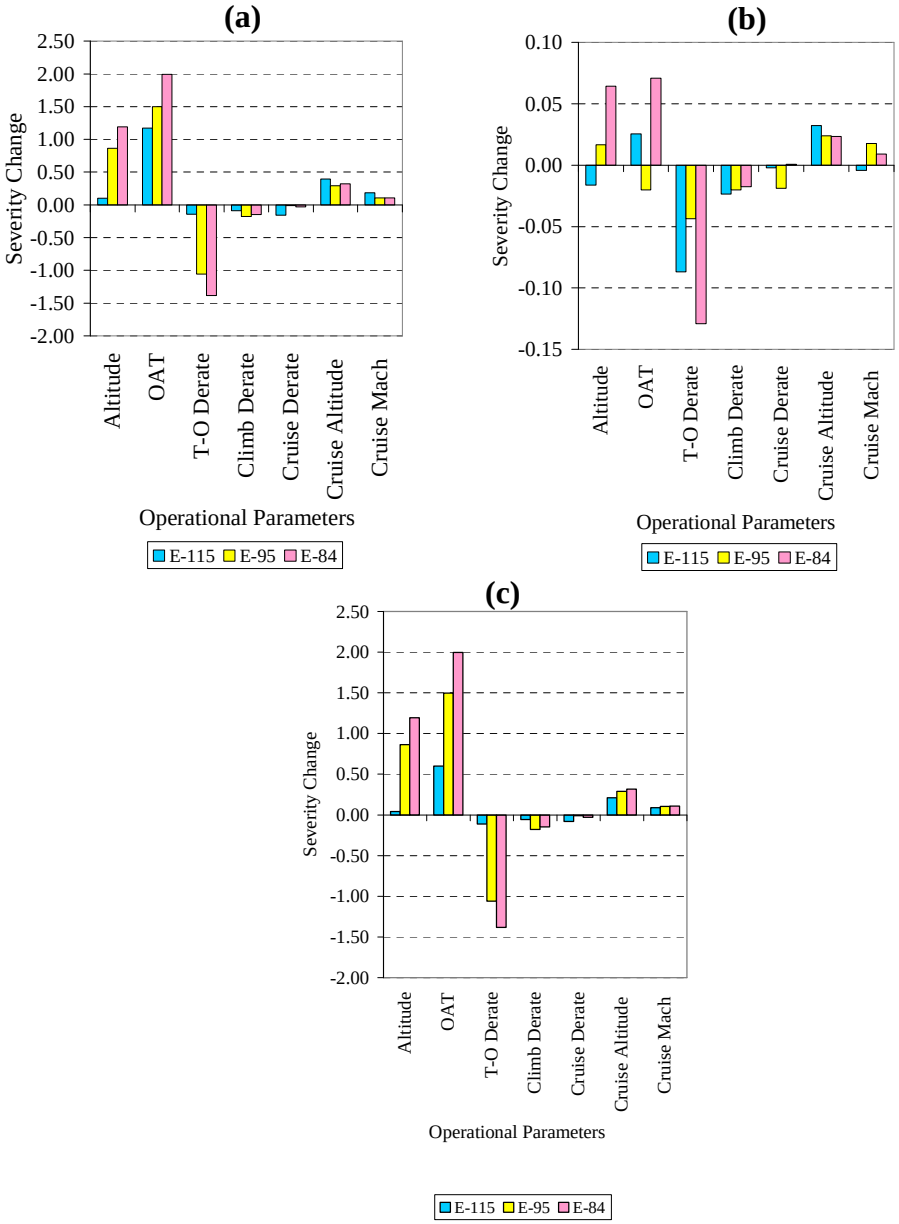

Figure 8.71 : Large thrust engine severity sensitivity on operational factors (a) Blade severity (b) Disc severity (c) HPT severity.

		E-115	E-95	E-84
Operational Parameters	Increment value	Severity Change	Severity Change	Severity Change
Altitude [m]	500	0.04	0.44	0.63
OAT [C]	5	0.60	0.74	1.03
TO Derate [%]	5	-0.11	-0.55	-0.76
Climb Derate [%]	5	-0.06	-0.10	-0.08
Cruise Derate [%]	5	-0.08	-0.01	-0.02
Cruise Altitude [m]	500	0.21	0.16	0.17
Cruise Mach	0.05	0.09	0.06	0.06

Table 8.11 : Large thrust engines severity sensitivity values for operational factors.

8.13 Severity Case Studies Summary

The severity factor estimated through the methodology is based on the information from the available literature, but could capture the trends and behaviour of aircraft engines from a relative perspective. The cascading of the data from aircraft performance as thrust variation into life consumption as severity estimate has been illustrated for the lower thrust and large thrust engines.

The impact of operational factors such as take-off derate, climb derate, cruise derate, OAT, airport altitude, cruise altitude and cruise Mach number has been observed for lower thrust and large thrust engines.

The concurrent technologies such as blade cooling and thermal barrier coating have been studied for the importance on severity of the component. Pattern factor and profile has been incorporated in the studies.

HPT blade and disc severity represents the engine severity to a larger part as observed to be a close match with the MRO curves for the reference mission.

Lower thrust engines have the life limiting phenomenon due to low cycle fatigue for the blade and disc. The large thrust engines experience creep as the limiting failure mode for the blade and low cycle fatigue for the disc.

The take-off derate and OAT are two important operational factors that will impact the maintenance cost as evident in the sensitivity on severity.

The airport altitude increases the severity on the engine however could be minimized through the use of take-off derate.

The climb derate will provide marginal benefits in lowering the maintenance cost. Three shaft engine will reap more benefits as compared to two shaft

engines.

The severity sensitivity is flatter for largest by-pass ratio engines. The effect of cruise derate will enhance the engine life for such engines.

Increase in the cruise altitude and Mach number for the same level of thrust will be detrimental to the engine life.

The blade cooling and thermal barrier coating are influencial in altering the sensitivity to severity. The engine manufacturers adopt suitable technology level, concurrent with the design to achieve a similar severity response characteristics for the aircraft engines.

9 Miscellaneous Case Studies on Severity

Additional studies have been addressed to extend the severity estimation to different components, capabilities and comparison. The high pressure compressor blade and disc assembly analyzed for the sensitivity on severity and hence towards the engine severity. Mesh convergence study has been carried out to substantiate the use of suitable number of nodes and elements on the finite element model. Further case studies on the high pressure turbine has been with respect to additional features such as tip shroud and blisk impacting component life. The severity obtained through the research methodology is compared with AN^2 approach, a traditional method in design normally used for sizing the blades. Hence through this chapter, the prospects of the methodology for analyzing competitive component designs has been demonstrated.

9.1 High Pressure Compressor Severity Estimation

The severity estimation process has been applied for the high pressure compressor that forms the high speed spool of the engine. The engine model under consideration for the demonstration has been E56 belonging to the lower thrust category. The steps followed are essentially identical with the high pressure turbine. The material Inconel 718 has been used for the blade and the disc to proceed with the analysis. The compressor sizing module has been developed to do preliminary sizing (Appendix B), and it is based on the design point condition, corresponding to the top-of-climb which is more demanding for the compressor. NACA 65A010 [52] profile has been used for the aerofoil.

The sized model is analyzed using finite element analysis through plane element with thickness variation for the blade, and axi-symmetric element for the disc region. The heat transfer correlations are applied at the different sections of the compressor model to simulate the transient temperature effects.

The leading edge uses a circular cylinder correlation, trailing edge a flat plate correlation, and the channel correlation for the tip. The disc is surrounded by cavities, experiencing rotating cavity with axial throughflow, hence a suitable correlation has been applied.

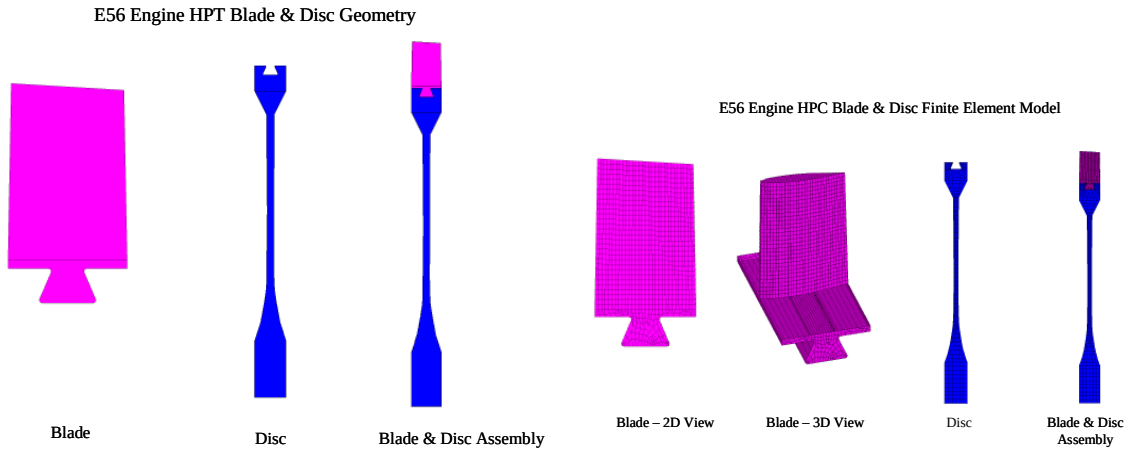

Figure 9.1 : Geometric and finite lement model of HPC blade and disc.

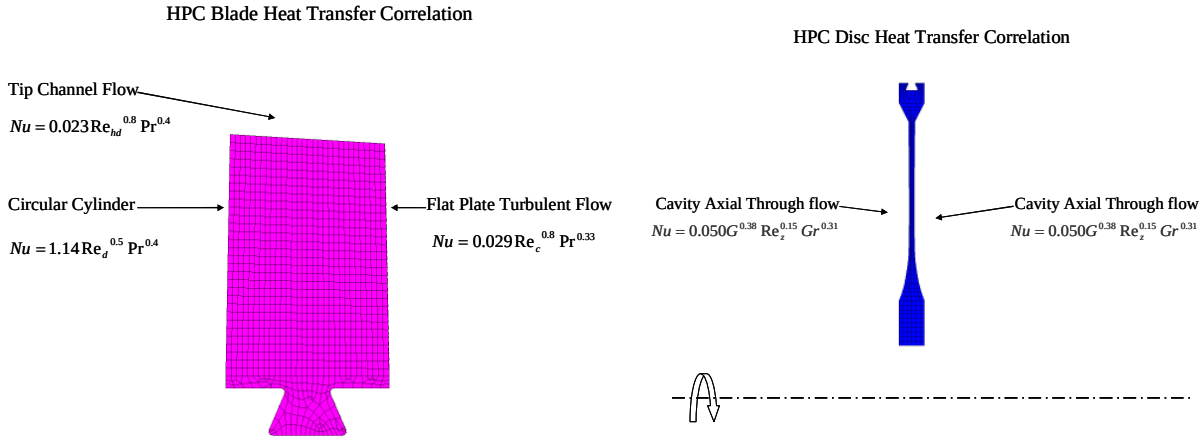

Figure 9.2 : Heat transfer correlations on HPC blade and disc.

The thermal analysis followed by thermo-mechanical analysis gives the metal temperature and stress variations during the mission for the HPC blade and the disc assembly.

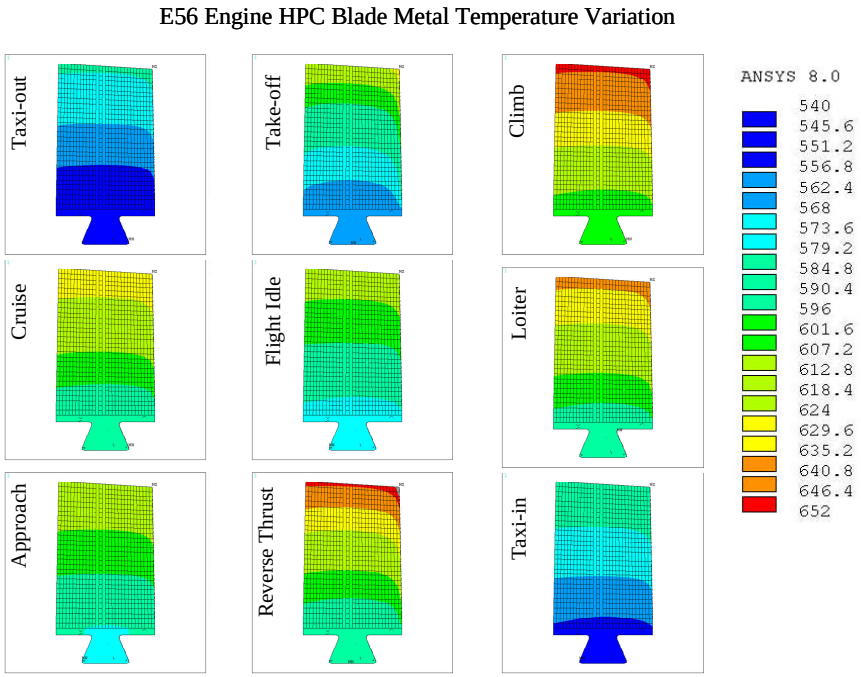

Figure 9.3 : Metal temperature variation on HPC blade.

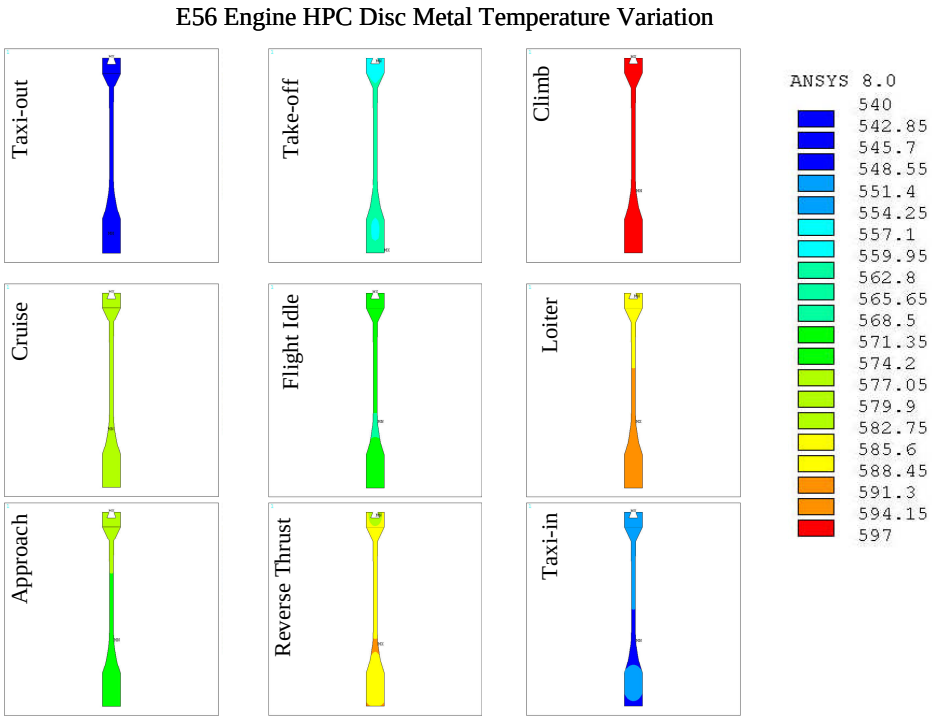

Figure 9.4 : Metal temperature variation on HPC disc.

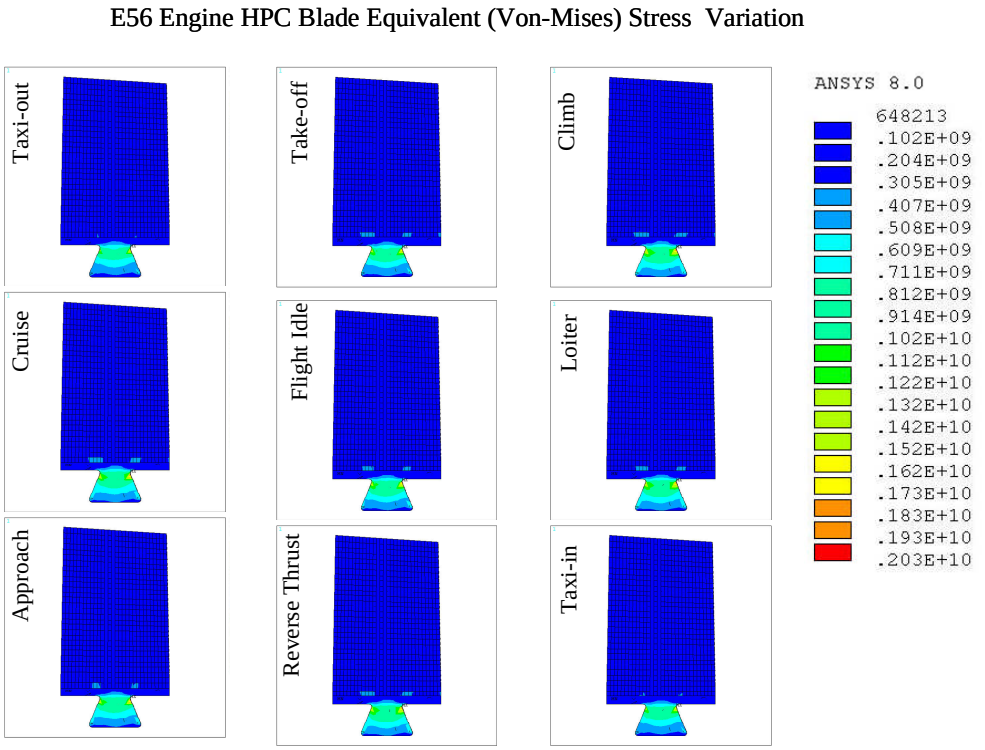

Figure 9.5 : Equivalent stress variation on HPC blade.

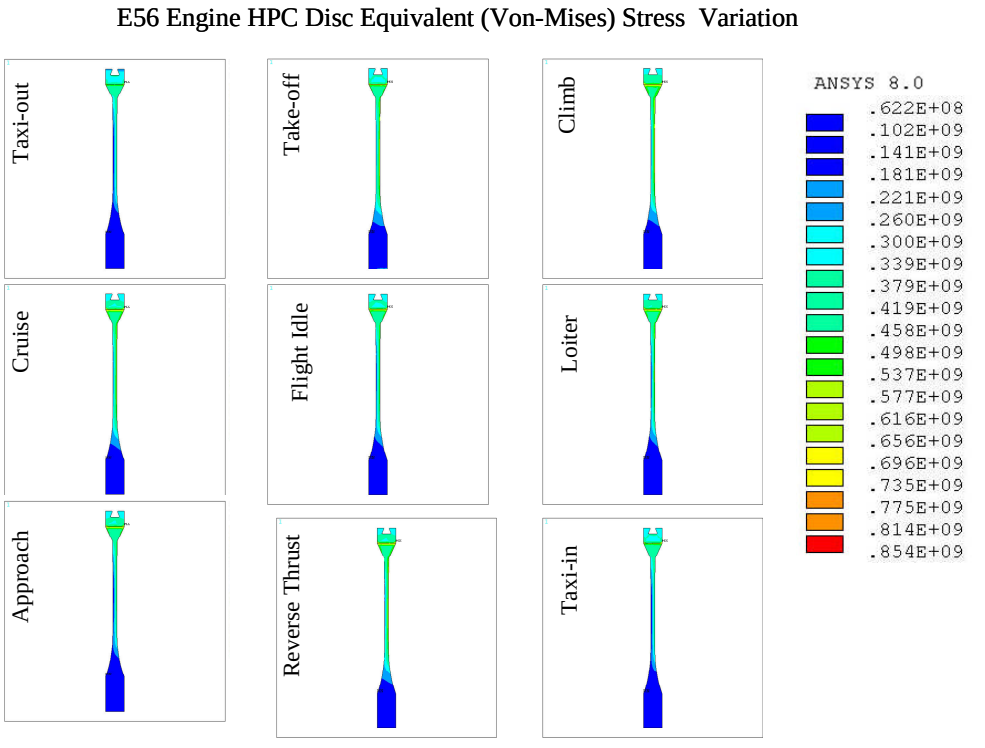

Figure 9.6 : Equivalent stress variation on HPC disc.

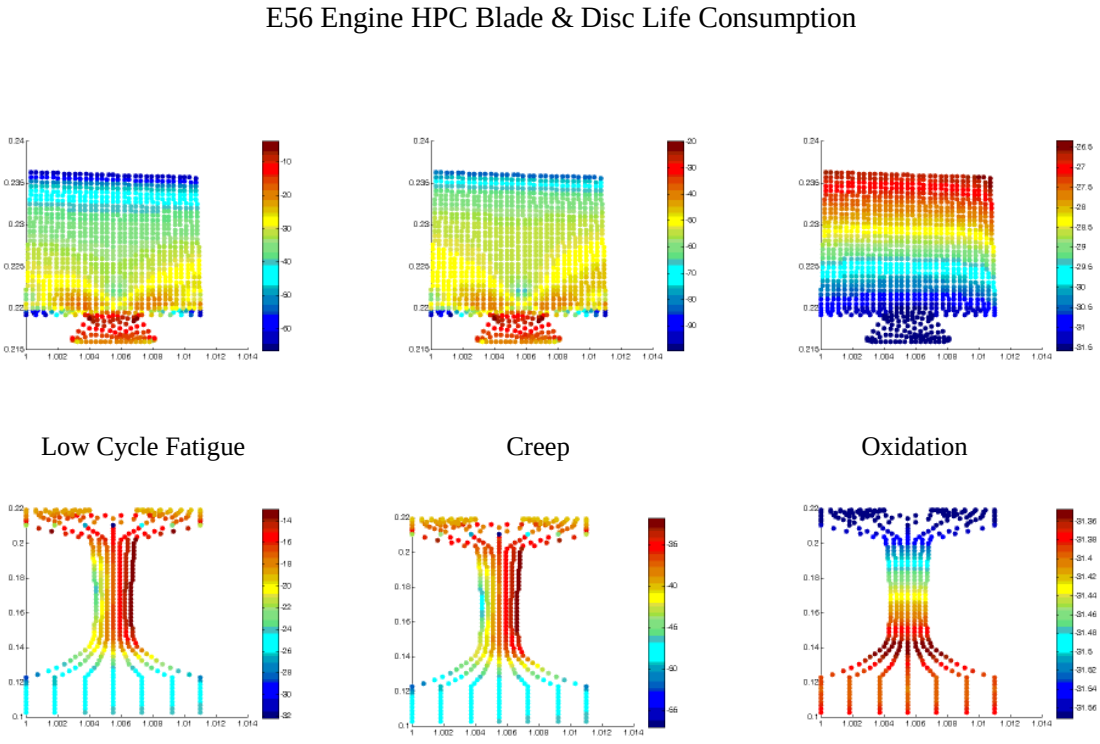

Figure 9.7 : Life plots for HPC blade and disc.

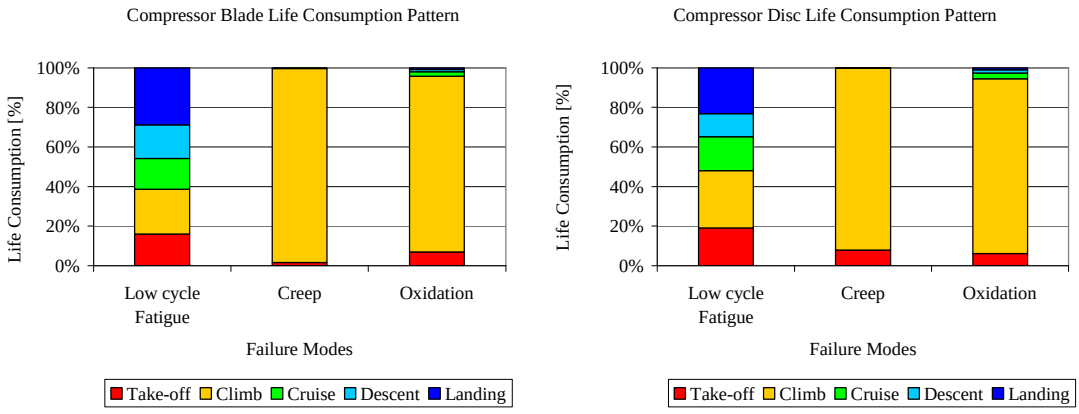

Figure 9.8 : Life consumption pattern for HPC blade and disc.

HPC Blade			
	Low cycle Fatigue	**Creep**	**Oxidation**
Units	cycles	hrs	hrs
Blade Life	7.57E+01	3.45E+08	2.75E+11
Take-off Life Consumption[%]	16.11	1.71	7.03
Climb Life Consumption [%]	22.50	97.84	88.67
Cruise Life Consumption [%]	15.62	0.41	2.32
Descent Life Consumption [%]	16.90	0.01	1.06
Landing Life Consumption [%]	28.88	0.02	0.92

HPC Disc			
	Low cycle Fatigue	**Creep**	**Oxidation**
Units	cycles	hrs	hrs
Blade Life	4.21E+05	6.60E+13	4.11E+13
Take-off Life Consumption[%]	19.05	7.97	6.04
Climb Life Consumption [%]	28.90	91.87	88.35
Cruise Life Consumption [%]	17.31	0.11	2.89
Descent Life Consumption [%]	11.60	0.01	1.65
Landing Life Consumption [%]	23.13	0.03	1.08

Table 9.1 : Life estimates for HPC blade and disc.

The blade and disc life summary, reveals the blade having very low value, this is due to the fact of the stress concentration (Figure 9.5) at the dovetail region of the blade. In actual designs the fillet radius are optimized to achieve the desired life limit of the component. The Figure 9.7 shows the evident zone of blade dovetail for low cycle fatigue and creep, as the operational temperatures are lower, and oxidation near the trailing edge experiencing high temperature during the mission. The HPC disc has the failure zone at the aft end of the web configuration for the failure modes under low cycle fatigue and creep, the oxidation life is quite the same over the entire disc. The steps in transforming the mission into the severity value is established for the high pressure compressor, and the case studies of interest has been conducted.

The operational parameters of take-off, climb and cruise derate have been varied to bring out the severity characteristics of the HPC blade and disc. The take-off derate has relatively more impact with the disc having more sensitivity to severity, as compared to the blade. This behaviour is quite different as compared to HPT, where the blade has high level of sensitivity due to exposure to high turbine entry temperature. Hence the take-off derate will enhance the life of the disc system marginally, as compared to the compressor blade.

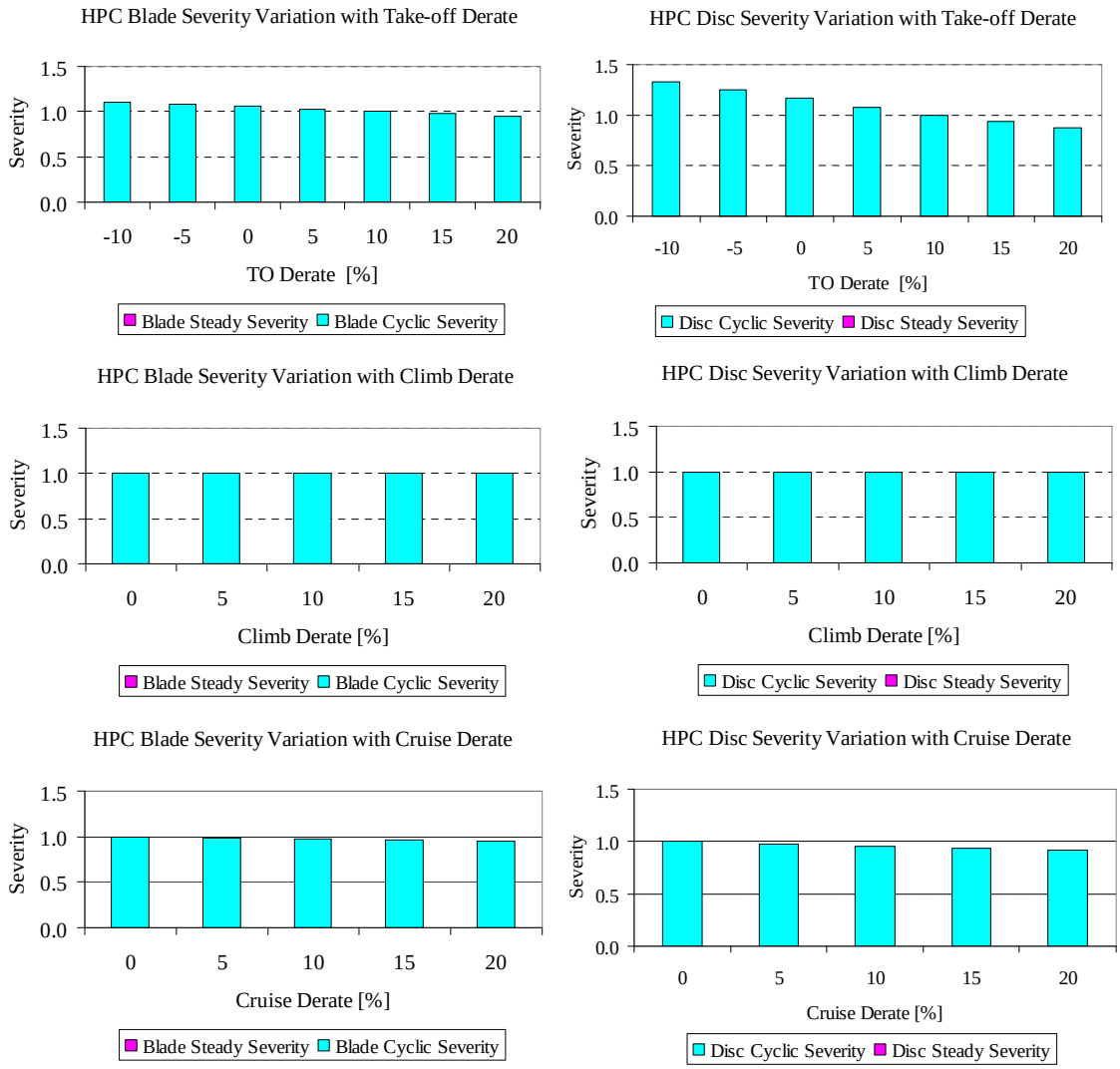

Figure 9.9 : Severity variation with take-off, climb and cruise derate variation for HPC blade and disc.

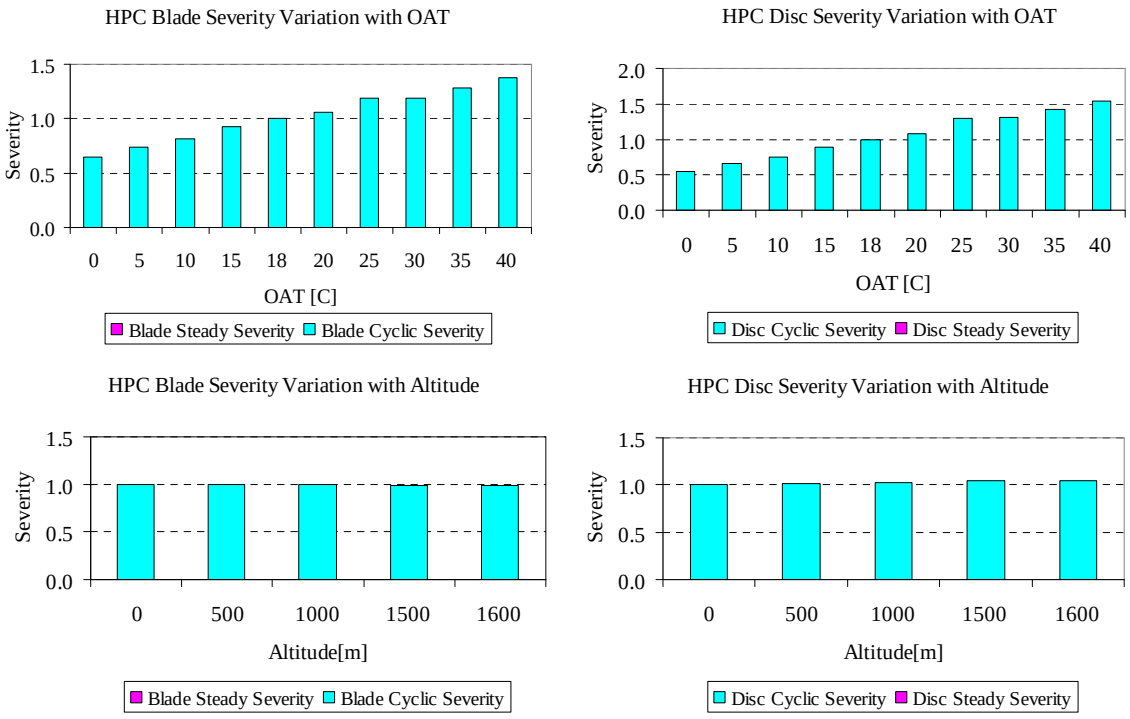

Figure 9.10 : Severity variation with OAT and airport altitude for HPC blade and disc.

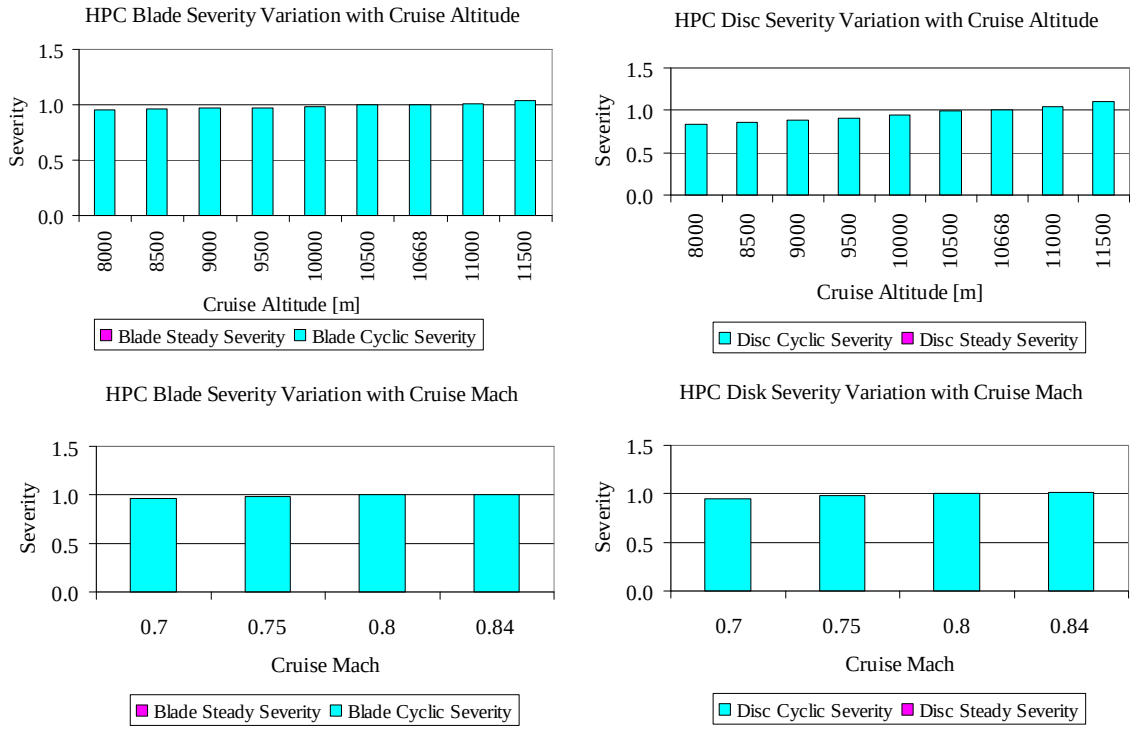

Figure 9.11 : Severity variation with cruise altitude and Mach number for HPC blade and disc.

The OAT has been observed to affect the severity of the HPC blade and the disc, while the other operational parameters are of no significance. Hence for the HPC the take-off derate and OAT will have minor impact on the severity of the component, prone to failure by low cycle fatigue.

9.2 Mesh Convergence Study

Mesh convergence study is carried out to identify the suitability of the finite element model, minimizing the numerical deviation due to approximations, in representing the geometry of the model. A refinement parameter has been utilized in the tool for maintaining the pattern of mesh, and refine them by increasing the divisions in a uniform fashion. The mesh refinement factor has been iterated between 0.5 to 1.5.

			HPT Blade Life			HPT Disc Life		
Refinement	Nodes	Elements	Low Cycle Fatigue	Creep	Oxidation	Low Cycle Fatigue	Creep	Oxidation
			cycles	hrs	hrs	cycles	hrs	hrs
0.5	1113	1020	5.85E+05	2.16E+07	9.55E+11	1.11E+04	3.82E+08	3.58E+10
0.75	1344	1240	5.95E+05	2.32E+07	9.41E+11	1.14E+04	3.61E+08	3.56E+10
1	1575	1460	6.47E+05	2.51E+07	9.41E+11	1.10E+04	3.53E+08	3.56E+10
1.25	1827	1700	6.44E+05	2.71E+07	9.45E+11	1.10E+04	3.50E+08	3.55E+10
1.5	2142	2000	6.43E+05	3.09E+07	9.45E+11	1.08E+04	3.46E+08	3.55E+10

Table 9.2 : Mesh convergence study for HPC blade and disc.

As the matrix size increases with increasing nodes for the life estimation, as it is built to estimate damage at every flight segment. Hence a very refined model, consumes sufficiently large time, while the tool should be capable of giving a quick and reliable estimate. Hence the refinement level of 1.25 with about 1827 nodes and 1700 elements, considered suitable for severity estimation.

9.3 Tip Shroud Design on HPT Blade Life

Tip shrouds have been used in aircraft engines to improve the efficiency of the turbine. But the use of tip shroud has a penalizing effect on the life of the component. The tip shroud effect has been tested on E115 engine HPT, indicating high level of sensitivity on the limiting life of creep failure. The life due to low cycle fatigue has been reduced, due to the additional centrifugal load on the turbine blade. Hence the engines with tip shroud tend to operate at lower shaft speed to reduce the impact on life consumption.

		HPT Blade Life			HPT Disc Life		
Engine	Design	Low Cycle Fatigue	Creep	Oxidation	Low Cycle Fatigue	Creep	Oxidation
		cycles	hrs	hrs	cycles	hrs	hrs
E115	Normal	1.03E+08	1.61E+04	1.18E+09	1.10E+04	3.50E+08	3.55E+10
E115	Tip Shroud	3.92E+07	7.11E+02	1.18E+09	6.42E+04	2.52E+09	3.55E+10

Table 9.3 : Tip shroud comparison on HPT blade life estimate.

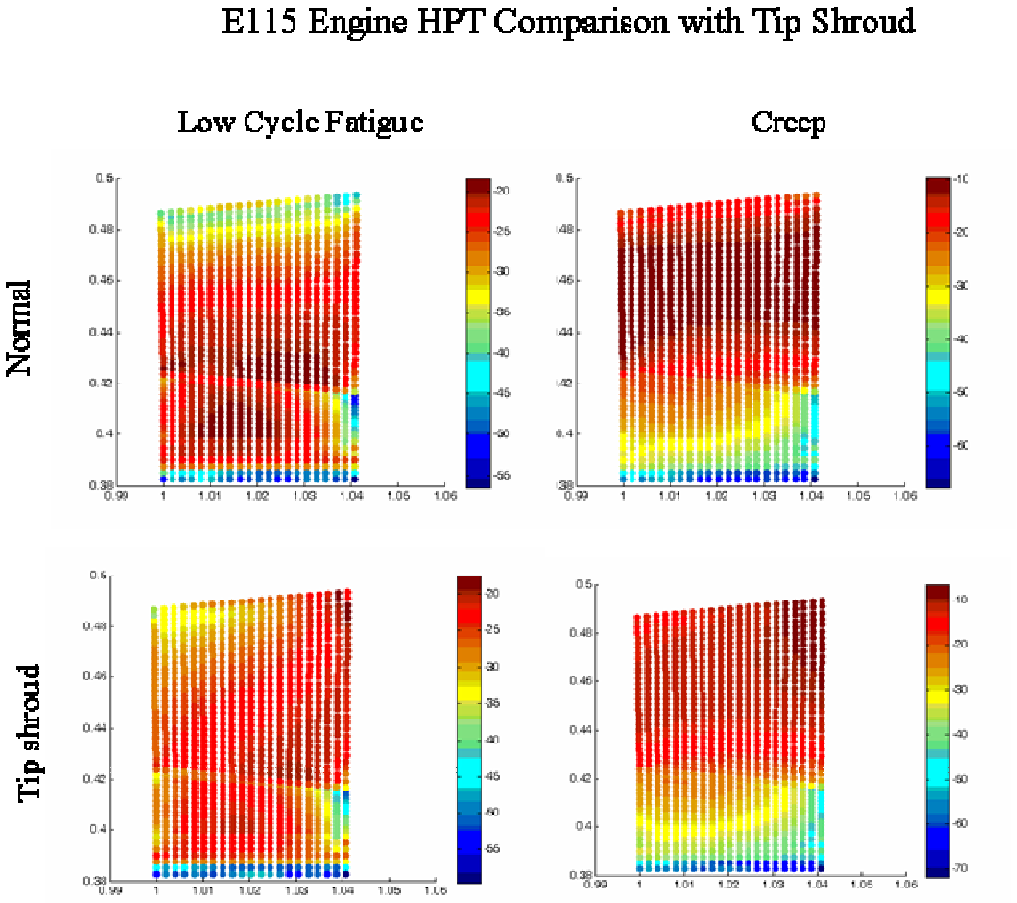

Figure 9.12 : HPT blade life plots comparison for tip shroud effect.

The tip shroud effects on the turbine blade could be analyzed using the severity methodology, and compare competitive designs from engine manufacturers.

9.4 Blisk Design on HPT Life

Bladed disc design is referred to as blisk, in gas turbine industry which aims at

integrating the blade and the disc as an integral component. The use of blisk design, eliminates the design of the blade root being prone to failure, due to stress concentration at the dovetail or fir-tree configuration. The blisk is achieved through advancement in the manufacturing technique, and have come into practice with the compressors stages, as the material for the blade and disc are similar, such as Inconel based alloys at the HPC end. The use in HPT could yield benefits, as evident from the lifing study, incorporating the blisk design. The improvement in the life will be appreciable for the disc, as compared to the blade, and depends on the life limiting zone of the design.

		HPT Blade Life			HPT Disc Life		
Engine	Design	Low Cycle Fatigue	Creep	Oxidation	Low Cycle Fatigue	Creep	Oxidation
		cycles	hrs	hrs	cycles	hrs	hrs
E115	Normal	1.03E+08	1.61E+04	1.18E+09	1.10E+04	3.50E+08	3.55E+10
E115	Blisk	5.19E+07	1.74E+04	1.18E+09	5.68E+04	6.00E+08	1.20E+10

Table 9.4 : Blisk comparison on HPT life estimate.

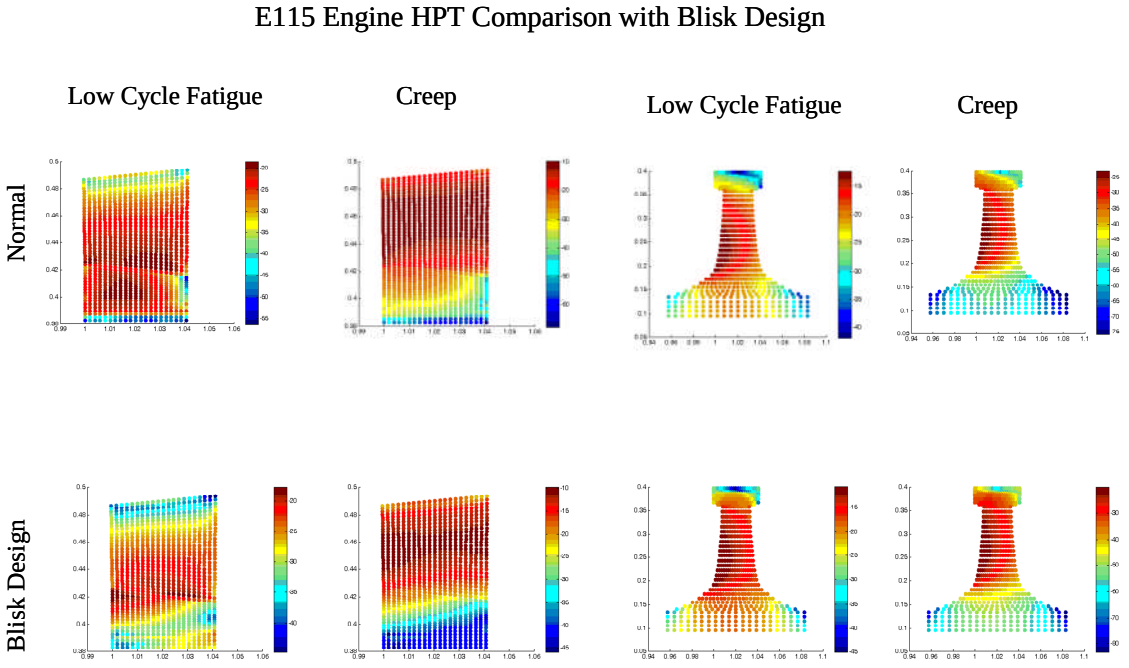

Figure 9.13 : HPT life plots comparison for blisk design.

From the lifing plots, it is evident that the root and shank region of the blade have improved as compared to the normal design. Hence the use of blisk will be beneficial for aircraft engines through component integration, and feasibility in terms of maintenance and repair being explored.

9.5 Comparison of AN^2 Approach with Severity Estimation Methodology

For the turbine blade design to estimate the feasibility with respect to mechanical design, the AN^2 approach has been used during the sizing of the blades. AN^2 is the characteristics of the centrifugal force on the blade as a function of the shaft speed. The severity methodology, involves higher degree of complexity in capturing the life consumption, and has been compared with the simplified methodology of AN^2 approach.

The AN^2 approach has been implemented, by assuming a stress level of 552MPa, and scaled with respect to the shaft speed scaling vector to capture the stress excursion during the mission. An average gas temperature has been assumed, based on inlet and outlet temperatures with the temperature offset due to cooling effectiveness and thermal barrier coating taken into account. The estimation process is done for the take-off derate study for comparison.

	E56 (AN^2 Approach)						E56 (Severity Method)					
T-O Derate	Low Cycle Fatigue [cycles]	Creep [hrs]	Oxidation [hrs]	Blade Cyclic Severity	Blade SS Severity	Blade Severity	Low Cycle Fatigue [cycles]	Creep [hrs]	Oxidation [hrs]	Blade Cyclic Severity	Blade SS Severity	Blade Severity
-10	4.49E+06	1.23E+05	9.61E+11	0.68	34.84	35.52	5.17E+05	5.38E+06	2.75E+11	1.21	0.16	1.37
-5	5.53E+06	2.59E+05	1.65E+12	0.56	16.61	17.17	5.41E+05	8.22E+06	3.82E+11	1.15	0.11	1.26
0	7.07E+06	7.99E+05	3.57E+12	0.43	5.38	5.82	5.72E+05	1.42E+07	5.66E+11	1.09	0.06	1.15
5	8.74E+06	2.49E+06	7.44E+12	0.35	1.73	2.08	6.06E+05	2.14E+07	7.73E+11	1.03	0.04	1.07
10	1.02E+07	6.16E+06	1.28E+13	0.30	0.70	1.00	6.44E+05	2.71E+07	9.45E+11	0.97	0.03	1.00

Table 9.5 : Comparison table on AN2 approach and severity method.

The severity level predicted through AN^2 approach is larger in magnitude as compared to the severity method. The comparison reveals, the severity method has lesser sensitivity, while the AN^2 due to coarse level of estimation, shows greater sensitivity with life.

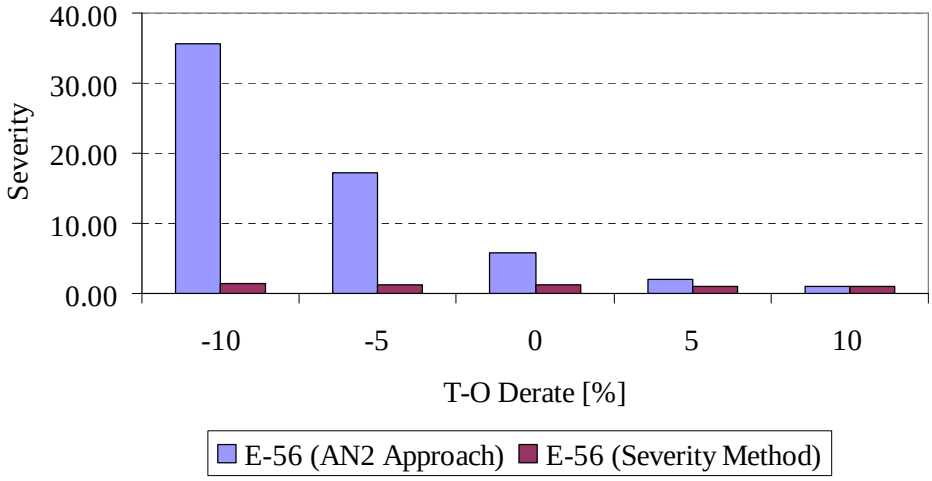

Figure 9.14 : Take-off derate severity characteristics comparison for AN^2 approach and severity method for engine E56.

Comparison of Methods		
Parameters	AN^2 Method	Severity Method
Design Phase	Conceptual	Preliminary Design
Complexity	Low	High
Temperature Effects	Gas Temperature	Metal Temperature
Transient Thermal Effects	Nil	Included
Stress	Assumed	Estimated
Effect of cooling effectiveness	Constant	Dynamic
Effect of TBC	Constant	Dynamic
Effect of Pattern Factor & Location	Nil	Included
Disk Rim Stress	Nil	Estimated
State of the Stress	Assumed	Elastic & Elasto-Plastic
Disk Lifing	Inefficient	Capable

Table 9.6 : Comparison of AN^2 approach with severity method in capturing the turbine blade severity.

The comparison table narrates the enhancement over the traditional AN^2 approach. The AN^2 will be a useful measure for preliminary sizing of the blades, but a finer behaviour needs to be captured for the life estimation and their relative sensitivity. Hence the severity method is in between the tradiational AN^2 approach and the design practice of OEMs.

9.6 Miscellaneous Case Studies on Severity – Summary

The severity estimation methodology has been extended to high pressure compressor blade and disc.

The HPC blade and disc are life limited by low cycle fatigue.

The severity of the HPC is less phenomenal as compared to HPT and hence lower sensitivity on engine severity.

Mesh convergence study has been adopted to avail suitable number of nodes and elements for the finite element analysis suitable for life estimation.

Tip shroud design will reduce the life of the HPT blade drastically, hence the operational requirement would be lower shaft speed to reduce the influence.

Blisk designs will improve the disc life, and a suitable design alternative for normal blade design with high level of stress concentration at the root region.

AN^2 approach due to coarseness of the methodology estimates high level of sensitivity, while the severity estimation method is inline with the finer level of details for appropriate estimation.

10 CASE STUDIES ON SHOP VISIT PREDICTION

The planned shop visit is predicted on the basis of performance degradation, and it is the task of the designers to match the EGT margin with the life limits of the components. The degradation of the components, leading to inefficiency in engine performance, causes an increase in the exhaust gas temperature, in maintaining the thrust has been captured using the methodology. The engine manufacturers specify the EGT margin, and often greater margin signifies reduced maintenance. The EGT margin is of paramount importance and engine manufacturers continuously strive to achieve better margins. The factor commonly used for characterizing the maintenance depends on the Mature Shop Visit Rate (MSVR). This factor is related to the Shop Visit Rate (SVR) and the severity. The severity has been captured as a part of this research and demonstrated on different engines. The shop visit rate that is predicted, based on the EGT margin consumption will be the core focus of this chapter as it unfolds.

10.1 Overview on Shop Visit Rate Prediction for Engine Models

The shop visit rate prediction methodology has been carried on two engine models, representing the short and long haul flight scenario. For the short haul flight, engine model E56 has been investigated, while for the long haul flight, engine model E115 has been explored. The degradation values are with respect to the reference [42], depicts levels of degradation as observed in the aircraft engines. Severe level of degradation has been considered for the current analysis. The simplified flight path analysis code along with Turbomatch has been synchronized using the Matlab software. The component degradation versus engine flight cycles definition is represented as change in the mass flow and efficiency of the components in the Turbomatch engine model. The thrust is kept constant causing continuous rise in the exhaust gas temperature, being observed at the take-off, climb and cruise.

Aircraft Engines for Shop Visit Study			
		Lower Thrust	Large Thrust
Parameter	**Units**	**E56**	**E115**
Spool		2	2
Fan Diameter	m	1.5494	3.256
Mass Flow	kg/s	355	1641
By- pass Ratio		5.1	8.9
Pressure Ratio		32.8	42
T-O Thrust	N	121430	512880
Shaft Speed	rpm	15183	11292
Overspeed	%	105	121
Cimb Thrust	N	26520	99565
Cruise Thrust	N	24376	98488

Table 10.1 : Engine models for shop visit study.

Hence with respect to engine flight cycles, the exhaust gas temperature characteristics is observed. The process is carried out for operational factors that are impactful on the shop visit rate. The operational factors included for the current study, involves the take-off derate, OAT and trip length. These characteristics are of importance as typically different mission requirements of the fleet involves varied settings. The variation of the shop visit rate and the severity level of the component with respect to the take-off derate is used in determining the Mature Shop Visit Rate (MSVR) as defined by MRO. The range of MSVR identified through the analysis are individually represented as a Weibull curve with a slope of 1.5 for estimating the age factor with respect to the engine flight hours. The age factor versus engine flight hours is commonly referred to as the aging curve. The aging curve provides the value for estimating the material maintenance cost of an aircraft engine. The other parameter used for the maintenance cost involves labour cost based on the Maintenance Repair and Overhaul (MRO) industry practice. The maintenace labour cost has not been addressed, as it is related to MRO strategy on time and effort for restoring the aircraft engines.

10.2 Degradation – Cycle Definition

The two engine models, E56 for lower thrust and E115 for large thrust are considered for predicting the shop visit. The critical piece of information for

predicting the shop visit is the degradation-cycle definition. The individual components of the performance model are subjected to different levels of degradation to obtain the EGT margin consumption. The components degrade to different proportion by the virtue of the design and environment. Predicting the pattern of degradation for individual components is not within the scope of work. The research is in proposing a performance model, capturing the assumed levels of degradation pattern used in literature, and predict the shop visit interval. A typical pattern as used for various studies is published in the reference [42]. The different levels of the degradation are obtained through scaling the pattern corresponding to the severe level, as per the reference. Hence the values imitating the typical degradation pattern has been used as a reference value for the case studies.

Fan Efficiency Change [%]	Fan Mass Flow Change [%]	LPC Efficiency Change [%]	LPC Mass Flow Change [%]	HPC Efficiency Change [%]	HPC Mass Flow Change [%]	HPT Efficiency Change [%]	HPT Mass Flow Change [%]	LPT Efficiency Change [%]	LPT Mass Flow Change [%]
-2.85	-3.65	-2.61	-4.00	-9.40	-14.06	-3.81	2.57	-1.08	0.42

Table 10.2 : Degradation values for the performance model.

The critical life limit for engine E56 is 10000 cycles, and for E115 is 3000 cycles. Hence the maximum level of degradation, assumed to be reached as the engine flight cycles tends to the critical life limit. The engine models are taken through different degradation studies to estimate the EGT margin consumption. The maximum degradation is scaled from 0% to 100% in increments of 25% to obtain the increase in the EGT at take-off and climb. A similar study is carried out by varying only the individual component degradation for insight on relative sensitivity towards the engine EGT margin consumption. However the individual component degradations leading to increase in the EGT, cannot be superimposed or added to obtain the resultant behaviour due to the

non-linearity, in the underlying engine performance characteristics. The pursuit of estimating the shop visit interval is established through the use of Weibull curve having slope value 1. The Weibull distribution is commonly used in representing the degradation characteristics, and adopted for the shop visit prediction methodology. The need for the Weibull distribution is to obtain an intermediate point of degradation cycle definition which will lead to the EGT characteristics with engine flight cycles. This characteristics as it crosses over the redline temperatue of the engine will highlight the shop visit interval.

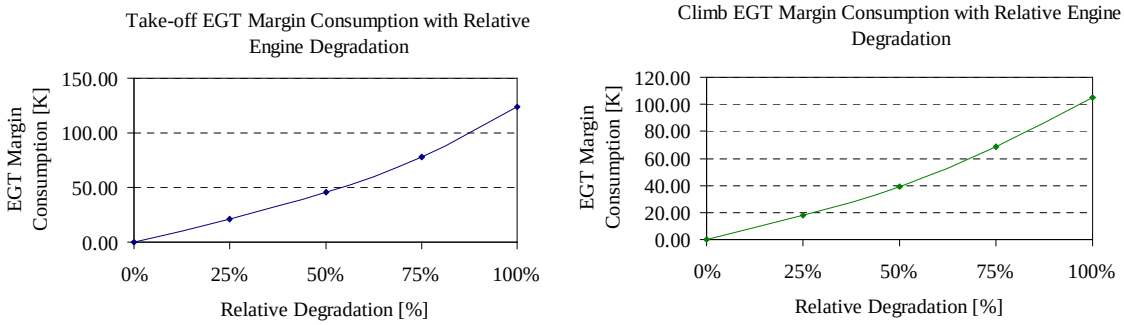

Figure 10.1 : EGT margin consumption for engine E56 through degradation scaling.

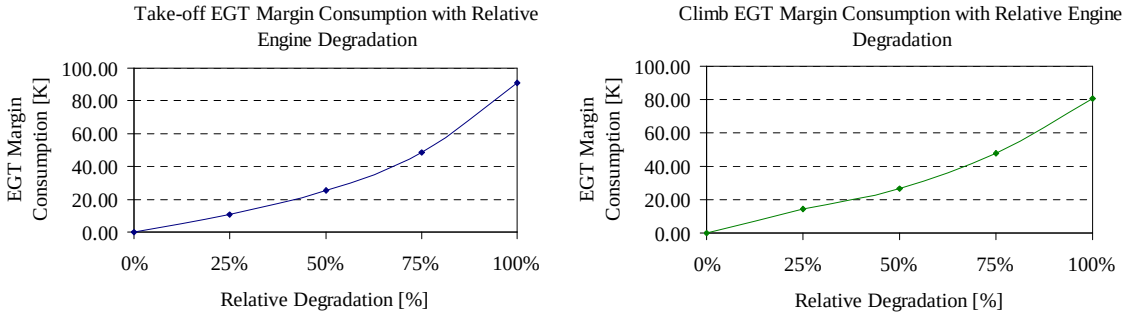

Figure 10.2 : EGT Margin Consumption for engine E115 through degradation scaling

The E56 engine is analyzed for take-off derate of 10% at 15 °C OAT for plotting the degradation characteristics. The E115 engine is analyzed for 4% take-off derate at 15 °C OAT. The rise in the EGT at take-off prevails to be dominant as compared to climb. The assumed level of degradation satisfy the requirement

of EGT margin of 120 K for E56 and 85 K for E115 engine models.

The component degradation characteristics with respect to the EGT margin consumption has been depicted for the engine E56 (Figure 10.3) and E115 (Figure 10.4), where a high level of sensitivity is observed with the high pressure compressor. The compression process achieved through fan, LPC and HPC, tend to dominate the EGT margin consumption, as compared to turbine degradation. Hence the engine wash that restores the performance of the compressor will yield appreciable benefits as observed in the aviation.

The intermediate point for the E56 engine (Figure 10.5) has been identified at 1500 cycles, having 0.7 as the scaling factor for the degradation. The intermediate cycle data has been fine tuned to achieve the required shop visit interval of 18500 hrs, yielding 1667 cycles. A similar degradation Weibull curve is constructed for the E115 model (Figure 10.6) which has an intermediate point of 300 cycles with 0.6 as the scaling factor for the degradation. Hence through the process of building the Weibull distribution for the degradation scale, the intermediate defining point portraying the EGT characteristics is obtained, and have been used for shop visit prediction.

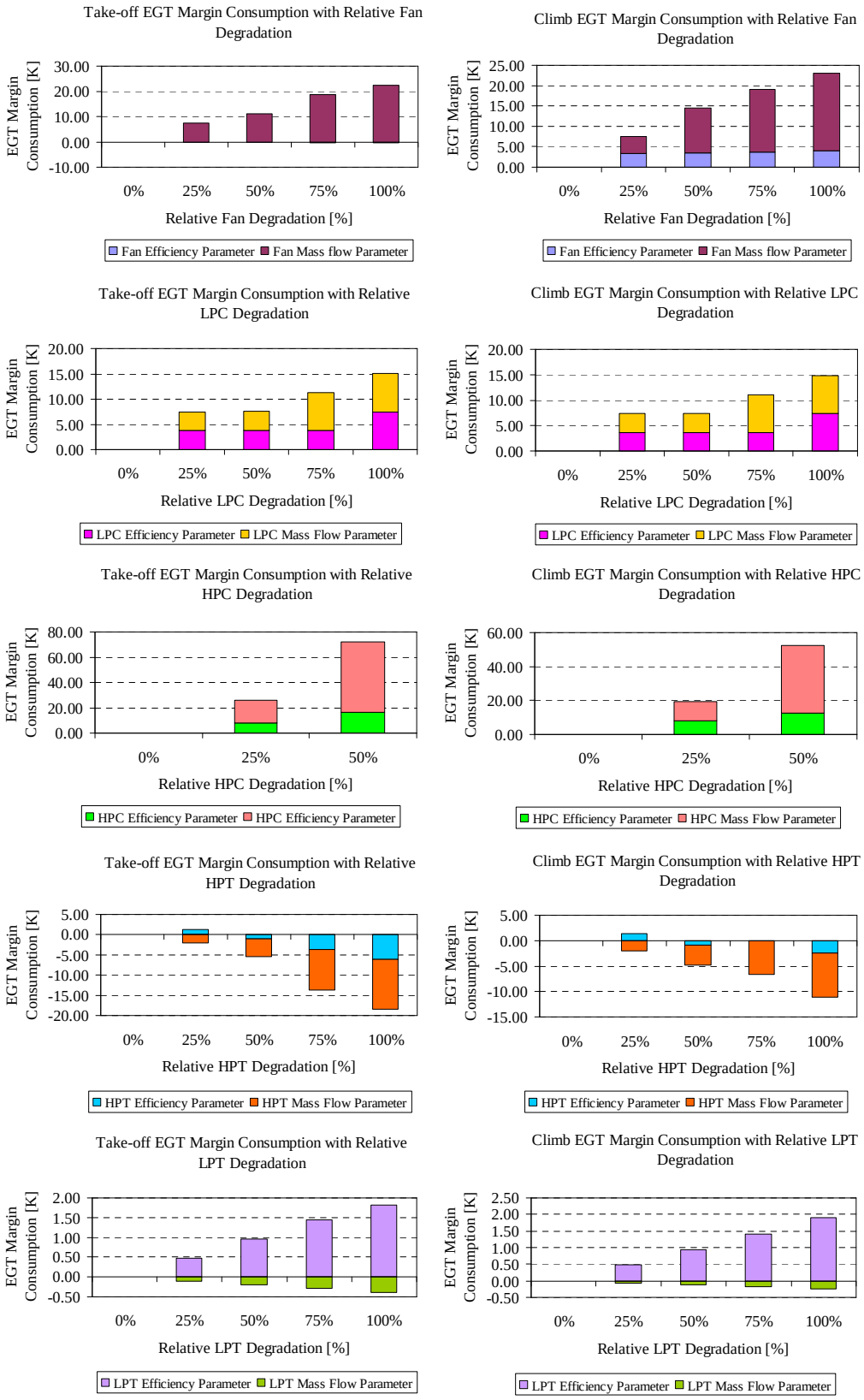

Figure 10.3 : EGT margin consumption due to individual component degradation for engine E56.

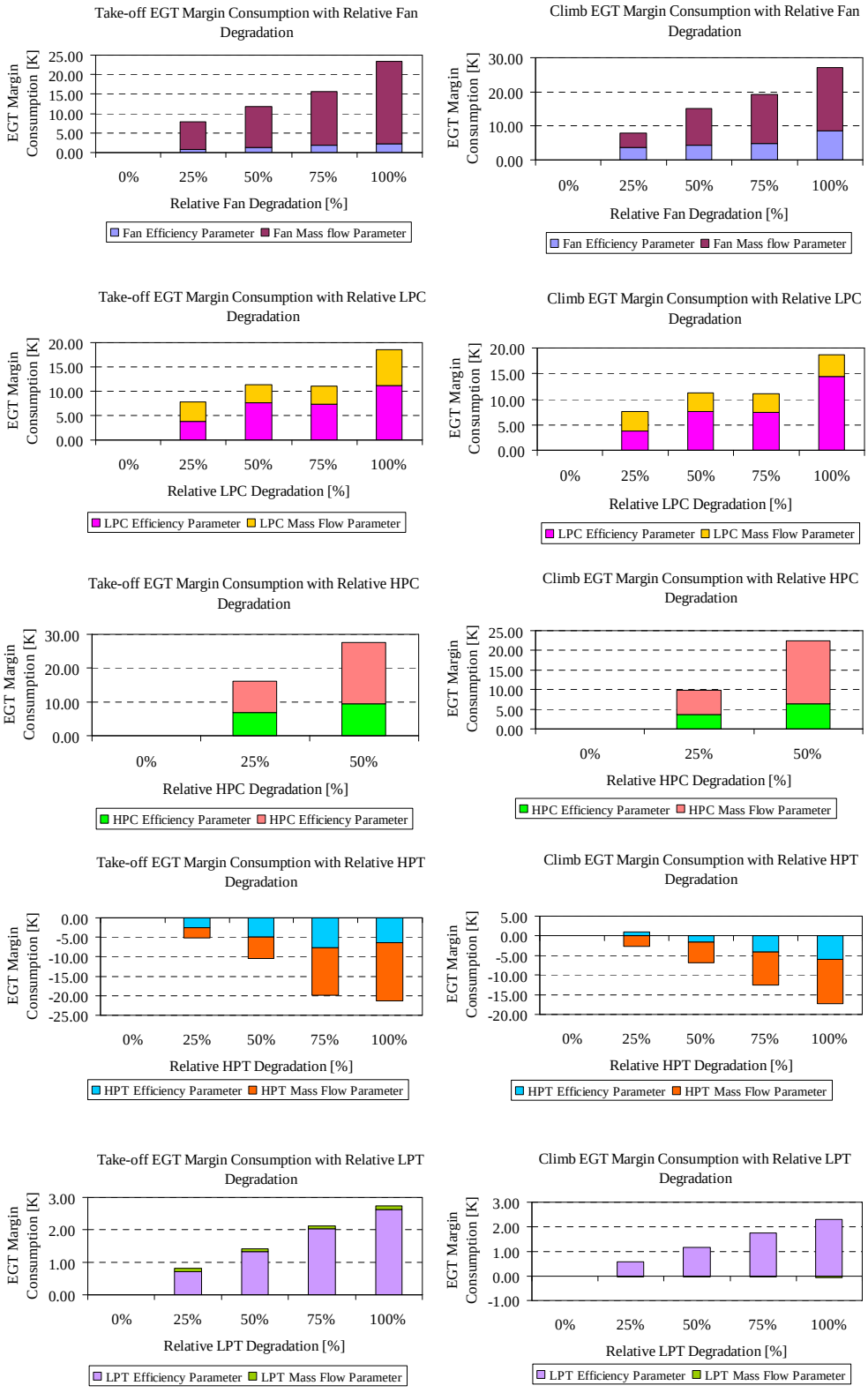

Figure 10.4 : EGT margin consumption due to individual component degradation for engine E115

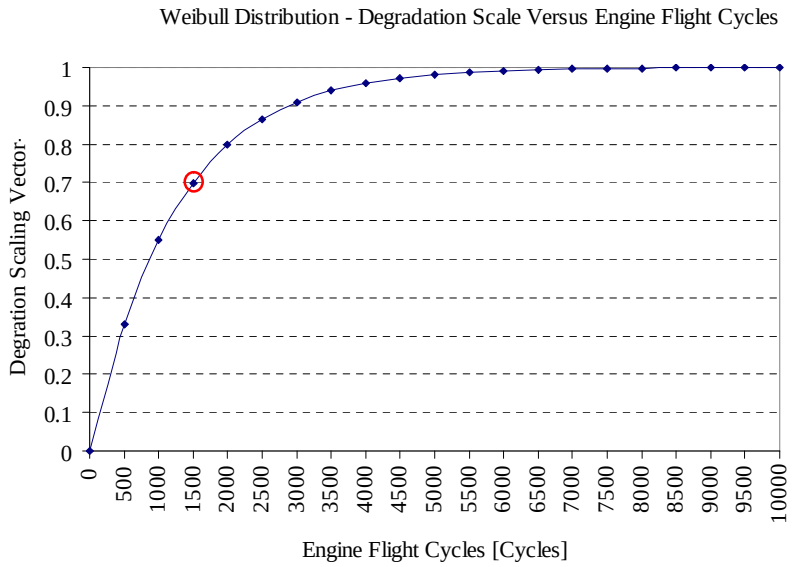

Figure 10.5 : Weibull curve for degradation scale of engine E56.

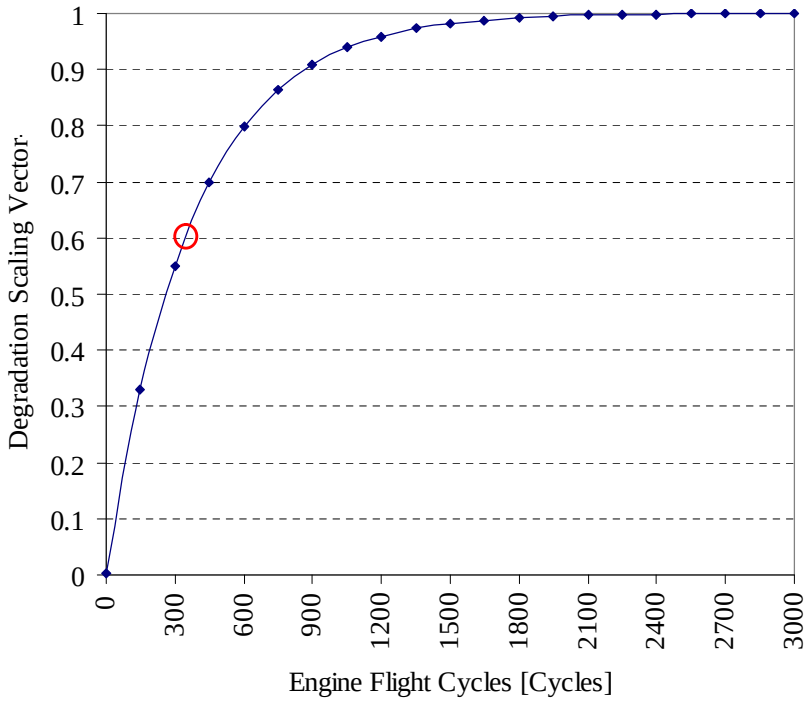

Figure 10.6 : Weibull curve for degradation scale of engine E115.

10.3 Short Haul Flight – Shop Visit Rate Prediction for Engine E56

The short haul flight mission having frequent take-off and landing, represented with the E56 engine. The engine model used for the severity estimation has been extended with the degradation for the component mass flow rate and efficiency. The compressor and turbine components have been simulated for the degradation levels specified in the Table 10.3.

The engine flight cycles definition is based on the turbine blade life or the critical Life Limited Part (LLP) of an aircraft engine. The lower thrust engines have a turbine blade life of 10000 cycles, and a disc life that are 15000 to 20000 cycles. The common industry practice is in having the disc life twice that of the turbine blade life, suitable for the shop visit strategy. During the first shop visit, the aerofoils in the gas path are replaced restoring the performance, and for the second shop visit the blades and the disc system are replaced. The casings are designed for the life of the aircraft, hence retained at different shop visits. This particular fact, the casings being conserved, leads to different clearance pattern with the rotating components, hence the performance cannot be restored to that of the engine as installed. This progressively leads to lesser EGT margins with successive shop visits. The engine flight cycle is specified with the maximum of 10000 cycles. An intermediate point has been identified at 1667 cycles using the Weibull curve.

Engine Flight Cycles	Fan Efficiency Change [%]	Fan Mass Flow Change [%]	LPC Efficiency Change [%]	LPC Mass Flow Change [%]	HPC Efficiency Change [%]	HPC Mass Flow Change [%]	HPT Efficiency Change [%]	HPT Mass Flow Change [%]	LPT Efficiency Change [%]	LPT Mass Flow Change [%]
1	0	0	0	0	0	0	0	0	0	0
1667	-1.995	-2.555	-1.827	-2.8	-6.58	-9.842	-2.667	1.799	-0.755	0.2958
10000	-2.85	-3.65	-2.61	-4	-9.4	-14.06	-3.81	2.57	-1.078	0.4226

Table 10.3 : Degradation cycle definition of engine E56.

Installed EGT Margin [K]	1st Shop Visit EGT Margin [K]	2nd Shop Visit EGT Margin [K]	3rd Shop Visit EGT Margin [K]
120	80	70	60

Table 10.4 : EGT margin settings for the shop visit prediction of engine E56.

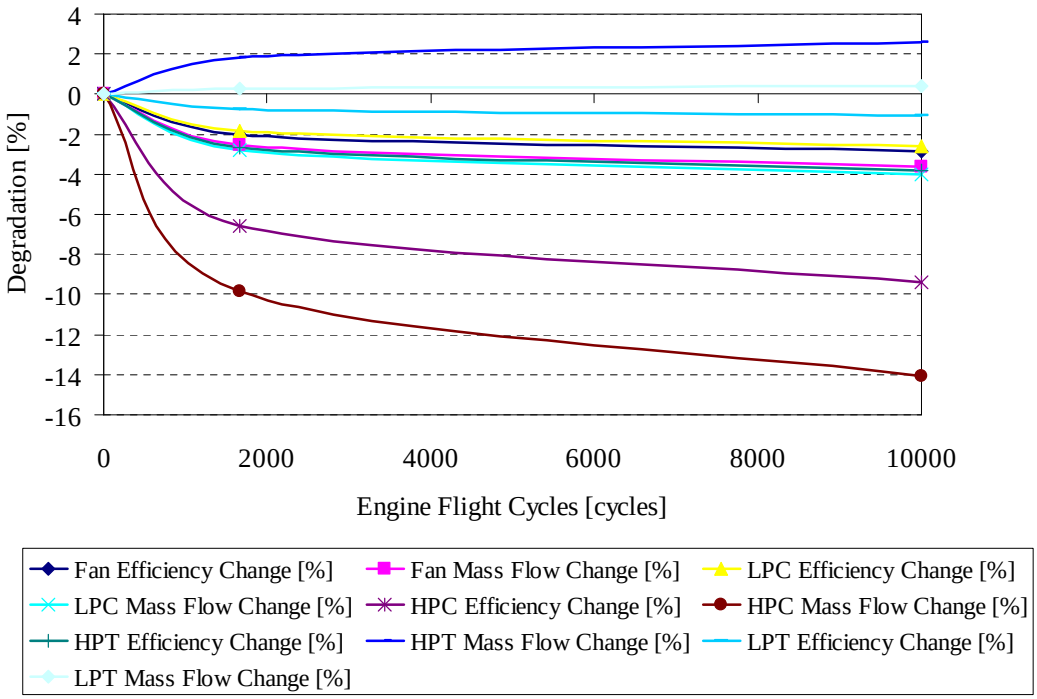

Figure 10.7 : Component degradation variation with engine flight cycles for engine E56.

The performance calculation has been carried out by changing the component degradation as specified in the Table 10.3. The exhaust gas temperatures at different engine flight cycles are extracted to predict the first shop visit interval.

The case under consideration, corresponds to 10% take-off derate at 15 °C OAT and a trip length of 2 hrs. The initial EGT margin for the engine E56 is 120 K, and the exhaust gas temperature is measured at the second stage LPT nozzle. The redline temperatures (Appendix D), the threshold temperature for identifying the proximity with the shop visit are 1193 K (920 °C) at take-off and 1168 K (895 °C) for continuous operation.

The EGT is observed at take-off, climb and cruise segment of the flight path.

The take-off is looked for maximum temperature, and regarding climb and cruise an average temperature is estimated, from the EGT variation during the mission.

The EGT curve crosses over the threshold considered as the redline temperature to identify the first shop visit interval. For prediction of the successive shop visit, the EGT characteristics is repeated with the offset in the EGT margin, leading to estimation of consequent shop visit interval. The different EGT margin is put up in the Table 10.4. The shop visit rate is predicted based on the shop visit interval expressed as per the MRO industry practice. Two parameters have been used part of this study which is the first SVR and SVR. The first SVR is with respect to the first shop visit interval and SVR represents the average shop visit interval for the entire life of the aircraft.

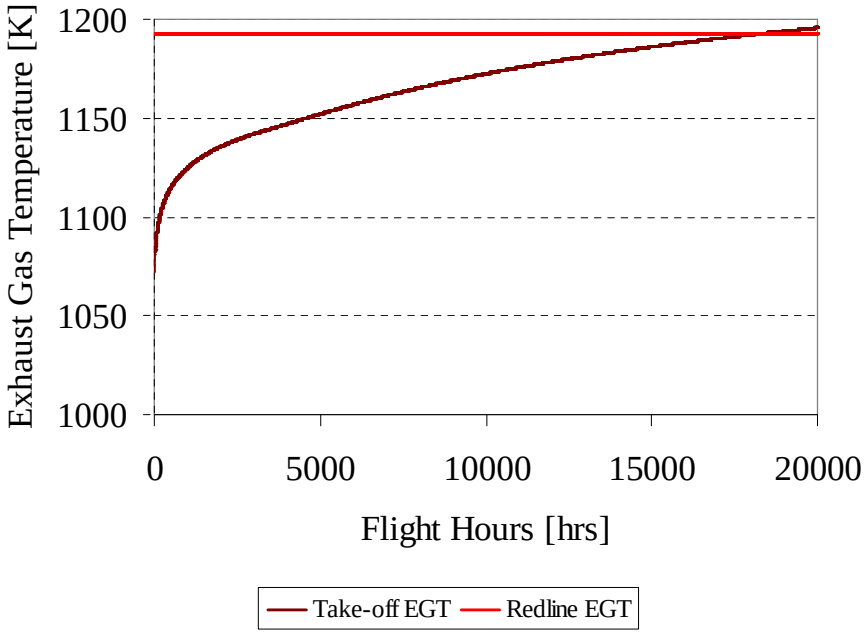

Figure 10.8 : Take-off EGT characteristics for first shop visit prediction of engine E56.

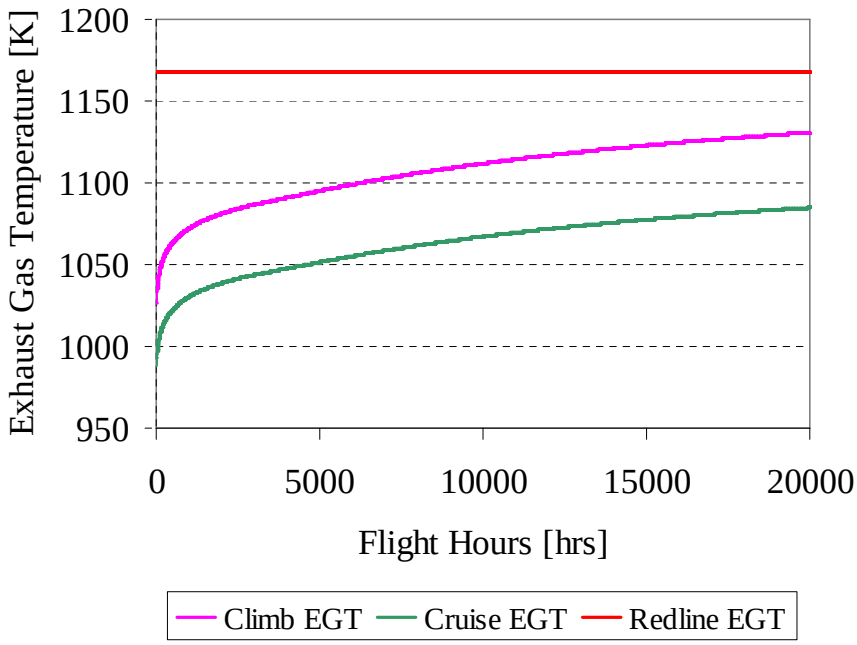

Figure 10.9 : Climb and cruise EGT characteristics for the shop visit prediction of engine E56.

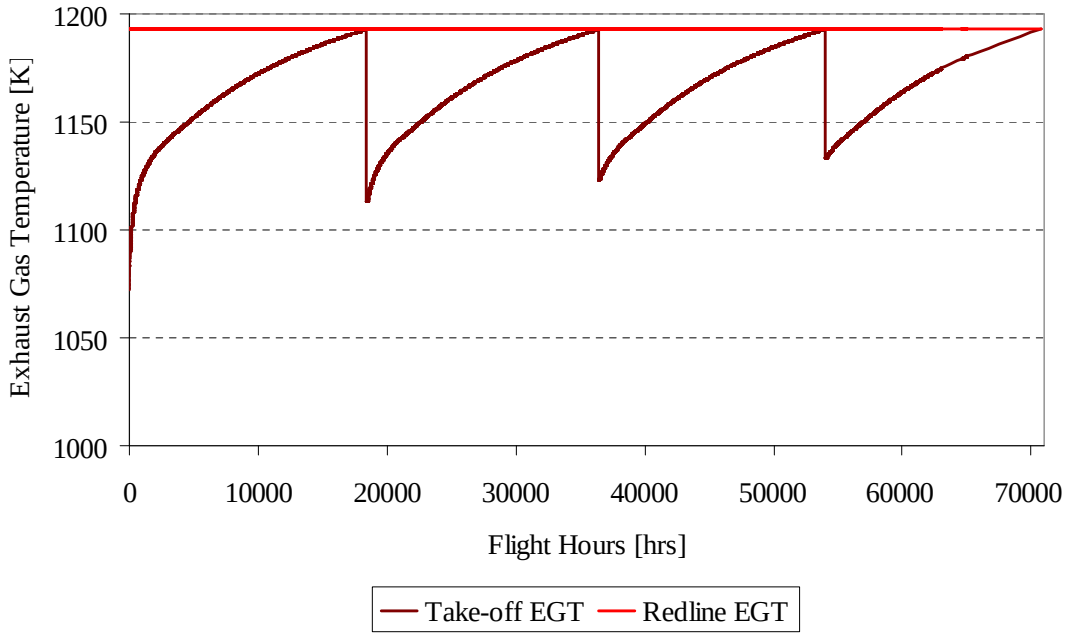

Figure 10.10 : EGT characteristics with successive shop visit for engine E56

First SVR	SVR	First Shop Visit [hrs]	Second Shop Visit [hrs]	Third Shop Visit [hrs]	End Life [hrs]
0.05	0.06	18438	36452	54024	70776

Table 10.5 : Shop visit interval for engine E56 through shop visit prediction.

The first shop visit interval for the E56 engine is at 18438 hrs which is inline with the industry observation (Appendix D) for a similar mission to make the first shop visit at 18500 hrs. The SVR for the engine E56 is 0.06 , the predicted value is evident in the application of a similar lower thrust engine.

10.4 Short Haul Flight – Operational Factors Study on Engine E56 Shop Visit Rate

The operational factors affect the shop visit interval, and the impact of the take-off derate, OAT and trip length has been considered in this study. The shop visit as percieved in the context of the EGT margin deterioration with engine flight hours, maintaining the thrust level, irrespective of the component degradation. Hence the significant factors tied with the thrust level is the take-off derate and OAT. Trip length affects the shop visit rate, as the degradations are based on cycles, and the shop visit interval is proportional to the ratio of Engine Flight Hours/Engine Flight Cycles ratio (EFH/EFC ratio), typically an average trip length. Hence the study has been with respect to the three opertional factors of prime interest in predicting the shop visit rate trends.

Effect of Take-off Derate

The take-off EGT has been observed to be the source of shop visit with respect to the study on E56 engine. The airliners use reduced thrust level at take-off referred as the take-off derate to increase the EGT margin extending the shop visit interval. The take-off derate has been varied from 0% to 10% during this parametric study for the degradation cycle definition of engine E56. The EGT margin deterioration characteristics for the different take-off derates have been plotted with respect to the take-off EGT.

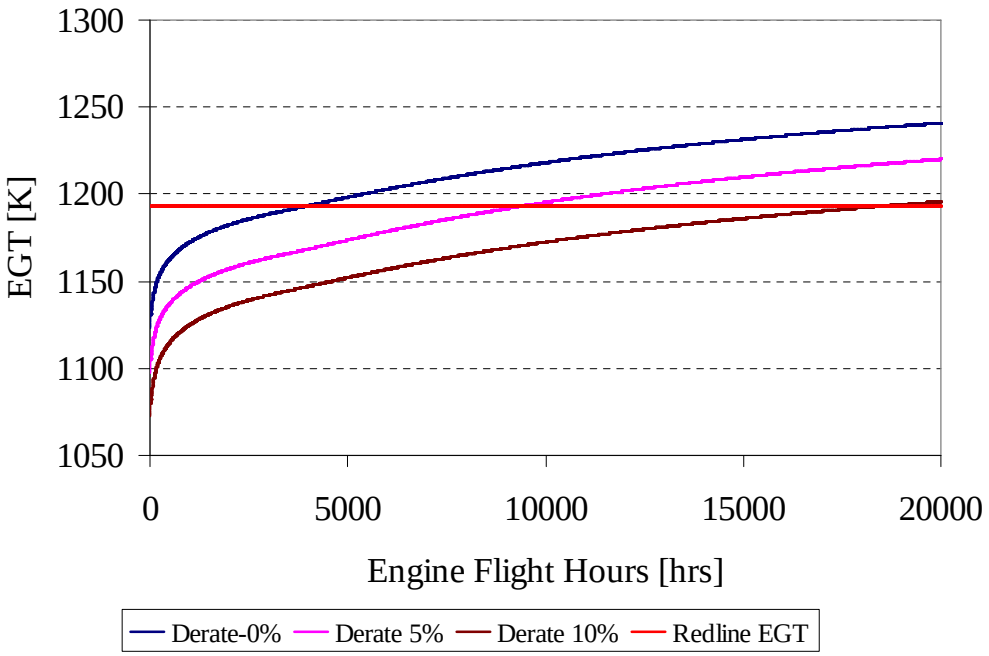

Figure 10.11 : Effect of take-off derate on shop visit interval of engine E56.

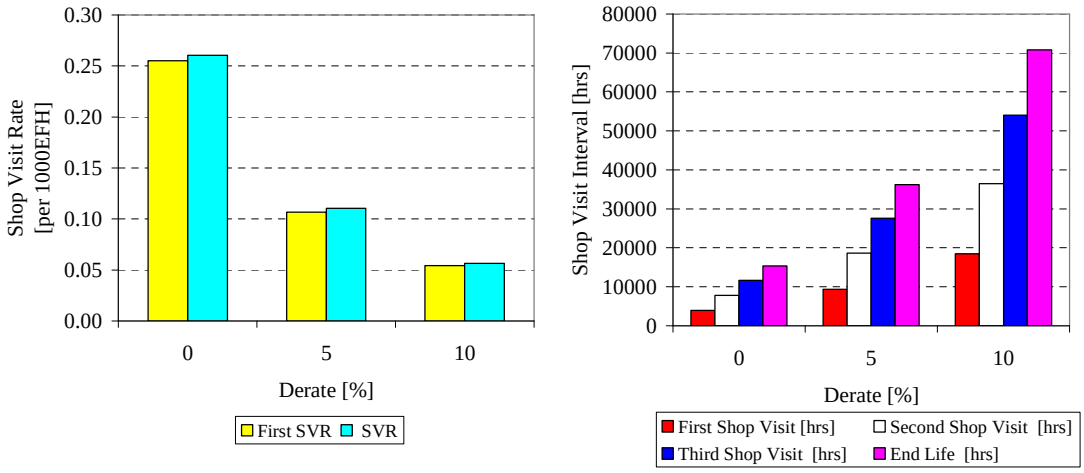

Figure 10.12 : Shop visit rate variation with take-off derate for engine E56.

The shop visit interval is improved with increasing take-off derate through the benefit of increasing the EGT margin with respect to the redline temperature. Hence the take-off derate has two fold benefits, such as one on the component severity, increasing the life of the components, and the other in increasing the EGT margin, a performance driver towards the shop visit.

Effect of Outside Air Temperature

The Outside Air Temperature (OAT) affects the crucial segment of take-off. The increase in the OAT, causes a fall in the thrust that is compensated by increasing the turbine entry temperature. This phenomenon encumbers continuous increase in the EGT with increasing level of degradation, as observed in the study, by varying the OAT from 18 °C to 30 °C to capture the effect on shop visit interval.

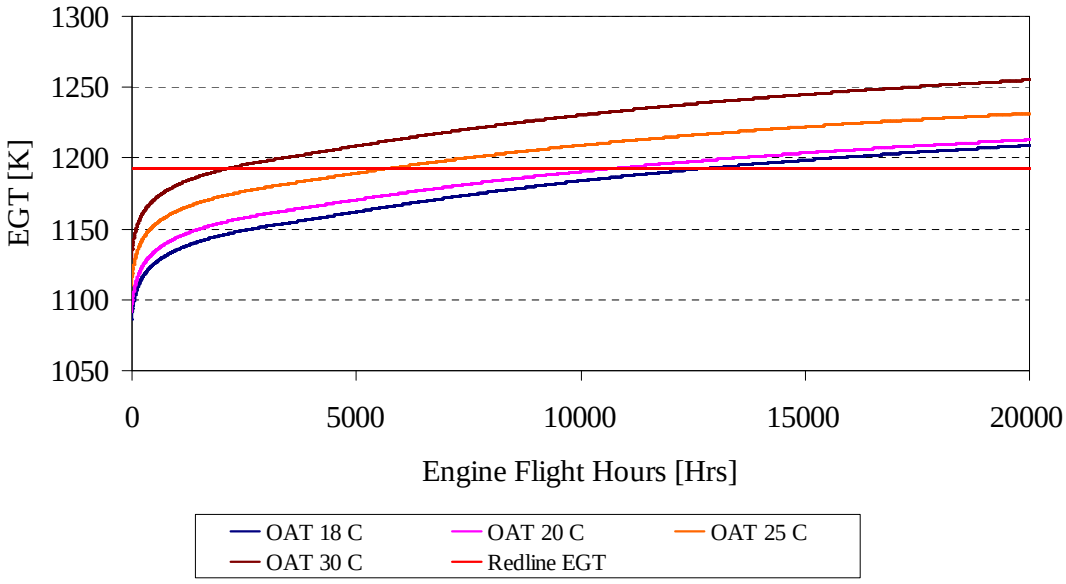

Figure 10.13 : Effect of OAT on shop visit interval for engine E56.

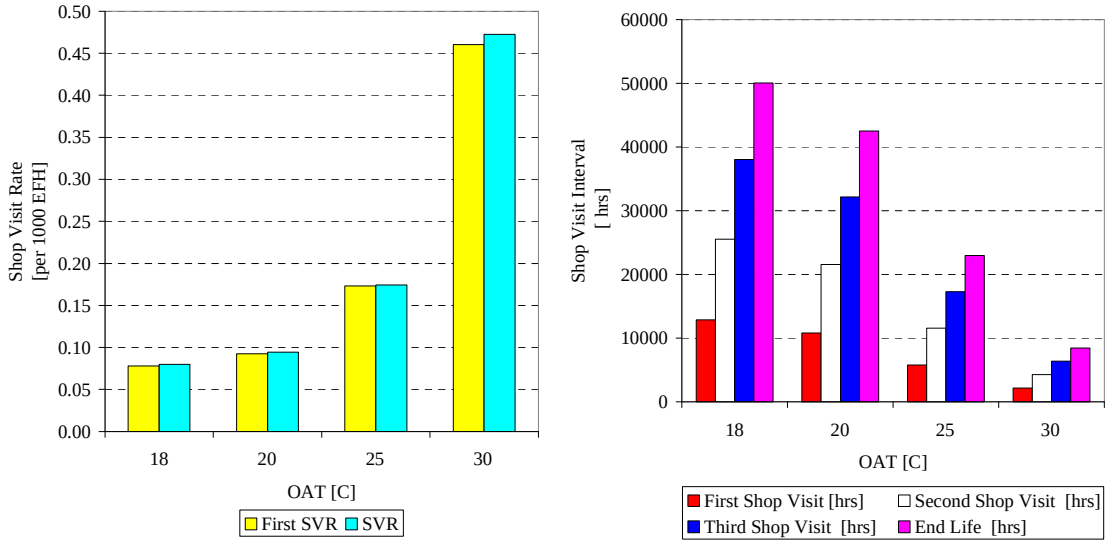

Figure 10.14 : Shop visit variation with OAT for engine E56.

The shop visit interval reduces with subsequent increase in the OAT, depicting greater sensitivity. Hence the factor of OAT affects the shop visit rate and varies with the geographical region.

Effect of Trip length

In the engine maintenance the the ratio of the EFH/EFC is important. The shorter trip lengths, reduce the engine flight hours as the life of the component is cycles limited. This is observed as per the derate-severity characteristics, having high level of severity for shorter trip lengths, due to underlying life limitation in cycles of operation. In the view of performance, the degradation being defined on the basis of cycles, gets scaled with the ratio of the EFH/EFC, specified as trip length of the mission. Hence the study involves the changes in the shop visit interval due to the trip lengths.

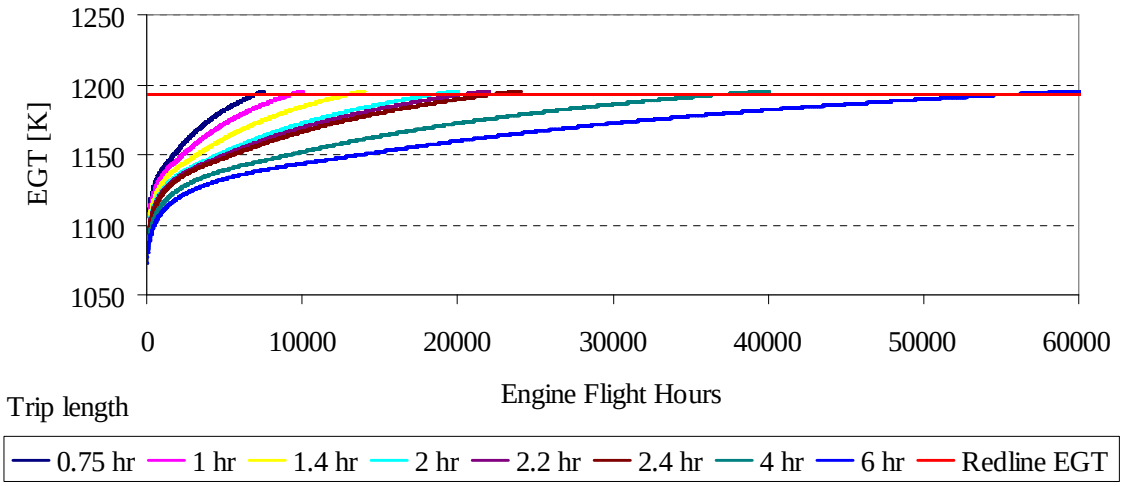

Figure 10.15 : EGT characteristics variation with trip lengths for engine E56.

The curves show the proportionality with respect to trip lengths, and the shop visit interval, increases for increasing trip lengths. Hence the trip lengths have importance for engine E56 with EFH/EFC ratio, as the short haul flights are limited by the cycles of operation.

10.5 Short Haul Flight – Aging Curve for E56 Engine

Towards the maintenance cost estimation, the age factor is needed. The age factor in maintenance is defined for the two basic aspects, such as the material and the labour. The labour is as per the industry practice, in restoration of the performance and reliability, or meeting the requirements for the shop visit, based on human effort and time. The age factor with respect to material is based on the shop visit interval, where the EGT margin is important. Since an airline operate on different derates and trip lengths for their fleet, the first SVR and SVR characteristics have been plotted, from the parametric studies, carried out on the E56 engine for short haul flight application.

The common use of E56 engine is in trip length range of 2 hrs to 6 hrs for which the range of the SVR factor is observed (Figure 10.16). The cruicial element of Mature Shop Visit Rate (MSVR) is estimated based on SVR and the severity. MSVR defines the shop visit interval, combining the component severity based on life consumption, and EGT margin consumption based on performance degradation.

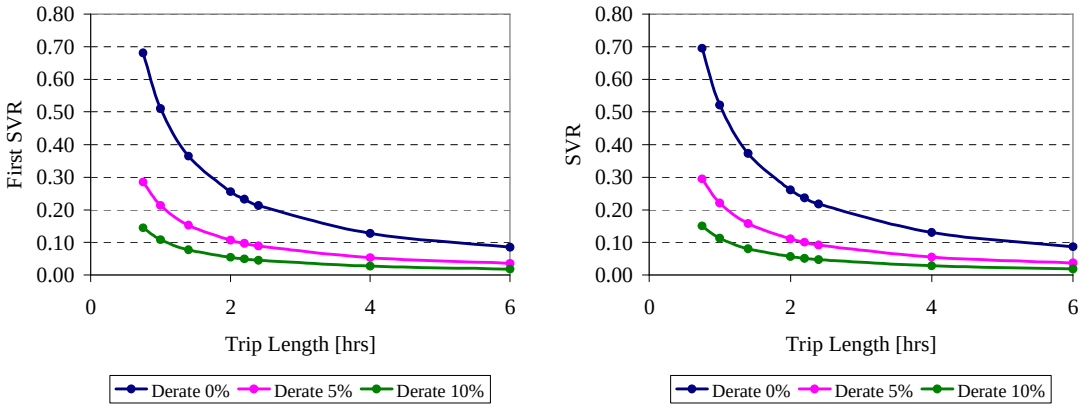

Figure 10.16 : Shop visit characteristics of engine E56.

MSVR	0.05	0.06	0.07	0.08	0.1	0.12	0.14	0.17	0.2	0.23	0.26	0.3
Effective Hours	76000	63333	54286	47500	38000	31667	27143	22353	19000	16522	14615	12667
Slope	1.5	1.5	1.5	1.5	1.5	1.5	1.5	1.5	1.5	1.5	1.5	1.5
Flight Hours	25333	21111	18095	15833	12667	10556	9048	7451	6333	5507	4872	4222
0	0.00	0.00	0.00	0.00	0.00	0.00	0.00	0.00	0.00	0.00	0.00	0.00
4000	0.06	0.08	0.10	0.12	0.16	0.21	0.25	0.33	0.39	0.46	0.52	0.60
8000	0.16	0.21	0.25	0.30	0.39	0.48	0.56	0.67	0.76	0.83	0.88	0.93
12000	0.28	0.35	0.42	0.48	0.60	0.70	0.78	0.87	0.93	0.96	0.98	0.99
16000	0.39	0.48	0.56	0.64	0.76	0.85	0.90	0.96	0.98	0.99	1.00	1.00
20000	0.50	0.60	0.69	0.76	0.86	0.93	0.96	0.99	1.00	1.00	1.00	1.00
24000	0.60	0.70	0.78	0.85	0.93	0.97	0.99	1.00	1.00	1.00	1.00	1.00
28000	0.69	0.78	0.85	0.90	0.96	0.99	1.00	1.00	1.00	1.00	1.00	1.00
32000	0.76	0.85	0.90	0.94	0.98	0.99	1.00	1.00	1.00	1.00	1.00	1.00
36000	0.82	0.89	0.94	0.97	0.99	1.00	1.00	1.00	1.00	1.00	1.00	1.00
40000	0.86	0.93	0.96	0.98	1.00	1.00	1.00	1.00	1.00	1.00	1.00	1.00
44000	0.90	0.95	0.98	0.99	1.00	1.00	1.00	1.00	1.00	1.00	1.00	1.00
48000	0.93	0.97	0.99	0.99	1.00	1.00	1.00	1.00	1.00	1.00	1.00	1.00
52000	0.95	0.98	0.99	1.00	1.00	1.00	1.00	1.00	1.00	1.00	1.00	1.00
56000	0.96	0.99	1.00	1.00	1.00	1.00	1.00	1.00	1.00	1.00	1.00	1.00
60000	0.97	0.99	1.00	1.00	1.00	1.00	1.00	1.00	1.00	1.00	1.00	1.00
64000	0.98	0.99	1.00	1.00	1.00	1.00	1.00	1.00	1.00	1.00	1.00	1.00
68000	0.99	1.00	1.00	1.00	1.00	1.00	1.00	1.00	1.00	1.00	1.00	1.00
72000	0.99	1.00	1.00	1.00	1.00	1.00	1.00	1.00	1.00	1.00	1.00	1.00
76000	0.99	1.00	1.00	1.00	1.00	1.00	1.00	1.00	1.00	1.00	1.00	1.00

Table 10.6 : Age factor estimation as Weibull distribution with respect to MSVR of engine E56.

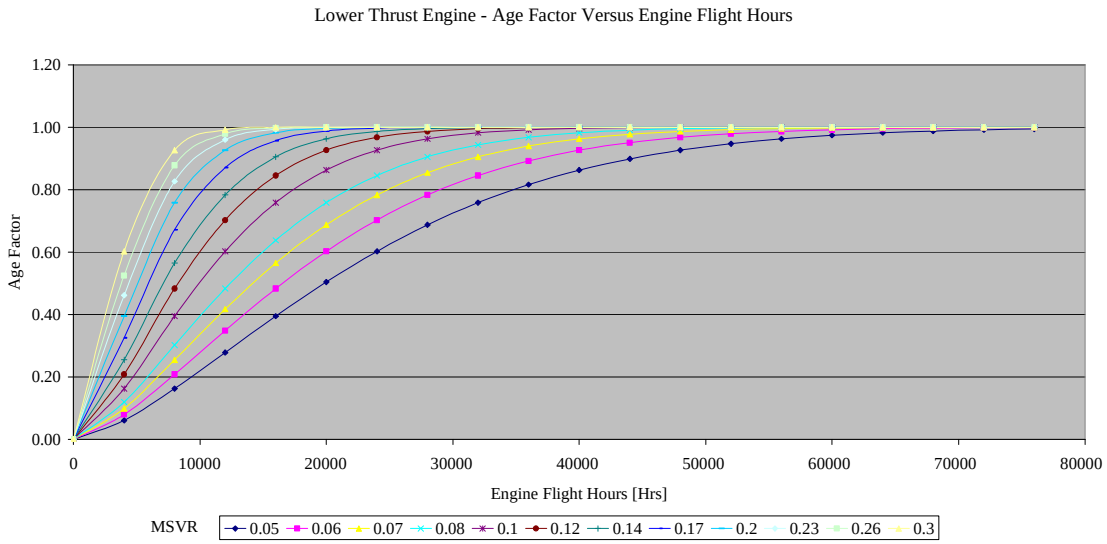

Figure 10.17 : Aging curves for engine E56.

The MSVR is fitted with a Weibull distribution to estimate the age factor variation with engine flight hours, referred to as the aging curve by the MRO. The aging curves reveal the spread of the age factor to longer time in service as the MSVR decreases.

10.6 Short Haul Flight – Effect of Engine Wash on Engine E56 Shop Visit Rate

Engine washing has been a current industry practice for partial restoration of the EGT margin, and thereby extending the shop visit interval. Engine washing helps in removing the deposits that degrade the performance of aerofoils. Hence the practice of engine wash has been aimed to achieve an EGT gain as high as 10 K per engine wash. However frequent engine wash with detergents and solvents mixed with water will lead to deterioration of the material surface and coatings, detrimental to the component life.

The benefits for the E56 engine, operated at take-off derate of 0 % has been estimated through the methodology. The shop visit interval is observed to be extended by 46 % through the use of engine wash for every 2000 flight hours. A considerable benefit that will help the engines, operated at lower take-off derates, due to demanding environment, so as to slow down the aging of the aircraft engine.

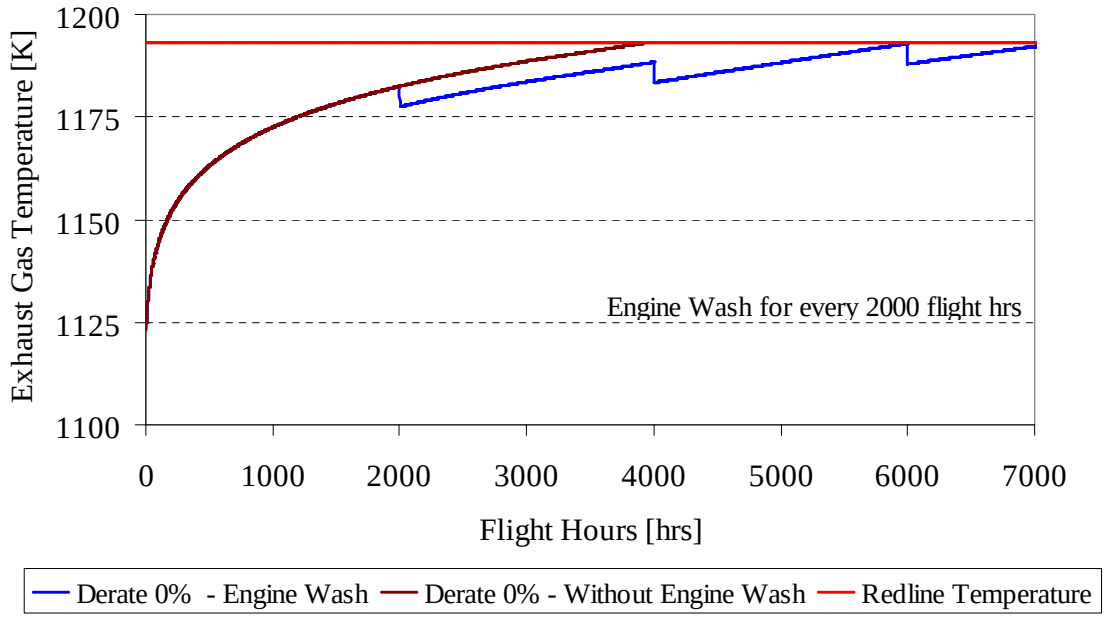

Figure 10.18 : Comparison of EGT characteristics due to engine wash for engine E56.

10.7 Long Haul Flight – Shop Visit Rate Prediction For Engine E115

The long haul flights use engines having more than 34000 lb thrust, and are considered as large thrust engines, suitably represented using engine model E115. The Turbomatch engine model built for the severity estimation has been adapted with the degradation characteristics for the shop visit prediction. The individual compressor and turbine components has been simulated for the degradation levels as specified in the Table10.7.

The limiting component life for the engine E115 is 3000 cycles for the interstage disc. The turbine blade is designed for useful life 15000 to 20000 hrs limited by the creep. Hence the EGT margin is balanced with the creep life of the turbine blade, and total number of cycles by the interstage disc with 3000 cycles. The degradation level is that of severe level as per the reference [42]. An intermediate point at 300 cycles has been assumed and the maximum degradation values are scaled down.

Engine Flight Cycles [cycles]	Fan Efficiency Change [%]	Fan Mass Flow Change [%]	LPC Efficiency Change [%]	LPC Mass Flow Change [%]	HPC Efficiency Change [%]	HPC Mass Flow Change [%]	HPT Efficiency Change [%]	HPT Mass Flow Change [%]	LPT Efficiency Change [%]	LPT Mass Flow Change [%]
1	0	0	0	0	0	0	0	0	0	0
300	-1.71	-2.19	-1.57	-2.40	-5.64	-8.44	-2.29	1.54	-0.65	0.25
3000	-2.85	-3.65	-2.61	-4.00	-9.40	-14.06	-3.81	2.57	-1.08	0.42

Table 10.7 : Degradation cycle definition of engine E115.

Installed EGT Margin [K]	1st Shop Visit EGT Margin [K]	2nd Shop Visit EGT Margin [K]	3rd Shop Visit EGT Margin [K]
85	50	45	40

Table 10.8 : EGT margin settings for shop visit prediction of engine E115.

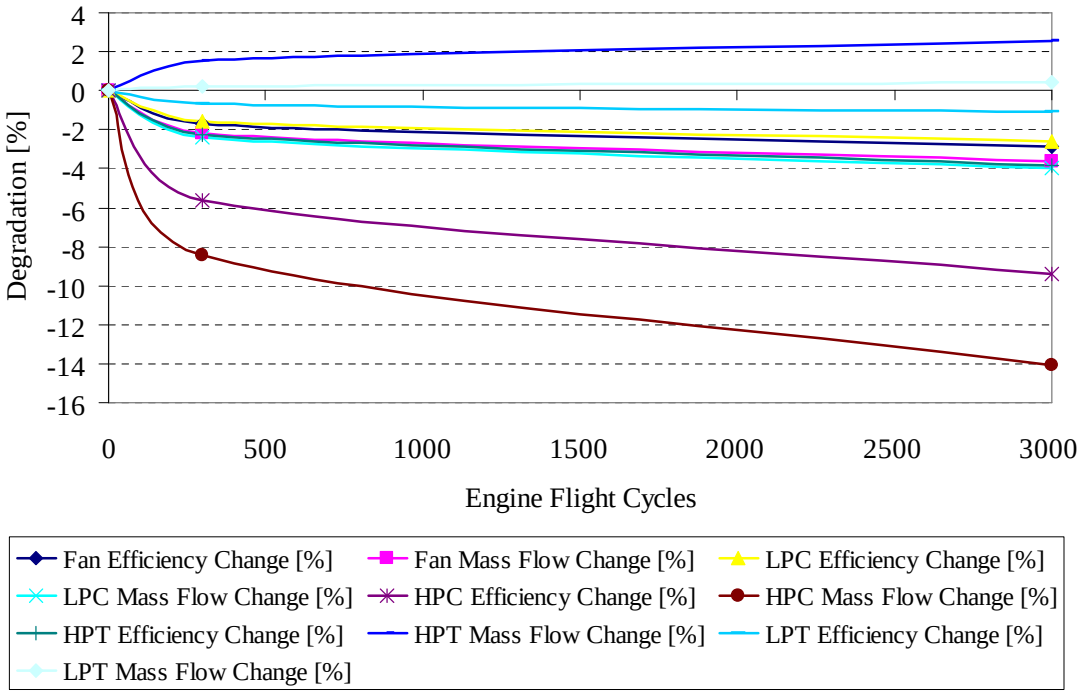

Figure 10.19 : Component degradation with engine flight cycles for engine E115.

The Turbomatch engine model is updated with component degradation as specified in the table. The exhaust gas temperature is tracked at the cycle definition points, so as to predict the first shop visit interval.

The case under consideration is for 4 % take-off derate at 15 °C OAT and a trip length of 8 hrs. The initial EGT margin for the engine E115 is 85 K and the exhaust gas temperature is measured at the 1st stage LPT nozzle. The redline temperatures (Appendix D) used for identifying the shop visits are 1363 K (1090 °C) at take-off and 1323 K (1050 °C) for continuous operation.

The EGT is tracked at take-off, climb and cruise segment of the flight path. The maximum temperature is observed at take-off, and an average temperature at climb and cruise, compared with the corresponding redline temperatures.

The intersection of the EGT curve with the redline temperature is considered as the first shop visit interval. Successive shop visits are tracked in a similar way,

using the EGT characteristics, by shifting the EGT margin, leading to different shop visit interval. The EGT margin during the shop visits is available in the Table 10.8.

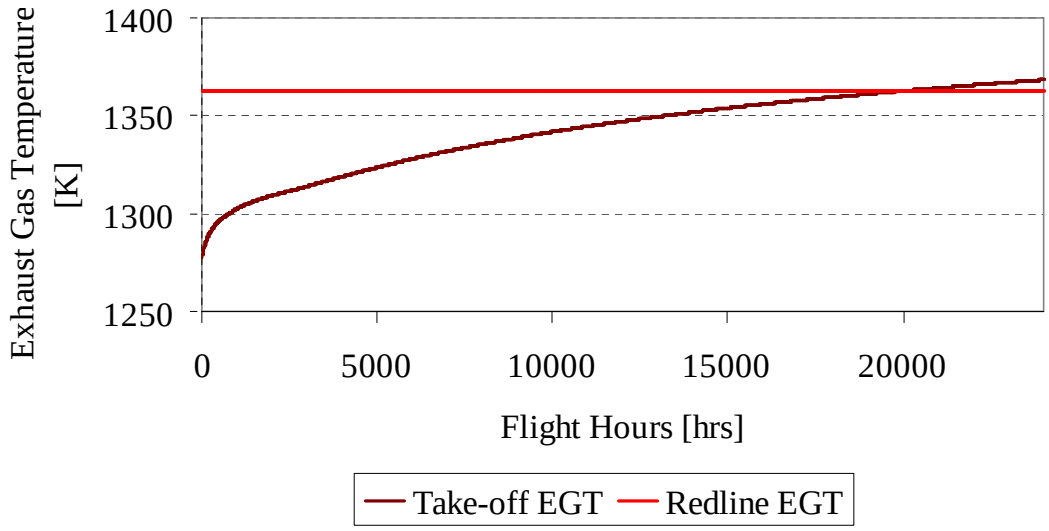

Figure 10.20 : Take-off EGT characteristics for engine E115.

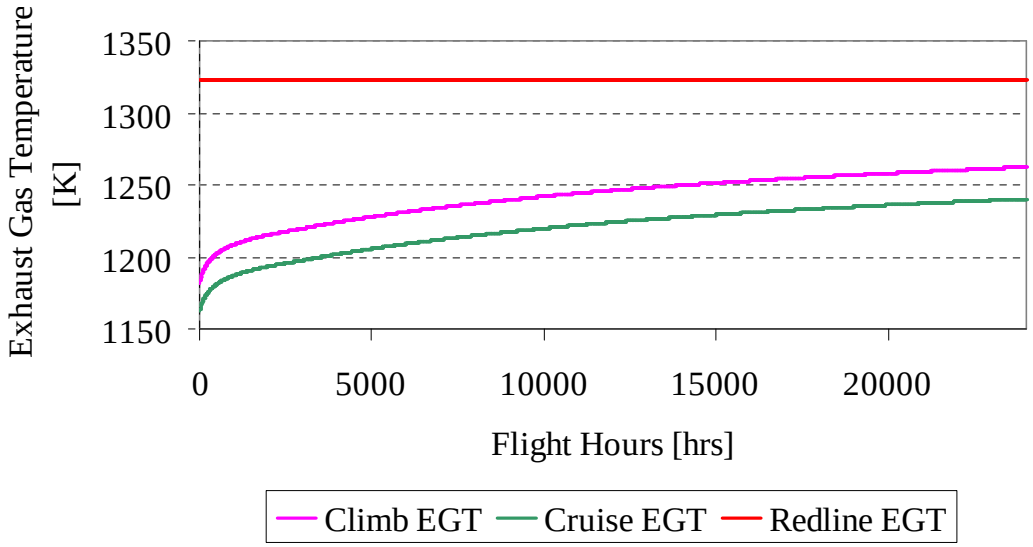

Figure 10.21 : Climb and cruise EGT characteristics for engine E115.

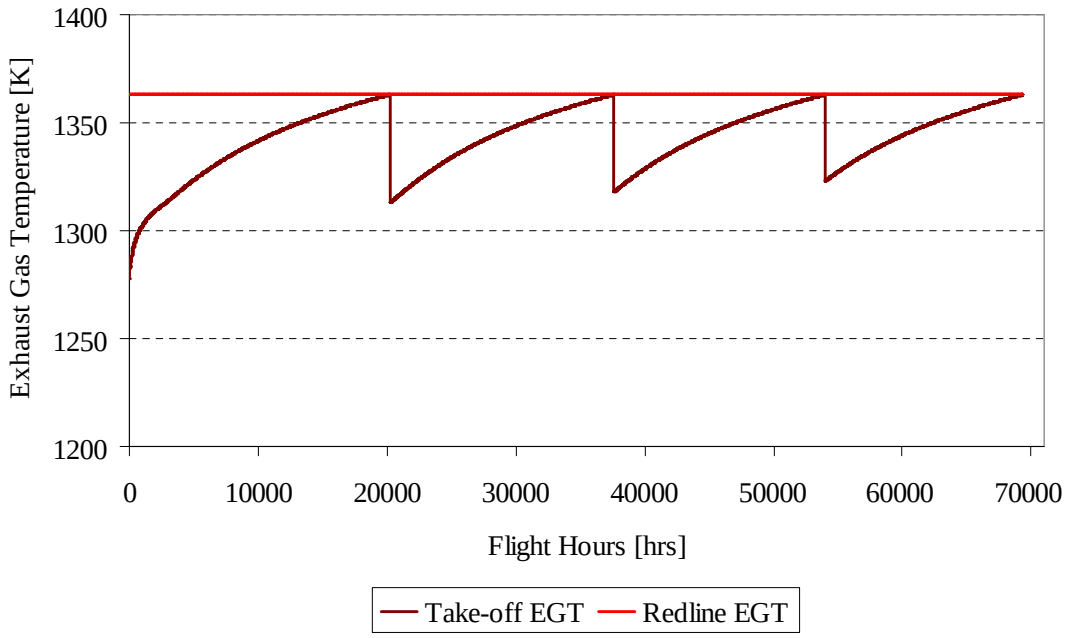

Figure 10.22 : Take-off EGT variation with successive shop visits for engine E115.

First SVR	SVR	First Shop Visit [hrs]	Second Shop Visit [hrs]	Third Shop Visit [hrs]	End Life [hrs]
0.05	0.06	20200	37600	53984	69312

Table 10.9 : Shop visit interval for engine E115 through shop visit prediction.

The first shop visit interval for the E115 engine is at 20200 hrs and SVR of 0.06 as observed for the large thrust engine. The values are concurrent with the MRO data (Appendix D) on SVR which portrays the suitablility of the methodology for predicting the shop visit .

10.8 Long Haul Flight – Operational Factors Study on Engine E115 Shop Visit Rate

The long haul flights are subjected to operational factors such as take-off derate, OAT and trip length causing relative shift in the shop visit interval. The significance of the individual factors has been portrayed for the lower thrust engines, and the large thrust engines follow a similar behaviour in consuming the EGT margin.

Effect of Take-off Derate

The take-off derate, a thrust reduction percentage, increases the EGT margin, and to identify the benefits on a large thrust engine, E115 has been studied. The take-off derate has been varied from 0 % to 4 % with the degradation cycle definition, as used for the shop visit prediction. The take-off EGT has been plotted, capturing the degradation characteristics with respect to different take-off derates.

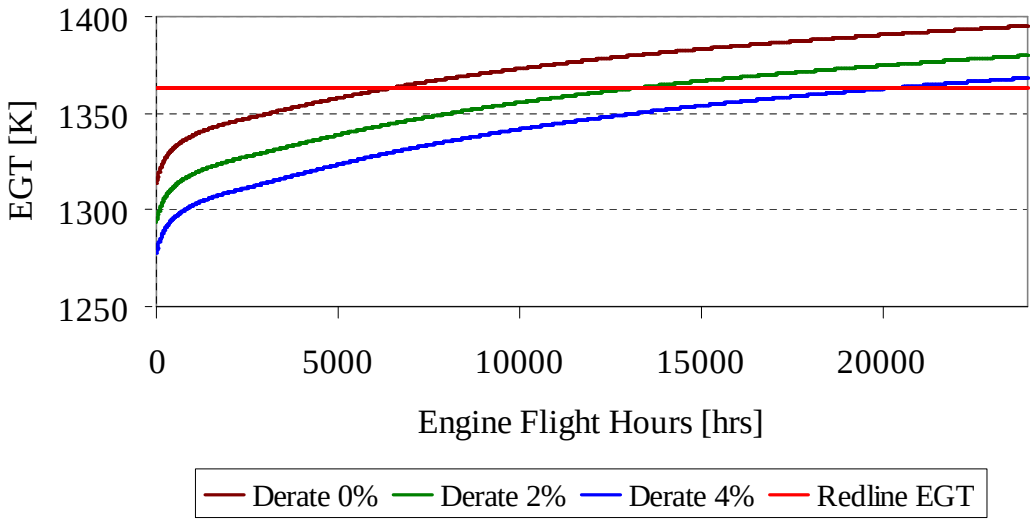

Figure 10.23 : Effect of take-off derate on EGT characteristics for engine E115.

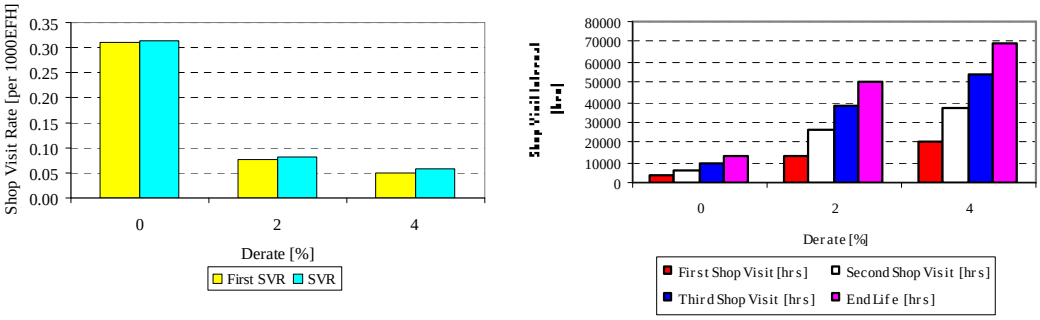

Figure 10.24 : Shop visit variation with take-off derate for engine E115.

The increasing take-off derate, reflects an increase in the shop visit interval, as larger EGT margin needs to be consumed. Take-off derate is said to improve the life of the components, and as well improving the shop visit interval through

larger EGT margin that plays a significant role in aircraft engine maintenance.

Effect of Outside Air Temperature

The increase in OAT is detrimental to the engine thrust, as the firing temperature is expected to be raised to achieve the desired thrust, especially at the crucial segment of take-off. The increase in the EGT due to variation in OAT from 15 °C to 25 °C has been carried out with the assumed degradation cycle .

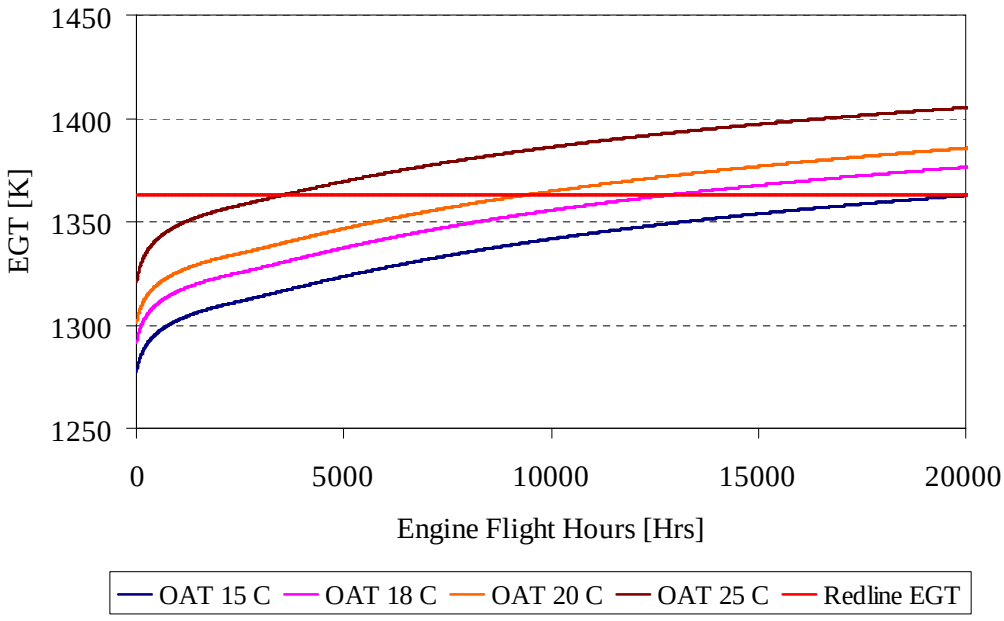

Figure 10.25 : Effect of OAT on EGT characteristics for engine E115.

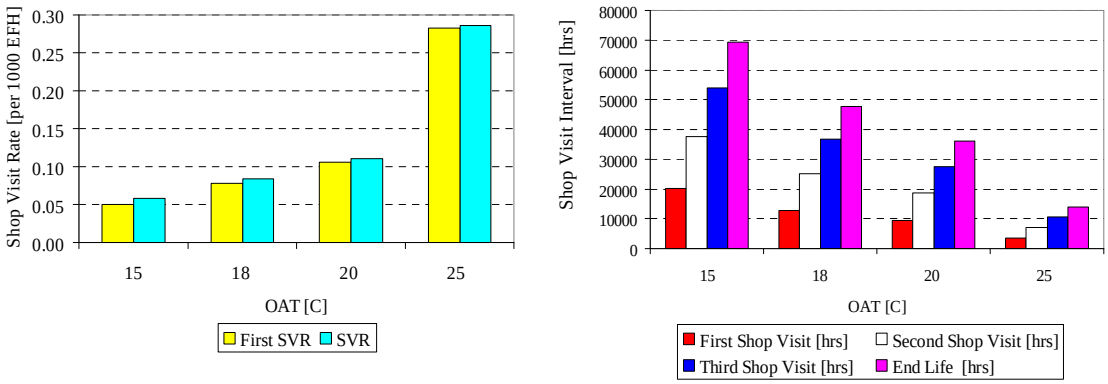

Figure 10.26 : Shop visit variation with OAT for engine E115.

The shop visit interval reduces significantly with the rise in OAT. A suitable take-off derate strategy has to be employed to counteract the reduction in the shop visit interval, and have a dominant role to play where aircraft engines operate at high OAT.

Effect of Trip length

The importance of the EFH/EFC ratio has been explored for the lower thrust engine, and holds good for the operation of the large thrust engines. The change in the behaviour is due to the use of large EFH/EFC ratio for the large thrust engines, as compared to the lower thrust engines that are much lower. This is quite evident in the longer trip mission purpose as the design requirement, and the dynamics shifts to engine flight hours due to creep limited component design. The study involves trip lengths from 1.4 hrs to 14 hrs to comprehend the benefits through the use of large EFH/EFC ratio.

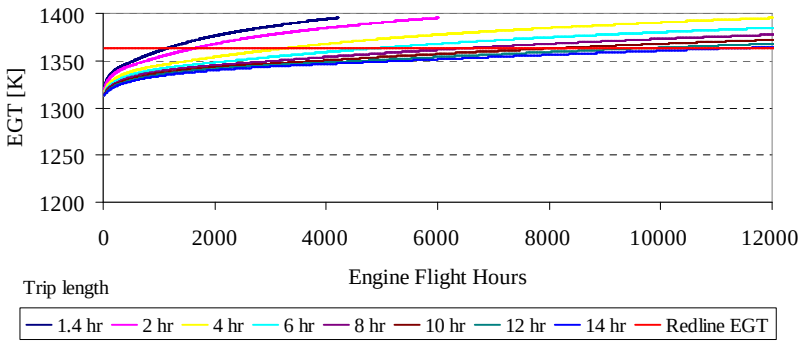

Figure 10.27 : Effect of trip length on the EGT characteristics of engine E115.

The shop visit interval increases with increasing trip lengths, hence the maintenance strategy depends on the choice of the EFH/EFC ratio for optimal use of the aircraft engines pertaining to the long haul flights. This points out the fact, that aircraft operated with fixed city pairs of low EFH/EFC ratio, needs to be swapped with aircraft of city pairs having higher EFH/EFC ratio, in order to maximize the fleet service life.

10.9 Long Haul Flight – Aging Curve for Engine E115

The aging curve of the large thrust engine E115 is estimated through the estimation of the MSVR. The SVR variation (Figure 10.28) with take-off derate and trip length, observed from the parametric study with respect to the operational scenario. The average SVR is used in the estimation of the MSVR with respect to the fleet under study. This estimated SVR with respect to the range of operational take-off derates provides the severity range, thereby the operational range of the MSVR being inferred.

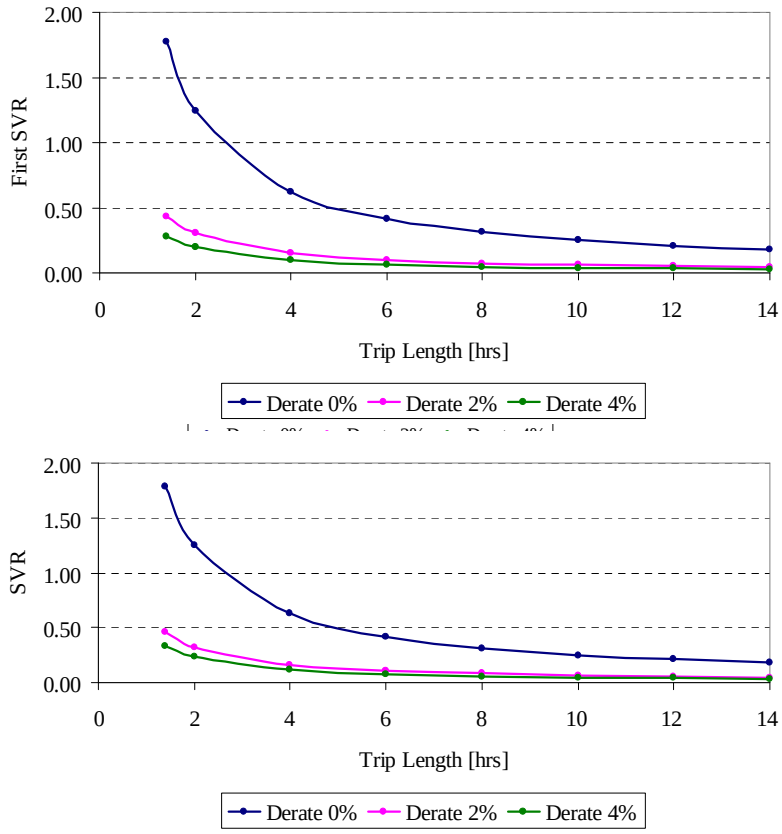

Figure 10.28 : Shop visit characteristics for engine E115.

MSVR	0.046	0.04	0.05	0.06	0.08	0.1	0.14	0.18	0.2	0.23	0.26	0.3
Effective Hours	82609	95000	76000	63333	47500	38000	27143	21111	19000	16522	14615	12667
Slope	1.5	1.5	1.5	1.5	1.5	1.5	1.5	1.5	1.5	1.5	1.5	1.5
Flight Hours	27536	31667	25333	21111	15833	12667	9048	7037	6333	5507	4872	4222
0	0	0	0	0	0	0	0	0	0	0	0	0
4000	0.05	0.04	0.06	0.08	0.12	0.16	0.25	0.35	0.39	0.46	0.52	0.60
8000	0.14	0.12	0.16	0.21	0.30	0.39	0.56	0.70	0.76	0.83	0.88	0.93
12000	0.25	0.21	0.28	0.35	0.48	0.60	0.78	0.89	0.93	0.96	0.98	0.99
16000	0.36	0.30	0.39	0.48	0.64	0.76	0.90	0.97	0.98	0.99	1.00	1.00
20000	0.46	0.39	0.50	0.60	0.76	0.86	0.96	0.99	1.00	1.00	1.00	1.00
24000	0.56	0.48	0.60	0.70	0.85	0.93	0.99	1.00	1.00	1.00	1.00	1.00
28000	0.64	0.56	0.69	0.78	0.90	0.96	1.00	1.00	1.00	1.00	1.00	1.00
32000	0.71	0.64	0.76	0.85	0.94	0.98	1.00	1.00	1.00	1.00	1.00	1.00
36000	0.78	0.70	0.82	0.89	0.97	0.99	1.00	1.00	1.00	1.00	1.00	1.00
40000	0.83	0.76	0.86	0.93	0.98	1.00	1.00	1.00	1.00	1.00	1.00	1.00
44000	0.87	0.81	0.90	0.95	0.99	1.00	1.00	1.00	1.00	1.00	1.00	1.00
48000	0.90	0.85	0.93	0.97	0.99	1.00	1.00	1.00	1.00	1.00	1.00	1.00
52000	0.93	0.88	0.95	0.98	1.00	1.00	1.00	1.00	1.00	1.00	1.00	1.00
56000	0.94	0.90	0.96	0.99	1.00	1.00	1.00	1.00	1.00	1.00	1.00	1.00
60000	0.96	0.93	0.97	0.99	1.00	1.00	1.00	1.00	1.00	1.00	1.00	1.00
64000	0.97	0.94	0.98	0.99	1.00	1.00	1.00	1.00	1.00	1.00	1.00	1.00
68000	0.98	0.96	0.99	1.00	1.00	1.00	1.00	1.00	1.00	1.00	1.00	1.00
72000	0.99	0.97	0.99	1.00	1.00	1.00	1.00	1.00	1.00	1.00	1.00	1.00
76000	0.99	0.98	0.99	1.00	1.00	1.00	1.00	1.00	1.00	1.00	1.00	1.00
80000	0.99	0.98	1.00	1.00	1.00	1.00	1.00	1.00	1.00	1.00	1.00	1.00

Table 10.10 : Age factor estimation as Weibull distribution with respect to MSVR of engine E115.

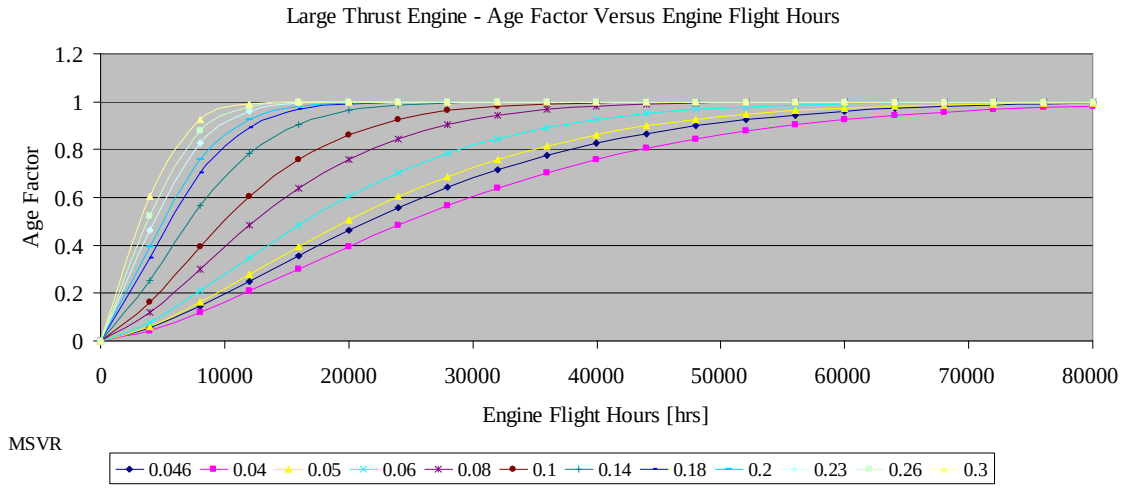

Figure 10.29 : Aging curves for engine E115.

The Weibull distribution with slope of 1.5, indicates the age factor with respect to the engine flight hours, from the MSVR values of interest yielding aging curves for the large thrust engines, as referred by MRO for maintenance cost estimation.

10.10 Long Haul Flight – Effect of Engine Wash on Engine E115 Shop Visit Rate

The engine washing entails the mechanism of restoring the performance, and hence reducing the exhaust gas temperature in the process. The mechanism of EGT margin benefit is explored for the large thrust engine E115, used for the long haul flights.

The un-derated engine EGT characteristics has been observed with the shop visit prediction methodology is analyzed with the EGT gain of 5 K for every engine wash, at an interval of 4000 flight hours. The shop visit interval is considerably increased through the gain in the EGT margin, as depicted in the Figure 10.30. Hence the scope of engine washing will have the benefit of increasing the shop visit interval for the large thrust engines operated at lower EGT margin.

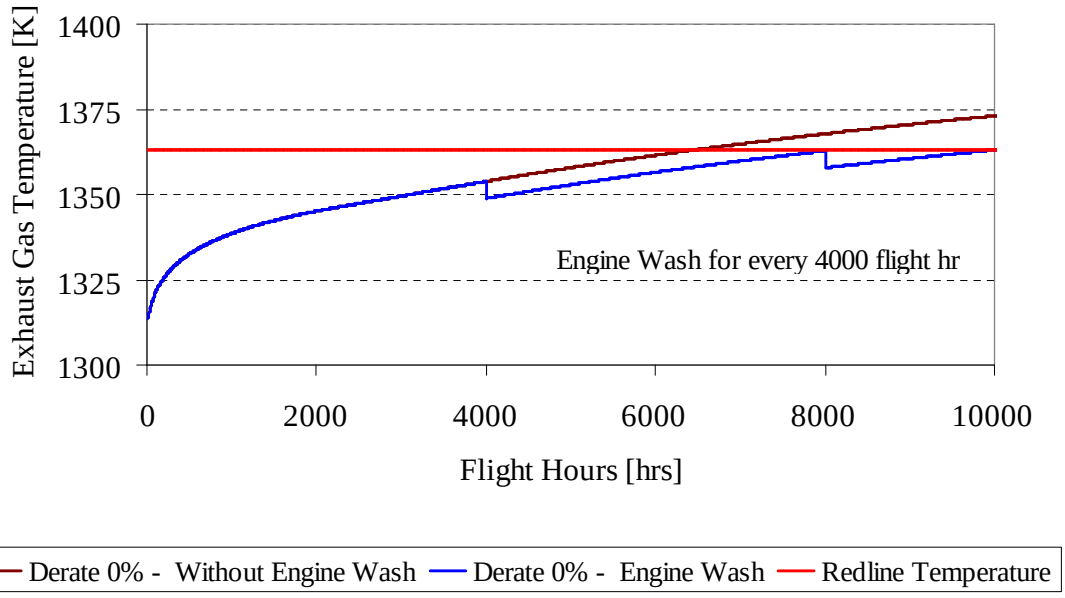

Figure 10.30 : Comparison of EGT characteristics due to engine wash for engine E115.

10.11 Shop Visit Rate Prediction Sensitivity Analysis

The sensitivity of the operational factors and engine wash has been characterized as change in SVR for every incremental value of the factors. This process of linearization will help in quantifying the benefits and the effect.

The take-off derate and OAT indicate larger sensitivity on shop visit rate of lower thrust and large thrust engines. This is due to the fact that EGT margin at take-off is a deciding factor in predicting the shop visit interval, and the use of take-off derate and outside OAT influence the consumption pattern considerably.

The EFH/EFC ratio or the trip length of the mission will be an important criterion as the sensitivity is magnified for larger trip lengths, reducing the SVR considerably for large thrust engines.

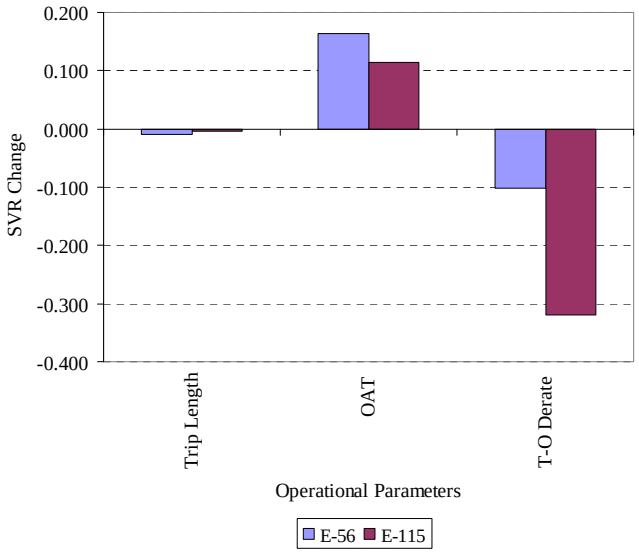

Figure 10.31 : Shop visit rate sensitivity plots for operational parameters.

		E-56	E-115
Operational Parameters	Increment	SVR Change	SVR Change
Trip Length [hrs]	1	-0.009	-0.004
OAT [C]	5	0.164	0.114
T-O Derate [%]	5	-0.102	-0.319

Table 10.11 : Shop visit rate sensitivity values for operational parameters.

The engine wash simulated as offset in the EGT margin, shows greater benefits in extending the shop visit interval, and hence a reduction in the SVR by 46% for lower thrust engines, and by 36% for the large thrust engines with respect to the assumed engine wash interval and EGT gain per wash.

Hence engine wash will be an enabling technology for reducing the maintenance cost, the interval for the engine wash will be of importance, and vary based on the engine EGT margin and degradation pattern.

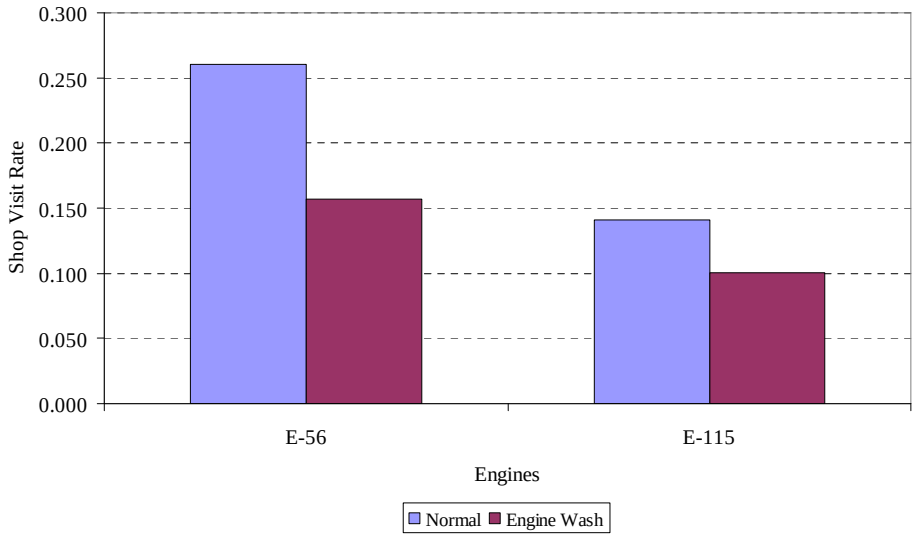

Figure 10.32 : Effect of engine wash for engine E56 and E115.

		SVR	
Engines	Normal	Engine Wash	Reduction [%]
E-56	0.261	0.141	46%
E-115	0.157	0.101	36%

Table 10.12 : Effect of engine wash on lower and large thrust engine..

10.12 Shop Visit Rate Prediction – Summary

The shop visit rate prediction methodology has been investigated on lower thrust (E56) and large thrust (E115) engine.

The degradation cycle definition is pivotal in determining the shop visit interval.

The shop visit rate observations are closer to the shop visit details of the engine, depicting the viability of the degradation pattern, and the suitability of the methodology for the prediction.

The three important operational factors, such as the take-off derate, OAT and EFH/EFC ratio have been analyzed through parametric studies on shop visit rate for the short haul and long haul flight engines.

The take-off derate and OAT, reveal high level of sensitivity on the SVR, and hence on the maintenance cost of civil aircraft engines.

The engine wash has significant contribution in extending the shop visit interval for the civil aircraft engines, and will be more beneficial for lower thrust engines working on low EFH/EFC ratio.

The age factor for maintenance cost estimation is derived through a Weibull distribution with respect to the MSVR, a the product of the SVR and the severity of the engine as defined by the MRO.

11 CONCLUSION

The research with the basic requirement of obtaining the engine characteristics of significance impacting the maintenance cost have been demonstrated through an integrated approach built on gas turbine fundementals. The two pivotal factors, such as *severity* in the realm of the relative life of the component, and *Shop Visit Rate (SVR)* in the realm of performance degradation has been obtained.

Through the severity estimation methodology, the engines belonging different thrust class have been studied to depict the severity characteristics with respect to operational and technological factors.

The following are the observations from the various studies on the basis of severity:

- The High Pressure Turbine (HPT) blade and disc are critical components dictating the severity factor on aircraft engines.
- The cooling effectiveness and thermal barrier coating are crucial factors controlling the life of the turbine blade.

Lower Thrust Engines

- The lower thrust engine HPT blade and disc are life limited due to cyclic damage (LCF). HPT blade dominates the derate-severity characteristics.
- Take-off derate and OAT have greater sensitivity on severity of lower thrust engines. A suitable choice of take-off derate will reduce the damage due to increase in OAT.
- The climb derate will improve the life of the HPT blade and the disc, irrespective of the taper and washout altitude.
- The effect of airport altitude on severity can be lowered through the use of suitable take-off derate.

Large Thrust Engines

- HPT blade is life limited by steady state damage (Creep) and disc by cyclic damage (LCF). HPT blade severity is always more than disc severity.
- Take-off derate and OAT prevail to be influencial factors on the severity of large thrust engines. Severity variation with take-off derate is flatter with increase in by-pass ratio of the engine.
- The climb derate will reduce the severity and prominent for three shaft engines as compared to two shaft engines.
- The cruise derate will lower the blade severity and two shaft design with larger by-pass ratio will benefit more.

The SVR prediction methodology has been implemented and the characteristic aging curves obtained for lower thrust and large thrust engines. The observations with respect to the shop visit prediction are:

Shop Visit Rate

- The shop visit interval could be predicted through EGT characteristics at take-off and climb with respect to component degradation, using Weibull curve representing the degradation variation with engine flight cycles.
- The take-off derate, OAT and EFH/EFC ratio affect the SVR.
- Engine washing will reduce the shop visit rate by 36 to 46 % based on the thrust class.
- The aging curve is a Weibull distribution of the estimated Mature Shop Visit Rate (MSVR).

12 Scope for Improvements and Further Research

The methodology phrased and demonstrated through the research is aimed to provide an insight on *severity* and *Shop Visit Rate (SVR),* as prominent parameters influencing maintenance cost of civil aircraft engines. The underlying steps to achieve the characteristics have been through different domains, such as aircraft performance model, gas turbine performance model, gas turbine design and life estimation methods. Hence the possibilities of improvement are prospective in different domains.

A simplified flight path analysis code has been built for the severity estimation which could be enhanced with advanced aircraft performance programs that deals with the detailed flight characteristics will be an advantage. For example, take-off and reverse thrust are important transient phenomenon, hence an integrated flight path analysis and gas turbine performance with transient capability will be useful in broadening the understanding on engine life consumption at the influencial segments. The variation in OAT with altitude, changes with different ambient temperatures at airport that will be closer to reality, as compared to the assumption of constant offset in OAT with altitude.

The performance model is built, based on the engine specification and certification documents which in certain respects lacks clarity, especially on the by-pass ratio, fan pressure ratio, overall pressure ratio data are corresponding to take-off top-of-climb or cruise is uncertain. Hence performance optimization based on cycle parameters, would enable identification of the performance parameters, at the critical mission points, making the design point data appropriate. The refinements on amount of cooling flows, bleed flow, splitting of the compressor pressure ratios, splitting cooling flows for stages of HPT will improve the suitability of engine performance model. The current level of coarse definition is good enough for gas turbine cycle definition, but needs to be

refined for providing inputs to gas turbine design and life estimation. The provision to split the efficiency change as depicted in the degradation cycle definition into the respective component efficiency, such as the high pressure compressor that is split up into more components needs to be accounted with respect to the net change in the efficiency will improve the degradation model for shop visit prediction.

Standard aerofoils have been used for the estimation of the blade thickness variation, could be extended to a wide range of profiles for the turbine and compressor blades. The NACA profiles with parbolic, circular arc and other prominent profiles, based on the industry practice will enable appropriate modeling of the geometry.

A comprehensive database on superalloy material properties and lifing data, would give the possibility of using the appropriate materials for the engine components, so as to identify the level of technology for different engines.

The heat transfer calculation module has only handfull of correlations for the preliminary calculation, and could be widened for more detailed investigation on heat transfer at the different sections of the components. The possible areas of improvement are, aerofoil heat transfer on pressure surface, suction surface and leading edge having different correlations. Based on the type of blade cooling technology the heat transfer to the blade surface and the tip shroud differs and could be captured through suitable correlations. Hence through the choice of appropriate correlations according to the heat transfer scenario will be important for severity estimation.

The prospective 3-D capability for fluid dynamics, thermal analysis and thermo-mechanical analysis as evident in research activities, could be synchronized along with the severity estimation for more finer modeling. The 2-D finite element analysis with thickness variation, could be extened into 3-D analysis of the blade geometry with a sector of the disc for detailed analysis capability on

the temperature and stress estimation. This will give room for modeling the blade cooling, thermal barrier coating and pattern factor effects towards more realistic simulation. However it could make the severity estimation more complex and computationally expensive.

The life estimation has been with respect to low cycle fatigue, creep and oxidation based on widely used approaches. The prospective theories such as Elasto-Plastic Fracture Mechanics (EPFM) for LCF and theta estimation approach for creep and many other theories could be experimented. This will provide a comparative view on life estimation techniques for severity estimation. Life estimation based on erosion of the blades and oxidation capturing fuel quality will form some of the future challenges.

The future scope in applying and extending the research towards maintenance aspects could be summarized as follows:

- Comprehensive engine severity estimation, inclusive of other components, such as fan and low speed spool systems (LPC and LPT).
- Variability in the material properties and manufacturing tolerances.
- Optimization of the fleet maintenace cost based on operational and environmental scenarios.
- Severity estimation for propfan and unducted fan LLP’s for future generation of narrow body aircraft engines.
- Monte Carlo simulation for fleet SVR prediction.
- Estimation of performance degradation mapped with actual engine fuel schedule or exhaust gas temperature for enhacement in SVR prediction.
- Engine wash strategy for engines.

The research has unlimited possibilities and avenues, receiving importance with focus of the industry and technology, while only a few have been outlined.

13 References

[1] ANDERSON, J. D.,JR. (1989), "*Introduction to flight",* 3rd ed, McGraw-Hill Book Company, Singapore.

[2] BERGER, JONATHAN N.,(2008), "*MRO 2008 – Efficient, Safe & Green"*, 2008 North American MRO Conference, Florida.

[3] BOSE, S. and DEMASI, J., "*Thermal barrier coating experience in gas turbine engine at Pratt & Whitney"*, 39559, Pratt & Whitney, East Hartford.

[4] BUNKER, R.S., "*Cooling design analysis"*.

[5] CANIERE, H. willCOKX, A., DICK, E. and DE PAEPE, M. (2006), "*Thermodynamic analysis of an air-cooled gas turbine with intercooling"*, 3265, AIAA, San Francisco. Report No: AIAA 2006-3265.

[6] CHAN, K. S., CHERUVU, N. S. and LEVERANT, G. R. (1999), "*Coating life prediction for combustion turbine blades"*, *ASME,* vol. 121, pp. 484-488.

[7] CHATTERJEE, S. and LITT, J. S. (2003), "*Online model parameter estimation of jet engine degradation for autonomous propulsion control"*, 5425, ASME, U.S. Paper No: GT2003-5425.

[8] CHOI, S. R., HUTCHINSON, J. W. and EVANS, A. G. (1999), "*Delamination of multilayer thermal barrier coatings*, *Mechanics of Materials",* vol. 31, no. 431-447, pp. 431-446.

[9] COHEN, H., ROGERS, G. F. C. and SARAVANAMUTTOO, H. I. H. (1996), "*Gas turbine theory",* 4th ed, Longman, Harlow.

[10] COLLINS, J. A. (1993), "*Failure of materials in mechanical design",* 2nd ed, John Wiley & Sons, United States of america.

[11] CRANFIELD SHORT COURSE LECTURE NOTES (2008), "*Gas turbine performance and design",* Cranfield University, UK.

[12] CROCKER, J. (1999), "*Effectiveness of maintenance"*, [Online], vol. 5, no. 4 available at: http://www.emerald-library.com.

[13] DAVIS, D. Y. and STEARNS, E. M. (1985), "*Energy efficient engine"*, 168219, NASA, Evandale. Report No: NASA CR-168219.

[14] DEMASI-MARCIN, J. T. and GUPTA, D. K. (1994), "*Protective coatings in the gas turbine engine*, *surface and coatings technology",* Surface & coatings technology, vol. 68-69, pp. 1-9.

[15] DESMORAT, R. (2002), "*Fast estimation of localised plasticity and damage by energetic methods"*, *International Journal of Solids and Structures,* vol. 39, pp. 3289-3310.

[16] DEVEREUX.B (1992), "*Improving life usage of the F404 engine through thrust rating",* MSc Thesis*,* Cranfield Institute of Technology, UK.

[17] DIETER, G. E. (1988), "*Mechanical metallurgy",* SI metric edition, McGraw-Hill, New York.

[18] DONALDSON, R., FISCHER, D., GOUGH, J. and RYSZ, M., (2007), "*Economic impact on derated climb on large commercial engines"*.

[19] ERASLAN, A. N. (2004), "*Tresca's yield criterion and linearly hardening rotating solid disks having hyperbolic profiles"*, Springer-Verlag, vol. 69, pp. 17-28.

[20] FIELDING, L. (2000), "*Turbine design : the effect on axial flow turbine performance of parameter variation",* ASME Press, New York.

[21] FONTANA, MARS GUY (1986), "*Corrosion engineering",* 3rd ed, McGraw-Hill, New York.

[22] GOMEZ, D. G. (2005), "*Variable cooling supply"*, MSc Thesis, Cranfield University, UK.

[23] GREEN, A. J. (1998), "*The development of engine health monitoring for gas turbine health and life management"*, 3544, AIAA, U.S. Report No: AIAA 98-3544.

[24] GUNSTON, B. (ED.) (1996), "*Jane's aero-engines",* .

[25] HALFORD, G. R., MEYER, T. T., NELSON, R. S. and NISSLEY, D. M. (1988), "*Fatigue life prediction modeling for turbine hot section materials"*, 100291, NASA, Washington. Report No: NASA-TM-100291.

[26] HILLERY, R. V. and PILSNER, B. H. (1985), *"Thermal barrier coating life prediction model"*, 175010, NASA, Washington. Report No: NASA CR-175010.

[27] HOLMAN, P. J. (2002), "*Heat transfer",* 9th ed, McGraw-Hill, Boston.

[28] HOLMS, A. G. and FALDETTA, R. D. (1947), *"Effects of temperature distribution and elastic properties of materials on gas turbine disk stresses"*, 1334, NACA, Washington. Technical Note No:1334.

[29] HORLOCK, J. H. (2001), *"The basic thermodynamics of turbine cooling"*, *Journal of Turbomachinery,* vol. 123, pp. 583-592.

[30] HORLOCK, J. H., WATSON, D. T. and JONES, T. V. (2001), *"Limitations on gas turbine performance imposed by large turbine cooling flows"*, *Journal of Engineering for Gas Turbines and Power,* vol. 123, pp. 487-494.

[31] HORLOCK, H. J. (1966), "*Axial flow turbines : fluid mechanics and thermodynamics",* Butterworths, London.

[32] HUTTER. (2006), *"Engine deterioration and maintenance actions"* (ICAO/Transport Canada Conference Aircraft Panel), Montreal.

[33] INFANTE, V., SILVA, J. M., DE FREITAS, M. and REIS, L. (2008), *"Failures analysis of compressor blades of aeroengines due to service"*, *Engineering Failure Analysis,* .

[34] JETENGINE CONSULTING, "*Operational cost",* Company presentation.

[35] ISSLER, S. and ROOS, E. (2003), *"Numerical and experimental investigations into life assessment of blade–disc connections of gas turbines"*, *Nuclear Engineering and Design,* vol. 226, no. 2, pp. 155-164.

[36] JAW, L. C. (2005), *"Recent advancements in aircraft engine health management (EHM) technologies and recommendations for the next*

step", *Proceedings of Turbo Exspo 2005: 50th ASME International Gas Turbine & Aeroengine Technical Congress,* June 6-9, 2005, ASME, .

[37] KERREBROCK, J. L. (1980), *"Flow in transonic compressors"*, *AIAA,* vol. 19, no. 1, pp. 4-19.

[38] KRAMER, W. H. and PAAS, J. E. (1980), *"CF6-6D engine short-term performance deterioration"*, 159830, NASA, U.S. Report No: NASA CR-159830.

[39] KURZ, R. and BRUN, K. (2007), *"Gas turbine tutorial - maintenance and operating practices - effects on degradation and life"*, *Proceedings of the thirty-sixth turbomachinery symposium,* pp. 173-185.

[40] LATTIME, S. B. and STEINETZ, B. M. (2002), *"Turbine engine clearance control systems: current practices and future directions"*, 211794, NASA, U.S. Report No: NASA/TM-2002-211794.

[41] LECTURE SERIES / VON KARMAN INSTITUTE FOR FLUID DYNAMICS (1995), "*Heat transfer and cooling in gas turbines",* Von Karman Institute for Fluid Dynamics, Rhode-Saint-Genese.

[42] LITT, J. S. and AYLWARD, E. M. (2003), *"Adaptive Detuning of a Multivariable Controller in Response to Turbofan Engine Degradation"*, 212723, NASA, Hanover. Report:NASA/TM-2003-212723.

[43] LITTLE, D. P. (1994), "*The effects of gas turbine engine degradation on life usage"*, MSc Thesis, Cranfield University, UK.

[44] LIU, H. W. and OSHIDA, Y. (1984), *"Literature survey on oxidations and fatigue lives at elevated temperatures"*, 174639, NASA, U.S. Report No: NASA CR-174639.

[45] LONG, C. A. (1994), *"Disk heat transfer in a rotating cavity with an axial throughflow of cooling air"*, *International Journal of Heat and Fluid Flow,* vol. 15, no. 4, pp. 307-316.

[46] LUKACHKO, S. P. and WAITZ, I. A. (1997), *"Effects of engine aging on aircraft nox emissions"*, 386, The American Society of Mechanical Engineers, New York.

[47] MAHADEVAN, S., MAO, H. and GHIOCEL, D. (2002), *"Probablistic simulation of engine blade creep-fatigue life"*, 1384, AIAA, Denver. Report No: AIAA 2002-1384.

[48] MAHASHABDE, A. (2006), "*Assessing selected technologies and operational strategies for improving the environmental performance of future aircraft",* MSc Thesis*,* Massachusetts Institute of Technology, U.S.

[49] MANSON, S. S. (1966), "*Thermal stress and low-cycle fatigue",* McGraw-Hill, New York.

[50] MANSON, S. S., *"Direct method of design and stress analysis of rotating disks with temperature gradient"*, 952, NACA, Washington. Report No:952.

[51] MARINAI, L., SINGH, R., CURNOCK, B. and PROBERT, D. (2003), "Detection and prediction of the performance deterioration of a turbofan engine", *Proceedings of the International Gas Turbine Congress,* November 2-7, 2003 tokyo, GTSJ, pp. 1-7.

[52] MATTINGLY, D. J. (2006), "*Elements of propulsion : gas turbines and rockets",* American Institute of Aeronautics and Astronautics, Reston, VA.

[53] METZGER, E. D. and AFGAN, H. N. (ED.) (1984), "*Heat and mass transfer in rotating machinery",* 9th ed, Hemisphere Pub. Corp, Washington.

[54] MOUSTAPHA, H. (2003), *"Axial and radial turbines",* Concepts NREC.

[55] NAEEM, M., SINGH, R. and PROBERT, D. (2001), *"Consequences of aero-engine deteriorations for military aircraft"*, *Applied Energy*, pp. 103-133.

[56] NAEEM, M., SINGH, R. and PROBERT, D. (1998), *"Implications of engine deterioration for fuel usage"*, *Applied Engineering,* vol. 59, no. 2, pp. 125-146.

[57] NAEEM, M., SINGH, R. and PROBERT, D. (1998), *"Implications of engine deterioration for operational effectiveness of a military aircraft"*, *Applied Energy,* vol. 60, pp. 115-152.

[58] OWEN, J. M. (1937), *"Heat transfer from turbine and compressor discs"*, 566, Aeronautical Research Council, U.K. Report No:566.

[59] OWEN, M. J. and ONUR, S. H. (APRIL 1983), *"Convective heat transfer in a rotating cylindrical cavity"*, *Transactions of ASME Journal of Engineering for Power,* Vol. 105, No. 2.

[60] PFOERTNER, H. and BROEDE, J. (2001), *"Statistical correlations for analysis and prediction of turbine engine component life usage"*, 34414, AIAA, U.S. Report No: AIAA 2001-34414.

[61] PILIDIS, PERICLES. (1983), "*Digital simulation of gas turbine performance",* PhD Thesis*,* University of Glasgow, UK.

[62] RAMSDEN, KENNETH, "*Turbomachinery",* Lecture Notes*,* Cranfield University, UK.

[63] RAO, J. S. (2000), "*Turbine blade life estimation",* Alpha Science.

[64] ROBERTS, M. L. (1978), *"Engine life, usage, and cycle selection"*, *Journal of Aircraft,* vol. 15, no. 4, pp. 240-245.

[65] SABOUR and BHAT, R. B. (2008), "*Lifetime prediction in creep-fatigue environment",* Materials Science, Vol.26, No.3, Poland.

[66] SARAVANAMUTTOO, H. I. H., ROGERS, G. F. C., COHEN, H., and STRAZNICKY, P. V.,(2009), "*Gas turbine theory",* 6th ed, Prentice Hall, Harlow.

[67] SHOEMAKER, W. W. (1980), *"Life cycle cost as a tool in the detail design of advanced propulsion systems"*, 1252, AIAA, New York. Report No: AIAA 80-1252.

[68] SIDWELL, C. V. (2004), "*On the impact of variability and assembly on turbine blade cooling flow and oxidation life",* PhD Thesis, Massachusetts Institute of Technology, US.

[69] SIMON, D. and SIMON, D. L. (2005), *"Aircraft turbofan engine health estimation using constrained kalman filtering"*, *Journal of Engineering for Gas Turbines and Power,* vol. 127, pp. 323-328.

[70] SPEAR, C. O. (1975), "*Turbine engine parts life improvement through thrust management"* , 0589, SAE, Hartford. Report No: 0589.

[71] SPIELER, S., STAUDACHER, S., FIOLA, R., SAHM, P. and WEIBSCHUH, M. (2008), "Probablistic engine performance scatter and deterioration modeling", *Journal of Engineering for Gas Turbines and Power,* vol. 130.

[72] STABRYLLA, G. R. and TROHA, A. W. (1980), *"Effect of aircraft power plant usage on turbine engine relative durability/life"*, 1115, AIAA, U.S. Report No: AIAA 80-1115.

[73] STECURA, S. and LEIBERT, C.H., (1977), "*Thermal barrier coating system"*, B32B, U.S. Patent No:4485151.

[74] STEPHENS, I. R. and OTTEN, H. F. (2001), "*Metal fatigue in engineering",* 2nd ed, John Wiley & Sons, New York.

[75] STERNER, S. C. and SAIGAL, S. (1994), "A unified numerical approach for the analysis of rotating disks including turbine rotors", *International Journal Solids Structures,* vol. 31, no. 2, pp. 269-277.

[76] SUAREZ, E., HANSEN, J., DUFFY, M. and GATLIN, P. (1997), "*New approach to tracking engine life"*, 2900, AIAA, U.S. Report No: AIAA 97-2900.

[77] SUAREZ, E. L., DUFFY, M. J., SETO, D. and COTE, S. M. (2003), "*Advanced life prediction systems for gas turbine engines"*, 4985, AIAA, U.S. Report No: AIAA 2003-4985.

[78] SUNDEN, B. (2001), "*Heat transfer in gas turbines",* WIT Press.

[79] SWAMINATHAN, P. V., ALEN, M. J. and TOUCHTON, L. G. (OCTOBER 1997), *"Temperature estimation and life prediction of turbine blades using post-service oxidation measurements"*, *Transactions of the ASME Journal of engineering for gas turbines and power,* vol.119, no.4,.

[80] TINGA,T.,VISSER,W.P.J.,DE WOLF,W.B and BROOMHEAD, M.J., (MAY 2000), *"Integrated lifing analysis tool for gas turbine components"*. National Aerospace Laboratory, NLR-TP-2000-049

[81] TONG, T. M., HALLIWELL, I. and GHOSN, J. L. (2004), *"A computer code for gas turbine engine weight and disk life estimation"*, *Transactions of the ASME Journal of engineering for gas turbines and power,* vol.126, no.2.

[82] TORBIDONI, L. and HORLOCK, J. H. (2005), *"A new method to calculate the coolant requirements of a high-temperature gas turbine blade"*, *Journal of Turbomachinery,* vol. 127, pp. 191-199.

[83] WALKER, G. I. and DONOVAN, R. M. (1979), *"Parts tracking and engine history recording for on-condition maintenance"*, 1280, AIAA, New York. Report No: AIAA 79-1280.

[84] WALSH, P. P. and FLETCHER, P. (2004), "*Gas turbine performance",* 2nd ed, Blackwell Science, Oxford.

[85] Website of ANSYS, available at: http://www.ansys.com/. (Finite element analysis software details)

[86] Website of CFM INTERNATIONAL, available at: http://www.cfm56.com/. (Engine Specifications)

[87] Website of EASA, available at: http://www.easa.eu.int/. (Engine Certification Documents)

[88] Website of ESDU, available at : www.esdu.com

[89] Website of GE AIRCRAFT ENGINES, available at: http://www.geae.com/. (Engine Specifications)

[90] Website of HAYNES INTERNATIONAL, available at: http://www.haynesintl.com/. (Superalloy Material Properties)

[91] Website of HIGH TEMP METALS, available at: http://www.hightempmetals.com/.(Superalloy Material Properties)

[92] Website of ICAO, available at: http://www.icao.int/. (Engine Certification Documents)

[93] Website of KNOVEL, available at : www.knovel.com (E-books)

[94] Website of MATLAB, available at: http://www.mathworks.com/. (Mathematical software details)

[95] Website of PRATT & WHITNEY, available at: http://www.pw.utc.com/. (Engine Specifications)

[96] Website of ROLLS-ROYCE, AVAILABLE AT: http://www.rolls-royce.com/civil/index.jsp. (Engine Specifications)

[97] Website of SPECIAL METALS, available at: http://www.specialmetals.com/. (Superalloy Material Properties)

[98] WING, R., (2000), "*White hot technology - a turbine revolution*".

[99] WITEK, L. (2006), *"Failure analysis of turbine disc of an aero engine"*, *Engineering Failure Analysis,* vol. 13, no. 1, pp. 9-17.

[100] YOUNG, J. B. and HORLOCK, J. H. (2006), *"Defining the efficiency of a cooled turbine"*, *Journal of Turbomachinery,* vol. 128, pp. 658-667.

[101] ZAITA, A. V., BULEY, G. and KARLSONS, G. (1998), *"Performance deterioration modeling in aircraft gas turbine engines"*, *Journal of Engineering for Gas Turbines and Power,* vol. 120, pp. 344-349.

[102] ZARETSKY, E. V. and HENDRICKS, R. C. (2002), *"Weibull-based design methodology for rotating aircraft engine structures"*, 211348, NASA, U.S. Report No: NASA/TM-2002-211348.

[103] ZHU, D., BANSAL, N. P., LEE, K. N. and MILLER, R. A. (2001), *"Thermal conductivity of ceramic thermal barrier and environmental*

barrier coating materials", 211122, NASA, Hanover. Report No: NASA/TM-2002-211122.

[104] ZIENKIEWICZ, O. C. and TAYLOR, R. L. (2000), "*The finite element method",* 5th ed, Butterworth-Heinemann, Oxford.

Appendix A

Turbomatch brick model representing the performance characteristics for engine E56 and E115.

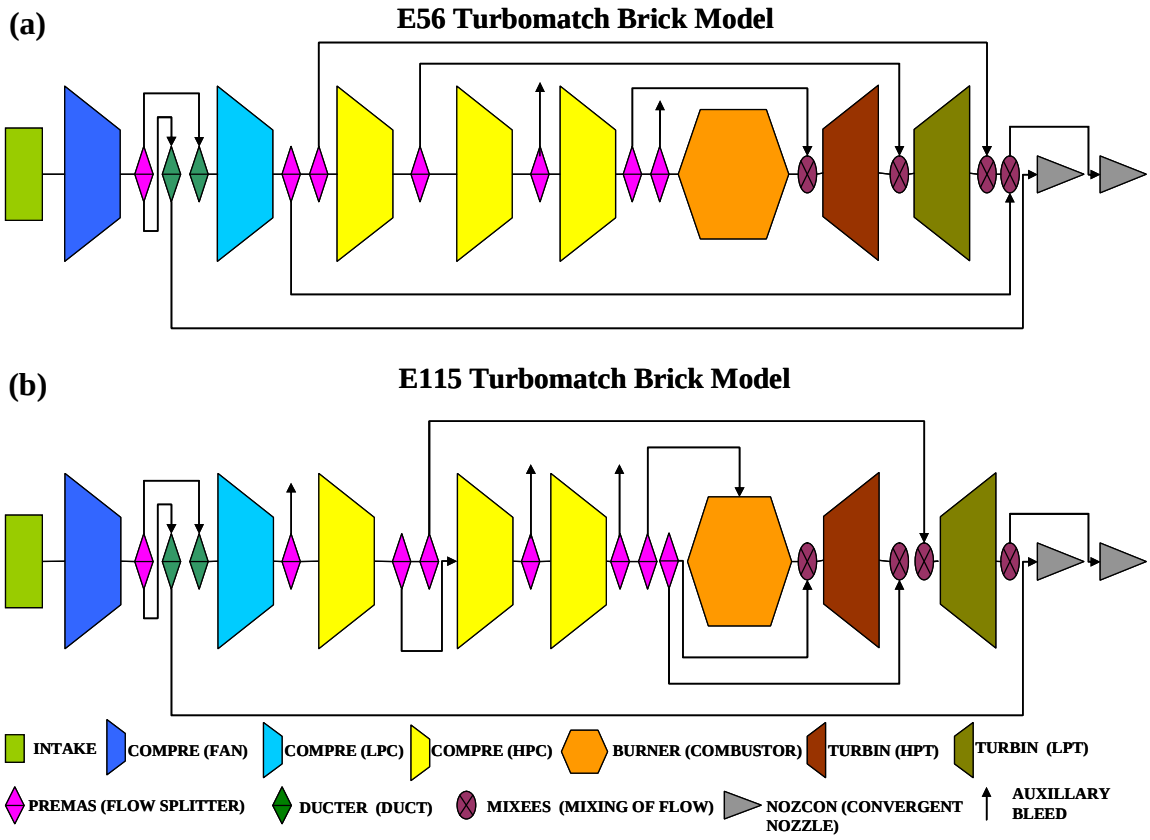

Figure A.1 : Turbomatch brick layout for engines (a) E56 (b) E115.

Appendix B

The flow path and blade sizing output from the sizing code. All dimensions are in metres.

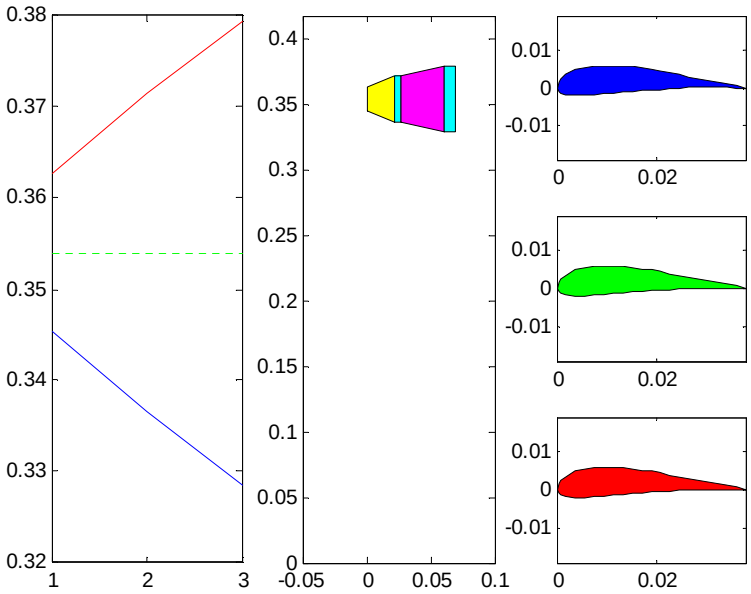

Figure B.1 : HPT flow path and blade sizing for E56.

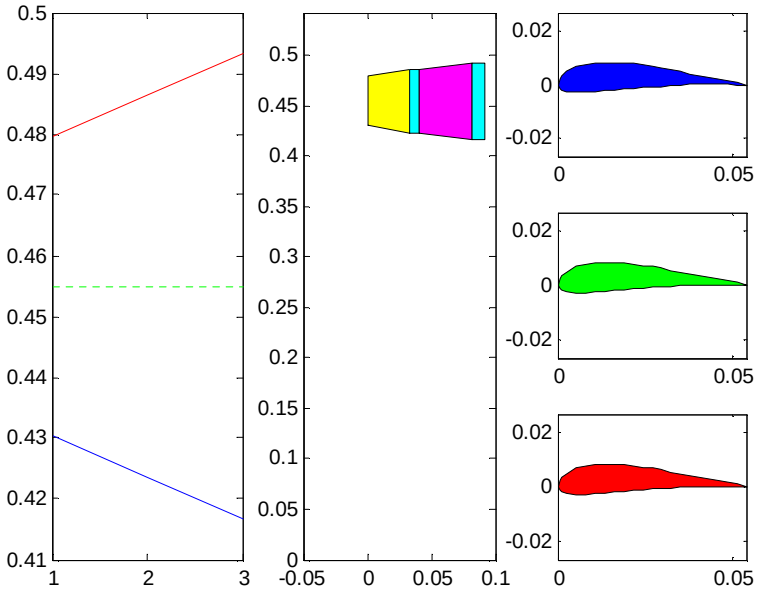

Figure B.2 : HPT flow path and blade sizing for E115.

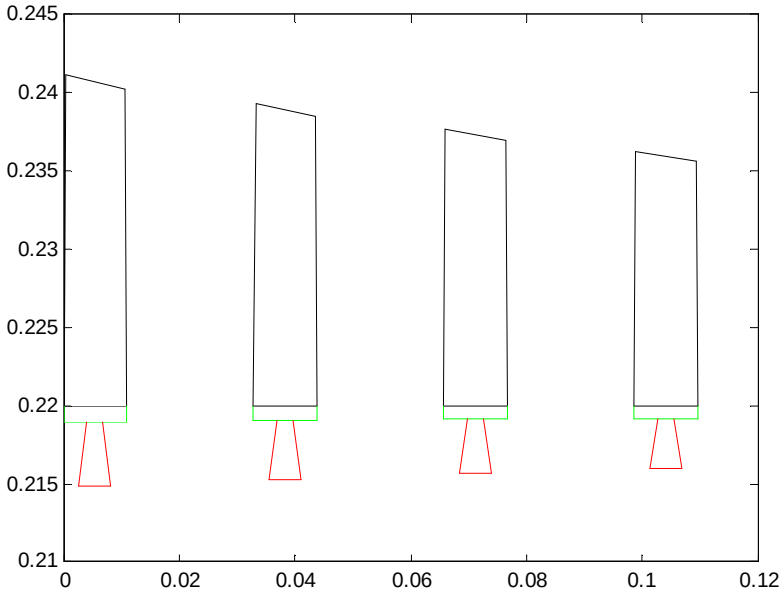

Figure B.3 : HPC flow path and blade sizing for E56.

Appendix C

The Larson Miller curve for Inconel 718 [97] and Rene 41 [90].

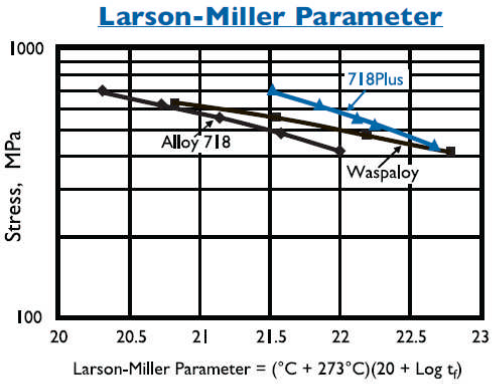

Larson-Miller Plot of Stress Rupture Life of Alloy 718Plus in Comparison with Alloy 718 and Waspaloy

Figure C.1 : Larson Miller curve for Inconel 718 [97].

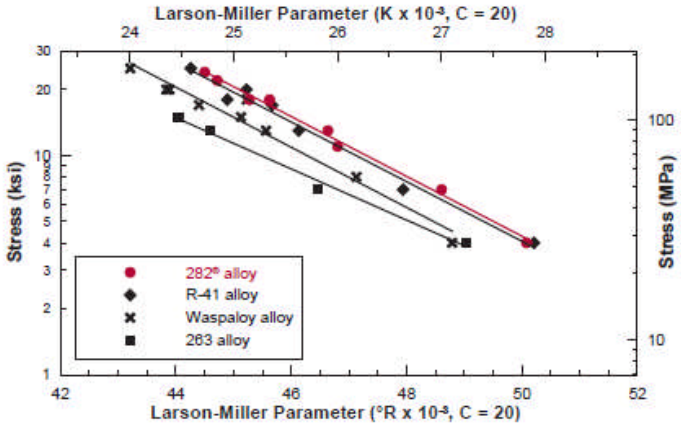

Figure C.2 : Larson Miller curve for R-41 (Rene 41) [90].

	Oxidation Constant	Depth of Oxidation	Activation Energy/Gas Constant
	C_{oxid}	d	Q/R
Component		[in]	[(ft-lb/lb)/(ft/R)]
Blade	4.3	0.0079	33608
Disc	4.3	0.0020	25700

Figure C.3 : Oxidation parameters for life estimation [79].

Appendix D

The MTBR data for CFM56-7 [34] comparable with E56 and GE90-115B [2] comparable with E115.

(a) **(b)**

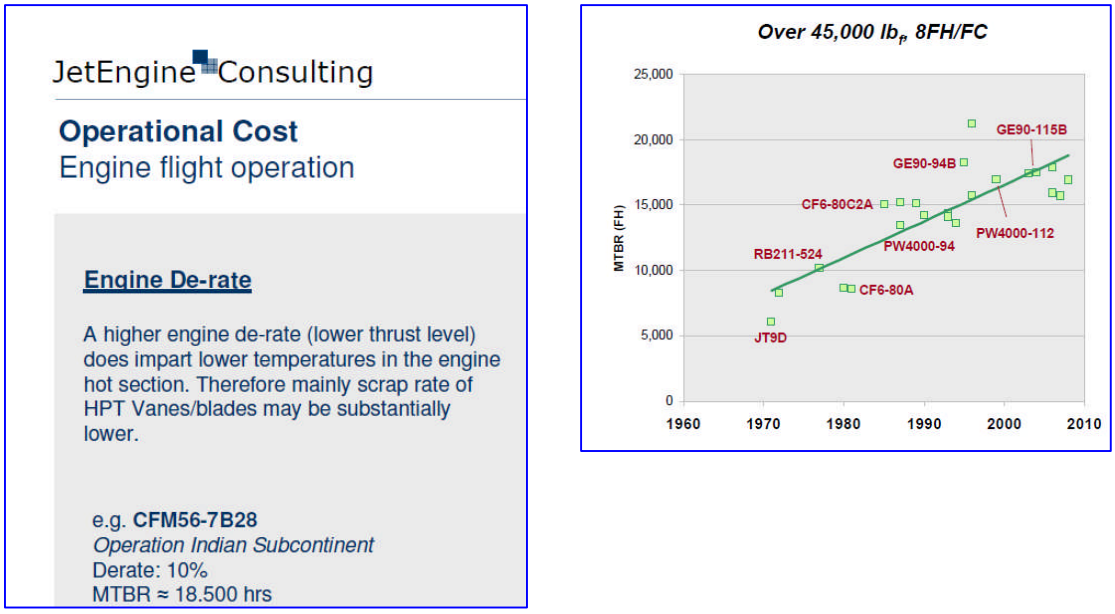

Figure D.1 : MTBR data for engines (a) CFM56-7 [87] (b) GE90-115B [87].

(a)

IV. Operational Limits:

1. Temperature Limits:

1.1 Exhaust Gas Temperature (°C):
The exhaust gas temperature is measured at station T49.5 (stage 2 LPT nozzle).

	Variants	Actual Temperature	Displayed Temperature
Take-Off	SAC and TI non "/F"	920	950
	DAC	930	
	TI "/F"	940	
Maximum Continuous	SAC and TI non "/F"	895	925
	DAC	905	
	TI "/F"	915	
Starting	All	725	725

(b)

IV.Operational Limits:

1. Temperature Limits:

1.1 Exhaust Gas Temperature (EGT), °C (°F):

	GE90-110B1, -113B, -115B
Take-off* (5 minutes, see note 3)	1090 (1994)
*: 30 seconds maximum transient	1095 (2003)
Maximum Continuous	1050 (1922)
Starting (Maximum on Ground)	750 (1382)
Starting (Maximum in Flight)	825 (1517)

EGT is measured at the inlet of the LP Turbine

Figure D.2 : Redline temperatures for engines (a) CFM56-7 [34] (b) GE90-115B [34].

Appendix E

The climb derate aimed at improving the engine life has the features of using the climb thrust reduction at the initial phase of the climb. After a certain altitude considered as taper altitude from which the climb thrust reduction is transitioned to the rated top-of-climb thrust (0 % climb thrust reduction) at an higher altitude called as the washout altitude. The climb derate study has been carried out for E56 and E115 with various combinations of taper and wash out altitude indicated for example as 50/90 signify taper altitude at 50% of the cruise altitude and washout altitude at 90% of the cruise altitude.

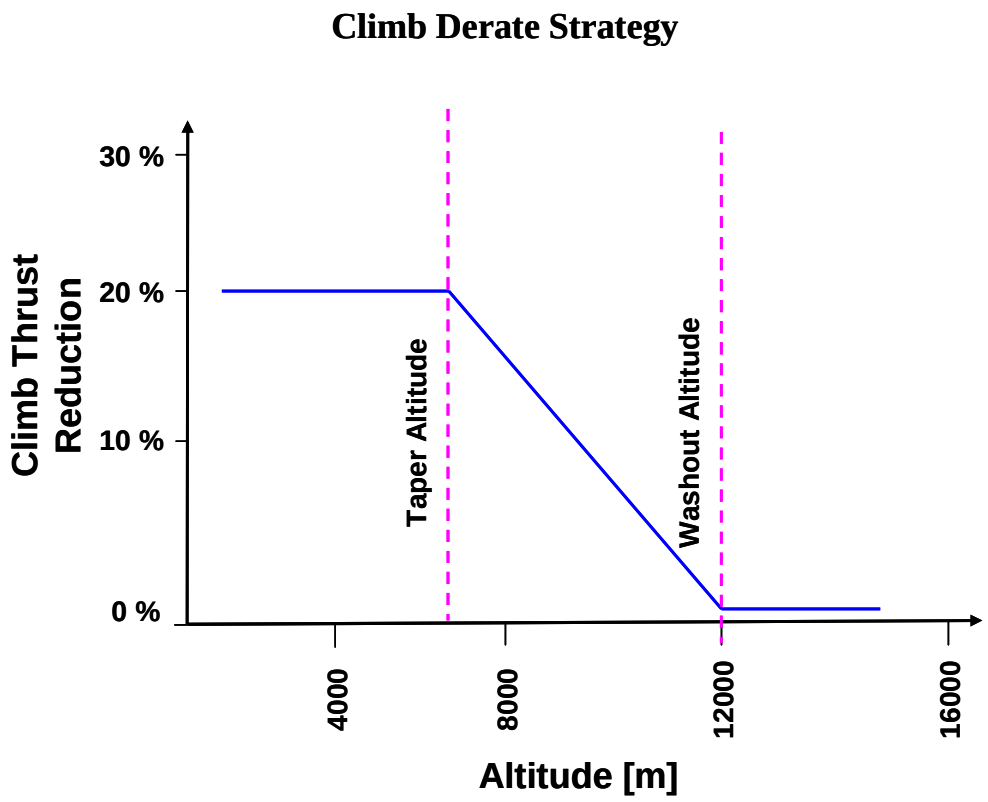

Figure E.1 : Typical climb derate characteristics.

Appendix F

The graphical user interface of the tool developed for the severity and shop visit prediction.

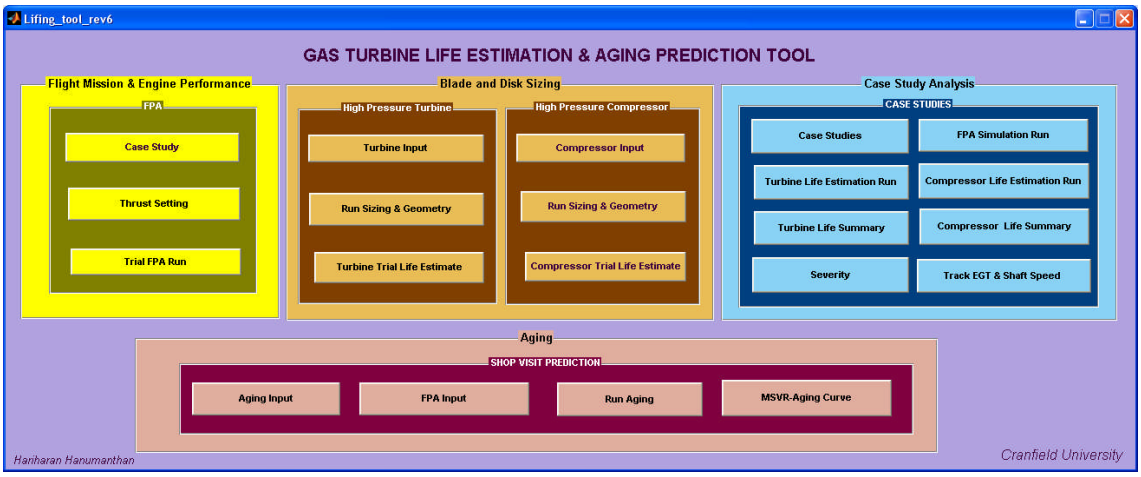

Figure F.1 : Graphical user interface of the tool.